Fixed-wing UAV Tracking of Evasive Targets in 3-Dimensional Space

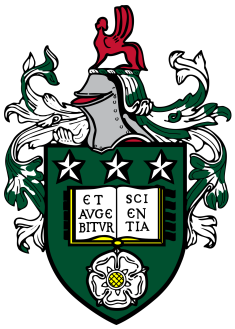

Chinedu Justice Mbam

Submitted in accordance with the requirements for the degree of *Doctor of Philosophy* in Mechanical Engineering

University of Leeds
Faculty of Engineering
School of Mechanical Engineering
Institute of Design, Robotics and Optimisation
January 2024

Declaration

The candidate confirms that the work submitted is his own and that appropriate credit has been given where reference has been made to the work of others.

This copy has been supplied on the understanding that it is copyright material and that no quotation from the thesis may be published without proper acknowledgement.

©2023 The University of Leeds and Chinedu Justice Mbam

Chinedu Justice Mbam
December 2023

Acknowledgements

I begin with gratitude to God, whose guidance and blessings have illuminated my path throughout this academic journey. Without divine guidance, none of this would have been possible.

Next, I extend my deepest appreciation to my thesis supervisor, Dr. Kim Jongrae. Your expertise, patience, and mentorship have been invaluable throughout this research endeavour, enhancing the quality of this thesis significantly. I'd also like to thank the other lecturers who have shared their knowledge and wisdom, enriching my understanding and perspective. To my fellow students, your camaraderie, discussions, and shared experiences have been a wellspring of motivation and inspiration. Our intellectual exchange and friendships have been invaluable. I also want to acknowledge the funding and support by the Petroleum Technology Development Fund, and the support by the Nigerian Air Force

On a personal note, I am profoundly thankful for my family. To my loving wife, Emem, your unwavering support, patience, and understanding have been my bedrock. Your sacrifices and unwavering belief in me have fuelled my determination. To my sons, Jayson and Jaden, and my daughter, Joanne, your enthusiasm, energy, and love have been a constant source of inspiration. You are my greatest joy, and your presence has kept me motivated.

Finally, I acknowledge the support of the academic community, the institution's staff, and its resources, which facilitated my research. This thesis stands as a testament to the collective efforts of all those mentioned above. Your contributions, whether big or small, have played a significant role in shaping this work. Thank you for being an integral part of this academic achievement.

Abstract

In this thesis, we explore the development of autonomous tracking and interception strategies for both single and multiple fixed-wing Unmanned Aerial Vehicle (UAV) pursuing single or multiple evasive targets in 3-dimensional (3D) space. We considered a scenario where we intend to protect high-value facilities from adversarial groups employing ground-based vehicles and quadrotor swarms and focused on solving the target tracking problem. Accordingly, we refined a min-max optimal control algorithm for fixed-wing UAVs tracking ground-based targets, by introducing constraints on bank angles and turn rates to enhance actuator reliability when pursuing agile and evasive targets. An intelligent and persistent evasive control strategy for the target was also devised to ensure robust performance testing and optimisation.

These strategies were extended to 3D space, incorporating three altitude control algorithms to facilitate flexible UAV altitude control, leveraging various parameters such as desired UAV altitude and image size on the tracking camera lens. A novel evasive quadrotor algorithm was introduced, systematically testing UAV tracking efficacy against a range of evasive scenarios while implementing anti-collision measures to ensure UAV safety and adaptive optimisation improve the achieved performance. Using decentralised control strategies, cooperative tracking by multiple UAVs of single evasive quadrotor-type and dynamic target clusters was developed along with a new altitude control strategy and task assignment logic for efficient target interception. Lastly, a countermeasure strategy for tracking and neutralising non-cooperative adversarial targets within restricted airspace was implemented, using both Nonlinear Model Predictive Control (NMPC) and optimal controllers.

The major contributions of this thesis include optimal control strategies, evasive target control, 3D target tracking, altitude control, cooperative multi-UAV tracking, adaptive optimisation, high-precision projectile algorithms, and countermeasures. We envision practical applications of the findings from this research in surveillance, security, search and rescue, agriculture, environmental monitoring, drone defence, and autonomous delivery systems. Future efforts to extend this research could explore adaptive evasion, enhanced collaborative UAV swarms, machine learning integration, sensor technologies, and real-world testing.

Table of Contents

List of Figures

List of Tables

List of Algorithms

List of Acronyms and Initialisms

2D	2-dimensional
3D	3-dimensional
6DOF	Six Degree of Freedom
AAR	Air to Air Refuelling
ABSC	Adaptive Backstepping Controller
ACLS	Automatic Carrier Landing System
ADMM	Alternating Direction Method of Multipliers
AoA	Angle of Attack
BA	Bat Algorithm
BSC	Backstepping Controller
BSiLQG	Belief Space iterative Linear Quadratic Gaussian
CBFs	Control Barrier Functions
CCOV	Chance-Constraints based on Obstacle Velocity
CMPC	Constrained MPC
C-UAS	Counter Unmanned Aircraft System
CW	Continuous Wave
DDPG	Deep Deterministic Policy Gradient
DEWs	Directed Energy Weapons
DO	Disturbance Observer
DMDP	Decentralised Markov Decision Process
EKF	Extended Kalman Filter

EMF Electromagnetic Field

EMPC Economic Model Predictive Controller

ESO Extended State Observer

FOA Fruit-Fly Optimisation Algorithm

FPA Flight Path Angle

FOV Field of View

GNS Global Navigation System

GPS Global Positioning System

GTT Group Target Tracking

HALE High Altitude Long Endurance

HPM High-power Microwave

IA Interval Avoidance

IBVS Image-Based Visual Servoing

IGWO Improvised Grey Wolf Optimiser

IMU Inertial Measurement Unit

IR Infra Red

iLQG iterative Linear Quadratic Gaussian

IoBT Internet of Battlefield Things

ITSMC Integral Terminal Sliding Mode Controller

KCF Kernelised Correlation Filter

LGVF Lyapunov Guidance Vector Field

LOS Line of Sight

LQG Linear Quadratic Gaussian

LMPC Linear MPC

LQR Linear Quadratic Regulator

LTI Linear Time Invariant

LTS Load Transfer Systems

LVF Lyapunov Vector Field

MALE Medium Altitude Long Endurance

MAV Micro Aerial vehicle

MDT Mode-Dependent dwell Time

MCMC-PF Markov Chain Monte Carlo Particle Filter

MLND Multi-Layer Neural Dynamics

MPC Model Predictive Control

MPF Moving Path Following

MPME Multiple-Pursuers Multiple-Evaders

MRAC Model Reference Adaptive Control

MTT Multi-Target Tracking

MUAVs Miniature UAVs

NBO Nominal Belief-State Optimisation

NMPC Nonlinear MPC

PTZ Pan-Tilt-Zoom

PD Proportional-Derivative

POMDP Partially Observable Markov Decision Process

PI Proportional-Integral

PID Proportional-Integral-Derivative

QP Quadratic Programming

QUAV Quadcopter UAV

QFHUAV Quadrotor Fixed-wing Hybrid UAV

RL Reinforcement Learning

SLAM Simultaneous Localisation & Mapping

SLMPC Successive Linearisation MPC

SMC Sliding Mode Control

SMPC Stochastic MPC

TCMPC Time-varying Constrained Model Predictive Controller

TMPC Tube MPC

UAS Unmanned Aerial Systems

UAV Unmanned Aerial Vehicle

UDE Uncertainty and Disturbance Estimator

UGVs Unmanned Ground Vehicles

UWB Ultra Wide Band

VTOL Vertical Takeoff and Landing

Nomenclature

Latin Letters

$(\hat{d}_r(\mathbf{x_{q_i}})$	Normalised UAV distance to i-th target
$(a_{gx},\ a_{gy},\ a_{gz})$	Target x, y and z acceleration components in world frame
(C_x, C_y)	Coordinates representing centre of polygon
(F_{xq}, F_{yq}, F_{zq})	Forces acting on the quadrotor in the body frame along the x, y, and z axes
(p, q, r)	Quadrotor body frame angular rates for roll, pitch, and yaw angles
$(u_{ax},\ u_{ay},\ u_{az})$	UAV x, y and z acceleration components in world frame
$(v_{ax},\ v_{ay},\ v_{az})$	UAV x, y and z velocities components in world frame
$(v_{gx},\ v_{gy},\ v_{gz})$	Target x, y and z velocities components in world frame
(x^{Bg}, y^{Bg}, z^{Bg})	Target x, y and z body-frame component
$(x_q,\ y_q,\ z_q)$	Quadrotor $x-y-z$ positions
$(x_a,\ y_a,\ z_a)$	UAV x, y and z components in world frame
$(x_g,\ y_g,\ z_g)$	Target x, y and z components in world frame
$(\mathbf{x}_m\ \mathbf{y}_m,\ \mathbf{z}_m)$	Moving frame unit vectors in x, y, z directions
$(\omega_{xq1}, \omega_{y_{q1}}, \omega_{z_{q1}})$	Angular velocities around the body-fixed x, y, and z axes
$(x^{Ba},\ y^{Ba},\ z^{Ba})$	UAV x, y and z body-frame component
α_a	UAV angle of attack
$\alpha_g, \beta_g, \gamma_g$	Functions of the UAV initial velocity and position, and target position

$\bar{J}$, $\bar{J}_g$	UAV and target equivalent cost functions
$\mathbf{d_{ij}}$	Distance between i-th and $j-th$ UAV
$\mathbf{d_{uav}}$	UAV displacement from target
$\mathbf{e_p}$	Position error vector
$\mathbf{e_{p,k}}$	Position error vector at time t_k
$\mathbf{e_{uav}}$	Direction of the quadrotor to the UAV
$\mathbf{s_{d_{it}}}$	Desired separation vector
$\mathbf{s_{e_{it}}}$	The i-th UAV to target separation vector error
$\mathbf{s_{ij}}$	Separation vector
$\mathbf{s_{it}}$	The i-th UAV to target separation vector
$\mathbf{U}$	Control input trajectory
$\mathbf{u_k}$	Control input vector at time t_k
$\mathbf{v_{qc}}$	Quadrotor velocity vector at current time step
$\mathbf{v_q}$	Quadrotor velocity vector
$\mathbf{X}$	State trajectory
$\mathbf{x_{a_m}}$	Mean of the various UAV positions
$\mathbf{x_{q_{des_i}}}$	Desired position for the i-th target
$\mathbf{x_{track}}$	Next target to track
$\ddot{x}_{sq1}$	Second derivative of position in quadrotor's body frame - first axis
$\ddot{x}_{sq2}$	Second derivative of position in quadrotor's body frame - second axis
$\ddot{x}_{sq3}$	Second derivative of position in quadrotor's body frame - third axis
Δ	Change
δ	Relationship between the quadrotors lift and drag

$\dot{\gamma}_p$	Projectile LOS rate
$\dot{\phi_{ua}}$, $\dot{\psi_{ua}}$, $\dot{\theta_{ua}}$	Time derivatives of UAV roll, pitch, and yaw angles respectively
$\dot{\psi}$	UAV turn rate
$\dot{\psi}_g$	Target turn rate
ε_f	Target tracking efficiency factor
$\hat{b}$	Bi-normal vector
$\hat{d}_{f_a}(\mathbf{x_{q_i}})$	Normalised distance of the i-th target to the protected facility
$\hat{n}$	Unit normal vector
$\hat{t}_{f_a}(\mathbf{x_{q_i}}))$	Normalised time of the i-th target to the facility
ϕ_a	UAV heading path angle
ϕ_g	Target heading path angle
ϕ_{ua}	Azimuth angle of the projectile
ψ_a	UAV bank angle
ψ_g	Ground target flight path angle
$\psi_{q_{des}}$	Desired yaw angle
ψ_q	Quadrotor yaw angle
$\psi_{tr}(t)$	Trajectory yaw angle
ψ_{ua}	Roll angle of the UAV
ρ_{lim}	Limit for angle between UAV and target
ρ_{q_i}	Angle made by the UAV and i-th target
σ_a	UAV flight path angle
σ_g	Target flight path angle
$\mathbf{x}_q$	Vector that represents the position of the quadrotor in the global frame

$\mathbf{x}_{tr}(t)$	Specified trajectory
$\mathbf{z}_{des}$	Desired trajectory
θ_a	Optimisation parameter for best-case UAV tracking minimisation
θ_{ci}	Heading angle correction for UAV i
θ_{d_i}	Desired heading angle
θ_{pa}	UAV pitch angle
$\theta_{q_{des}}$	Desired pitch angle
θ_q	Quadrotor pitch angle
θ_{ua}	Pitch angle of the UAV
θ_{ua}	UAV yaw angle
$\varphi_{q_{des}}$	Desired roll angle
φ_q	Quadrotor roll angle
A_p	Area of target cluster polygon
A_a	UAV state space A matrix
A_g	Target state space A matrix
B_a	UAV state space B matrix
B_g	Target state space B matrix
C_a	UAV state space C matrix
C_g	Target state space C matrix
$d_(\mathbf{x_{q_i}})$	Relative distance between the UAV and a target $\mathbf{x_{q_i}}$
d_h	Horizontal distance between the UAV and the target
d_p	Diameter of target cluster polygon
d_r	Distance function between a target and a restricted area

$d_r(x_{q_i})$	Distance of i-th target to restricted area
d_{cur}	Distance in the current step
d_{eng}	Engagement distance of the UAV to the target
d_{prd}	Predicted UAV distance
d_{prv}	Distance covered in the previous time step
d_{dec}	Deceleration distance
d_{drd}	Remaining distance after deceleration and the target radius
$d_{e_{it}}$	The i-th UAV to target distance error
$d_{f_a}(\mathbf{x_{q_i}})$	Distance between the target and the facility
d_{f_o}	Threshold distance to the protected facility
$d_{f_{c_i}}$	Ratio of target distance to UAV focal length
D_{mR}	Direction cosine matrix reference to moving frame
d_{q_i}	Euclidean distance between UAV and i-th target
d_{rel}	Average relative distance of the UAV to the target
d_{rem}	Distance remaining from the current position to the target position
D_{Rm}	Direction cosine matrix moving to reference frame
d_{safe}	Minimum safe distance
d_{trv}	Distance travelled during the travel phase
d_{c_w}	Euclidean distance between UAV and target centre in world frame
d_{c_i}	Euclidean distance between midpoints of UAV camera and target image
d_{ig_i}	Magnitude of target cluster diameter on the i-th UAV camera plane
d_{it_o}	Optimal distance between UAV i and the target
e_x	Coefficient for optical range optimisation

e_ρ	Coefficient weighting term for J_{ρ_i}
E_B	Quadrotor centre of mass
E_{dec}	Energy consumed during the deceleration phase
e_{p_c}, e_{p_c}	Quadrotor position and velocity errors with respect to the desired trajectory
e_{p_q}	Quadrotor position error
e_{si}	Image size error
E_{tgt}	Energy consumed during a close manoeuvre to the target
E_{tot}	Total energy consumed in the various phases of travel
E_{trv}	Energy consumed during the travel phase
e_{v_q}	Quadrotor velocity error
e_{za}	Altitude error
$E_{v_{\max}}$	Energy dissipated at maximum velocity
f_c	Camera focal length
F_i	Forces exerted by each quadrotor rotor (F_1, F_2, F_3, F_4)
$F_{\text{int}}(U_j)$	Function that measures the UAV's capability to intercept the target
$F_{\text{pos}}(U_j)$	Function that assesses the position-related suitability of the UAV based on its proximity to the target
$F_{\text{vel}}(U_j)$	Function that evaluates the suitability related to the UAV's velocity
F_a	UAV state discretization matrix
f_{c_i}	Focal length of the i-th tracking UAV
F_g	Target state discretization matrix
g	Acceleration due to gravity
G_a	UAV control input discretization matrix

G_g	Target control input discretization matrix
h	Height
$h_{\max}$	Maximum altitude that maximises visibility coverage
$h_{\min}$	Minimum altitude that optimises observation and image quality
h_{tc}	Altitude of the target cluster, measured from its centre point
h_{u_i}	Altitude of the i-th UAV
$i,\ j$	The i-th and j-th term
$J,\ J_g$	UAV and target cost functions
J_{ρ_i}	Vertical control cost dependent on angle made by UAV and i-th target
$J_{adv_{ij}}$	Cost for preventing collision between the i-th and $j-th$ UAV
$J_{adv_{it}}$	Cost for preventing collision between the i-th UAV and target
J_{alt}	Cost function for control of UAV altitudes
J_{avd}	Collision avoidance function
J_{comb}	Combined cost function for cooperative UAV tracking
$J_{g_{bd}}$	Minimal cost along the constraint boundary for target
$J_{g_{in}}$	Minimal control effort within target constraints circle
J_{hi}	Cost function for determining the altitude of the i-th UAV
J_h	Cost function for UAV altitude
J_{tr}	UAV min-max cost function for tracking the evasive quadrotor
J_{um}	Cost function for UAV NMPC
J_{x_i}	Cost function for optimal optical range
k	Time step
k_a	Constant for the avoidance acceleration

K_{p_i}, K_{d_i}	Proportional and derivative respective gains for x_{i_l}
$K_{p_{za}}$, $K_{d_{za}}$	Proportional and derivative respective gains for z_a
k_{pr}	Constant that determines the strength of the retardation effect
L	Axis of rotation of the rotors
l_a, l_g	Lengths for UAV and target 2-step schematics
m	Mass
M_i	Moment perpendicular to the quadrotor blade's plane of rotation (M_1, M_2, M_3, M_4)
N_p	Projectile proportional navigation constant
N_q	Number of quadrotors in the evasive drone swarm
N_u	Number of UAVs
$n_{sam_{Op}}$	Adaptively optimised number of samples in control space
p_{met}	UAV performance metric
p_{des}	Desired angular roll rate
$p_{r_{\min}}$	Projection ratio limits
Q_p	Adaptive weighting matrix for UAV position
q_{des}	Desired angular pitch rate
$R(x_{q_i})$	Risk factor for each of the quadrotor target
R_u	Adaptive weighting matrix for UAV control input
r_{a_d}	Length of line connecting the UAV and the desired altitude
r_{a_g}	Length of line connecting the UAV and the target
$r_{min_{Op}}$	Adaptively optimised minimum turn radius
r_q	Actual position and yaw angle of the quadrotor
r_{tgt}	Target radius

r_{tr}	Desired trajectory vector for quadrotor position and yaw angle
r_w	Distance measured along the line of sight between UAV and target
$S(U_j)$	Suitability score for each UAV
S_i	Tracking decision score
$s_q(t)$	Target paths at each time t
$s_u(t)$	UAV paths at each time t
t	Time
t_0	Initial time
t_{nt}	Total time taken to neutralise all targets
t_{tot}	Total time
$t_{a_{\textbf{score}}}$	Performance of the UAV in tracking the target over time
$t_{c_{ij}}$	Time to the collision between UAVs i and j
$t_{f_a}(\mathbf{x_{q_i}})$	Estimated time for target i to reach the protected facility
t_{f_o}	Threshold time to the protected facility
t_f	Final time
t_{ttg}	Time to target
t_{vmx}	Time during which the UAV is operating at maximum velocity
U	Set of all available UAVs
U_p	Set for assignment of pursuit task to UAV
u_{areq}	Required acceleration of the UAV
u_p	Acceleration command for countermeasure projectile
u_{q1}, u_{q2}	Quadrotor first and second control inputs
$u_{avd_{ij}}$	Avoidance acceleration between UAVs i and j

u_{si}	Image size control input
$u_{x_{it}}$, $u_{y_{it}}$	Respective x and y collision avoidance control input
v_{aerrp}	Previous velocity error
v_{aerr}	Error between the predicted velocity and the current velocity
v_{rpr}	Predicted UAV relative velocity
v_{r}	Relative velocity
$v_{a_{\text{opt}}}$	Optimal UAV velocity
$v_{c_{ij}}$	Closing velocity between UAVs i and j
$v_{max_{Op}}$	Adaptively optimised maximum velocity
$v_{min_{Op}}$	Adaptively optimised minimum velocity
v_{xy}	UAV horizontal plane velocity magnitude
$v_{avd_{ij}}$	Velocity correction
w_0, w_n	Pair of waypoints
w_d, w_f, w_t	Weights for UAV distance, target distance to facility and time to facility
w_1, w_2, w_3	Weights of the functions are represented by the constants
W_{comb}	Combined weight
X_q	Set of all quadrotor targets
x_{prd}	Predicted UAV position
$x_{i_{cen}}$	Centre of the target on the image plane
$x_{i_{min}}$, $x_{i_{max}}$	Extreme corners of the longer diagonal of the image box
$x_{p_{cen}}$	Midpoint of the image plane
x_{s_i}	Size of the target box frame on the image plane
x_{s_w}	Size of the ground target box frame in the world plane

z_d	Desired UAV altitude
z_a, z_g	UAV and target altitudes
$\mathbf{r}a$, $\mathbf{r}_g$	UAV and target schematic displacement vector at each time step
$\mathbf{u}_a^m$	Tracking command in 2D body frame expressed in the moving frame
$\mathbf{U}_a$	Set of feasible UAV control inputs
$\mathbf{u}_a$	UAV acceleration vector
$\mathbf{U}_g$	Set of feasible target control inputs
$\mathbf{V}_a$	Set of feasible UAV velocities
$\mathbf{V}_g$	Set of feasible target velocities
$\mathbf{v}_a$	UAV velocity vector
$\mathbf{v}_{r_{ij}}$	Relative velocity
$\mathbf{v}_{r_{it}}$	i-th UAV to target relative velocity
$\mathbf{x}$	UAV state
$\mathbf{x}_a$	UAV state vector
$\mathbf{z}$	Target state
$\mathbf{x}_{sq}$	Quadrotor six-dimensional state vector
$r_{\min}$	Minimum turn radius of UAV
t_{stp}	Time taken to decelerate from maximum to minimum velocity
x_B, y_B, z_B	Quadrotor body frame directions
$\mathbf{v}_{des}$	Desired velocity
$\mathbf{v}_{err}$	Velocity error
$x_{s_i}{}^{des}$	Desired size of the target on image plane

Chapter 1

Introduction

1.1 Motivation

The continuous effort by mankind to find better and more efficient ways of performing vital tasks has in led to an accelerated technological advancement [1]. One such effort by man to solve the problem of faster travel by air led to research into powered aerial flights in the late 1800s. Since the first powered flight by the Wright brothers in 1903, the field of powered aerial vehicles has experienced increasing research and development [2]. One area that has benefited from the rapid technological growth is the design and production of autonomous vehicles such as the Unmanned Aerial Vehicle (UAV) [3]. UAVs have attracted increasing attention in the literature and have been applied for surveillance, intelligence gathering, transportation of goods, agricultural activities, and target tracking [4, 5]. In particular, the field of target tracking has attracted the interest of the research community due to the real-world application of autonomously tracking moving targets over land and sea [6]. Due to the potential for misuse of drones for malicious and illegal activities to support terrorism, conduct organised crime and disrupt critical national infrastructure, the tracking of uncooperative aerial targets has become a paramount research area [7]. For instance between 2016 to 2018, about 771 drone-related crimes were documented in which criminal gangs used drones to smuggle illegal substances to UK prisons [8–10]. Additional statistics of illegal drone incidences such as the disruption at Gatwick Airport in December 2018, highlight the magnitude of the evolving risks posed by the malicious and nefarious use of drones [9, 10]. Furthermore, the nature of these evasive drone targets presents critical challenges in the deployment of UAVs for efficient and robust tracking within dynamic and unpredictable environments. Moreover, as UAVs become increasingly integrated into civilian and military operations, the need for optimal and adaptive tracking systems capable of handling agile and elusive targets has become paramount [11].

The pursuit of highly evasive targets, such as agile drones or manoeuvrable airborne threats, poses a significant challenge due to their erratic movement patterns, swift changes in trajectory, and rapid speed variations [12, 13]. Current literature on the subject of evasive target tracking falls short in adequately modelling evasive targets as researchers commonly use simple models to mimic real-world target evasion [14–16]. At the time of conducting this research, we could not find any literature that implemented a 3D dynamics and smart evasion strategy for aerial drone-type targets to evade a fixed-winged tracking UAV. This leaves a gap as the robustness of the tracking algorithm is tested against the evasive capabilities of the target being tracked. This research addresses this important gap by designing and optimising algorithms for both UAV tracking and target evasion in various scenarios and mission configurations.

The research aims to develop algorithms for single and coordinated UAVs to track agile, manoeuvring, and evasive ground and aerial targets by investigating various approaches and methods for effectively and persistently maintaining the targets in the UAVs Field of View (FOV) while considering the physical and dynamic limits of the tracking vehicle(s). This study starts by investigating the tracking problem using a 2-dimensional (2D) scenario and solving it by assuming a randomly moving target, then extending it to a 3-dimensional (3D) scenario. To capture the problem realistically, and to test the robustness of the tracking algorithm being developed, this research will introduce evasive target(s) with peculiar dynamic capabilities and constraints to that of the UAV, in the form of mobile ground vehicles and fast-moving quadrotors.

The tracking UAV will use the information provided by onboard sensors like cameras to identify and track the mobile target, constrained by limited FOV, control inputs and turn radius [14]. The type of targets considered for the tracking algorithm design includes intruder vehicles encroaching a restricted area, single or swarm of aerial quadrotor-type targets violating a restricted area or a drone controlled by a mischievous actor, intending to cause harm or havoc to a protected facility of building. Considering that these types of target-tracking missions are time-sensitive and often unplanned, they would require the quick intervention of tracking UAVs. Accordingly, this research also intends to address UAV coordination to ensure that the target is persistently tracked, captured, or neutralised.

The outcomes of this research endeavour are anticipated to contribute to advancing the field of UAV-based target tracking, offering robust and scalable solutions that can be applied across various domains including security operations, surveillance, search and rescue, precision agriculture and commercial transportation. The potential impact of this work therefore extends to enhancing tactical operations, improving civilian safety, and facilitating advancements in autonomous UAV systems, thereby contributing to the broader technological evolution in aerial robotics and unmanned systems.

1.2 Problem Statement

Tracking single or multiple manoeuvring targets using lone or cooperative UAVs is a dynamically challenging task [13]. Designing a realistic model of the tracking and evasion vehicles will require solving different challenges at the different stages of design [17]. Firstly, we need to mathematically design models of the aerial and ground vehicles that accurately describe the behaviour of the vehicles in real-life scenarios while allowing for simplicity for the design of robust controllers and navigation algorithms. Secondly, we stabilise the translational and rotational dynamics of the UAV to cope with tracking active and evasive targets. The last step is designing guidance systems to track moving targets and, if cooperative aerial vehicles are utilised, to coordinate them.

1.2.1 Dynamics consideration

As a result of the considerations above, the issue is split into the following main axes:

- UAV dynamics: This research focuses on fixed-wing models when analysing the dynamics of UAVs. These aircraft have distinct motion constraints and dynamic constraints, causing them to behave like non-holonomic vehicles. Unlike ground targets, fixed-wing UAVs have more difficulty stopping or changing direction, which often results in difficulty when attempting to outmanoeuvre targets.
- Target dynamics: Non-smart manoeuvring targets are frequently designed by researchers to mimic evasive target manoeuvres. In this study, the target's behaviour and dynamics are critical factors that must be carefully considered. The target can move on an open field or a road network, and its movement is constrained by the dynamics of a car model. Furthermore, the target may behave neutrally or employ evasive tactics, introducing a tracking-evasion scenario. This tracking-evasion scenario is analogous to game theoretic pursuit and evasion problems, in which the UAV operator must make strategic decisions. As a result, understanding the target's dynamics and behaviour is critical in developing effective UAV tracking and pursuit strategies.
- Cooperative UAV tracking of aerial targets: Cooperative tracking of aerial targets considers the collaboration among multiple UAVs, to ensure efficient tracking efforts. Understanding the dynamics of the UAVs as well as that of single and multiple targets is vital for predicting trajectories and adapting tracking strategies in real time. Utilising appropriate tracking algorithms and information sharing will enhance accuracy and tracking robustness. Additionally, adaptive control algorithms empower UAVs to dynamically manoeuvre and respond to the unpredictable movements of

aerial targets. In general, cooperative decision-making processes will enable proper task assignment and overall mission success.

1.2.2 Research questions

The main focus of this research is on enhancing evasive target tracking and contributing to the field of UAV design and operations. Accordingly, the main research question is as follows: How can we effectively track a single or multiple evasive ground or aerial targets using single or multiple fixed-wing UAVs while considering the dynamics and limitations of the tracking and evasion vehicles? To enable us to address the above question thoroughly, it is broken down into four sub-research questions as follows:

a. What tracking algorithm is best suited for tracking a single or group evasive target while considering the limitation of the tracking vehicles?

b. What consideration should be made in designing a smart target that can persistently evade the tracking UAV?

c. What optimisation parameters need to be adjusted to enable a UAV to track an evasive target effectively?

d. How can cooperative UAVs make a joint decision and task assignment during active target tracking scenarios to ensure optimal tracking of targets?

1.3 Research Aim and Objectives

This research aims to develop a 3D target tracking algorithm for single and cooperative fixed-wing UAV tracking of smart evasive ground or aerial targets while accounting for the dynamic constraints of tracking and evading vehicles. The research objectives are outlined below to address the research questions identified above:

a. Develop a UAV tracking and evasion model using optimal and other control concepts and extend the UAV tracking model from 2D to 3D (addresses research question **a**).

b. Implement a quadrotor target algorithm that can persistently evade the fixed-wing UAV tracking UAV 3D (addresses research question **b**).

c. Develop an adaptive control algorithm that selectively adjusts various optimisation parameters online to enhance UAV target tracking (addresses research question **c**).

d. Implement UAV algorithm for cooperative tracking of single and multiple evasive aerial targets (addresses research question **d**).

1.4 Summary of Contributions

The main contributions of this research are outlined as follows:

- Comprehensive survey of up-to-date literature on fixed-wing UAV evasive ground and aerial targets tracking (research objective **a**).
- The turn rate and bank angle limits are used to solve the 2-step prediction fixed-winged UAV optimal control strategy by [14]. This allows for smoother target tracking while limiting the UAV's ability to turn excessively (research objective **a**).
- We extend the 2D algorithm in [14] to a 3D target tracking algorithm, accounting for changes in terrain (research objective **a**).
- A Flight Path Angle (FPA) for controlling the UAV's vertical movement is calculated using an altitude control rule that takes into account the relationship between the velocity vector in the 2D plane and the desired altitude above the target. A second altitude controller is also designed using the relationship between the real and project size of the target image on the tracking camera plane (research objective **a**).
- An evasive target control method is developed by solving a two-step maximisation problem, offering realistic target movements (research objective **b**).
- A modified controller is developed for organising and tracking a group of evasive, uncooperative aerial targets while avoiding mid-air collisions (research objective **c**).
- Using the size of the target cluster, the distances between individual targets, and balancing the requirements for image quality and FOV coverage and autonomously controlling the altitude for each UAV on a cooperative search mission (research objective **c**).
- A task assignment and switching logic is developed to aid the tracking UAV in choosing the sequence of targets to track (research objective **d**).
- To neutralise or interdict an adversarial quadrotor drone targets, we developed a novel proportional navigation-based projectile algorithm with a retardation component (research objective **d**).

From Fig. 1.1, it can be observed that contribution 1 is a result of the survey conducted in Chapter 2. Similarly, contributions 2, 3 and 4 are from Chapter 3 while contribution 5 results from Chapter 4. Also, the research presented in Chapter 5 makes the 6th contribution while contribution 7 is derived from Chapter 6. The last two contributions are the results of the work presented in Chapter 7. Collectively, Chapters 2, 3 and 4 address Objective 1 of this thesis while Chapter 5 addresses Objectives 2 and 3. In the same vein, Chapters 6

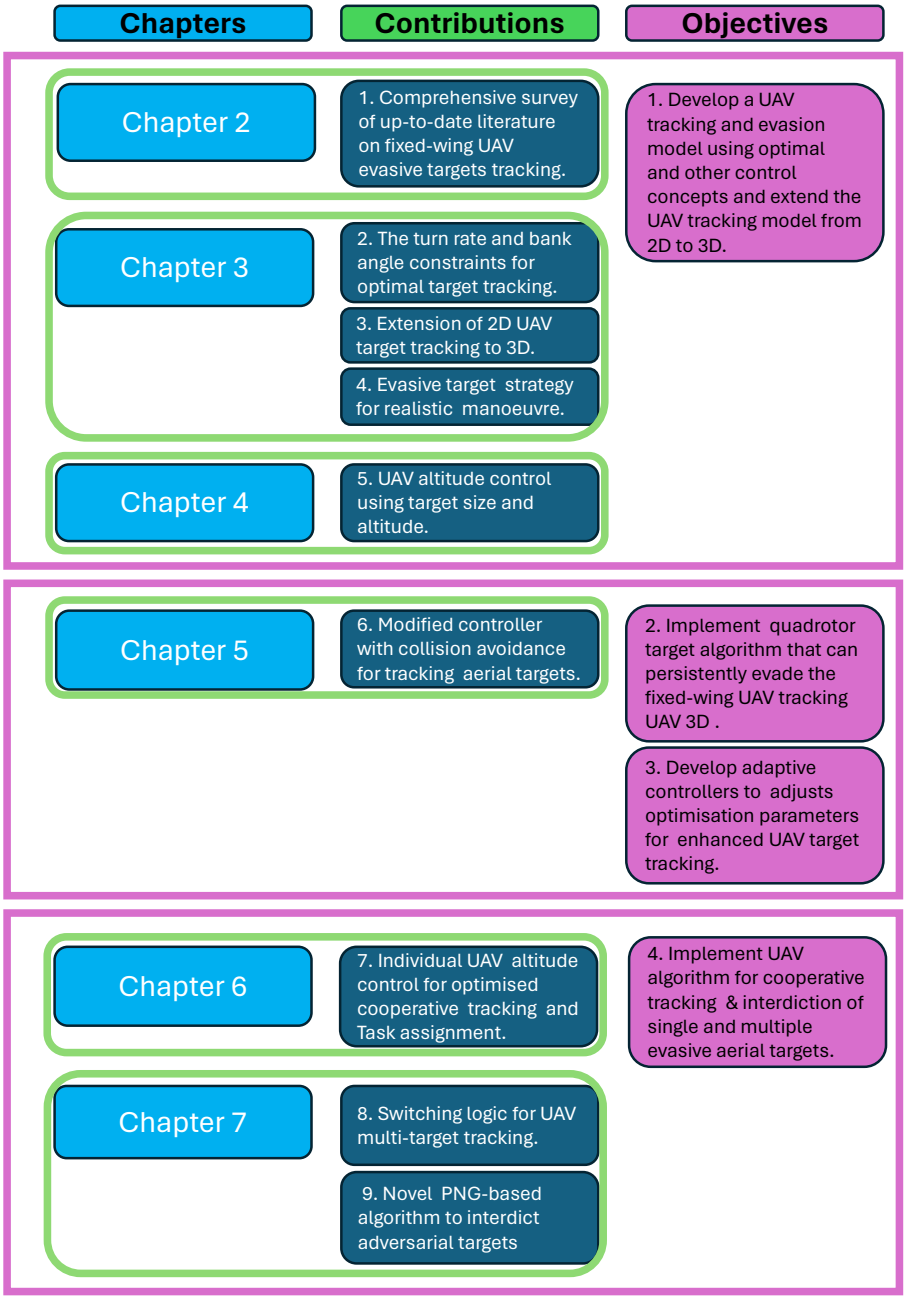

Fig. 1.1 Link between thesis chapters, contributions and objectives.

and 7 address objective 4 of this thesis. The chart in Fig.. 1.1 shows that the research work presented in all the chapters is related to the thesis objectives and overall aim of designing a fixed-wing tracking algorithm for single and cooperative tracking of both ground and aerial evasive targets.

1.5 Thesis Organisation

This thesis presents various modified and novel algorithms for tracking both single and multiple evasive ground and aerial targets using single and cooperative fixed-wing UAVs. The design considers the physical limits of small and medium-sized UAVs in deciding the dynamics constraints and smart target control. The thesis is structured as outlined in Fig. 1.2 while the brief description of the research focus of the technical chapters is provided in the following paragraphs.

Chapter 2 explored of recent advancements and applications in UAV target tracking before presenting an in-depth analysis of the factors influencing target tracking. The factors identified include environmental, dynamics, target types, and the number of targets tracked. This chapter also reviewed state-of-the-art target tracking guidance and control methodologies, including optimal control strategies and adaptive online control methods that aid the effective tracking of evasive targets. Cooperative target-tracking control strategies were also examined, highlighting collaborative efforts among multiple UAVs in complex environments. Lastly, the chapter explored recent literature on countermeasures against adversarial targets. The chapter identified key insights, gaps, and avenues for further research, and laid a robust foundation for subsequent investigations into UAV target tracking.

Chapter 3 discusses a UAV tracking algorithm to track an evasive ground-moving target using optimal control law. The UAV tracking algorithm modified the work of [14] by considering additional constraints that ensured smooth target tracking. Additionally, an evasive target is designed to intelligently evade the tracking UAV. Both algorithms were extended to 3D space to simulate more realistic UAV and target engagement scenarios.

Chapter 4 developed various altitude control algorithms aimed at automatically adjusting the altitude of the UAV to operate within an upper and lower altitude band above ground or aerial targets. The altitude equations and algorithm assume that the UAV will adjust its altitude in response to the altitude or elevation of the target and is used in combination with the tracking algorithm in Chapter 3 to develop various aerial target tracking scenarios

Chapter 5 outlines the modification and development of UAV controllers for tracking evasive quadrotor-type targets that are designed to constantly take evasive action to manoeuvre away from the tracking UAV. The UAV algorithm developed in Chapter 3 is adaptively optimised to track and keep the aerial target within the UAV's FOV while maintaining a

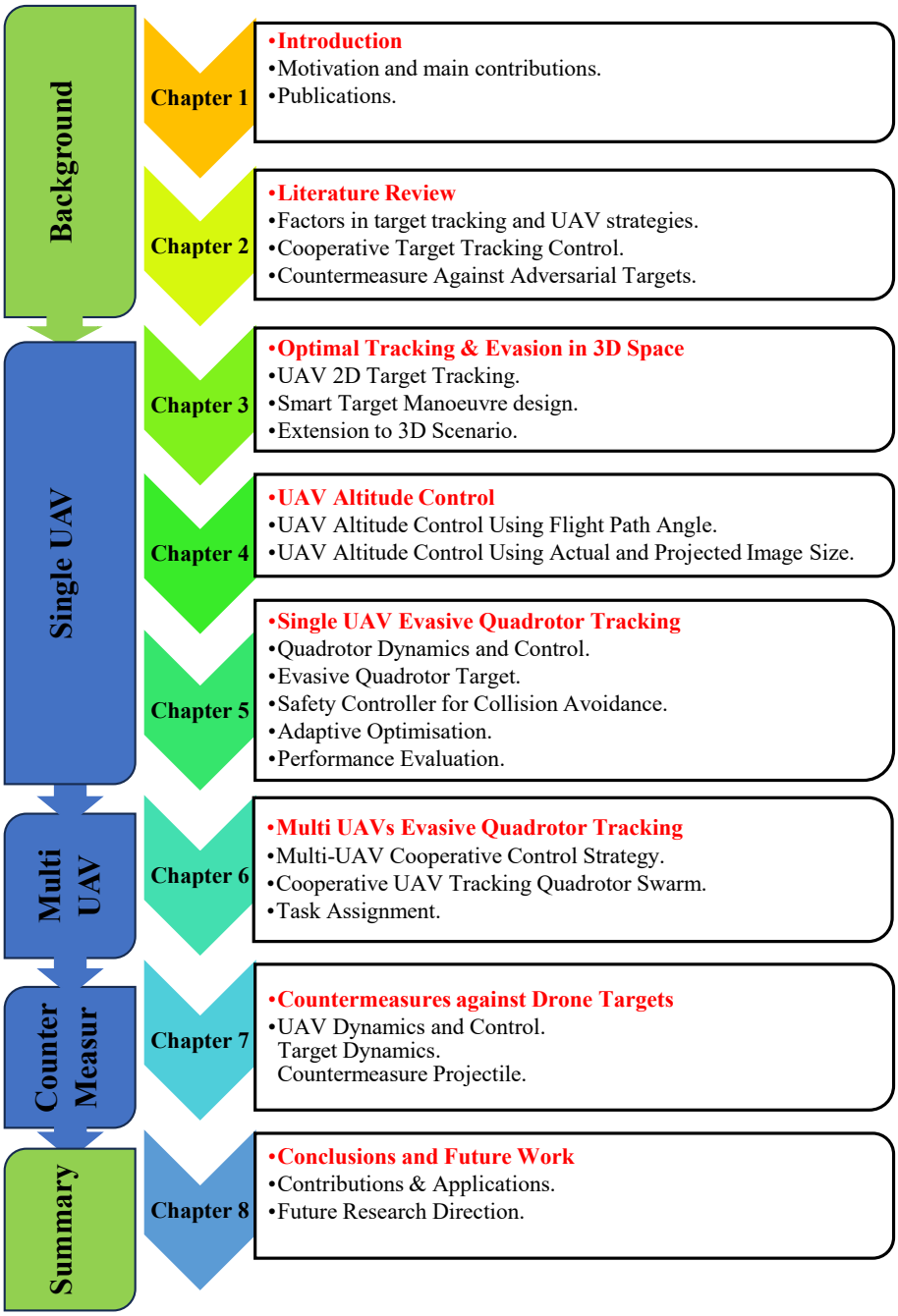

Fig. 1.2 Outline of thesis structure

predefined optimal altitude band.

Chapter 6: This chapter discusses the cooperative tracking of a single quadrotor target by multiple UAVs. The UAV control algorithm in this chapter is developed by modifying the algorithm presented in Chapter 3 to cooperatively track the evasive target while avoiding collision between the UAVs and the target. The tracking algorithm is designed as decentralised cooperative tracking where each UAV tracks the target independently, keeping the

target in their respective FOVs while maintaining a safe distance between the UAVs and the target

Chapter 7 considers a scenario where a fixed-wing UAV is tracking 3 independently manoeuvring quadrotor-type adversarial targets, attempting to intrude on a restricted facility and cause havoc. These targets are assumed to be aware of the tracking UAV and are continuously performing evasive manoeuvres to evade the UAVs. The goal of the UAV algorithm is to track the 3 targets independently and neutralise each target using the onboard countermeasure. A task assignment computation is also presented to aid the UAV in deciding which target to track first and the next target in the tracking and neutralisation sequence. We also implement some performance metrics to compare the tracking and neutralisation performance of our algorithm against optimal solutions in the same scenario.

Chapter 8 summarises the thesis, outlines the main contributions of this research and presents considerations for future research.

1.6 Methodology

The methodology used for the fixed-wing tracking UAV in this research is developed using a 2-step, min-max optimal control strategy that explores and minimises the worst-case target evasion. This study developed a smart target evasion strategy using a similar cost function to evade the UAV persistently, modifying the dynamics and constraints to suit a moving ground target. To autonomously control the altitude of the UAV, this research devised a method that computes flight path angle using velocity vectors from the 2D plane and a PD controller that utilises the relationship between the size of the image on the UAV camera and the actual size of the target on the ground to control the UAV to a desired altitude.

To utilise the UAV algorithm for aerial target tracking, the research applied an adaptive optimisation control method and designed an evasively manoeuvring quadrotor target using PID control. To explore multiple UAV tracking of a single target, collision avoidance computations are incorporated to prevent mid-air collision between the UAVs and the target. This is extended to multiple target tracking by devising a method that views the target cluster as a polygon and utilising the position of the various targets and cluster size to develop a dynamic altitude control strategy that optimises coverage while compensating for image quality. To complete the research, a methodology for assigning tasks to the tracking UAVs is presented, and NMPC & optimal control methods of driving the UAV to intercept an adversarial target. Where direct interception by the UAV would be limited,

this research also presented a proportional navigation guidance algorithm that allows a projectile to close up with the target and retard as it gets closer to the target to allow for the deployment of a countermeasure net.

1.7 Publications

Parts of the research presented in this thesis have been published as a peer-reviewed contributed paper to an international conference, while other aspects are in the process of preparation for submission. Details of the published paper are as follows.

1.7.1 Published Article

Mbam, C.J., and Kim, J. "Optimal Tracking & Evasive Algorithms for Fixed-Wing UAV & Target in 3D Space", In *Proceedings of IFAC World Congress. Yokohama, Japan*: Japan IFAC-PapersOnLine. 2023. pp.4938 - 4943

The above publication consists mainly of the research work presented in Chapter 3 of this thesis.

1.7.2 Unpublished Articles

Mbam, C.J., and Kim, J. "Comprehensive survey of up-to-date literature on fixed-wing UAV evasive targets tracking.", In preparation for submission to Multidisciplinary Digital Publishing Institute (MDPI) *Systems*.

Mbam, C.J., and Kim, J. "Single & Multiple Fixed-wing UAV Adaptive Tracking of Evasive Aerial Target", In preparation for submission to IEEE Transactions on *Journal of the Franklin Institute*.

Mbam, C.J., and Kim, J. "Fixed-wing Cooperative Tracking and Interception of Agile Quadrotor Swarm", In preparation for submission to *IEEE Transactions on Automatic Control*.

The content of the first paper in this subsection is drawn from a combination of the research effort covered in Chapters 4 and 5, while the second paper presents a concise write-up of the research covered in Chapters 6 and 7 of this thesis.

Chapter 2

Literature Review

2.1 Introduction

This Chapter reviews related work in the area of autonomous UAV target tracking in recent years. My interest in this field of research stems from my work experience in operations related to tracking evasive targets using aerial surveillance platforms and the challenges observed in various mission scenarios. Furthermore, we believe that the research would advance the development of better UAVs and algorithms to protect vital facilities and security operations. Accordingly, this Chapter explores state-of-the-art UAV tracking of various types of targets using different environments, UAVs, sensors, and target types. The reviewed literature also explored the common control strategies implemented by researchers in tracking aerial and ground targets, ranging from optimal control to adaptive online controls. The purpose of the review in this Chapter is to explore available information in target tracking, identify current techniques, methodologies, ideas, and theories, and establish relationships in terms of similarities, differences, and gaps in the existing literature to be covered in our research. Before exploring the various aspects of the UAV target tracking problem, let's first highlight the various applications where tracking paths or target objects are being applied.

Military Operations. UAV target tracking is essential in the following areas of military applications such as defence operations for surveillance, reconnaissance, and target tracking [18].

Search and Rescue. UAVs equipped with thermal cameras and other sensors to locate and track missing persons or disaster survivors [19, 20].

Law Enforcement. UAVs have also been employed for tracking suspects, monitoring crowds, and enhancing situational awareness in law enforcement operations. This is essential in locations where tracking with human eyes or fixed assets is limited [21–23].

Environmental Monitoring. When applying target tracking in environmental monitoring, UAVs are used to track wildlife, monitor ecosystems, and survey natural disasters or environmental changes [24–26].

Infrastructure Inspection. UAVs equipped with cameras and sensors could also be used to inspect infrastructure like power lines, pipelines, and buildings for defects, and damage or to track changes [27–29].

Agriculture. UAVs are being applied for tracking crop health, pest detection, precision agriculture, and harvesting of fruits using multi-rotor drones. This agricultural application saves time in terms of man-hour and cost by using sensors to detect and analyse images of leaves, fruits, and stems[30–32].

Film and Photography. Another area that has benefited from UAV target tracking is the film and photography industry. UAVs are used in the entertainment industry for tracking shots, aerial cinematography, and other forms of coverage that would be difficult or impossible to film using fixed structures of manned aerial vehicles [33–35].

Having established the various applications of target tracking research efforts, the rest of the Chapter is organised as follows. In Section 2.2, we review factors that affect target tracking using UAVs while Section 2.3 explores target tracking guidance & Control. In Section 2.4, we carefully review cooperative target tracking control efforts. This is followed by exploring research efforts on countermeasures against adversarial targets in 2.5. A summary of the findings and deductions from the reviewed studies is provided in 2.6. The process of planning, selecting appropriate literature, extracting relevant information, and executing the literature review is depicted in Fig. 2.1.

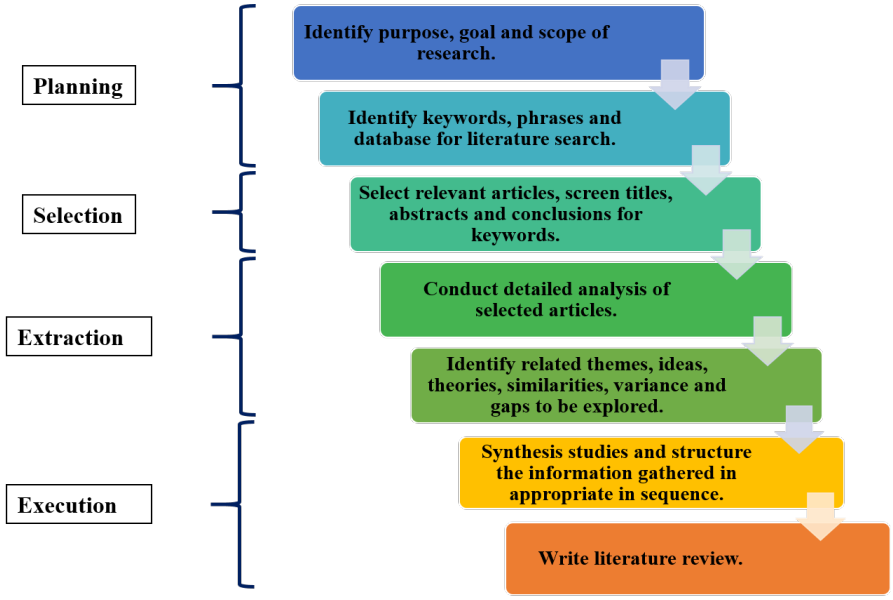

Fig. 2.1 Depiction of literature selection and review process

2.2 Factors in target tracking using UAVs

As outlined in the previous section, target tracking using UAVs applies to and is essential for executing vital tasks in different settings. When employing UAVs for the aforementioned roles, they could encounter non-cooperative targets, and either randomly or evasively manoeuvring. Therefore, developing a UAV target tracking algorithm that is capable of tracking intelligently evading targets is worth considering. To autonomously perform target tracking roles, the UAV must be capable of predicting and responding to evasive manoeuvres from agile targets. Accordingly, some factors need to be taken into consideration when modelling a target tracking scenario. These factors include simulation environment, target characteristics, UAV dynamics & characteristics, navigation, as well as guidance and control algorithms for tracking UAVs. Therefore, a review of these factors and how they affect target tracking implementation is presented in the succeeding subsections with reference to recent literature on target tracking. A flowchart of the various factors reviewed is shown in Fig. 2.2.

2.2.1 Tracking environment

In modelling a tracking scenario, the UAV must operate in a physical environment that accommodates the target and defines the confines of its operation. UAVs typically operate in the air when tracking targets and can fly at low or high altitudes, depending on the environment of operation. The environment also determines the complexity of the UAV control strategy and the constraints that need to be taken into consideration in their implementation. This subsection, therefore, discusses the characteristics of the environment

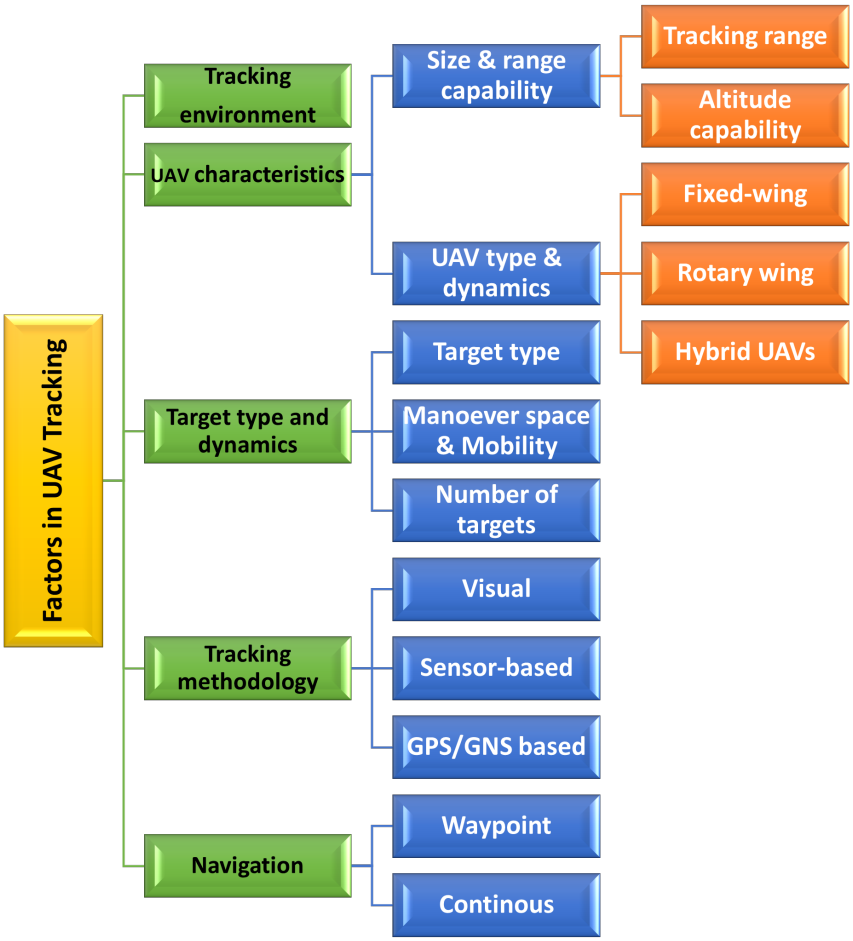

Fig. 2.2 Factors considered in target tracking review

and how it affects our UAV tracking problem. The environment of operation affects the way the UAV observes the target and how it is represented in the UAV camera FOV.

Physical and mathematical modelling of operating environment. The tracking by a UAV and evasion by a target can only take place in an environment that allows both vehicles to travel from an initial starting point to a desired endpoint. The operating environment can be processed by first considering the physical environment attributes and secondly mathematically modelling the environmental space by defining constraints utilised for the path planning algorithm. The translation of the physical environment into a navigable space can be achieved using graph theory. For instance, [36] designed a mathematically complex environment in which 2 UAVs will cooperatively operate, by modelling moving airflow, adversary radar, mountain area and anti-aircraft weapon positions into the environment in combination with game playoff functions. Similarly, Jones et al. [37], presented a comprehensive survey that classified the complexity of various methods of modelling a tracking environment. Their study also highlighted challenges in the existing methods of modelling the complexity of tracking environment, UAV path planning approaches and suggested possible research questions and future directions. While the environmental

models are useful, the complexity or otherwise is not the subject of this thesis. Accordingly, we explore the physical attributes of a target tracking environment to present a broad overview of the various aspects to consider when deciding on a tracking environment. These physical considerations are presented in the succeeding subsections.

Bounded and continuous environment. The environment could be bounded discrete [38–42] or a continuous environment [43–45]. In addition, the state of the environment can be limited to 2D or 3D space. When the UAV target tracking is implemented in a 2D environment, the common assumption is that the target moves on a flat ground plane while the UAV operates at a fixed optimal altitude throughout the tracking scenario [14]. The UAV 2D environment can be viewed as a square plane observed from a plane directly above the camera of the tracking UAV [46]. While the 2D plane simplifies the tracking and evasion problem, it does not allow for the altitude and some attitude changes that the 3D environment provides [47, 48]. In the 3D environment, a more detailed operation of the UAV aerial and target motion is facilitated, with the environment represented as a box [49]. Despite the difficulty of modelling irregular or complex environments such as spheres, some research exists in the literature [50] with irregular environments.

Terrain. The next consideration for the UAV target tracking control environment is the terrain of the ground. This may be flat terrain, Irregular or undulating [51]. The terrain can also be obstacle-cluttered [52, 53], or obstacle-free surfaces [54]. The terrain type affects the mobility of the target as well as the UAV's tracking capability to effectively track the target [55]. A table classifying the related research based on the characteristics of the environment is given in Table 2.1.

Table 2.1 Types of UAV target tracking environments

Environment	**Discrete**	**Continuous**	**Hybrid**
2D	[45, 43, 39, 41]	[43–45]	[56]
3D	[42, 40, 38, 44]	[44]	[57]

When the ground environment is cluttered with obstacles, it affects the FOV of the UAV and restricts the movement of the target around the various obstacles [55]. In such environments, the obstacles may be mapped to enable the UAV and target to plan their trajectories [58–60] or without a map of obstacle positions to test how the UAV can navigate the unknown obstacles [61–63]. Furthermore, the obstacles in a target tracking environment could be confined or unconfined obstacles. In the confined scenario, the obstacles are restricted to fixed positions like road paths where the targets are constrained to move on [64]. In other scenarios, the obstacles could have fixed predefined positions, shape, and size. The shape of the obstacles can also be used to classify the tracking environment. The common shapes

of obstacles modelled in UAV tracking research include cylindrical [65–70], square-shaped pillars [71–73], rectangular-shaped obstacles [74–76], and circular [74, 77–79]. Some studies have also designed spherically shaped obstacles [80–82] and irregular obstacles [83, 84]. In research works where the UAV tracking goal includes manoeuvring through hoops [85, 86], tube-shaped, square, rectangular, and parallelogram openings have been used to design the UAV tracking or navigation paths or waypoints [45]. These could be considered as forms of obstacles in the operating environment as the UAV must manoeuvre its way through these hoops to get to the target or a desired endpoint. On the other hand, obstacle-free or unconfined environments do not have defined paths or obstacles in the tracking, mission scenario. However, boundaries may be set to prevent the target or UAV from moving in unrealistic spaces [87]. In this research, the environment used throughout is the undefined type with no obstacles on the ground surface. This is because the scenario being modelled is that of UAV tracking a freely evasive ground or aerial target. The use of obstacles will limit the target manoeuvre and as such, we utilise an obstacle-free environment to explore the limits of the UAV tracking and target evasion strategies.

Environment dynamics. The operating environment can also be static or one that evolves dynamically. Static environments have either none or fixed obstacles within an unchanging environment throughout the mission scenario [63, 84]. On the contrary, dynamic environments are designed to have either moving or changing obstacles that are modified in either shape, size, or location during the mission scenario [66, 88–90]. Typically predefined shapes and positions of the obstacles and a changing sequence will be provided to test the UAV tracking capability in the dynamic environment. However, there are studies in which the UAV tracking problem is executed in random or abruptly dynamic environments. Operating in these types of environments requires the tracking UAV to dynamically adapt to the changing environmental situation during the mission thus introducing more complexity into the UAV tracking algorithm development [91–93]. A classification of UAV target tracking literature based on their operating environment is given in Table 2.2.

Table 2.2 Cited references by environment type and obstacle presence

Environment Type	**Obstacle Presence**	**Cited References**
Static Environment	Obstacle	[58–60, 63, 84]
	No Obstacle	[91–93]
Dynamic Environment	Obstacle	[66, 88–90]
	No Obstacle	[87]

The table above shows that both static and dynamic environments have been designed for target-tracking problems. However, a larger number of studies lean towards the static

environment due to the less complexity and design considerations. While the various environments in the reviewed literature are useful for various mission scenarios, in this research, we focused on the 3D environment with no obstacles. This environmental type represents our mission space for the target tracking problem using fixed-wing UAVs which would normally be in an open space with limited or no obstacles. We therefore believe that this type of environment is sufficient for this research.

2.2.2 Target type and dynamics

The target tracked by a UAV in a mission scenario can be classified into 3 categories. These are target type, manoeuvre design and target dynamics.

Target Type. The target could be classified into cooperating and non-cooperating [94–96]. With cooperating targets, information from the target is transmitted to the tracking UAV. This information may include position coordinates, speed, acceleration or identification frequency, thus making it easier for the UAV to locate and keep track of the moving target [97]. The target may also be fed with information about the UAV position and communication frequency [98]. On the other hand, non-cooperating targets could be grouped into passive and active targets. Passive non-cooperating targets will normally manoeuvre independently, without considering the UAV tracking [99]. The target may take abrupt or pre-designed manoeuvres to accomplish its desired objective of arriving at a destination by following some path [100, 101]. The active non-cooperating target is designed to actively and smartly evade, or randomly manoeuvre away from the tracking UAV. These types of targets would normally have some onboard sensor to detect when the UAV is closing up on their location and then take evasive action to manoeuvre away from the pursuing UAV [99]. The non-cooperative target is more difficult to track by the UAV as it must adapt to the possible evasion by the target during the tracking scenario [102, 96, 103, 104]. For instance, [14] developed a 2D control strategy for fixed-winged UAV autonomous tracking of a randomly manoeuvring ground target. Unlike the random manoeuvre, [15], presented a control algorithm designed to track a smart evading target that utilises a dipole-type vector field around the tracking UAV to actively execute evasive action. However, these were only implemented for 2D engagement dynamics with the main focus being on the UAV control strategy. The reviewed literature showed that only a few UAV target tracking studies considered active non-cooperative target dynamics and control strategy models. Our research addresses this gap by designing and simulating active and non-cooperative ground and aerial targets in 3D space to enable adequate simulation of the UAV tracking algorithm developed.

Target manoeuvre space and mobility. Targets in UAV tracking missions are constrained by the environmental space of their operation either ground or aerial. Some research focuses on tracking ground-moving single or multiple independent targets while others design a group of targets that move as a dynamic cluster which changes in shape and size depending on how close or far apart the targets are from each other. These clusters could be in the form of cars moving a straight-line convoy, diamond shape clusters [105–109] or even a smarm of aerial mini-drone targets [110, 111]. Tracking clustered groups of targets requires the UAV to actively adjust its altitude to enable its camera to keep the cluster within its FOV. Targets can also be classified based on their manoeuvre types. This could be a simple target manoeuvre in a straight line [112, 113], along curved[114–116], circular [117, 118], zig-zag [119, 120] or sinusoidal paths [121, 120, 122]. Other researchers design random target movements to simulate target evasion [123–126, 79, 127, 65]. This could be useful to assess the UAV tracking performance against unpredictable target manoeuvres. In other cases, targets have been designed to evade the tracking UAV using either predefined evasion strategies or intelligent manoeuvres [12]. Evasive manoeuvres from targets are designed with the capability to use the UAV parameters in their evasion strategy [128–131]. Despite several research efforts from different studies reviewed, more understanding is still needed in the area of fixed-wing UAV tracking of various types of single and clustered evasive targets. Accordingly, this research presents an algorithm for a smart evasive target that is capable of persistently evading the tracking UAV during a mission scenario. With the non-manoeuvring target moving in a straight line. We assume a scenario where the UAV is tracking a ground target moving on a straight road path. The other type of target implemented is the evasive type, which uses information about the UAV's position and speed to manoeuvre away from the pursuer UAV. We also implemented both aerial and ground targets and multiple evasive quadrotor-type targets to test the UAV's ability to persistently track the evasive aerial vehicles.

Number of targets. In terms of the number of targets being tracked by the UAV, most research implements a fixed number of targets while a few studies have explored a dynamic number of targets. For studies with a fixed number of targets, single or constant multiple targets are maintained in the tracking environment throughout the mission simulation [132, 106, 133, 134]. In other studies, a dynamic target set where the number of targets could increase or decrease during a mission scenario has been explored [135–139]. In such cases, new targets may be inserted or removed from the tracking environment at a preset time or predefined entry or exit points. Alternatively, the scenario could design targets to appear at a random position within the UAV's tracking range. To keep track of the targets in these scenarios, the UAV needs to continuously scan the environment to detect changes such as the appearance of a new target in the simulation environment.

Table 2.3 Structured reference table of target manoeuvre space and mMobility

Category	Target Type	Manoeuvre Type	References
Target Space	Single Targets	-	-
	Multiple Targets	-	-
	Clustered Targets	-	[105–109]
	Mini-Drone Targets	-	[110, 111]
Target Movement	-	Simple Manoeuvres	[112, 113]
	-	Complex Manoeuvres	[114–122]
	-	Random Manoeuvres	[123–126, 79, 127, 65]
	-	Evasive Manoeuvres	[12, 128–131]
Target Dynamics	Fixed Number of Targets	-	[132, 106, 133, 134]
	Variable Number of Targets	-	[135–139]

While it may be interesting for the UAV to track targets that change in number during a mission scenario, it will only occur in real-world scenarios where the UAV is constrained to track targets within a defined space beyond which it loses track of the target. In this research work, the number of targets is constant during the tracking mission. However, in Chapter 7 of this thesis, we present a scenario where a target tracking mission starts with multiple aerial targets which reduce in number as the UAV neutralises the targets in sequence.

2.2.3 UAV characteristics

UAVs have emerged as versatile tools for various applications due to their ability to navigate complex environments, access remote or hazardous areas, and perform tasks either with human assistance or autonomously. One crucial application domain is target tracking, where UAVs are employed to follow and monitor dynamic subjects such as vehicles, individuals, or wildlife. The effectiveness of UAV-based target tracking hinges on the understanding of UAV dynamics, which involves factors like agility, stability, and control precision. In this subsection, we review the characteristics of UAVs based on their size, capabilities, and dynamics.

UAV Size. UAVs are often categorised based on their physical dimensions and payload capabilities. Miniature UAVs (MUAVs) are characterised by their small size and lightweight construction, making them suitable for indoor or confined space tracking scenarios. They offer advantages such as manoeuvrability and low cost, but may be limited in terms of flight duration and sensing capabilities [140–144]. On the other hand, Medium Altitude

Long Endurance (MALE) [145–151] and High Altitude Long Endurance (HALE) UAVs, which are larger and equipped with advanced sensors, are capable of prolonged flights over vast areas. These platforms excel in tracking scenarios in which extended mission duration and comprehensive surveillance coverage are needed [152–156].

Tracking range. Short-range UAVs are designed for tracking targets within a relatively close distance, often in the range of a few kilometres [157–159], while medium-range UAVs can track targets over longer distances, typically up to several tens of kilometres [160]. Long-range UAVs can track targets over extended ranges, sometimes even hundreds of kilometres away [161, 162]. The range of a target tracking UAV is roughly proportional to the wingspan size as shown in Fig. 2.3.

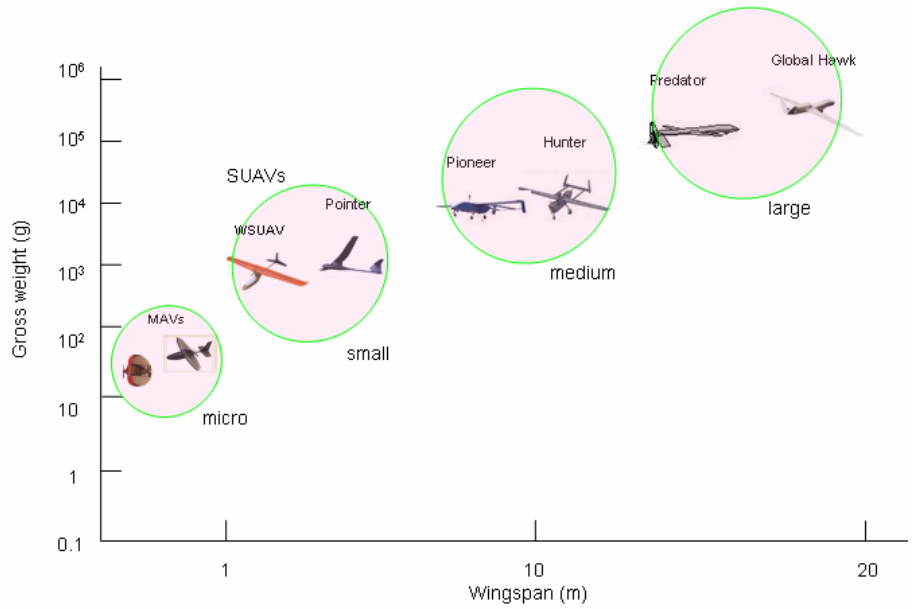

Fig. 2.3 UAV classification by size and weight [163]

Operating altitude classification. Target-tracking UAVs are also categorised by their operating altitudes, ranging from low-altitude to high-altitude platforms. Low-altitude UAVs, such as micro and mini UAVs, are well-suited for close-range target tracking, enabling detailed observations and interactions [164–167]. Medium [168, 169] and high-altitude UAVs are more suitable for tracking targets across larger geographic areas, where altitude provides a vantage point for broader coverage and extended line-of-sight communication [170, 171]. A table showing target tracking UAV literature based on the sizes and capabilities is shown in Table 2.4.

In this research, we consider a lightweight, medium-range fixed-wing UAV operating at low altitudes for our tracking scenario. This is because these types of UAVs would be best suited for the mission of intercepting and preventing adversarial targets from gaining access to a protected facility.

Table 2.4 Table of UAV size, altitude, and range capabilities

Category	**Size**	**Range**	**Altitude**
Small UAVs	Small [140] Lightweight [141] MUAVs [142] Manoeuvrability [143] Low Cost [144]	Short-Range [157]	Low-Altitude [164]
Large UAVs	Large [145] Advanced Sensors [146] Prolonged Flights [147] Long Surveillance [148]	Medium-Range [160] Long-Range [161] Extended Durations [170]	Medium Altitude [168] High Altitude [169] Extended Coverage [170]

2.2.4 UAV type and dynamics

Another way of classifying UAVs used in target tracking is by their design and propulsion mechanisms. The type of UAV designed and employed for a target tracking problem depends on various factors such as target type, operating environment, and tracking range. A brief review of recent target tracking literature using various UAV dynamic configurations is presented below.

Fixed-wing UAVs. Fixed-wing UAVs have a traditional aeroplane-like configuration and are known for their efficient long-endurance flight capabilities. They are suitable for covering large areas and conducting short, medium or extended surveillance missions, covering long distances, and maintaining stable flight paths, which is beneficial for tracking targets that traverse expansive areas [172, 173]. Their dynamics are optimised for efficient cruising and high-speed dynamics. Fixed-wing UAVs must however maintain a minimum velocity above-stall speed, below which the aircraft will stall and fall to the ground [174]. Some target-tracking research that employed fixed-wing UAVs is highlighted below.

Liao et al., [176] designed a fixed-wing UAV flight at a constant altitude and speed to track a moving target. In [177], the fixed-wing UAV was designed to follow a circular part while tracking a ground-moving target using loitering and following patterns. To enable stand-off target tracking, [178] developed a small fixed-wing UAV, equipped with target-tracking radar and addressed the challenge of designing a fixed-wing UAV flowing from theory to practical tracking of mobile ground targets. Similarly, Pei et al., [179] implemented fuzzy-controlled, V-empennage fixed-wing UAV for target tracking. The UAV type was chosen due to the advantage of speed and endurance available to fixed-wing UAVs while [180] designed a UAV algorithm for tracking a moving ground target

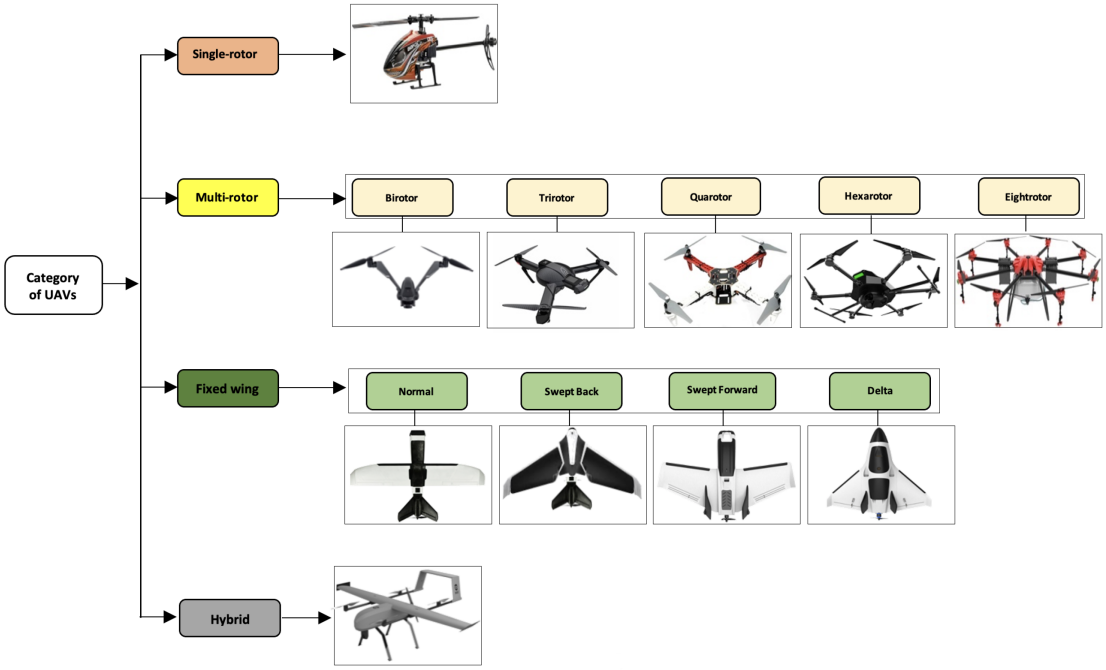

Fig. 2.4 UAV types categorised by dynamics [175]

with a fixed-mounted camera. To address the issue of energy consumption by fixed-wing UAVs during a target tracking mission, [181] developed an economic Model Predictive Control (MPC) controlled UAV with a camera mounted on a gimbal to track moving ground targets in a built-up urban environment. Similarly, [182] implemented an online vision-based localisation and trajectory smoothing for a fixed-wing UAV tracking a moving target. In a related study, [183] implemented a small low-cost fixed-wing UAV to track moving targets. A method of conducting field experiments to integrate formation flying, target identification, and tracking tasks within a unified structure for fixed-wing UAV swarms was also implemented by [184, 185]. A diagrammatic chart of UAVs classified by their design types is shown in Fig. 2.4. In this research, we implemented fixed-wing UAVs because of their advantage of speed and endurance in tracking evasive manoeuvring targets in 3D space.

Rotary-wing UAVs. Rotary-wing UAVs include helicopters, quadcopters, hexacopters, and other multirotor UAVs. Several research has applied multi-rotor UAVs due to their excellent manoeuvrability and vertical takeoff and landing capabilities, making them suitable for tracking targets in tight spaces or areas with obstacles, cluttered environments or areas with limited access. The choice of UAV type depends on the specific tracking requirements and environmental constraints, which may require peculiar capabilities for the UAV to either hover for short periods or be capable of agile manoeuvres [186]. Zhang et al., [187] employed rotary-wing UAVs for their target tracking research due to the reduced trajectory,

power consumption costs and patrol efficiency. Two unique capabilities of rotary wing UAVs are reviewed below:

- 1. *Hovering Dynamics*: Rotary-wing UAVs, such as quadcopters and hexacopters, have the unique ability to hover in place and perform vertical takeoff & landing. This hovering capability allows for precise tracking and observation of targets in confined spaces or areas with limited access. Hu et al., [188] compared the disguised or camouflaged tracking capabilities for fixed and rotary-wing UAVs. They observed that while limited in its maximum velocity and acceleration in comparison to the fixed-wing, the rotary-wing UAV was capable of making sudden changes in direction and velocity, and the ability to hover at a spot and when performing tasks that require precise control, stationary motion, and stability. This is possible due to the different propulsion and thrust power models available for ascending and descending in rotary-wing UAVs. The unique dynamics of rotary wings like quadrotors make them suitable for autonomous navigation and tracking in agricultural settings, such as following plantation rows, crop-monitoring, and scouting operations [189].
- 2. *Agile Manoeuvrability*: Rotary-wing UAVs exhibit agile and responsive manoeuvrability, enabling them to track targets with quick changes in direction and altitude. This makes them well-suited for tracking dynamic targets or objects in complex environments. Due to their agility, [190] designed a rotary-wing UAV for target-tracking military missions. Other researchers have designed quadcopters and quadrotors, a type of UAV propelled and lifted by four rotors due to their high manoeuvrability and capability of performing complex tasks in crowded and static or dynamic environments [191, 192]. Quadrotors can also be designed as small or lightweight miniature UAVs for tracking active targets [193–195]. Xue et al., [196] designed an underactuated quadrotor UAV to track moving targets using passive control and artificial potential field for fixed distance target tracking.

Hybrid UAVs with Adaptive Configuration. With recent advancements in technology, advancements, a new breed of UAVs known as hybrid UAVs are increasingly being employed for target tracking tasks. These innovative aircraft types possess the remarkable ability to seamlessly transition between fixed-wing and rotary-wing configurations and as such benefit from the advantages of both [197]. Due to this adaptability, hybrid UAVs have a unique blend of capabilities, allowing them to excel in diverse operational scenarios as they are engineered with transformative mechanisms that enable them to change their propulsion and wing configurations on the fly. This gives them the advantages of both fixed-wing and rotary-wing UAVs, making the hybrid platforms versatile for various tracking and surveillance missions. One example of the hybrid UAV used for target tracking is the Vertical Takeoff and Landing (VTOL) UAV. The common types of VTOL hybrid UAVs are

the tail-sitter and quad-plane and are capable of landing vertically in a confined space [197].

Hybrid UAVs can transition between fixed-wing and rotary-wing configurations, combining the advantages of both dynamics. In fixed-wing mode, they can efficiently cover long distances, and while in rotary-wing mode, they offer agile manoeuvrability and vertical operations. This adaptability allows them to adjust their dynamics based on the tracking requirements and environment. Dalwadi et al., [198] designed a hybrid UAV, using a biplane quadrotor model to track stationary and moving targets while [199] developed a conceptual design for a solar-powered MALE hybrid UAV that utilises both solar and conventional energy sources. The hybrid-powered UAV exploited solar-powered to fly the UAV and conventional power sources to provide the system with increased versatility and reliability. Zhang et al., [200] also developed a Quadrotor Fixed-wing Hybrid UAV (QFHUAV). The adaptability of the UAV allowed for vertical take-off in quadrotor mode, cruise tracking in fixed-wing mode, and landing in quadrotor mode [201]. In [202], they developed a simplified hybrid UAV that combines multirotor and fixed-wing UAV characteristics using 3 electric power-train propeller sets for VTOL and a fixed-wing with a single combustion power-train set for long-range missions. Systematic categorisation of various types of miniature hybrid UAVs based on their designs and target tracking capabilities was presented in [203].

The UAV type used in target tracking problems, whether fixed-wing, rotary-wing, or hybrid, depends on the specific tracking requirements and environmental constraints of a given mission. Hybrid UAVs bridge the gap between these traditional configurations, offering mission planners and operators enhanced flexibility in adapting to various operational scenarios. This adaptability also leads to potential improvements in mission efficiency, as a single hybrid UAV can fulfil roles that previously required multiple specialised platforms. The choice of UAV also has direct implications for target tracking effectiveness. In scenarios requiring rapid response and tight manoeuvres, rotary-wing UAVs excel due to their agility and ability to hover. Fixed-wing UAVs, while less agile, offer efficient endurance and can cover extensive distances. The altitude of operation impacts the FOV, sensor resolution, and communication range, influencing the quality of tracking data and the overall tracking process [204]. A categorisation of the literature on various UAV types designed and employed for target tracking missions is shown in Table 2.5.

The classification of UAVs based on size, type, and operating altitude serves as a foundational framework for tailoring UAV selection to specific tracking requirements. The synergy between UAV dynamics and the chosen classification aids in optimising the tracking process, enabling UAVs to effectively and autonomously pursue and monitor moving

Table 2.5 UAV type and dynamics for target tracking

UAV Type	Dynamics	References
Fixed-wing UAVs	Efficient Long-endurance	[172, 173, 4]
	High-speed Cruising	[174, 176, 177]
	Stable Flight Paths	[179, 178]
	Speed and Endurance	[117, 180]
Rotary-wing UAVs	Hovering Dynamics	[188, 189]
	Agile Manoeuvrability	[190–192]
	Confined Spaces	[187, 186]
	Precision Control	[196, 205, 206]
Hybrid UAVs	Adaptability of Fixed-wing and Rotary-wing	[197, 198, 203]
	Long-distance and Agile	[199–201]
	Hybrid Power Sources	[202]
	Enhanced Mission Flexibility	

targets across diverse scenarios. In this research, we implemented the medium-range fixed-wing UAV. We assume that the UAV is already airborne at the start of the simulation and has the range and endurance to remain airborne throughout the tracking period. Accordingly, our research does not model the takeoff and landing phases of the UAV flight.

2.2.5 Tracking methodology

The tracking methodology employed by the UAV influences its capability to track and can be grouped into visual, sensor-based and system-based. These are reviewed in the paragraphs below:

Visual tracking. UAVs equipped with cameras can visually track targets using computer vision algorithms. This includes object detection, recognition, and tracking techniques. These UAVs are equipped with high-resolution cameras for visual tracking and surveillance, mounted on single-axis gimbals [179]. Zhou et al., [182] implemented an online vision-based target tracking, while [172, 207] and [179] presented variants of the vision-based UAV target tracking. A long-term visual tracking algorithm for UAVs based on kernel correlation was utilised by [208]. In a related study to correct the errors resulting from UAV visual tracking, [209] developed a spatial attention aberration repressed correlation filter to stabilise tracking video feeds while [210] applied deep reinforcement learning to optimise visual tracking images from onboard UAV cameras. In similar efforts, [211, 212] utilised embedded visual object detection and tracking for UAV real-time tracking.

Sensor-based tracking and Multi-sensor payloads. This involves using sensors such as radar, lidar, or thermal imaging to detect and track targets based on their characteristics like movement, heat signatures, or reflective properties. The UAVs carry a combination of sensors such as cameras, thermal sensors, lidar, and radar for multi-modal tracking

[186]. For instance, [213] used a monocular Infra Red (IR) camera, to detect and track IR emitting targets in low illuminance or at night. Similarly, [214] implemented a dual-axis rotary tracking UAV that utilises a combination of thermal imager and full-colour camera for aerial scanning reconnaissance. The UAV sensor tracking device also has 3 sets of laser range finders, Global Positioning System (GPS), and a long-range antenna to ensure accurate tracking. Chi et al., [215] developed a UAV target recognition and tracking using a single photon array imaging lidar, while [185] used an adaptive sensor for UAV motion and tracking control. The adaptive sensor dynamically combines visible light cameras, infrared thermal & hyperspectral imagers, laser radar, and image transmission technology. In another related study, the authors used intelligent waveforms based on reinforcement learning and cognitive radar for UAV target tracking [216].

Global Positioning System/Global Navigation Satellite System tracking. Another methodology of UAV tracking is the GPS or Global Navigation System (GNS). The GPS and GNS-based tracking algorithms track targets based on their geographical coordinates. This tracking method was implemented by [197], using a monocular vision camera to estimate the relative target position and a GPS sensor to provide position measurement to a hybrid UAV. These UAVs were equipped with communication equipment for relaying tracking data to ground or airborne stations. In [217], the researchers implemented an Extended Kalman Filter (EKF)-based GNS/Ultra Wide Band (UWB) tight integration with online time synchronisation for improved outdoor target tracking. A review of UAV target tracking employing GPS and GNS-based Iridium and Orbcomm satellites in the VHF-L band was presented in [218]. The study showed that UAV target tracking and localisation could be achieved for various scenarios using UAV-RFI detection/tracking and GPS data from multiple UAVs. To improve the accuracy of multiple target drone tracking, [219] developed a Markov Chain Monte Carlo Particle Filter (MCMC-PF) that overcomes data errors and offers real-time suitability. In a related survey study, [220] explored the application of UAV Simultaneous Localisation & Mapping (SLAM) techniques and data fusion for target detection and navigation. A table of recent literature on UAVs and tracking methodologies is shown in Table 2.6 below:

Table 2.6 References on various tracking sensors

Category	**References**
Visual tracking	[172, 207, 179, 182, 208–212]
Sensor-based tracking and Multi-sensor payloads	[186, 213–215, 185, 216]
GPS/GNSS tracking	[197, 217–220]

The use of sensor-based tracking could be viewed as a way of enhancing the basic visual tracking method by making the tracking system more robust for tracking targets at night

and in adverse weather. Additional sensors and or GPS/GNS systems could be incorporated. Accordingly, the UAV in this thesis is designed to utilise methods that ensure it persistently tracks the target using a visual tracking method with the assumption that its camera is capable of identifying and isolating the tracked target. We assume that the camera is mounted under the fuselage of the tracking UAV and uses visual and other navigation equipment to track ground or aerial targets, using a combination of Kalman filters and Inertial Measurement Unit (IMU) to effectively estimate the target position during a tracking mission. Future studies will explore the use of more sophisticated tracking sensors highlighted in the review.

2.2.6 Navigation

We now dive into key aspects of navigation within the framework of UAV operations with the goal of robust and precise target tracking. Tracking a moving target necessitates not just good control tactics, but also precise guidance and navigation systems that ensure the target is always inside the UAV's FOV [221]. Two essential factors are involved in enabling the smooth movement of a UAV between different points or directing its continuous trajectory toward specific targets. These factors consist of a precisely defined guidance and a navigation system which are both seamlessly incorporated into the operational structure of the UAV [222]. The guidance law refers to a set of mathematical rules or algorithms that dictate how a vehicle should move from its current state to a desired state. It defines the logic or rules governing the trajectory or path the vehicle should follow to reach its intended destination. On the other hand, navigation is the process of determining the UAV's position, orientation, velocity, and trajectory of the tracking UAV relative to its environment [222]. Navigation involves the use of various sensors, systems, and algorithms to ensure accurate and efficient movement of the UAV during its operation. We discuss the guidance and control in the next subsection but first, let's address the two common types of navigation used by target-tracking UAVs.

Waypoint navigation. Waypoint navigation is based on segmenting the UAV's trajectory into a sequence of carefully placed waypoints. This method requires the UAV to move from one waypoint to another in a specified sequence. However, the waypoint-based strategy has inherent rigidity, as it may fail to adapt to dynamic scenarios involving agile or evasive targets [223]. Tracking manoeuvring objects that can rapidly change direction during missions can be difficult under this system. Although GPS-based waypoint navigation is available for automating UAV flight operations, it does not provide the accuracy required for the exact placement of sensor payloads on structures [223, 224]. Since the waypoint navigation does not suit the evasive target tracking, we consider the continuous navigation alternative in the next subsection.

Continuous navigation. The continuous navigation method takes an alternative approach by removing the dependency on predetermined waypoints. Instead, a steady stream of guiding inputs is generated based on specified design characteristics and limits [225]. This method enables the UAV to dynamically navigate a trajectory aimed at obtaining desirable positions. The adaptability of continuous navigation allows for real-time adjustments, making it more sensitive to the complexity of monitoring agile targets [223, 225, 226].

The navigation system applied in this research is the continuous type which allows for evasive target tracking and abrupt manoeuvres. The next subsection will explore the control strategies used in directing the UAV toward tracking the moving target. This will provide an understanding of the interplay between guidance, navigation, and control in UAV target tracking settings.

2.3 UAV Target Tracking Guidance & Control

There are various strategies in the literature for tracking meandering paths as well as moving aerial and ground targets. In this section, we review the various control methodologies applied in recent target-tracking research to guide our decision on which system works best and also aid the design of strategies employed in this research. The two broad categories of target tracking control are analytical and data-driven strategies. The main focus of the review presented in this chapter is on analytical control. However, we review a few literature on data-driven control here to show the broad spectrum of UAV control strategies and to serve as a reference for future research.

2.3.1 Machine learning and data-driven control strategies

Machine learning and data-based control algorithms seek to leverage on statistics data and reinforcement learning models to optimise conventional tracking control strategies to achieve enhanced and high-quality tracking performance [206]. For instance, the study by [227, 228] proposed a data-guided that embeds observation data learned from local linear models to improve tracking performance for a fixed-wing target tracking UAV. The learning agent was guided by vision-based sensors to learn optimal policies for tracking reference trajectories. The performance of their controller was compared with Linear Quadratic Regulator (LQR) in the presence of sensor noise and erroneous datasets. while this work makes a valuable contribution to data-driven research on UAV target tracking, the controller was only implemented for 2D scenarios and the target being tracked was a moving trajectory to mimic a moving ground target. In another related work, Tang et al. [229] proposed a fixed-wing UAV tracking strategy using Reinforcement Learning (RL) Deep Deterministic Policy Gradient (DDPG) framework. The RL package was trained and

optimised for tracking a 3D trajectory environment by controlling the UAV state of flight and rudder control input. The study also considered uncertainties such as measurement-induced noise and sensor delays and verified the performance of the RL controller using proportional-integral-derivative Proportional-Integral-Derivative (PID) control. While this research considered 3D tracking, like [228] it was implemented for trajectory tracking and did not consider evasive target dynamics.

A similar research conducted by [230] proposed RL-based UAV control for autonomous UAV tracking and landing on a moving ground or sea-based target in a harsh environment. A model-free Partially Observable Markov Decision Process (POMDP) was designed to automatically learn tracking and landing manoeuvres using a neural network that combines DDPG and heuristic rules. Simulation results from the study showed that the proposed RL-based algorithm performed better than a PID controller in the same scenario method. However, this study was designed for a quadrotor type UAV as opposed to the fixed-wing UAV and the research focused more on landing on the target than tracking. In the research carried out by [206], they presented an innovative deep RL-based strategy for correcting the position, velocity and angular errors of a VTOL UAV despite wind disturbances. The embedded neural networks obtained and eliminated real-time tracking control errors during the target tracking mission. The UAV controllers were formulated as a Markov decision process (MDP) with an appropriately designed system state, reward functions and soft update method. To enhance tracking control in the presence of wind disturbances, the research modelled constant, dynamic and strong gust winds into the learning environment. Furthermore, a quantum-based experience replay strategy was implemented to improve tracking accuracy for practical applications. The simulations in this research explored computer-based, hardware-in-the-loop experimentation, and actual real-world flight missions to evaluate the performance and validate the proposed method. The controller was reported to effectively perform standoff tracking of a real-life aerial target while maintaining flight stability.

The control strategies reviewed in this chapter are presented in the subsequent subsections and a chart of the control strategies reviewed is shown in Fig. 2.5. For the conventional control strategies, we start from simple PID control and move on to more complex controllers.

2.3.2 Proportional-Integral-Derivative control

In the context of UAV control for target tracking, the utilisation of PID controllers for UAV target tracking has been implemented by various studies. With the increasing

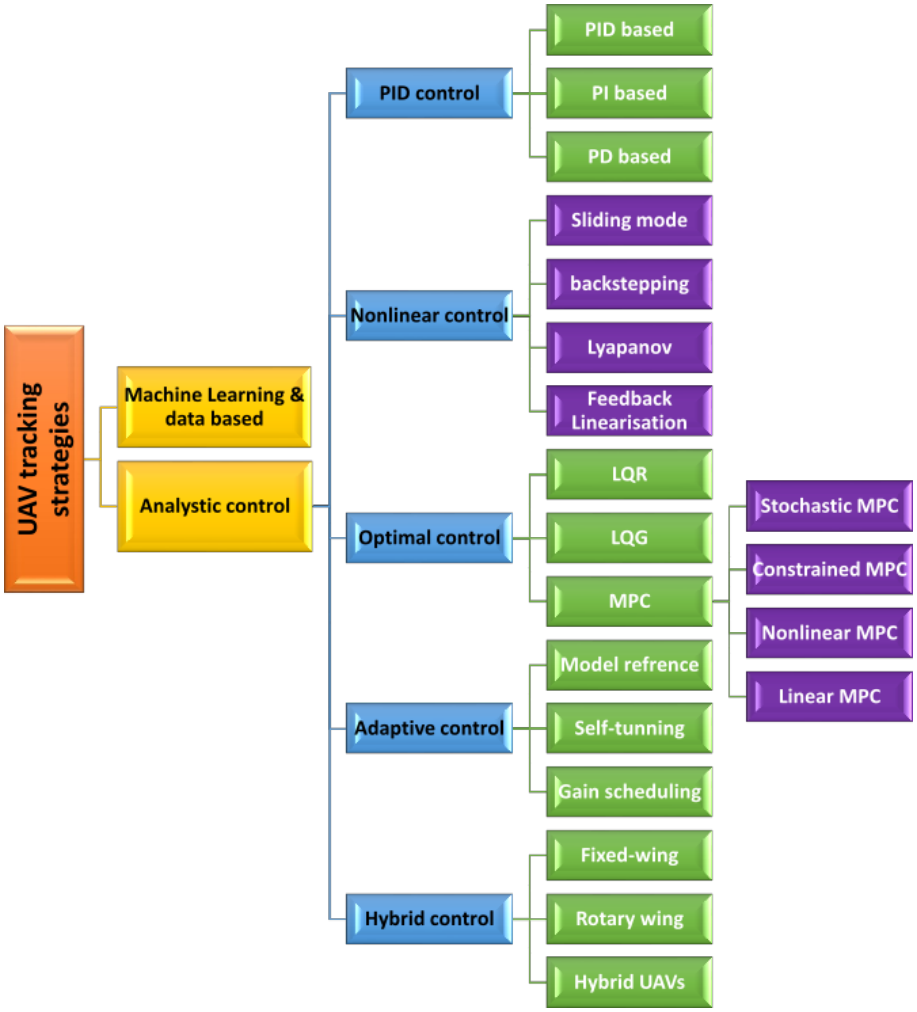

Fig. 2.5 Chart of common control strategies used in target tracking

need for autonomous UAV control algorithms based on Proportional-Derivative (PD), principles have also been used to enhance the integration of intelligent systems into tracking algorithms. A few studies using the PID, PD, and Proportional-Integral (PI) control strategies in target tracking are presented below:

PID Control. PID controllers have been applied for several target-tracking problems. For example, Altan et al., [231] proposed an MPC controller with a Hammerstein model for controlling a 3-axis gimballed UAV camera and compared the performance with conventional PID while [232] designed a PID-based control and guidance algorithm for a novel rotorcraft UAV, enhancing target tracking efficiency using simplified image-based visual servoing. A PID controller was implemented to compare the tracking performance of the vision-based feedback controller tracking system developed for a rotorcraft UAV using Kernelised Correlation Filter (KCF) tracker and a re-detection algorithm to handle occlusions and real-time tracking challenges [233]. Similarly, [234] presented a fuzzy PID control-based attitude control method for quadrotor UAVs and compared it with standard

PID control via simulation experiments. The Fuzzy PID was reported to offer reduced overshoot, quicker regulation, and better anti-interference adaptability [235]. Apart from the PID control strategy, the PI controllers have also been applied to target tracking problems as discussed in the next subsection.

PI control. Rabah et al., [191] created a target-tracking method based on a Fuzzy-PI controller to track a moving target with variable speed. In [196], a tri-copter UAV with individually tilted main wings for improved manoeuvres, using PID and PI controllers was presented. To analyse flight control effects using PI controllers, a target tracking problem was designed and simulated using experiments by [204]. To overcome the challenges faced by quadcopter UAVs in tracking moving targets due to their complex dynamics and changing target speeds, a PI controller was proposed by [236], that uses rotation matrices to centre the target in the tracking UAV camera FOV. The control algorithm demonstrated successful real-time tracking and disturbance rejection. Like PI controllers, some researchers have also used PD controllers for target tracking with good tracking results.

PD control. The PD controller utilises only the proportional and derivative gains to control UAVs. A PD controller was employed to compare target tracking using finite time for uncooperative vision-based UAV target tracking, subject to actuator saturation [237]. Similarly [12] developed a long-term UAV target tracking in an urban environment using intention inference and deep reinforcement learning. When the target moves outside the UAV's FOV, the position-tracking mode of the UAV is guided by a PD controller to pursue the target. In some cases, the PD controller can be used as a supporting control and a reference for assessing the performance of the main tracking control law. For instance, [238] utilised a UAV bounding box area and PD controller to reduce target tracking error and create accurate control signals. The PD controller simplified the PID control by using only the proportional and derivative terms to adjust output and predict future errors for stability.

As showcased in the reviewed literature, the PID controllers have been extensively applied in target-tracking scenarios due to their efficacy in various UAV control applications [231–233]. However, while PID controllers exhibit complexity and their inherent integral action may lead to overshoot and oscillations, prompting exploration of alternative control strategies. Our review also showed that PI controllers have been utilized in target tracking systems [191]. However, studies by [196, 204, 236] suggest limitations of the PI control in addressing complex dynamics and varying target speeds. In contrast, PD control emerged as an effective control option as highlighted by [237, 12]. Additionally, [238] utilized the PD controller as a supporting control, simplifying PID control by leveraging proportional and derivative terms for enhanced stability and reduced tracking error. Given the above, we

implemented the PD control over PID and PI control in subsequent chapters of this thesis due to its simplicity, reduced oscillations, and effective handling of specific target tracking scenarios. In particular, Chapter 4 of this research presented a PD altitude controller that uses a control bounding box formed by the relationship between the actual target size, the size of the image formed on the camera image plane, and the camera focal length. Additionally, the evasive quadrotor targets in Chapters 5 and 6 of this research work are implemented using variations of PD control. Other types of controllers are reviewed in succeeding paragraphs.

2.3.3 Nonlinear control

The next controller type considered in this review is nonlinear control strategies. Various types of nonlinear control have been applied for UAV tracking of manoeuvring or evasive targets as they offer a versatile approach by accommodating complex dynamics and nonlinearities often encountered in real-world scenarios [239]. These methods focus on designing control laws that capture the intricate relationships between the UAV's state variables and the target's dynamics. Nonlinear control strategies include sliding mode, feedback linearisation, backstepping, and Lyapunov-based control. We review a few research that employed these control types in relation to target tracking.

Sliding mode control. Due to its versatility in handling uncertainties and disturbances, the Sliding Mode Control (SMC) is considered a robust control approach widely employed in UAV target tracking [240]. SMC creates a sliding surface for target tracking that directs the system's states in the direction of the intended trajectory while guaranteeing robustness against disruptions [241, 242]. An SMC approach for tracking moving targets and avoiding obstacles with an under-actuated quadrotor UAV was implemented by [243]. The method combines artificial potential fields and SMC for position tracking. Additionally, they employ SMC with radial basis function networks for attitude control. The stability of both subsystems was validated using Lyapunov theory [243]. Similar research was carried out by [205] and [206] where SMC was utilised for various tracking mission considerations. In [244], a target-tracking multi-rotor drone that utilises model-based integral SMC was implemented by as a velocity controller for practical industrial UAV tracking applications. The SMC showed reliable performance results for practical scenarios with robustness against parameter uncertainty in comparison to an LQR-based integral SMC. In similar research, [245] investigated tracking of mobile targets in a monitored area by a Quadcopter UAV (QUAV). The study utilises a robust vision-based approach using Image-Based Visual Servoing (IBVS) and SMC was proposed. Circular search and SMC ensured effective tracking against disturbances. This was extended in another research

to address uncooperative ground target tracking by modifying the QUAV control with enhanced IBVS, a virtual camera, and robust control that exploits prior target information. The modified SMC considered flight heterogeneity, uncertainties, and manoeuvrability to improve tracking performance [246].

Feedback linearization. Feedback linearization is an approach that transforms the nonlinear system dynamics into a linear one by applying a suitable change of coordinates [247]. In [248], a vision-based tracking and landing of Micro Aerial vehicle (MAV) on a moving ground target vehicle was implemented using a supervised learning algorithm that detects the ground target while the feedback linearization controller enables effective tracking and landing of the UAV on the moving target [248]. The research by [249] addressed the challenge of the quadrotor's under-actuation using static feedback linearization, focusing on attitude and trajectory control. The simulation confirmed superior performance over dynamic feedback, showcasing the value of feedback linearization. We now consider the backstepping nonlinear control in the next subsection.

Backstepping control. This control type constructs a series of interconnected subsystems, each stabilising a part of the overall system [250]. Sconyers et al., [251] designed a rotorcraft control and trajectory generation for mobile target tracking. The flight controller employed a backstepping approach, while the trajectory generator enhanced autonomy in tracking to control the UAV such that it seeks out a desired position and heading. The backstepping controller was designed using the nonlinear system model of the UAV rotorcraft. In related research, [252] presented an approach utilising backstepping nonlinear control for time-varying trajectory tracking in a quadrotor UAV, accounting for its full Six Degree of Freedom (6DOF) dynamics. The control law incorporated integral action on controlled velocities to ensure convergence to reference signals. Stability analysis was carried out using Lyapunov Theory to validate the system stability. To reduce chattering during tracking, [253] developed a fractional-order backstepping SMC approach that, enhances robustness, and addresses strongly coupled dynamics. This method was reported to have shown better UAV trajectory tracking and robustness against disturbances. A similar problem was solved for multi-UAV tracking of targets with opposing movements. Using backstepping control, neural network, and Uncertainty and Disturbance Estimator (UDE) were also applied to manage uncertainties, improve precision, and reduce chattering for the cooperative target tracking in [254]. In the next subsection, we take a Lyapunov-based control.

Lyapunov-based control. The Lyapunov control method has been also applied for target tracking to ensure stability and convergence to the desired trajectory. Oliveira et al., [255] developed a Moving Path Following (MPF) control to guide UAVs to follow 3D paths with time-varying velocities in an inertial frame. The MPF error space and Lyapunov-based

control law were developed for fixed-wing UAVs with the control law providing the angular velocity vector to compute the UAV's vertical velocity and bank angle commands. In another related research, [256], presented a controller for UAVs, using range and bearing data for circular trajectories around constant velocity targets using Lyapunov theory and feedback linearization proofs. Another research modified sliding mode guidance law for fixed-wing UAVs to track ground moving target tracking, achieving finite-time convergence through Lyapunov theory [177]. Also, [257] implemented Lyapunov Vector Field (LVF) with curvature constraint for standoff target tracking while [258] presented a guidance law based on Lyapunov theory for tracking reference trajectories using a centre of oscillation. These approaches were reported to provide steady cruise speed, making them useful for a variety of applications.

As highlighted in the review above, nonlinear control strategies, encompassing SMC, Feedback Linearization, Backstepping, and Lyapunov-based control, present versatile approaches accommodating the complexities and nonlinearities inherent in real-world UAV target tracking scenarios [239]. The SMC showed robustness against uncertainties and disturbances[240], while Feedback Linearization, transforms nonlinear system dynamics into a linear form, exhibiting successful performance in vision-based tracking and landing of MAVs on moving targets [248]. Similarly, Backstepping control addressed system stability via interconnected subsystems and proved effective in rotorcraft trajectory generation and quadrotor trajectory tracking [251, 252]. Furthermore, the Lyapunov-based control method was reported to be instrumental in ensuring stability and convergence to desired trajectories [255, 257].

While the nonlinear controls demonstrate robust performance in various tracking missions, challenges persist in scenarios involving parameter uncertainty [245, 243, 205, 244]. Therefore, we consider optimal control methods over these nonlinear approaches as they offer precise trajectory optimisation, achieving superior performance in trajectory tracking tasks. Hence, despite the benefits exhibited by nonlinear control methods in handling complex dynamics, the specialised requirements for precise trajectory optimisation in UAV target tracking systems drive the choice towards optimal control strategies. Although nonlinear controllers were not implemented in this research, the reviewed literature was considered as a reference for comparing the performance of the optimal control strategy applied in our research and also as an option for future application. The next section reviews optimal control literature.

2.3.4 Optimal control strategies

Optimal control strategies are policies designed to optimise a certain performance objective, by determining the best control inputs over a specific time horizon while considering system

dynamics, constraints, and various costs or objectives [259]. UAV optimal control aims to compute control inputs that minimize or maximize a defined objective function while accounting for the UAV's dynamics, limitations, and mission-specific requirements [260]. Optimal control strategies have been widely applied to solving target tracking problems, due to their advantage of providing a near-optimal result. A few pieces of literature on target-tracking UAVs developed using optimal control methods are presented below:

Linear Quadratic regulator. The LQR is a control design technique used in control theory to determine optimal control strategies for Linear Time Invariant (LTI) systems subject to quadratic performance criteria [261]. Closed-loop control strategies were developed for a tilting-rotor UAV using cascade PD and LQR controllers. Both controllers were applied to both simplified and fully nonlinear models, with a focus on vision-based target tracking using LQR control. Simulation results highlight the efficacy of the LQR controller in enabling the VTOL UAV to track moving targets via vision-based navigation within linearization limits [262]. An LQR control law was also employed to achieve stable quadrotor flight along the planned path while carrying a payload for a quadrotor-based search and rescue, using kinematic and dynamic analysis. Initial static and dynamic path planning techniques were used, transitioning to centralised control for swarm formations and payload lifting [263]. In a similar study, [264] presented an Air to Air Refuelling (AAR) docking control approach by a UAV using a novel reference and disturbance observer for enhancing LQR-based state-feedback control performance for precise trajectory tracking amid external disturbances in complex flow conditions. An LQR control was also employed for trajectory tracking by a quadrotor UAV filming of a moving target with adjustable positioning, maximising visibility along the trajectory [265]. Similarly, [261] presented a hybrid PD-LQR controller, optimised with Improvised Grey Wolf Optimiser (IGWO) for quadrotor control which demonstrated better performance in target tracking and stability compared to conventional methods. In a related study, [266] developed control strategies for interconnected load-carrying drones using LQR and compared their results using an MPC control while considering execution time and physical constraints.

Linear Quadratic Gaussian control. The Linear Quadratic Gaussian (LQG) is a form of a linear optimal control technique that minimises quadratic state error and control effort costs while considering Gaussian disturbances and model deviations [267]. The LQG controller is mostly made up of the LQR and the Kalman Filter [268]. Hendrix et al., [267] designed an LQG control for a small hovering aerial vehicle with the utilisation of an optical tracking system. The proposed non-GPS control system employs LQG with UKF for control and estimation, validated through simulation and flight tests. In another study, [269] explored the use of an LQG controller with a 3D Kalman filter for target tracking and intelligent trajectory optimisation, while [270] proposed a fast response, low overshoots,

disturbances/noise resistant LQG controller for their motion control module to track a reference velocity direction developed in the planning module of the UAV system. The LQG control input was further transformed in terms of thrust acceleration to UAV attitude, for real-world UAV systems application. In [271], an LQG controller was designed to compute control commands for the target movements. The controller minimises target localisation uncertainty via UAV collaboration, updating the pose measurements. In a similar study by [272], they utilised an iterative Linear Quadratic Gaussian (iLQG) in combination with the distributed Alternating Direction Method of Multipliers (ADMM) to solve multi-UAV trajectory optimisation problems for tracking clustered targets.

The reviewed literature on UAV optimal control shows the prevalence of LQR and LQG in target tracking applications due to their advantages. The LQR demonstrated effectiveness in vision-based navigation and trajectory tracking, showcasing stability and usefulness for in search and rescue missions, precise trajectory tracking and enhanced performance [262–265, 261]. Similarly, the LQG integration of LQR and Kalman Filter components was instrumental in non-GPS control systems, path planning, fast response motion control modules, and multi-UAV trajectory optimization for tracking clustered targets [267, 269–272].

Despite these strengths, we will be considering the MPC UAV target tracking systems due to its unique advantages of operating on the receding horizon theory, enabling future state predictions and optimal control determination over a defined time horizon, accommodating system dynamics and constraints while optimising a specified objective function [273, 274]. Unlike LQR and LQG, MPC can effectively handle nonlinearities, offering the ability to minimise an objective function and generate optimal control signals [275]. Accordingly, we prioritise MPC over LQR and LQG for the UAV target tracking systems in this study based on MPC's capability to handle nonlinearities, robustness in diverse scenarios, and its adaptability across different types of MPC controllers, aligning closely with the requirements of UAV target tracking systems. Therefore, while LQR and LQG offer significant advantages, the specialised features of MPC in handling nonlinearities and its versatile nature make it the preferred choice for UAV target tracking applications.

Model predictive control . Model predictive control is another form of optimal control strategy that employs the receding horizon theory. The algorithm employs a process model for predicting future states and determining optimal system inputs by optimising a linear or quadratic open-loop objective with linear constraints over a defined time horizon [273]. It can handle nonlinearities and minimises an objective function to create the optimal control signals [274]. The Model MPC belongs to a class of optimal-control techniques known as open-loop optimal feedback control [275]. The common types of MPC-related tracking controllers in the literature include linear, nonlinear, constrained, and stochastic. These are

discussed below:

- *Linear MPC*: Linear MPC (LMPC) aims to optimise a linear objective function subject to linear equality and inequality constraints[276]. Pereira et al., [66] proposed an MPC with feedback linearisation to ensure accurate velocity following for fixed-wing UAVs that use a two-layer guidance and tracking strategy. The vector field approach was used to switch between converging to a target curve and avoiding obstacles. The approach was validated with simulations while accounting for aircraft constraints, wind, and measurement uncertainties. A study that explores the use of MPC for tail-sitter VTOL UAVs, was also proposed by [277] for addressing flight control challenges. A Successive Linearisation MPC (SLMPC) was designed and applied to indoor flight experiments, which outperformed traditional LMPC in terms of precision and stable position holding in non-uniform windy conditions. A controller switching mechanism and warm-up mechanism were employed to enhance envelope control during forward and backward transitions. The research by [278] investigated a decentralised control for a leader-follower multi-agent system using graph theory and Tube MPC (TMPC). The study proposed a controller that tracks predefined trajectories in the presence of noise and disturbances, enhancing robustness and stability. Similarly, [279] presented an algorithmic architecture for systematic risk management in autonomous transportation vehicles, encompassing low-level control, trajectory tracking, and multi-vehicle coordination, utilising an adaptable MPC. In related research, an autonomous UAV landing system was introduced for moving platforms with uncertainties and disturbances. The system combined a vision-based target detection method, EKF for position estimation, and an LMPC-based control scheme for UAV motion coordination [273, 275].

- *Nonlinear MPC*: The Nonlinear MPC (NMPC) is designed for systems with nonlinear dynamics and constraints. It optimises a nonlinear objective function subject to nonlinear equality and inequality constraints [280]. In terms of NMPC, [278] proposed a system for coordination in autonomous systems, focusing on Unmanned Aerial Systems (UAS). Also, a novel "Polycopter" UAS platform was developed by exploring the challenges of local trajectory generation for multi-agent collision avoidance, using an Interval Avoidance (IA) method. An NMPC was also implemented for fixed-wing UAV attitude control during ground target tracking by [280]. The approach accommodated real-world constraints, optimising input via a quadratic cost function. Simulations across various scenarios demonstrated NMPC's superiority over LMPC in handling constraints and nonlinearities. Employing a cooperative non-inertial MPC controller, a quadrotor controller to orbit a UGV

along a pre-computed circular trajectory [281]. An Economic Model Predictive Controller (EMPC) was introduced to effectively track a target while minimising energy consumption. EMPC's performance was reported to surpass MPC and greedy approaches, tracking persistently with optimal energy use [181].

- *Constrained MPC*: The Constrained MPC (CMPC) applies to systems where constraints on the state, input, or both need to be enforced during control. In UAV target tracking, the constrained MPC incorporates dynamics constraints in the control algorithm. For instance, Wakabayashi et al., [89] developed an MPC that considers multiple collision avoidance constraints in a constrained optimisation framework was implemented to control multi-rotor UAVs flying in urban airspace. The control strategy was developed to safely and autonomously avoid collisions with unpredictable moving obstacles, like birds, the UAV's relative position and the velocity of the aerial obstacles. A Chance-Constraints based on Obstacle Velocity (CCOV) method, was proposed that combined with previous positional chance constraint methods to account for uncertainty in both position and velocity. Another study researched a robust Time-varying Constrained Model Predictive Controller (TCMPC) for real quadrotor control, accounting for various constraints. The controller was reported to outperform PID, as well as advanced error and efficient MPC controls in wind conditions, showcasing its robustness [282]. In similar research, [276] developed a two-layered constrained MPC strategy to address trajectory tracking for tilt-rotor UAVs. The first layer employs a constrained LMPC for transnational dynamics, ensuring adherence to a reference trajectory. This enabled the generation of feasible rotational set-points while respecting physical limitations. The second layer utilises a constrained robust switching MPC with Mode-Dependent dwell Time (MDT) to follow the generated trajectories from the first layer. The design also integrates actuator constraints using an augmented dynamic model to enhance trajectory tracking performance and energy efficiency.

- *Stochastic MPC*: The Stochastic MPC (SMPC) approach accounts for uncertainties or stochastic disturbances in the system dynamics, constraints, or external disturbances affecting the system. The study by [283] presented a vision-based guidance command for a UAV, that uses a SMPC approach to ensure that the tracked target is located within the camera FOV. The visual servoing problem was modelled as an SMPC framework by regarding the x and y axes' rotational velocities as stochastic variables. Also, [284] proposed an integrated framework for autonomous vehicle control, accounting for uncertainties that combine predictive manoeuvre and trajectory planning using SMPC to optimise decisions. Simulation experiments were reported to demonstrate improved adaptability and robustness without added computational

complexity. In a similar study, [285] implemented a solution to enhance target tracking reliability using a framework that employs multiple pan-tilt cameras, inspired by the chameleon visual system and MPC approach. Their scanning algorithm optimally scanned using SMPC, while a switched controller that employs min-max and minimum-time MPC theories was applied for the target tracking design.

While LMPC, as demonstrated in various studies [66, 277, 279], showcases effectiveness in specific UAV control scenarios, its limitation in handling nonlinearities and constraints compared to NMPC is apparent. NMPC, designed explicitly for systems with nonlinear dynamics and constraints, demonstrated superior performance, as evidenced by research works [280, 278, 281, 181]. NMPC's optimisation of nonlinear objectives under nonlinear constraints showcased its superiority over LMPC in handling real-world constraints and nonlinear dynamics, a crucial factor in the dynamic and uncertain environments of UAV control systems. Accordingly, we utilised the NMPC as a preferred control option for the UAV target tracking algorithm presented in Chapter 3 and the countermeasure design in Chapter 7 based on its capability to address systems characterised by nonlinear dynamics and constraints. Additionally, we robustify the target tracking UAV control using adaptive control strategies to handle uncertainties and disturbances.

2.3.5 Adaptive control strategies

Unlike the predictive strategy applied to the MPC as seen in the previous section, the adaptive control strategy utilises the current information from the system to improve performance output. Adaptive controllers can be either model-based or non-model-based. We review a few related model-based adaptive control literature before considering the other types.

Model reference adaptive control. Shastry et al., [286] developed a Model Reference Adaptive Control (MRAC) applied to Load Transfer Systems (LTS) for accurate real-time payload delivery by UAVs. Simulations within the constraints of the LTS's physical properties on the moving UAV were conducted to evaluate MRAC's mission performance effects. Similarly, an MRAC controller was also applied to VTOL UAV for LTS in [287]. A similar strategy was implemented by [198], where an adaptive control was developed for a hybrid UAV using multiple observers to enhance control stability in tracking a MAV. When the interceptor UAV nears an intruding MAV, a speed-damping scheme was used to adjust its forward speed based on a bounding box area. An adaptive model calibration method was employed to mathematically estimate the needed speed reduction relative to changes in distance to the target distance [288]. A related research by, [289] developed a multivariable MRAC scheme based on an Automatic Carrier Landing System (ACLS) proposed to manage UAV dynamics with parametric and structural uncertainties. The approach was

employed to develop longitudinal and lateral flight controllers for carrier-based UAVs. The study established a realistic UAV model and obtained a linear representation for control design. In a related target tracking study, a state feedback output tracking MRAC scheme was implemented to ensure accurate tracking during carrier landing, even in the presence of flight deck motion disturbances. The study by [290] employed an adaptive approach for controlling fixed-wing UAV landing by optimising output error through real-time parameter adjustments using MRAC.

Machine learning based adaptive control. In machine learning adaptive control, a neural network model is used to learn the behaviour of a controller with the goal of adaptively optimising performance using carefully crafted reward functions. For example, a novel adaptive control approach was introduced for motion prediction by implementing a control fusion of deep learning and adaptive reference derivatives estimation to autonomously detect and track high-speed ground vehicles. The utilised platform involved a quadrotor UAV equipped with minimal sensors, a stereo camera, and an IMU. Deep learning was used to aid object detection, while adaptive reference derivatives estimation-based control predicts movement and compensation [286]. Non-model-based adaptive control strategies can be divided into model reference, self-tuning, and gain scheduling methods. These subdivisions are discussed with reference to UAV target tracking in the next subsections.

Self-tuning control. Self-tuning adaptive control has also been applied to target tracking. For instance, [291] designed a controller for fixed-wing UAV swarm formations with coordinated flocking along a non-uniform circular path. The adaptive self-tuning algorithm addressed parameter uncertainties, ensuring stability and practicality in diverse initial conditions. While multi-rotor UAV using Multi-Layer Neural Dynamics (MLND) controllers can achieve trajectory tracking, uncertainties in UAV parameters degrade control quality. To address this problem, adaptive self-tuning methods were incorporated to improve control accuracy by [292].

Gain scheduling. Gain scheduling is another important method of adaptively optimising the target tracking algorithms. Cesetti et al., [293], presented a real-time gain scheduling approach for controller tuning. It proposed a vision-based method for guiding and landing UAVs in a partially known environment. Natural landmarks were detected through feature-based image matching, enhancing an autonomous behaviour-based control system for navigation and landing. The Gain-Scheduled PID controller gave better control output than the typical fixed gains PID controller for target tracking [191]. A novel fuzzy-gain scheduling strategy for PID control adjustment was also developed to enhance stability under various conditions and disturbances by maintaining effectiveness in the presence of altitude-related errors [294]. The method enabled successful trajectory tracking and robustness in noisy environments, outperforming conventional PID.

While gain scheduling and model reference adaptive control methods, as highlighted in the literature by various studies [286, 287, 289, 290, 293, 191, 294], offer significant benefits, including precise payload delivery, addressing uncertainties in UAV dynamics, and enhancing stability in diverse conditions, the context of UAV target tracking demands a strategy more aligned with real-time adjustments based on observed system behaviour. The self-tuning adaptive control strategy, as exemplified in studies such as [291, 292], demonstrated practicality in handling parameter uncertainties and achieving stability in varying initial conditions which are essential when dealing with real-time UAV target tracking scenarios. The ability to dynamically adjust parameters without explicit reference to a model or pre-defined scheduling mechanism allows for adaptability in rapidly changing scenarios, such as those encountered in UAV target tracking missions.

In contrast, model reference adaptive control methods, while robust and offering accurate control in specific applications like UAV landing optimisation [290], often rely on accurate system models and might face challenges in situations with dynamic changes or uncertainties. Gain scheduling methods, though effective in controller tuning and trajectory tracking [293, 191, 294], might require extensive prior knowledge about the system behaviour or environment. This reliance on a priori knowledge can limit their adaptability in scenarios where real-time adjustments based on observed system behaviour are necessary, as in the case of UAV target tracking. Therefore, considering the dynamic and real-time nature of UAV target tracking scenarios, the decision to implement a self-tuning adaptive control strategy was driven by its inherent adaptability and practicality in handling uncertainties and diverse conditions, enabling the UAV system to dynamically adjust and optimize its performance based on observed behaviour without strict dependencies on predefined models or scheduling mechanisms.

2.3.6 Hybrid control

In some circumstances, UAV target tracking problems may require the combination of two or more control strategies to effectively execute the tracking task. These types of combined algorithms are presented as hybrid controls. Hybrid controllers combine different control strategies to leverage their complementary strengths. For instance, a hybrid autonomous visual tracking algorithm for micro aerial vehicles was implemented by [295]. Similarly, a hybrid controller developed by [278] uses tube model MPC to track predefined paths in the presence of noise and disturbances. In a related study, [198] presented a hybrid control algorithm that incorporated a dual observer system consisting of an Extended State Observer (ESO) for state approximation and a nonlinear Disturbance Observer (DO) for external disturbance estimation to control a hybrid UAV, biplane quadrotor, applicable in diverse fields such as agriculture, disaster management, and relief operations. The control

strategies encompassed a Backstepping Controller (BSC), Integral Terminal Sliding Mode Controller (ITSMC), and a Hybrid Controller (ITSMC + BSC). Additional solutions were devised to manage variable mass changes during flight and wind gusts, employing an Adaptive Backstepping Controller (ABSC) and an Adaptive Hybrid Controller combined with ESO and DO.

Hybrid controllers may be designed to switch between control strategies at different phases of a target-tracking mission or when some preset threshold is reached. For instance, an adaptive exponential switching control that improves transient response, and yields smoother control compared to conventional adaptive SMC was applied for a UAV-GMT tracking by estimating uncertainties using adaptive rules [296]. Wang et al., 9[297] also utilised switching control for hybrid UAV tracking of a ground vehicle in motion. A non-chattering sliding mode guidance law for hybrid UAV-ground vehicle tracking that employed adaptive second-order sliding mode switching control was implemented for robustness and finite-time tracking by [298]. The adaptive estimation part of the hybrid controller handled uncertainties and enhanced command state generation. In [299], a UAV stabilisation approach using computer vision and adaptive switching controllers to track moving ground targets was proposed. A quadrotor equipped with a camera captures real-time images processed by a computer vision algorithm while a vision-based estimator computes the UAV's relative 3D position and velocity with reference to the target. These measurements guide a microcontroller for stabilisation. The switching controllers enabled enhanced decisions during temporary target loss or when out of the camera's view.

The reviewed literature shows that the integration of different control strategies into hybrid controllers allows for leveraging their complementary strengths to address complex UAV target-tracking problems effectively. For instance, the hybrid autonomous visual tracking algorithm for MAV by [295] and the TMPC-based controller by [278] demonstrated the efficacy of combining strategies to achieve predefined path tracking in noisy and disturbed environments. Moreover, the hybrid control algorithm presented by [198] showcased the versatility of hybrid controls. Additionally, hybrid controllers also facilitate dynamic switching between control strategies at different phases of a mission or upon reaching preset thresholds, as exemplified in studies such as [296–299]. These switching controllers improve transient response, robustness, and decision-making during uncertain or changing conditions that are essential in real-time UAV target tracking scenarios. Due to these unique attributes, we implement a hybrid optimal-adaptive control strategy in Chapter 5 of this thesis to exploit the complementary strengths of different control methods, ensuring robustness, adaptability, and effective performance in complex and dynamic UAV target tracking scenarios.

2.4 Cooperative Target Tracking Control

The use of multiple UAVs to cooperatively track a ground or aerial target would be vital in some peculiar tracking scenarios. Accordingly, we review a few research on target tracking using multi-UAV platforms. For instance, [300] designed a multi-UAV LVF cooperative UAV guidance to track an intelligent target that evades detection by mathematically maximising the UAV estimation error. Similarly, [301] devolved an evasive target tracking algorithm using two dynamic control optimisation strategies for different target models of evasive and stochastic motion. However, the target control policies were essentially lookup tables of any combination of UAV and target engagement. Wolfe et al., [302] also designed an EKF and T-Test selection model to track a target with random behaviour, while [303] developed a non-equilibrium game theoretic algorithm for tracking an active evasive target by two coordinated UAVs with the capability of estimating the level of target intelligence to deploy countermeasures. The pursuer-evader game was designed to minimise relative distance for the pursuing team of UAVs and maximise the evading target. The UAVs in these researches were, however, assumed to fly at a constant speed and the pursuit-evasion game was implemented for only 2D scenarios. The idea for countermeasure deployment as highlighted in this review was presented in Chapter 7 of this thesis. Multi-UAV tracking could be applied to single and multiple target tracking as reviewed in the following subsections.

2.4.1 Mult-UAV tracking of single target

In [117], a self-tuning, fuzzy MRAC was employed in developing a multi-UAV, ground target tracking algorithm for decentralised and centralised consensus based on Lyapunov guidance vector fields. The study explored an open chain control with each UAV only interacting with its next neighbours, cooperative leader control with a UAV formation. Similarly, Zhou et al., [304] proposed a UAV swarm-based cooperative tracking approach for multiple targets. Intelligent algorithms enhance accuracy, reduce tracking delay, reduce energy consumed by the UAV, and ensure collision avoidance, surpassing deep Q-network solutions. In a related study, [272] adopted a Belief Space iterative Linear Quadratic Gaussian (BSiLQG) for UAV trajectory optimisation to track clustered multiple targets. The study by [305] proposed a multi-UAV cooperative target tracking. To establish a system, a multi-agent deep reinforcement learning approach was introduced for intelligent flight decisions. The method used past and present target position information, alongside spatial information entropy to enhance detection coverage.

2.4.2 Mult-UAV tracking of multiple targets

To bolster Group Target Tracking (GTT) in UAV swarms, [306] designed an automatic measurement partitioning method with deep learning-based manoeuvre modelling and 3D shape estimation to enhance performance. In [306], a set of optimised criteria was proposed for tracking group target tracking, while [307], presented a novel decentralised control strategy, that employs a Decentralised Markov Decision Process (DMDP) framework for UAV swarm formation and multi-target tracking control. Nominal Belief-State Optimisation (NBO) was used to counteract the curse of dimensionality, enabling approximate dynamic programming. Coordinating multiple UAVs to consecutively track diverse targets presents challenges. To address this challenge, a cooperative tracking intelligent algorithm was developed for consecutive tracking and collision avoidance and validated through stable swarm behaviour in realistic scenarios [304].

The review of studies like [300, 301] highlighted the success of cooperative guidance algorithms and dynamic control optimisations, enhancing tracking accuracy and adaptability. Further insights from research by [302, 303] demonstrated the potential of multiple UAVs in tracking elusive targets, estimating target intelligence levels, and deploying countermeasures. In single-target scenarios, methods from [117, 304] leveraging fuzzy MRAC and intelligent algorithms significantly improved accuracy, reduced delay, and ensured collision avoidance, surpassing traditional solutions. For multiple targets, strategies proposed by [306, 307] focused on enhancing group target tracking and stable swarm behaviour, overcoming dimensionality issues, and employing decentralised control strategies. Due to the highlighted advantages, we implement multi-UAV tracking in Chapter 6, emphasising improved accuracy, adaptability, collision avoidance, and enhanced tracking performance, particularly in scenarios involving intelligent or evasive targets.

2.5 Countermeasure Against Adversarial Targets

The end goal of a target tracking mission is either to continuously track and record target movements or to execute some interception action against an intruding target. Therefore, it may be necessary to incorporate air-to-ground or air-to-air countermeasure capability into the tracking UAV. The development of countermeasure systems to identify and neutralise malicious drones has gained significance as a result of the proliferation of drones. With the increasing need for efficient counter-UAV measures, the tracking of UAVs is identified as a vital aspect of these countermeasures [308]. Additionally, identifying the target drones is a crucial initial phase in formulating effective counteractions [309, 310]. Counter-UAV systems vary widely and interdicting unauthorised UAVs involves various approaches based on vulnerabilities. These measures include hand-held devices, and anti-aircraft

missile systems, which include laser, electronic, and kinetic systems [311]. A holistic survey for anti-drone systems encompassing detection, tracking, and interception was presented by [312].

In [313], they explored a multi-platform Counter Unmanned Aircraft System (C-UAS) concept using a cooperative team of mini-drones as a countermeasure defence. Similarly, [314], outlined the various types of countermeasures that could be applied to detect, track, neutralise, and or destroy swarm unmanned aerial system UAS. These include Ground lasers, anti-laser weapons, high-powered microwaves, surface-to-air missiles, and armed & hybrid C-UAS systems equipped with jammer guns and electronic hacking, signal jamming, de-authentication and cyber-attack methods. Other countermeasure considerations include swarm versus swarm engagement, escort swarm UAVs and UAVs mounted with net-capturing projectile systems for entangling rotors. Tokyo police have also employed larger net-carrying UAVs to trap smaller drones. In other cases, trained eagles have been deployed to intercept drones as employed by police in Scotland and the Netherlands [315].

Rogers et al, [316] designed a comprehensive approach that incorporates preventive and reactive C-UAS countermeasures. The preventive measures include deterrence, suppression, and avoidance, while the reactive measure deploys detection, decision-making, and neutralisation [317]. Additionally, the article explores a coverage-based algorithm for defending against adversarial swarms using fixed-wing UAVs equipped with explosives. This method encompasses impact point optimisation and MPC-driven impact time control, with the goal of both maximising coverage within the adversary swarm and minimising impact time, by guaranteeing the coordinated arrival of multiple UAVs at dynamically changing impact points [318]. A novel distributed control system was also proposed by [319] for tracking and jamming rogue drones in 3D space using a team of pursuer UAVs equipped with radio jammers. Their approach involved estimating target existence probability, spatial density, and optimal radio transmission levels to enhance target jamming while preventing the jamming of friendly UAVs.

2.5.1 Task assignment and aerial targets countermeasure

When a group of UAVs are cooperatively tracking targets, there may be a need to assign a UAV to track one or some of the targets during the mission scenario. To address the issue of task assignment when intercepting adversarial targets, the research by [320] explored task assignment in cooperative air combat with timing continuity constraints. They established task assignment and integer programming models, that solve the problem using integrated linear programming software which showed viability and efficiency for enhanced cooperative aerial countermeasure tasks. In a similar study, task allocation and path planning

for heterogeneous UAVs in search and destroy missions were explored by [321]. Their approach optimised system utility by considering targets and proposing resource-aware task allocation and coalition-based path planning using distributed cooperative particle swarm optimisation. The path planning algorithm developed ensured safe trajectories, satisfying kinematic and collision avoidance constraints. In [322], they proposed a solution to address safety concerns caused by unlicensed UAVs by employing high-speed interception UAVs to neutralise rogue drones. Their approach involved precise target tracking and optimal interceptor control through a navigation, guidance, and control architecture. They utilised Kalman filter estimation for navigation and proportional navigation-based guidance that incorporated thrust vectoring control. In related research, they presented a countermeasure UCAV that launches a projectile upon operator command or time elapse in simulations to hit an aerial target within a preset time [323].

2.5.2 Countermeasures decision processes

A novel UAV-based method for tracking dynamic targets invading an oilfield was developed by employing trajectory prediction technique, swarm intelligence optimisation, and an improved algorithm developed by the fusion of Fruit-Fly Optimisation Algorithm (FOA) and Bat Algorithm (BA), termed as FOBA to maintain effective target tracking distances [323]. In related literature, a circular formation control was implemented by [324] to create a decentralised guidance law that commands a tracking UAV to encircle the target, using adaptable instructions that limit the target's movement and neutralise it by rendering it ineffective. Similarly, [325], proposed a countermeasure that uses a swarm of surveillance UAVs to track targets back to their origin. Reactive tracking and predictive pre-positioning strategies were considered in their algorithm development which revealed that the circular swarm outperforms the reference randomly moving swarm, especially when using predictive pre-positioning with a smaller number of surveillance UAVs.

In the context of countermeasures against adversarial UAVs, various methods have been explored, encompassing a wide range of techniques and technologies [308, 311, 312]. The common counter-UAV systems highlighted from our review include ground lasers, high-powered microwaves, surface-to-air missiles, and armed C-UAS systems, showcasing diverse approaches [314]. Studies such as [316, 318, 319] propose preventive and reactive countermeasures using fixed-wing UAVs equipped with explosives, coverage-based algorithms, and distributed control systems. These methods aim to deter, suppress, detect, and neutralise adversarial swarms, presenting multifaceted approaches to counter adversarial threats [316, 318, 319]. However, within this array of approaches, the utilisation of a countermeasure UCAV launching a projectile, as detailed by [323], stands out due to its precision targeting and optimal control mechanisms. This method involves employing

high-speed interception UAVs equipped with guidance and control architecture, utilising Kalman filter estimation for navigation, and proportional navigation-based guidance with thrust vectoring control, demonstrating precision and effectiveness in neutralising aerial targets [323]. While various countermeasure approaches offer comprehensive coverage and diverse functionalities, the precision targeting, optimal control, and efficacy in neutralising targets portrayed by the projectile-based countermeasure method informed our choice for its utilisation.

2.6 Summary

This Chapter provided a comprehensive summary of up-to-date literature related to target tracking using UAVs. We highlighted the need to establish the type of environment in which the tracking mission is taking place to enhance intended scenario simulations. The environment types identified were either discreet or continuous and could be modelled in 2D planar of 3D space. The environment could also be cluttered with or free of obstacles that are either static or dynamic. We also reviewed various types of targets employed in a tracking mission and categorised them according to operating space, manoeuvre type, and dynamics. The tracking UAV types used in tracking missions were also reviewed and grouped by their size & range capabilities and dynamics of either fixed or rotary wing. We also explored tracking methodologies that have been employed in the recent literature for target tracking simulations, including visual, sensor-based as well as GPS/GNS. We then considered guidance and navigation literature by highlighting the differences and unique applications of waypoint and continuous navigation.

The reviewed literature explored a broad spectrum of control strategies applied in Unmanned Aerial Vehicle (UAV) target-tracking scenarios. It juxtaposes the efficacy and limitations of various control methodologies, emphasising their suitability concerning UAV dynamics, complexities, and adaptability. The literature extensively covers PID, PI, PD controllers, nonlinear controls, optimal control strategies, adaptive controls, hybrid control approaches, cooperative guidance, and countermeasure methodologies. The review converges on the effectiveness of PID controllers in UAV target tracking due to their widespread application but acknowledges their limitations, such as overshoot and oscillations. PI controllers are considered, yet studies suggest their inadequacy in addressing complex dynamics and varying target speeds. PD control emerges as a viable alternative, offering reduced oscillations and effective handling of specific target-tracking scenarios. The literature extensively covers nonlinear controls, emphasising their robustness but acknowledges challenges in scenarios involving parameter uncertainty.

The Optimal control methods were selected as a preferred control strategy due to their precision in trajectory optimisation, aligning closely with the requirements of UAV target tracking systems. Adaptive control strategies, particularly self-tuning adaptive control, stand out for their adaptability in handling uncertainties, contrasting with model reference adaptive control, and gain scheduling methods that may rely on extensive prior knowledge. The choice of control strategies in this thesis is justified by aligning the requirements of UAV target tracking scenarios with the strengths of each control methodology. The implementation of PD control over PID and PI in the research chapters is driven by its simplicity, reduced oscillations, and effectiveness in handling specific scenarios. We favoured the optimal control methodologies, particularly MPC, as the preferred controller due to their adaptability, handling of nonlinearities, and precision in trajectory optimisation, which align with UAV target tracking system requirements. The literature review informed the selection of NMPC over LMPC due to the former's superior handling of nonlinear dynamics and constraints, crucial in uncertain UAV control environments. Adaptive control strategies, specifically self-tuning adaptive control, were chosen for their dynamic parameter adjustment capability in real-time, crucial in rapidly changing UAV target tracking scenarios.

We also explored cooperative target tracking of single and multiple targets as well as countermeasures against adversarial targets and target-tracking decision processes. The reviewed literature provided a background for the platforms, dynamics, and control strategies implemented in the various Chapters of this thesis. Within the introductory section of the technical Chapters, we also provide more specific literature related to highlighting gaps and aiding problem formulation. Regarding countermeasures against adversarial UAVs, the review encompasses various techniques, emphasising precision targeting and optimal control mechanisms demonstrated by a countermeasure UCAV launching a projectile. This method stands out for its efficacy in neutralising aerial targets, informing its utilisation despite the array of comprehensive countermeasure approaches. Overall, the review critically analyses diverse control strategies' strengths and limitations in UAV target tracking. It rationalises the selection of control methodologies in the thesis by aligning their specific advantages with the demands of UAV target tracking scenarios. The comprehensive review aids in highlighting the need for adaptable, precise, and robust control strategies, justifying the preference for certain methodologies over others. The literature informs a strategic choice of control methods in subsequent research chapters, advocating for a robust and adaptable control strategy combining optimal and adaptive control methods, and acknowledging the necessity of dynamic adjustments in real-time scenarios. Additionally, it guides the utilisation of countermeasure methodologies, favouring precision and efficacy in neutralising adversarial UAVs.

Chapter 3

Optimal Tracking & Evasion in 3D Space

3.1 Introduction

The UAV is increasingly being employed as an alternative to manned platforms for autonomous target tracking missions as it provides better manoeuvrability, reduced operational cost and less burden on human operators [15]. To autonomously perform this role, a fixed-winged UAV must be capable of predicting and responding to evasive manoeuvres from agile targets. Several UAV control law designs for fixed-winged UAV tracking of manoeuvring targets exist. However, researchers commonly design non-smart manoeuvring targets to mimic evasive manoeuvres. To design a realistic UAV tracking engagement to continuously track a smart evasive target, the dynamic constraints of the UAV and target need to be taken into consideration. Additionally, the undulating nature of the ground terrain would require a 3D model that enables the UAV to adjust its altitude in response to target manoeuvre and terrain. This chapter addresses these design considerations, by implementing an evasive ground-moving target that is optimally controlled to persistently evade the tracking UAV. To account for the effect of target evasion and tracking performance of the UAV in environments with undulating ground surfaces, we also implemented a strategy to extend the target tracking simulation to 3D space.

3.1.1 UAV tracking-related work

Chen et al. [326] implemented a single UAV tracking in 2D space, with the target manoeuvre designed as a fixed velocity moving curve. In [14], Kim developed a 2D control strategy for fixed-winged UAV autonomous tracking of a randomly manoeuvring ground target while [48] developed a reinforcement learning-based UAV tracking of an

aerial evading target that uses a state-dependent statistical control policy. Although this strategy was implemented for 3D engagement, the control actions were heuristically determined. In [15], a control algorithm was designed to track a smart evading target that utilises a dipole-type vector field around the tracking UAV to execute evasive action. However, this was only implemented for 2D engagement dynamics.

Multiple and cooperative UAV controls for target tracking have also been designed and tested. For instance, [300] designed a multi-UAV Lyapunov vector field cooperative UAV guidance to track an intelligent target that evades detection by mathematically maximising the UAV estimation error. [301] also devolved an evasive target tracking algorithm using two dynamic control optimisation strategies for different target models of evasive and stochastic motion. However, the target control policies were essentially lookup tables of any combination of UAV and target engagement. [302] also designed an EKF and T-Test selection model to track a target with random behaviour. Similarly, [303] developed a non-equilibrium game theoretic algorithm for tracking an active evasive target by two coordinated UAVs with the capability of estimating the level of target intelligence to deploy countermeasures. The pursuer-evader game was designed to minimise relative distance for the pursuing team of UAVs and maximise the evading target. The UAVs in these researches were, however, assumed to fly at a constant speed and the pursuit-evasion game was implemented for only 2D scenarios.

Despite efforts in developing UAV control strategies to track evasive targets, limited attention has been paid to the implementation of smart evasive targets capable of initiating intelligent evasive manoeuvres against the tracking UAV. Furthermore, the dynamic nature of the pursuit-evasion requires that both platforms are designed with the capability to either accelerate or decelerate within design limits while allowing the UAV to adjust its altitude with changes in target states [327]. This Chapter addresses this gap by developing a 3D optimal control for a UAV tracking an evasive smart ground target and accounting for the associated dynamic constraints.

3.1.2 Contributions

The contributions of this Chapter are as follows:

- The 2-step prediction fixed-winged UAV optimal control strategy by [14], is solved with the turn rate and bank angle constraints, enabling smoother target tracking while restricting excessive turns of the UAV.
- An evasive target control strategy is introduced by solving the maximisation problem and providing realistic target movements.

- The 2D algorithm in [14] is extended to a 3D target tracking algorithm, taking into account the terrain changes.

The rest of the Chapter is outlined as follows. In section 3.2, the UAV target tracking problem is formulated using simplified dynamics and mathematical models of constraints considered in the development of optimal target tracking. In section 3.2.2, the solution for the UAV optimal target tracking problem and its cost function development is presented while Section, 3.3 discusses the target manoeuvre control design, incorporating vehicle constraints and cost function evaluation. A method for extending from a 2D to 3D target tracking algorithm is presented in Section 3.4 while a simulation of sample engagement scenarios and discussion of results is presented in Section 3.5. Section 3.6 presents concluding remarks and plans.

3.2 UAV 2D Target Tracking

Consider a UAV with the task of tracking an evasive ground target in a 3D engagement space. The UAV can accelerate or decelerate within specified bounds and is constrained by a maximum turn radius. We assume that the UAV can identify the target in its camera field of view at all times.

3.2.1 Dynamics

The UAV and target dynamics are represented as shown in Fig. 3.1. The UAV positions are represented by x_a, y_a and z_a. and the dynamic equation of the UAV is represented by

$$\dot{x}_a = v_{ax}, \dot{y}_a = v_{ay}, \dot{z}_a = v_{az}, \tag{3.1a}$$

$$v_{ax} = \|\mathbf{v}_a\| \cos\sigma_a \sin\phi_a \tag{3.1b}$$

$$v_{ay} = \|\mathbf{v}_a\| \sin\sigma_a \cos\phi_a \tag{3.1c}$$

$$v_{az} = \|\mathbf{v}_a\| \sin\sigma_a \tag{3.1d}$$

$$\dot{v}_{ax} = u_{ax}, \dot{v}_{ay} = u_{ay}, \dot{v}_{az} = u_{az} \tag{3.1e}$$

where $(\dot{})$ is the derivative with respect to time, $\mathbf{v}_a$ is the UAV velocity vector with respective components as v_{ax}, v_{ay} and v_{az} in the global reference frame, indicated by x-y-z in Fig. 3.1. The global frame used in this research is the East-North-Up coordinate frame.

Furthermore, σ_a and ϕ_a are the flight path and heading (course) angles respectively [328], while u_{ax}, u_{ay} and u_{az} are the control acceleration input of the UAV. The body frame is defined by x^{Ba}, y^{Ba} and z^{Ba} as shown in Fig. 3.1, where x^{Ba} is aligned with the UAV

velocity vector, y^{Ba} is towards the right-hand-side of the wing, and z^{Ba} is given by the cross product of x^{Ba} and y^{Ba}.

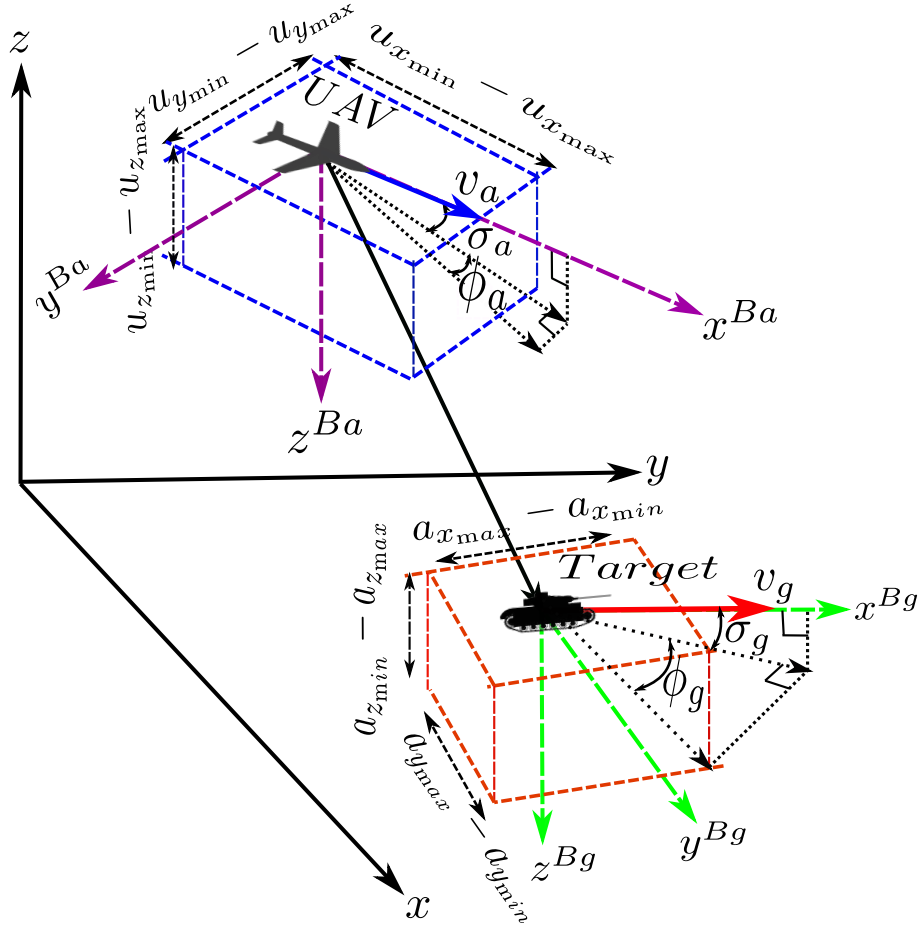

Fig. 3.1 UAV and target engagement dynamics. The coordinates (x,y,z) are global while (x^{Ba},y^{Ba},z^{Ba}) and (x^{Bg},y^{Bg},z^{Bg}) are local. The dotted boxes around the UAV and target indicate their respective control input magnitude constraints.

The state space representation is given by

$$\dot{\mathbf{x}}_a = A_a\mathbf{x}_a + B_a\mathbf{u}_a = \begin{bmatrix} 0_3 & I_3 \\ 0_3 & 0_3 \end{bmatrix}\mathbf{x}_a + \begin{bmatrix} 0_3 \\ I_3 \end{bmatrix}\mathbf{u}_a \tag{3.2a}$$

$$\mathbf{x} = C_a\mathbf{x}_a = [I_3\, 0_3]\mathbf{x}_a \tag{3.2b}$$

where 0_3 is the 3×3 zero matrix, I_3 is the 3×3 identity matrix, A_a, B_a and C_a are defined appropriately in the above equation, $\mathbf{x}_a = [x_a, y_a, z_a, v_{ax}, v_{ay}, v_{az}]^T$ and $\mathbf{u}_a = [u_{ax}, u_{ay}, u_{az}]^T$.

The target dynamics are given by

$$\dot{x}_g = v_{gx}, \dot{y}_g = v_{gy}, \dot{z}_g = v_{gz}, \tag{3.3a}$$
$$v_{gx} = \|\mathbf{v}_g\| \cos\sigma_g \sin\phi_g \tag{3.3b}$$
$$v_{gy} = \|\mathbf{v}_g\| \sin\sigma_g \cos\phi_g \tag{3.3c}$$
$$v_{gz} = \|\mathbf{v}_g\| \sin\sigma_g \tag{3.3d}$$
$$\dot{v}_{gx} = a_{gx}, \dot{v}_{gy} = a_{gy}, \dot{v}_{gz} = a_{gz} \tag{3.3e}$$

where x_g, y_g and z_g represent the position of the target and v_{gx}, v_{gy} and v_{gz} represent the respective components of the target velocity vector $\mathbf{v}_g$. The target flight path angle is σ_g, and its heading angle is ϕ_g. Additionally, the target acceleration components are a_{gx}, a_{gy} and a_{gz} respectively while its state space representation is given by:

$$\dot{\mathbf{x}}_g = A_g\mathbf{x}_g + B_g\mathbf{u}_g = \begin{bmatrix} 0_3 & I_3 \\ 0_3 & 0_3 \end{bmatrix} \mathbf{x}_g + \begin{bmatrix} 0_3 \\ I_3 \end{bmatrix} \mathbf{a}_g \tag{3.4a}$$
$$\mathbf{z} = C_g\mathbf{x}_g = [I_3\, 0_3]\mathbf{x}_g \tag{3.4b}$$

where, A_g, B_g and C_g are defined appropriately in the above equation, $\mathbf{x}_g = [x_g, y_g, z_g, v_{gx}, v_{gy}, v_{gz}]^T$ and $\mathbf{a}_g = [a_{gx}, a_{gy}, a_{gz}]^T$.

We discretise the governing differential equation with the time step, Δt, for the UAV and target as follows:

$$\mathbf{x}_a(k+1) = F_a\mathbf{x}_a + G_a\mathbf{u}_a(k) \tag{3.5a}$$
$$\mathbf{x}_g(k+1) = F_g\mathbf{x}_g + G_g\mathbf{a}_g(k) \tag{3.5b}$$
$$\mathbf{x}(k) = C_a\mathbf{x}_a(k) \tag{3.5c}$$
$$\mathbf{z}(k) = C_g\mathbf{x}_g(k) \tag{3.5d}$$

where $\mathbf{x}$ and $\mathbf{z}$ represent the UAV and target position state vectors, while C_a and C_g are the respective output matrices for the UAV and target state equations.

$$F_a = \begin{bmatrix} I_3 & \Delta t I_3 \\ 0_3 & I_3 \end{bmatrix}, G_a = \begin{bmatrix} 0_3 \\ \Delta t I_3 \end{bmatrix}, F_g = F_a, G_a = G_g \tag{3.6}$$

The control input space of the UAV is confined by

$$u_{ax_{\min}} \leq u^B_{ax} \leq u_{ax_{\max}} \tag{3.7a}$$
$$u_{ay_{\min}} \leq u^B_{ay} \leq u_{ay_{\max}} \tag{3.7b}$$
$$u_{az_{\min}} \leq u^B_{az} \leq u_{az_{\max}} \tag{3.7c}$$

where u^B_{ax}, u^B_{ay}, and u^B_{az} are the control input of UAV in the UAV's body coordinates. The control input acceleration of the ground vehicle is given by

$$a_{gx_{\min}} \leq a^B_{gx} \leq a_{gx_{\max}} \tag{3.8a}$$
$$a_{gy_{\min}} \leq a^B_{gy} \leq a_{gy_{\max}} \tag{3.8b}$$
$$a_{gz_{\min}} \leq a^B_{gz} \leq a_{gz_{\max}} \tag{3.8c}$$

where a^B_{gx}, a^B_{gy}, and a^B_{gz} are the control input of the target in the body coordinates.

To simplify the tracking optimisation problem, we assume that the altitude of the UAV is fixed and the terrain where the ground vehicle moves is flat [14]. Hence, the corresponding dynamics given by (3.1) is used excluding z_a and v_{az} making it a 2D tracking problem, with a simplified engagement diagram as shown in 3.2.

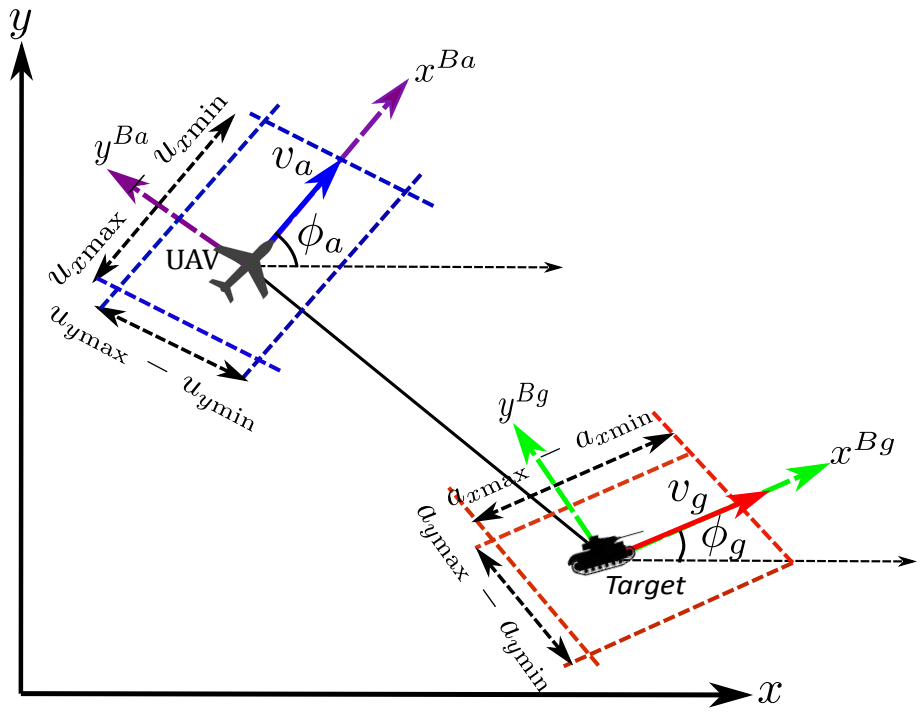

Fig. 3.2 Simplified 2D UAV and target engagement diagram

The velocity and control vectors in the global coordinate must satisfy the constraint, while its turn radius must be larger than its minimum radius of turn given as $r_{\min}$. The curvature

of the UAV flight path in 2D space must be smaller than the inverse of the minimum turn radius. These constraints are summarised as follows:

$$v_{a_{\min}} \leq \sqrt{v_{ax}^2 + v_{ay}^2} \leq v_{a_{\max}} \tag{3.9a}$$

$$u_{ax_{\min}} \leq u_{ax}\cos\phi_a + u_{ay}\sin\phi_a \leq u_{ax_{\max}} \tag{3.9b}$$

$$u_{ay_{\min}} \leq -u_{ax}\sin\phi_a + u_{ay}\cos\phi_a \leq u_{ay_{\max}} \tag{3.9c}$$

$$0 \leq v_{gx}^2 + v_{gy}^2 \leq v_{g_{\max}}^2 \tag{3.9d}$$

$$\frac{|v_{ax}u_{ay} - v_{ay}u_{ax}|}{(v_{ax}^2 + v_{ay}^2)^{(3/2)}} \leq \frac{1}{r_{\min}} \tag{3.9e}$$

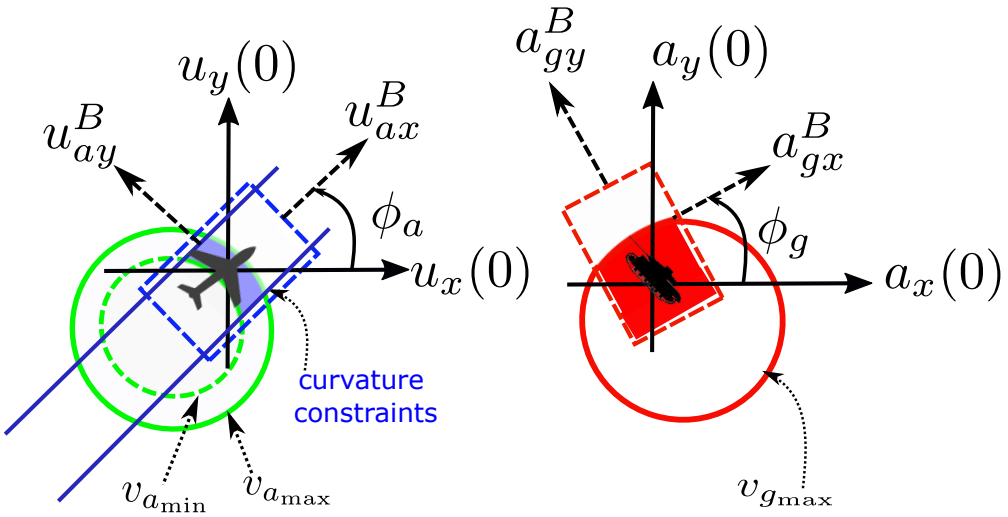

(a) UAV control input constraint (b) Target control input constraint

Fig. 3.3 UAV and target constraints and feasible control spaces

where $v_{a_{\min}}$ and $v_{a_{\max}}$ are the respective minimum and maximum allowed UAV velocities, ϕ_a is the aircraft heading angle measured with respect to x-axis in the global frame, while $v_{g_{\max}}$ is the maximum target velocity. Similarly, $u_{ax_{\min}}$, $u_{ax_{\max}}$, $u_{ay_{\min}}$ and $u_{ay_{\max}}$ are the minimum and maximum control inputs of the UAV along the x-y axes in body frame.

As shown in Figure 3.3, the UAV is constrained by an outer maximum velocity solid thick line and a minimum constraint circle represented by a dashed line. The control input constraint box is represented by the rectangular dashed line, while the two blue parallel lines represent the UAV curvature constraint limits. The shaded area at the intersection of the various constraints defines the allowable control input space for the UAV. Unlike the UAV the ground target is only constrained to a maximum velocity limit since it can operate with zero or negative velocity by coming to a full stop or reversing backwards during a

simulation. The control input magnitude is represented by the red dashed rectangular line and the red shade area represents its allowable;e control input space.

In addition, sharp turns by the UAV could result in high loading to the structure of the UAV. To prevent excessive loading,the UAV bank angle, γ_a, and the turn rate, $\dot{\psi}$, are constrained as follows [257]:

$$\gamma_{a_{\min}} \leq \gamma_a \leq \gamma_{a_{\max}} \tag{3.10a}$$

$$\dot{\psi}_{\min} \leq \dot{\psi} \leq \dot{\psi}_{\max} \tag{3.10b}$$

where $\gamma_{a_{\min}}$ and $\gamma_{a_{\max}}$ are the minimum and maximum allowed bank angles respectively, while $\dot{\psi}_{\min}$ and $\dot{\psi}_{\max}$ are the respective minimum and maximum turn rates with constraints defined as $-\pi/4 \leq \gamma_a \leq +\pi/4$ [257]. The bank angle and the turn rate are related to the speed of UAV, $\|\mathbf{v}_a\|$, and $r_{\min}$ as follows [329]:

$$\gamma_a = \frac{\dot{\psi}\|\mathbf{v}_a\|}{g}, \ \dot{\psi} = \frac{\|\mathbf{v}_a\|}{r_{\min}} \tag{3.11}$$

where g is the acceleration due to gravity. The UAV turn rate is represented as $\dot{\psi}$ in rad/s.

3.2.2 UAV target tracking algorithm

To ensure the UAV tracks the target, the two-step cost function to be minimised is given by;

$$\underset{\mathbf{v}_g(t)\in\mathbb{V}_g}{\text{Maximise}} \ \underset{\mathbf{u}_a(t)\in\mathbb{U}_a}{\text{Minimise}} \ J = \int_{t_f}^{t_0} [\mathbf{x}(t) - \mathbf{z}(t)]^T [\mathbf{x}(t) - \mathbf{z}(t)] \, dt \tag{3.12}$$

subject to (3.5), (3.7), (3.9) and (3.10), where t_f and t_0 represent the initial and final time t while $\mathbb{V}_g$ and $\mathbb{U}_a$ represent the feasible control input sets of the target and the UAV, respectively. This cost function can be reduced to:

$$\underset{\mathbf{v}_g(0),\mathbf{v}_g(1)\in\mathbb{V}_g}{\text{Maximise}} \ \underset{\mathbf{u}_a(0)\in\mathbb{U}_a}{\text{Minimise}} \ J = \sum_{k=1}^{2} [l_a(k)]^2 \tag{3.13}$$

where $l_a(k)$ is equal to $\|\mathbf{x}(k) - \mathbf{z}(k)\|$. Note that the ground target acceleration capability as in (3.8) is omitted in the UAV tracking algorithm design phase allowing the target to change its velocity instantaneously. This provides an advantage for the target to evade from the tracking algorithm's point of view. The two-step is chosen as it is the minimum

number of steps for providing the control input in the cost function, i.e., the relative degree of the system.

To design a worst-case scenario, consider the problem from the target perspective and assume the UAV has an unknown optimal tracking algorithm. The best evasive option for the target is to maximise the sum of the relative distance from the UAV. As the UAV approaches to the target, the evading ground target moves with maximum speed providing the biggest advantage to maximising the distance from the UAV.

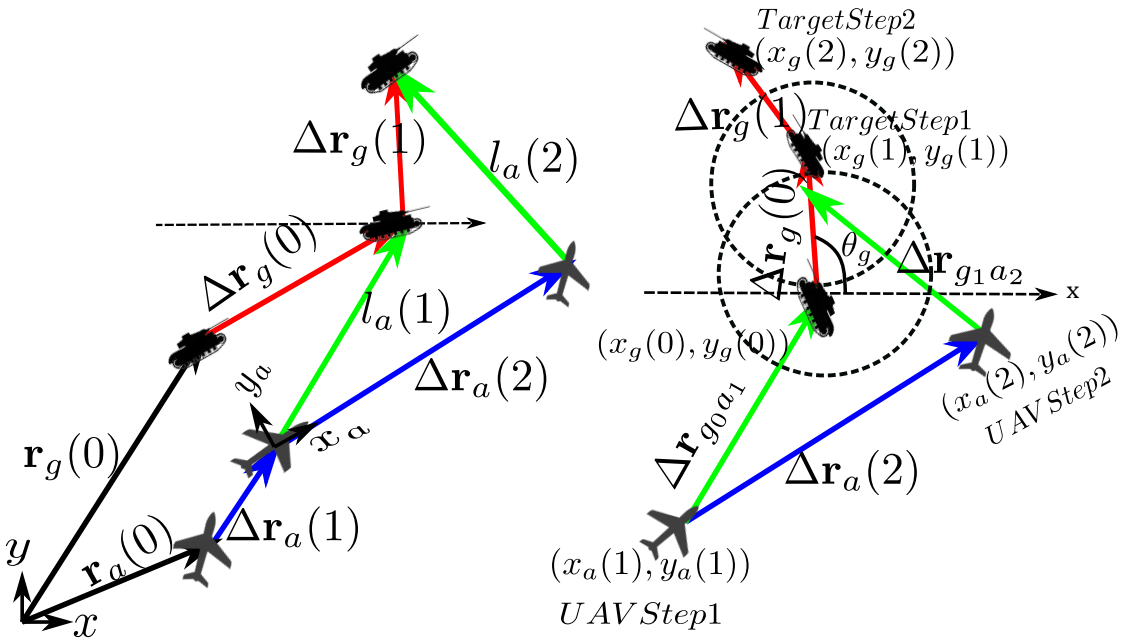

Fig. 3.4 UAV 2-Step tracking prediction

The two circles drawn around the target at $k = 1$ and $k = 2$ in Fig. 3.4, indicate that the next position of the target with the maximum speed can lie in any position at the boundary of the circles. It is assumed that the UAV will also move in a direction that minimises its relative distance to the target. At $k = 1$, the distance between UAV and target is a function of θ_g, the maximisation parameter used in computing the worst-case scenario for the UAV tracking minimisation, i.e.,

$$l_a(1) = \|\Delta\mathbf{r}g_o a_1 + v_{g_{\max}}\Delta t(\cos\theta_g\mathbf{i} + \sin\theta_g\mathbf{j})\| \tag{3.14}$$

At $k = 2$, the target simply tries to drive away from the UAV with maximum velocity in an opposite direction to the UAV velocity. The distance at $k = 2$ is given by

$$l_a(2) = \|\Delta\mathbf{r}g_1 a_1\| + v_{g_{\max}}\Delta t \tag{3.15}$$

Once the worst θ_g is determined by solving the maximisation problem, the minimisation problem for the UAV is obtained. The details of the 2D tracking algorithm are found in [14].

3.3 Smart Target Manoeuvre design

The target cost function was designed using the min-max concept to maximise its distance from the best-case UAV minimisation effort. Similar to the UAV tracking algorithm design, the smart target is assumed to have the position and velocity information of the UAV. The target control cost function is given by (3.16).

$$\underset{\mathbf{v}_a(t)\in\mathbb{V}_a}{\text{Maximise}}\ \underset{\mathbf{a}_g(t)\in\mathbb{U}_g}{\text{Minimise}}\ J_g = \int_{t_f}^{t_0} [\mathbf{z}(t)-\mathbf{x}(t)]^T [\mathbf{z}(t)-\mathbf{x}(t)]\, dt \tag{3.16a}$$

The above equation can summarised as (3.17).

$$\underset{\mathbf{v}_a(0),\mathbf{v}_a(1)\in\mathbb{V}_a}{\text{Minimise}}\ \underset{\mathbf{a}_g(0)\in\mathbb{U}_g}{\text{Maximise}}\ J_g = \sum_{k=1}^{2} [l_g(k)]^2 \tag{3.17}$$

subject to (3.5) and

$$v_{gx}^2 + v_{gy}^2 \leq v_{g_{\max}}^2 \tag{3.18a}$$

$$a_{gx_{\min}} \leq a_{gx}\cos\phi_g + a_{gy}\sin\phi_g \leq a_{gx_{\max}} \tag{3.18b}$$

$$a_{gy_{\min}} \leq -a_{gx}\sin\phi_g + a_{gy}\cos\phi_g \leq a_{gy_{\max}} \tag{3.18c}$$

$$v_{a_{\min}}^2 \leq v_{ax}^2 + v_{ay}^2 \leq v_{a_{\max}}^2 \tag{3.18d}$$

$$\dot{\psi}_{a_{\min}} \leq \dot{\psi}_g \leq \dot{\psi}_{a_{\max}} \tag{3.18e}$$

where $\mathbb{V}_a$ and $\mathbb{U}_g$ represent the feasible control input sets of the UAV velocity and the target acceleration, $v_{g_{\max}}$ is the maximum velocities of the target, $a_{gx_{\min}}$, $a_{gx_{\max}}$, $a_{gy_{\min}}$ and $a_{gy_{\max}}$ are its respective minimum and maximum control input components. The target turn rate, $\dot{\psi}_g$, is restricted by the minimum and the maximum bounds, $\dot{\psi}_{a_{\min}}$ and $\dot{\psi}_{a_{\max}}$.

In comparison to the tracking UAV, the target is designed with the consideration that it can stop, and move backwards. Accordingly, the target is not restricted by curvature and minimum velocity constraints as shown by the shaded feasible control space for the UAV and target in Fig. 3.3.

Substituting and expanding all the expressions into the cost function for the target, the following compact function, $\bar{J}_g$, equivalent to the original cost function is obtained:

$$\bar{J}_g = a_{gx}^2(0) + \alpha_g a_{gx}(0) + a_{gy}^2(0) + \beta_g a_{gy}(0) + \gamma_g \tag{3.19}$$

where α_g, β_g and γ_g are functions of the UAV initial velocity and the initial positions of the UAV and the target.

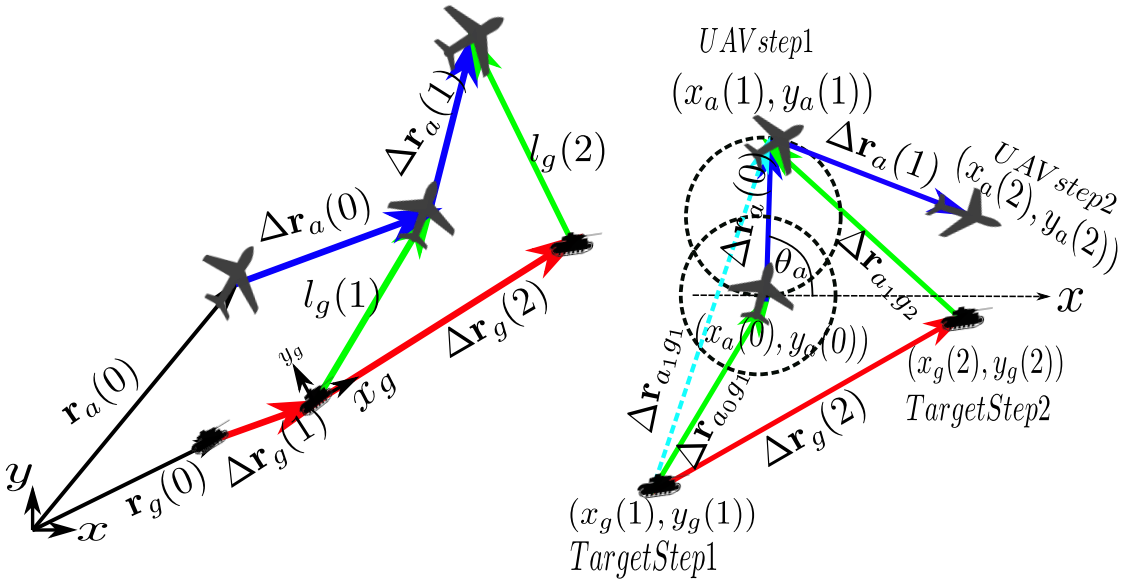

Fig. 3.5 Target 2-Step evasion manoeuvre

Similar to the worst-case scenario for the UAV tracking algorithm design, consider the worst-case scenario for the ground vehicle evasion manoeuvre. As shown in Fig. 3.5, the distance between UAV and target at $k = 1$, is equal to $l_g(1)$ and be calculated with respect to, θ_a, an optimisation parameter introduced to obtain best-case UAV tracking minimisation.

$$l_g(1) = \|\Delta \mathbf{r} a_o g_1 + v_{a_{\text{opt}}}(1)\Delta t(\cos\theta_a \mathbf{i} + \sin\theta_a \mathbf{j})\| \tag{3.20}$$

where $v_{a_{\text{opt}}}(1)$ is the UAV's optimal speed determined by the relative distance from the target. At $k = 2$, the UAV tries to close the relative distance between the two vehicles depicted as $l_g(2)$, which is calculated by

$$l_g(2) = \|\Delta \mathbf{r} a_1 g_1 + \Delta \mathbf{r}_a(1)\| = \|\Delta \mathbf{r} a_1 g_1\| + v_{a_{\text{opt}}}(2)\Delta t \tag{3.21}$$

where $v_{a_{\text{opt}}}(2)$ is the optimal speed applied by the UAV at $k = 2$ to close up with the target, dependent on the relative distance from the target given by $\|\Delta \mathbf{r}_a(1)\|$.

To simplify the worst-case scenario for the target, we assume that both of the optimal UAV speeds are equal to the UAV's maximum speed. Then, the minimisation of $l_g(2)$ is

equivalent to the minimising the following length:

$$\bar{l}_g(2) = \|\Delta\mathbf{r}a_1g_1\| = \|\Delta\mathbf{r}a_0g_1 - \Delta\mathbf{r}_g(2) + \Delta\mathbf{r}_a(0)\| \tag{3.22}$$

The original cost function can now be represented by the following minimisation problem:

$$\bar{J}_g = [l_g(1)]^2 + [\bar{l}_g(2)]^2 \tag{3.23}$$

The evasive control input is obtained by solving the maximisation of $\bar{J}_g$. The target optimal control is obtained using the same sampling or maximisation approaches used for the UAV optimal acceleration, i.e., search for the maximisation solution at the boundary or the inside of the control input constraints. The sampling approach enables finding optimal control corresponding to the minimal cost along the constraint boundary, $J_{g_{bd}}$. Similarly, optimal cost, $J_{g_{in}}$ corresponding to minimal control effort within the constraints circle is obtained. If $J_{g_{in}} \leq J_{g_{bd}}$, then $u_{gx}(0)$ and $u_{gy}(0)$, corresponding to $J_{g_{in}}$ are optimal. Otherwise, these values are used as an initial guess and solved using the Armijo gradient descent rule to obtain the optimal control input [14]. To test the control feasibility of the UAV and target, their cost functions were compared by simulating a sample scenario of the UAV and target engagement and their cost and constraints. Fig. 3.6 shows the cost function contours, constraints, and the corresponding control inputs for the UAV and the target for a sample scenario. The plot shows that the UAV and target control limits lie within the feasible control space and control algorithms are implementable.

The contour plot is used to visualise and analyse the optimal control trajectory. It signifies the optimal control trajectory for the UAV in tracking the manoeuvring target and shows the cost values for different values of the state and control variables [330, 331]. The contour lines indicate the optimal trajectory is the one that minimises the maximum possible cost over all possible target trajectories and can be found by tracing the minimum cost path on the contour plot. In Fig. 3.6, the cost functions of the tracking UAV and the evasive target are plotted by overlaying the two cost functions in the same contour plot. The resulting contour plot shows the trade-off between the control objectives of the UAV and the target. As indicated contour plot legend, the lines and map colours represent the values of the cost function at different points in the control space. The contours are closer together in areas of high cost, and farther apart in areas of low cost. The intersection of the two cost function contour plots represents the set of control inputs that achieve a balance between the control objectives of the UAV and the target. This shows the control inputs are for both the UAV and the target, allowing the UAV to track the target while the target attempts to evade the UAV.

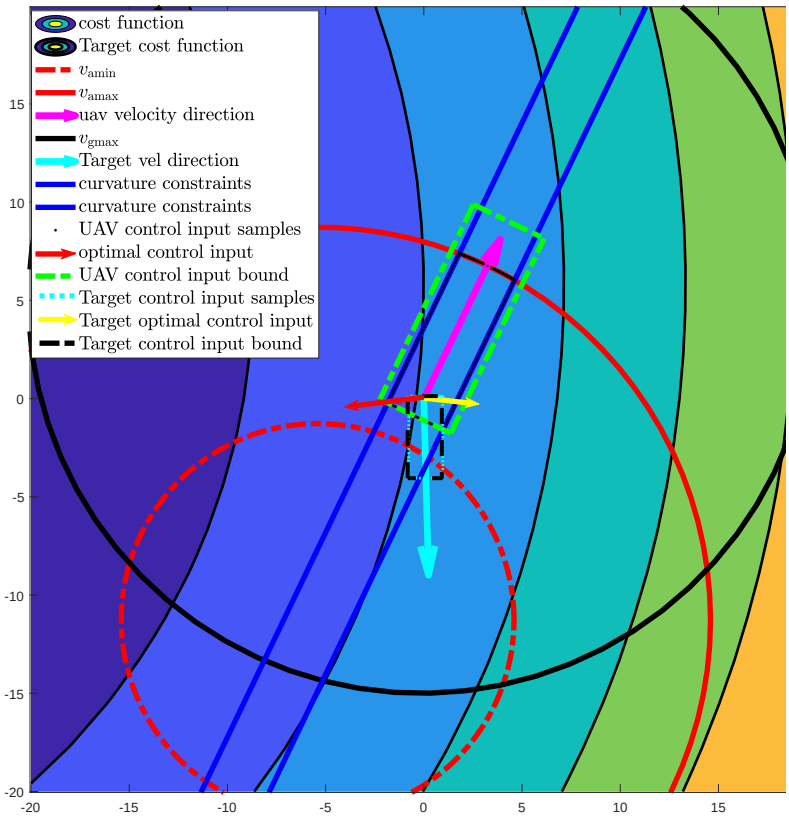

Fig. 3.6 Optimal control inputs and cost function contours for UAV minimisation and target maximisation

The position of the contours in the contour plot also affects the control vectors of the UAV and the target. When the contours of the UAV's cost function are farther away from the origin, it implies that the cost of the control inputs is higher, and the UAV needs more aggressive manoeuvres to track the evasive target. Conversely, when the target cost contours are closer to the origin, it indicates the target is more vulnerable to being tracked, and the UAV needs to execute less aggressive manoeuvres. When the contours of the two cost functions intersect at a point where both costs are high, it indicates that both the UAV and the target are in a highly disadvantageous position, and the control inputs need to be adjusted to improve the situation. However, if the contours of the two cost functions intersect at a point where both are low, this implies that both UAV and target are in a highly

advantageous position, and the control inputs can be maintained.

The pseudocode explaining the main step in the target evasion algorithm is presented in a summarised format in Algorithm 1. It begins by initialising various parameters and constraints for the UAV and the target. These parameters include time intervals Δt, maximum and minimum velocity limits and, minimum turn radius for the target $r_{g_{\min}}$. Conditional checks are performed to ensure that the UAV's velocity and acceleration stay within specified limits. If these limits are exceeded, the algorithm adjusts the bounds to ensure they comply with the constraints, which involves modifying the acceleration bounds. The algorithm samples point along the constraint boundary and calculate the cost for each sample to obtain optimal control input for the target evasion corresponding to the minimum cost, $J^*_{\text{g-bd}}$. Similarly, it samples points inside the boundary of the constraints and calculates the cost for those samples to find the optimal control input corresponding to the minimum cost, $J^*_{\text{g-in}}$.

A decision point is reached to compare $J^*_{\text{g-bd}}$ with $J^*_{\text{g-in}}$. If $J^*_{\text{g-bd}}$ is less than or equal to $J^*_{\text{g-in}}$, it means that the optimal control inputs for the boundary samples are sufficient, and the algorithm selects $a_{gx}(0)$ and $a_{gy}(0)$ corresponding to $J^*_{\text{g-bd}}$ as the optimal controls. However, if $J^*_{\text{g-bd}}$ is greater than $J^*_{\text{g-in}}$, the algorithm proceeds to a minimisation step. It takes $a_{gx}(0)$ and $a_{gy}(0)$ corresponding to $J^*_{\text{g-in}}$ as an initial guess for the minimisation of the objective function and uses the gradient descent method with Armijo's rule to solve the optimisation problem. The gradient descent approach is applied in conjunction with Armijo's rule to solve the minimisation inside the cost function constraint of the boundary. Armijo's rule establishes direction by modifying the search variables α_{amj}.

Algorithm 1 Optimal Target Evasion Control

Initialise the prediction interval and the UAV/target constraints: $\Delta t, v_{g\max}, v_{g\min}, a_{x_{g\max}}, a_{x_{g\min}}, a_{y_{g\max}}, a_{y_{g\min}}, r_{g\min}, v_{a\max}$
Set the initial position/velocity of UAV and the target position: $x_g(0), y_g(0), v_{gx}(0), v_{gy}(0), x_a(0), y_a(0)$
Calculate $v_g(0) = \sqrt{v_{gx}(0)^2 + v_{gy}(0)^2}$
if $\frac{v_g(0)}{\Delta t} + a_{x_{g\max}} > \frac{v_{g\max}}{\Delta t}$ **then**
    Replace $a_{gx\max}$ bound by the arc given by the larger circle intersecting with the control constraint box
end if
if $\frac{v_g(0)}{\Delta t} + a_{x_{g\min}} < \frac{v_{g\min}}{\Delta t}$ **then**
    Replace $a_{gx\min}$ bound by the arc given by the smaller circle intersecting with the control constraint box
end if
Sample points along the boundary of the constraints and calculate the cost for the samples; Find the optimal control corresponding to the minimum cost, $J^*_{\text{g-bd}}$, among the samples
Sample points inside the boundary of the constraints and calculate the cost for the samples; Find the optimal control corresponding to the minimum cost, $J^*_{\text{g-in}}$, among the samples
if $J^*_{\text{g-bd}} \leq J^*_{\text{g-in}}$ **then**
    $a_{gx}(0)$ and $a_{gy}(0)$ corresponding to $J^*_{\text{g-bd}}$ are optimal
else
    Let $a_{gx}(0)$ and $a_{gy}(0)$ corresponding to $J^*_{\text{g-in}}$ be the initial guess of the minimisation of the objective function. Solve the optimisation using the gradient descent method with Armijo's rule to modify search variables α_{amj}.
end if

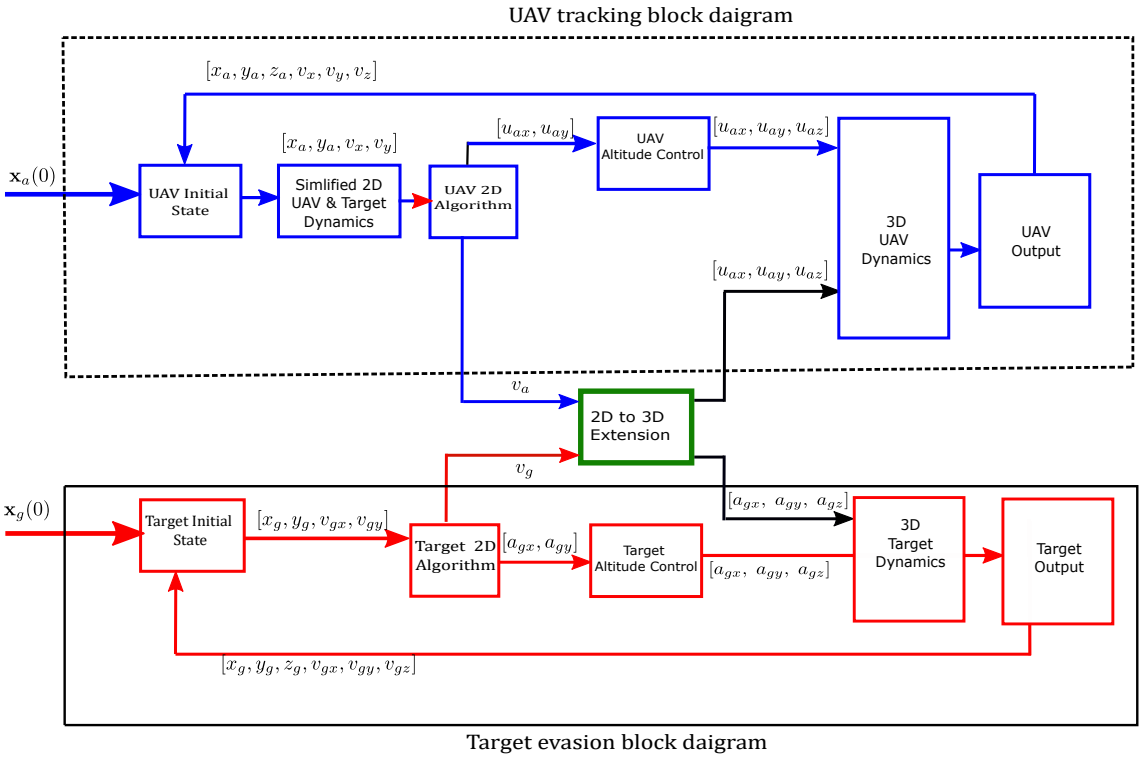

Fig. 3.7 UAV tracking and target evasion block daigram

3.4 Extension to 3D Scenario

3.4.1 2D to 3D related research

A few research literature on UAV tracking extension from 2D to 3D is presented. Mellinger et al. [332] and [333] implemented a 2D to 3D algorithm extension by estimating future points on a 2D tracking trajectory, closest to the current position at each time instant. Then a unit tangent vector of the trajectory and the desired velocity vector was derived to compute the position and velocity errors needed to calculate the commanded acceleration, using PD feedback of the position and velocity errors. In a related research, [334] developed a UAV path generation and tracking algorithm, by extending a 2D Dubins suboptimal tracking algorithm to 3D, using empirical calculations. An optimal 2D path was generated on the xy-plane and the path length within a short time interval was used to compute command output for 3D path tracking. A similar extension from 2D to 3D motion planning algorithm was implemented by [335], by developing a new planning heuristic algorithm for fixed-wing UAVs using the shortest path on 2D Dubins curves, and precomputed sets of motion primitives derived from the vehicle dynamics model. An autonomous navigation 3D algorithm was also developed for an unmanned helicopter using a 2D extension of reactive fuzzy sensor data-based navigation [336]. The simple 2-D navigation subsystems simultaneously combine the desired flying direction based on seven 2D subsystems to form a 3-D solution space that is suitable for UAV tracking motion.

In [337], a 3D Path tracking algorithm for a UAV operating in a cluttered environment was developed by mapping a path smoothing algorithm using consecutive triplets of waypoints in a homogeneous coordinate transformation to a 2D plane. A previously developed 2D path smoothing algorithm was then applied and the generated command output in the 2D plane mapped back into 3D space. Similarly, a 2D Dubins path algorithm was extended to 3D path tracking by incorporating a flight-path angle constrained by the physical limit of the path-tracking UAV [338]. The reviewed literature all focused on 2D to 3D extension for UAV path planning or trajectory optimisation without mention of ground or aerial targets. This gap is addressed in this section by developing a 2D to 3D algorithm extension that takes the tracking UAV and evasive target into consideration.

3.4.2 Application of 2D to 3D extension in target tracking algorithm

The extension of UAV tracking from 2D to 3D has significant implications and applications. Some of them include:

- Application of UAV tracking in various scenarios beyond the initial 2D context.
- Mapping the 2D solution to a 3D context provides a practical approach to solving tracking problems in three-dimensional space, especially when analytical solutions in 3D are not feasible [337].
- Leveraging existing numerically attractive, well-established, and proven 2D navigation methods allows for the simulation of 3D scenarios [336] and the development of solutions in the 3D domain.

These implications and applications highlight the importance and benefits of extending UAV tracking from 2D to 3D, opening up new possibilities and opportunities in the field of UAV navigation and tracking. Given the aforementioned benefits, the 2D target tracking in [14] is extended for 3D tracking scenarios. Considering the UAV and target velocity vectors $\mathbf{v}_a$ and $\mathbf{v}_g$ as shown in Fig. 3.8, if the two vectors are parallel, the angle between them is zero and can not be used for a vector transformation. However, if we assume that the vectors are never parallel, then the angle between the two vectors can be defined as θ_{ag} and used in the formulation of a direction cosine matrix for our transformation.

We establish an instantaneous moving frame, x_m-y_m with the unit vector in x_m-axis, aligned to the target velocity vector $\mathbf{v}_g$ while the unit vector towards $\mathbf{z}_m$-axis is orthogonal to the plane formed by the cross product, $\mathbf{v}_g \times \mathbf{v}_a$ as follows:

$$\mathbf{x}_m = \frac{\mathbf{v}_g}{\|\mathbf{v}_g\|}, \quad \mathbf{z}_m = \frac{\mathbf{v}_a \times \mathbf{v}_g}{\|\mathbf{v}_a \times \mathbf{v}_g\|} \tag{3.24}$$

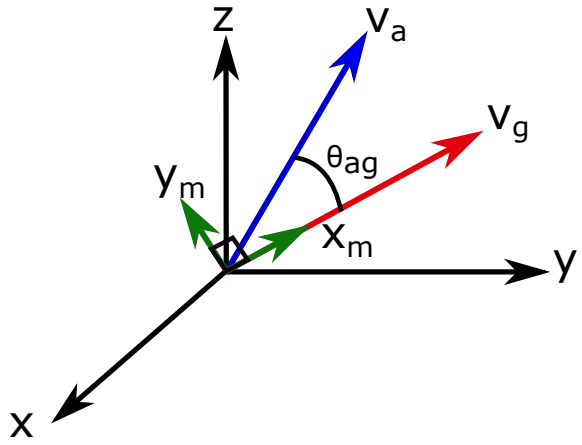

Fig. 3.8 2D to 3D vector transformation diagram

The unit vector $\mathbf{y}_m$ is equal to $\mathbf{z}_m \times \mathbf{x}_m$. The direction cosine matrix, D_{Rm}, transforming the vectors in the moving frame to the reference frame is given by:

$$D_{Rm} = \begin{bmatrix} \mathbf{x}_m^R & \mathbf{y}_m^R & \mathbf{z}_m^R \end{bmatrix} \tag{3.25}$$

where $\mathbf{x}_m^R$, $\mathbf{y}_m^R$ and $\mathbf{z}_m^R$ are the moving frame unit vectors expressed in the reference frame and D_{Rm} is the orthonormal matrix satisfying $D_{Rm}D_{Rm}^T = I_3$, i.e., $D_{mR} = D_{Rm}^T$.

The target tracking control input in the moving frame is the same algorithm solution as the 2D tracking problem. Once the 2D algorithm calculates the optimal tracking control input in the moving frame, the following equation maps the 2D control input into the 3D space.

$$\mathbf{u}_a = D_{Rm}\mathbf{u}_a^m \tag{3.26}$$

where $\mathbf{u}_a$ is the UAV global frame acceleration in 3D and $\mathbf{u}_a^m$ is the UAV tracking command in 2D body frame expressed in the moving frame. The control output for z-axis generated from the mapping of the 2d control input to 3D needs to be constrained to enable the UAV to maintain a desired altitude above the target. A pseudo-code detailing the 2D to 3D extension is summarised in Algorithm 2.

Algorithm 2 2D TO 3D Algorithm

Require: 2D current position, velocity of UAV and target

1: **for** Every time step **do**
2: Obtain the control input $\mathbf{u}_a^m = [u_{ax}^B \;\; u_{ay}^B \;\; 0]$
3: Compute transformation $D_{Rm} = \begin{bmatrix} \mathbf{x}_m^R & \mathbf{y}_m^R & \mathbf{z}_m^R \end{bmatrix}$
4: Convert 2D control to 3D frame $\mathbf{u}_a^R = D_{Rm}\mathbf{u}_a^m$
5: Perform UAV & target manoeuvre in 3D
6: **end for**

In 3D space, the target can manoeuvre in any direction, including upwards and downwards. To ensure the UAV is able to track and keep the target within its FOV, the assumption used for the 2D case that the UAV always operates at an optimal altitude no longer holds. Depending on the UAV camera resolution and cloud base, the UAV cannot operate above a certain altitude ceiling. Similarly, due to obstacles in the operating environment, the UAV's altitude must exceed some threshold above the target. As a result, the UAV must be restricted to operating within an upper and lower optimal altitude band. Altitude control was implemented in Chapter 4.

3.5 Simulations and Results

To simulate the tracking capability of our algorithm against various target scenarios, we first assess the effect of modifying the control using bank angle and turn rate constraints. Relying on the assumption that the UAV can detect and estimate the position of the target, we implement 3 scenarios. In the first scenario, the target is unaware it is being tracked and is moving at a constant speed. In the second scenario, the UAV is tracking a target that is aware it is being tracked and initiates a predefined zig-zag manoeuvre to escape the tracking UAV. In the third scenario, the target is fully aware it is being tracked and is also intelligently evading, having information about the UAV's position, velocity, and estimated acceleration. These simulation results for the scenarios highlighted are presented in the following subsections.

3.5.1 Bank angle and turn rate constraint assessment

We implemented a scenario to track a manoeuvring target using a UAV algorithm without bank angle and turn rate constraints and another UAV with the modified control. The UAVs were initiated at the same initial position $\mathbf{x}_a = [0,\ 0,\ 0]$, and the target commenced manoeuvre from position $\mathbf{x}_g = [500,\ 60,\ 0]$. A UAV minimum turn radius of $r_{\min} = 100$, and velocity limits of $v_{a_{\min}} = 10$m/s and $v_{a_{\max}} = 15$m/s is used in this scenario while the

respective minimum and maximum acceleration limits of the UAV along x, y, and z axes are as follows:

$$u_{ax_{\min}} = -2\ [\text{m/s}^2],\ u_{ax_{\max}} = 4\ [\text{m/s}^2],$$
$$u_{ay_{\min}} = -3\ [\text{m/s}^2]\ , u_{ay_{\max}} = 3\ [\text{m/s}^2],$$
$$u_{az_{\min}} = -0.5\ [\text{m/s}^2],\ u_{az_{\max}} = 0.5\ [\text{m/s}^2]$$

In this scenario, the maximum target velocity of $v_{g_{\max}} = 10$m/s, and the tracking and evasion scenario is simulated for 100s. The control input magnitude limits of the target are as follows:

$$a_{gx_{\min}} = 0\ [\text{m/s}^2],\ a_{gx_{\max}} = 0\ [\text{m/s}^2],$$
$$a_{gy_{\min}} = 0\ [\text{m/s}^2],\ a_{gy_{\max}} = 0\ [\text{m/s}^2],$$
$$a_{gz_{\min}} = 0\ [\text{m/s}^2],\ a_{gz_{\max}} = 0\ [\text{m/s}^2]$$

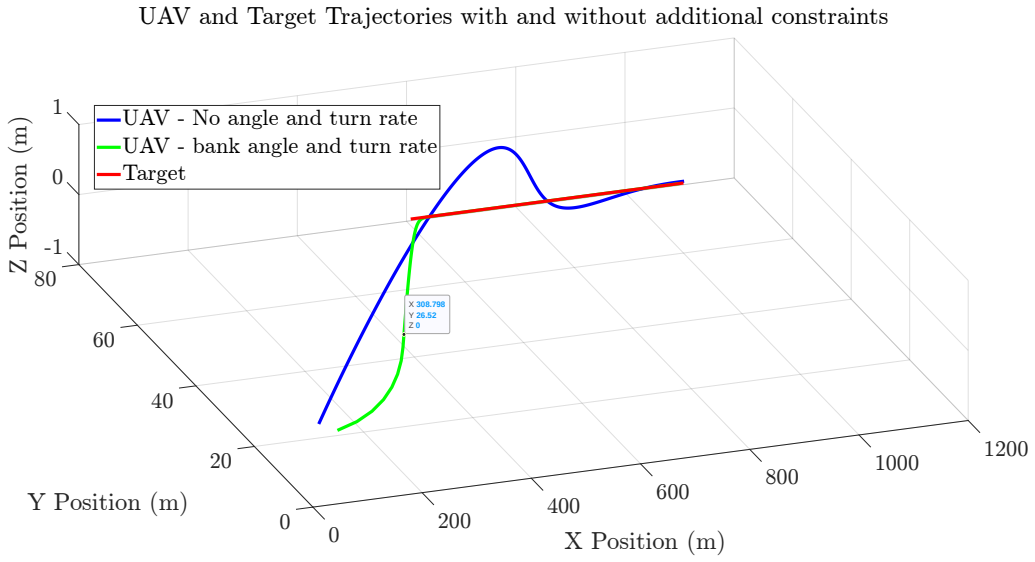

Fig. 3.9 UAV and target trajectories with and without additional constraints

As shown in Figure 3.9, both UAVs can track the target, closing up and keeping the target within their FOVs for the entire duration of the simulation. Their trajectories are almost identical except for the responses to sharp target manoeuvres. This shows that the constraints restricted the second UAV from taking very sharp manoeuvres in response to target evasion. This is a useful safety consideration as rapid turns at high speed could lead to wear and tear, causing mechanical damage to the control surfaces and actuators in live tracking situations.

3.5.2 Non-manoeuvring target

In the first scenario, we implement a constant velocity target to observe how the UAV tracks the target moving in a straight line. The UAV is initiated at position $\mathbf{x}_a = [4000,\ 1000,\ 500]$, while the target initiated at $\mathbf{x}_g = [0,\ 0,\ 50]$. The UAV minimum turn radius, $r_{\min}$, is set at 100m with the velocity limits of $v_{a_{\min}} = 10$m/s and $v_{a_{\max}} = 20$m/s, while the respective minimum and maximum acceleration limits of the UAV along x, y, and z axes are as follows:

$$
\begin{aligned}
u_{ax_{\min}} &= -5\ [\text{m/s}^2],\ u_{ax_{\max}} = 6\ [\text{m/s}^2],\\
u_{ay_{\min}} &= -5\ [\text{m/s}^2]\ , u_{ay_{\max}} = 5\ [\text{m/s}^2],\\
u_{az_{\min}} &= -0.5\ [\text{m/s}^2],\ u_{az_{\max}} = 0.5\ [\text{m/s}^2]
\end{aligned}
$$

The target velocity limits are set to $v_{g_{\max}} = 10.7m/s$, while its respective acceleration was constrained to zero, with the target essentially moving at constant velocity. The simulation was run for $100s$

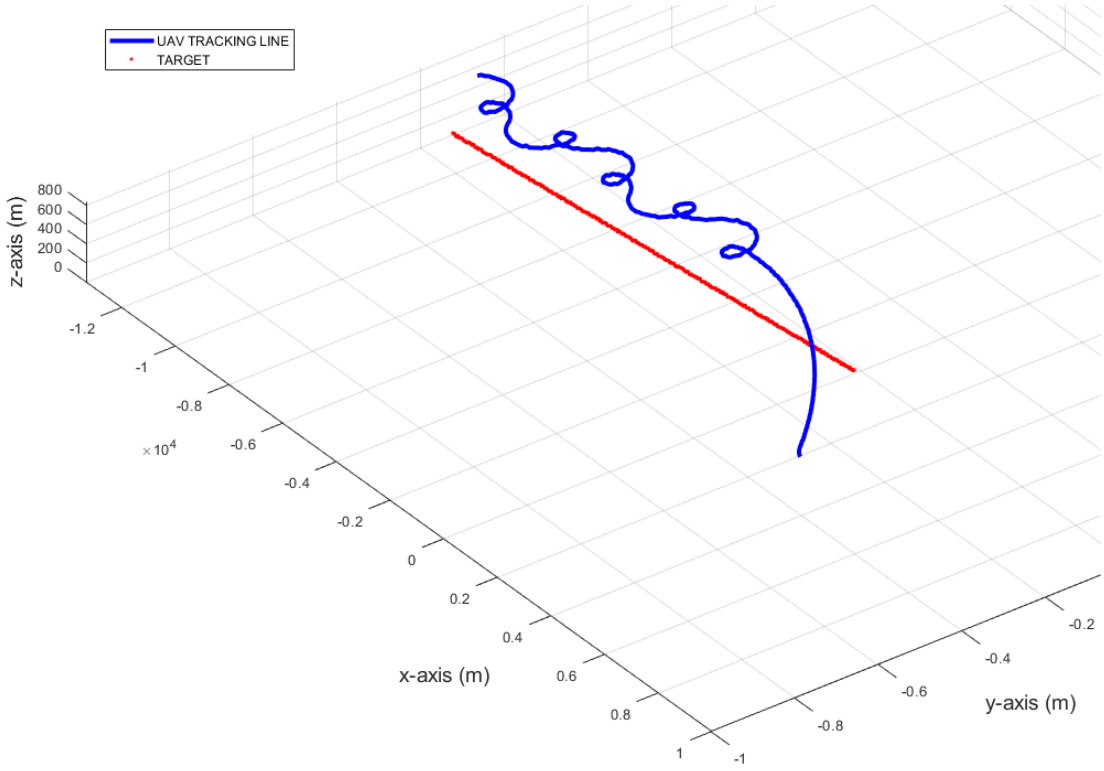

Fig. 3.10 3D plot of UAV tracking a smart manoeuvring target

As shown in 3.10, for a straight-line target, the UAV follows a trajectory that ensures it is kept within a favourable tracking distance throughout the tracking scenario. Due to the small turn radius constraint on the UAV, it was able to follow the tight circular path,

preventing it from outrunning the target and ensuring that it was kept within its camera FOV.

3.5.3 Simple manoeuvring target

To simulate the UAV tracking performance when tracking a target that manoeuvres in predefined paths, we implemented a scenario where the target can accelerate while following a somewhat zig-zag path. The UAV and target are initiated at positions $\mathbf{x}_a = [200,\ 200,\ 500]$ and $\mathbf{x}_g = [0,\ 0,\ 50]$ respectively. The UAV minimum turn radius was adjusted to, $r_{\min}$, is set at 200m to see how its trajectory is affected and the velocity limits are set to $v_{a_{\min}} = 10$m/s and $v_{a_{\max}} = 20$m/s. The UAV respective minimum and maximum acceleration limits of the UAV along x, y, and z axes are set to:

$$
\begin{aligned}
u_{ax_{\min}} &= -10\ [\text{m/s}^2],\ u_{ax_{\max}} = 8\ [\text{m/s}^2],\\
u_{ay_{\min}} &= -4\ [\text{m/s}^2]\ , u_{ay_{\max}} = 4\ [\text{m/s}^2],\\
u_{az_{\min}} &= -0.2\ [\text{m/s}^2],\ u_{az_{\max}} = 0.5\ [\text{m/s}^2]
\end{aligned}
$$

Similarly, the target velocity limits is set to $v_{g_{\max}} = 12.5m/s$, while its respective acceleration limits along x, y,and z axes are as follows:

$$
\begin{aligned}
a_{gx_{\min}} &= -4\ [\text{m/s}^2],\ a_{gx_{\max}} = 6\ [\text{m/s}^2],\\
a_{gy_{\min}} &= -4\ [\text{m/s}^2],\ a_{gy_{\max}} = 6\ [\text{m/s}^2],\\
a_{gz_{\min}} &= -0.4\ [\text{m/s}^2],\ a_{gz_{\max}} = 0.4\ [\text{m/s}^2]
\end{aligned}
$$

similar to the constant target velocity scenario above, the simulation was run for $100secs$.

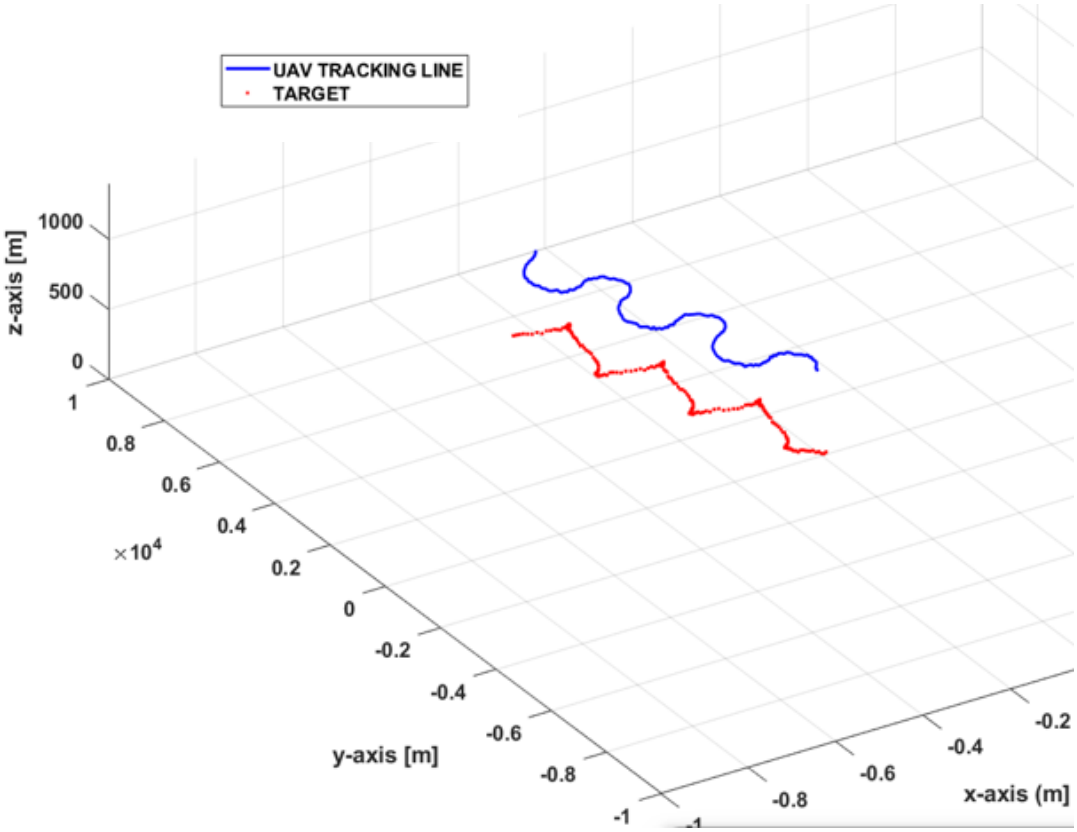

Fig. 3.11 3D plot of UAV tracking target following a manoeuvring pattern

As shown in 3.11, when the UAV tracks a target manoeuvring in a simple pattern, it follows a trajectory that enables it to keep the target within tracking proximity. In this case, the UAV executed a sinusoidal trajectory pattern, autonomously adjusting its acceleration and velocity within its control bounds to keep the target within its camera FOV. The UAV trajectory is also affected by the increased turn radius constraint which enables the UAV to follow a less restrictive trajectory path.

3.5.4 3D evasive target

The UAV minimum turn radius, $r_{\min}$, is set at 400m with the velocity limits of $v_{a_{\min}} = 20$m/s and $v_{a_{\max}} = 40$m/s. Similarly, the respective minimum and maximum acceleration limits of the UAV along x, y, and z axes are as follows:

$$
\begin{aligned}
u_{ax_{\min}} &= -10\ [\mathrm{m/s^2}],\ u_{ax_{\max}} = 8\ [\mathrm{m/s^2}],\\
u_{ay_{\min}} &= -4\ [\mathrm{m/s^2}]\ , u_{ay_{\max}} = 4\ [\mathrm{m/s^2}],\\
u_{az_{\min}} &= -0.2\ [\mathrm{m/s^2}],\ u_{az_{\max}} = 0.5\ [\mathrm{m/s^2}]
\end{aligned}
$$

The target velocity limits is set to $v_{g_{\max}} = 16.7m/s$, while its respective acceleration limits along x, y,and z axes are as follows:

$$a_{gx_{\min}} = -2\ [\text{m/s}^2],\ a_{gx_{\max}} = 4\ [\text{m/s}^2],$$
$$a_{gy_{\min}} = -2\ [\text{m/s}^2],\ a_{gy_{\max}} = 2\ [\text{m/s}^2],$$
$$a_{gz_{\min}} = -0.2\ [\text{m/s}^2],\ a_{gz_{\max}} = 0.4\ [\text{m/s}^2]$$

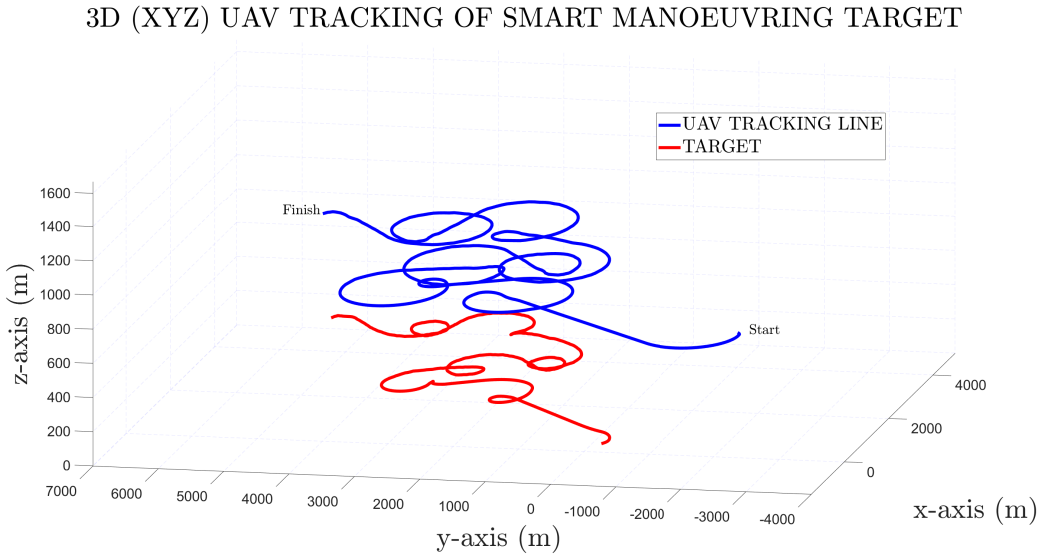

Fig. 3.12 3D plot of UAV tracking a persistently evading target

The initial UAV position is set to (2000m, -2000m, 500m) while the initial target position is set to (50m,-50m, 50m) in x-y-z respectively. As shown in Fig. 3.12, the UAV and target manoeuvre trajectory indicate that the UAV responds to the target's evasive manoeuvres. The target performs an evasive manoeuvre when the UAV closes up to its location. Then, the evasive manoeuvre results in a corresponding change in the velocity and position of the UAV. When the target moves in a straight line, the UAV manoeuvre ensures the target is kept within a favourable tracking distance.

Comparing the x, y and z positions with the corresponding control input responses of the UAV and target for various engagement scenarios, we observe that the increase or decrease of the acceleration in response to manoeuvres by the other vehicle as shown in Figs. 3.13a, 3.14a and 3.15a. Sharp spikes resulting from sudden evasive target manoeuvres and a corresponding increase in UAV acceleration to close up with the target are shown in the figure. These abrupt UAV manoeuvres are restricted by the turn rate and bank angle constraints.

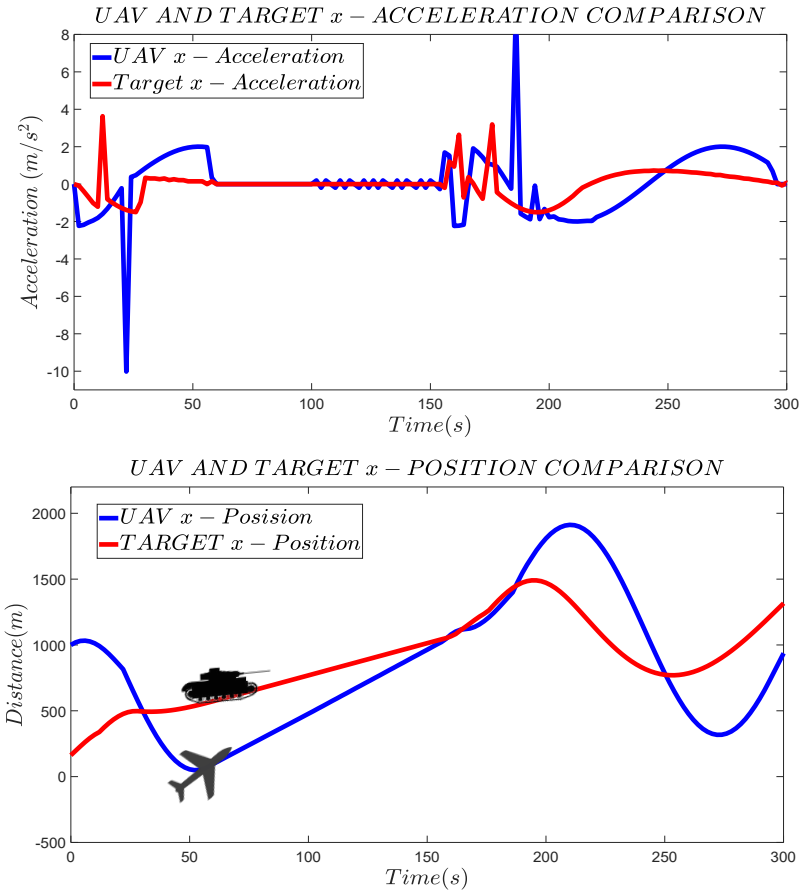

(a) x-direction accelerations & positions

Fig. 3.13 UAV and target accelerations & positions - X direction

A closer look at a sample plot comparing the UAV and target position, velocity, and acceleration as shown in 3.16 indicates that the direction of the target control input spike is in sync with the direction of its velocity and position. A similar pattern is also observed when the UAV responds with the direction of the control input spike corresponding to the velocity and position turns. We also observed that the response time of the UAV to the target manoeuvre is dependent on the time interval of the evasive manoeuvre. The plot shows that when the target executes a sharp turn, the response time from the UAV is short to enable the UAV to close up to the target. However, when the target executes a slow manoeuvre, the response from the UAV was also slower. This implies that the UAV algorithm adjusts its control input and velocity to ensure the target is kept within a favourable distance throughout the tracking scenario.

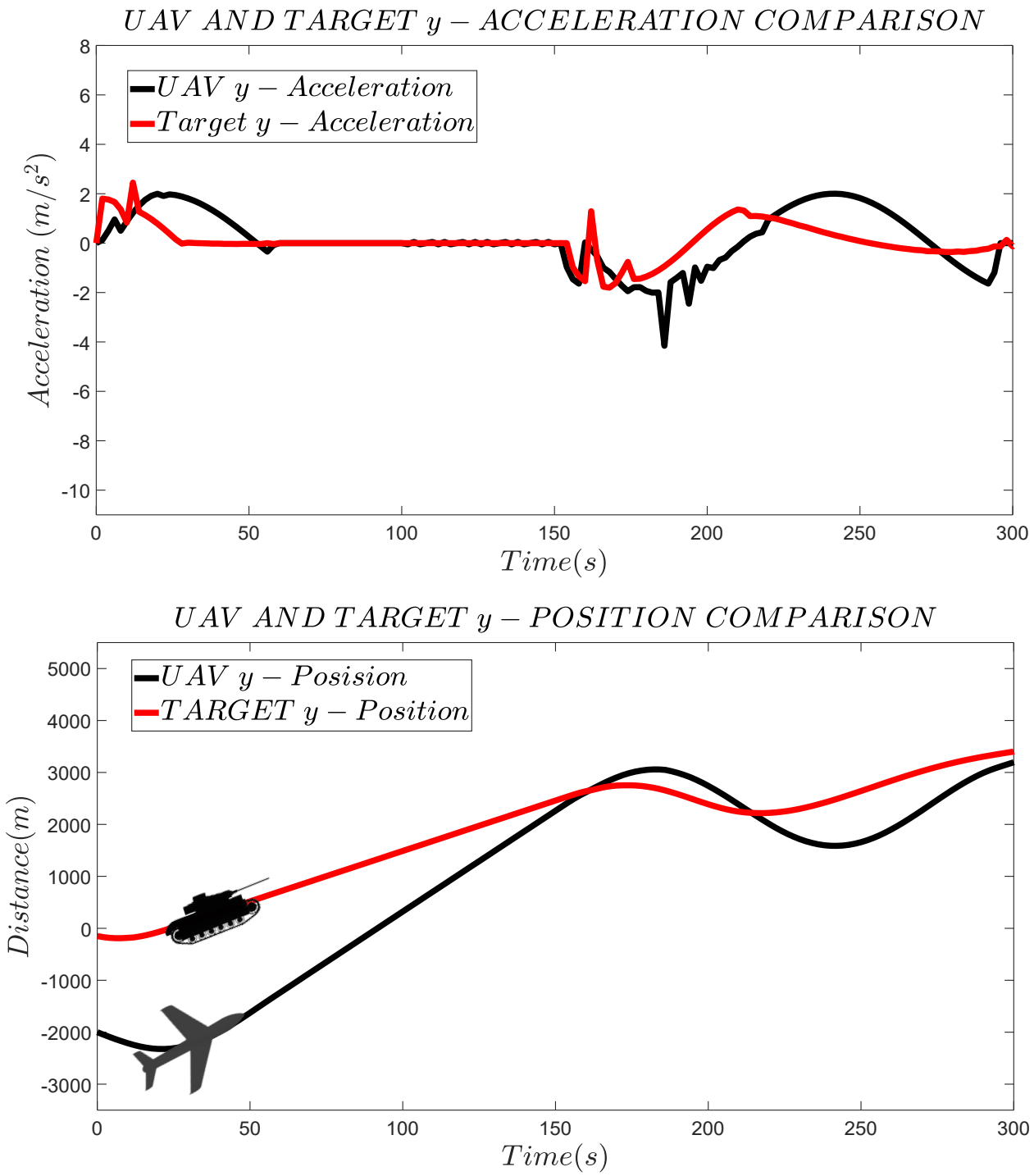

(a) *y*-direction accelerations & positions

Fig. 3.14 UAV and target accelerations & positions - Y direction

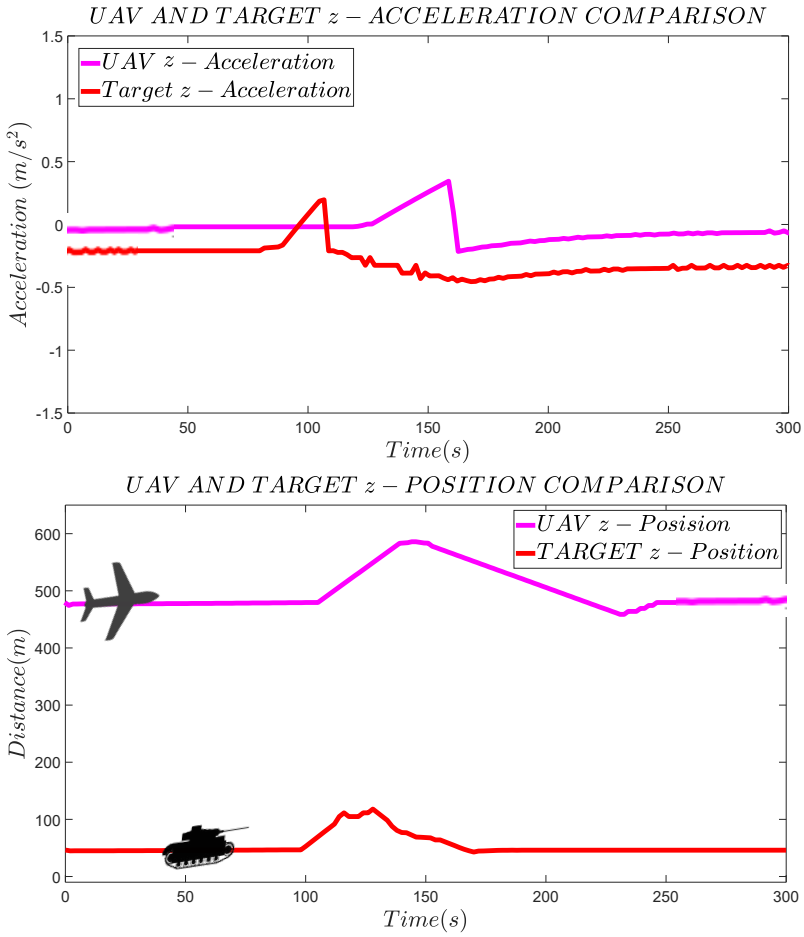

(a) z-direction accelerations & positions

Fig. 3.15 UAV and target accelerations & positions - Z direction

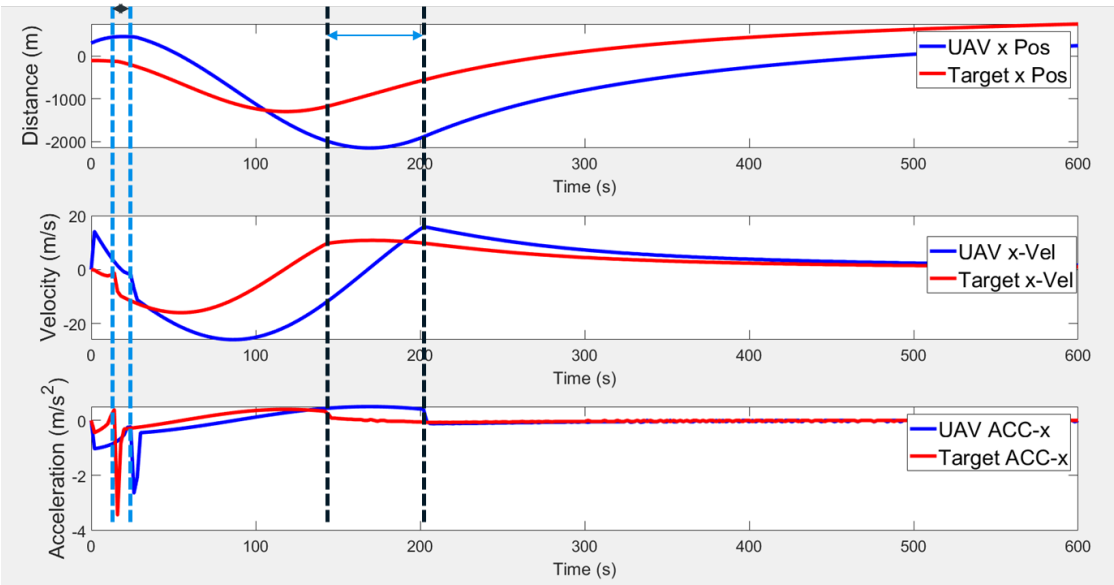

Fig. 3.16 Comparison of UAV and target position, velocity and acceleration for a sample scenario

3.6 Summary

This Chapter provides a fixed-wing UAV optimal target tracking strategy with the minimum turn radius varying with the bank angle, which enables the generation of realistic tracking paths for the tracking UAV. The UAV control is based on a 2 step predictive min-max cost function where the UAV tries to persistently minimise its relative distance to the track a target that is assumed to be evading with its best control effort within the limits of the design constraints. In addition to the UAV control, we developed an evasive target control strategy by maximising the same cost function, which produces smart evasive manoeuvres for the target. The evasion cost function is designed is to continuously evade the UAV which assumed to be optimally tracking the target. Both the dynamics of the UAV and target are mathematically modelled and constrained to operate within allowable limits of the tracking and evasion scenarios. We also extended the 2D target tracking algorithm to 3D cases using a vector transformation and direction cosine matrix derived from the UAV and the target instantaneous velocity vectors. The 2D to 3D extension enables the utilisation of the 2D algorithm for 3D scenarios while avoiding the complexity of implementing a new design and fills a gap in the evasive target-tracking literature. The simulation results obtained show that the UAV persistently tracked the evading target in various combinations of scenarios and mission configurations.

Considering the importance of UAV vertical control with variation in target altitude in an aerial pursuit, Chapter 4 implements various options for altitude control that can be applied to the control strategy presented for the UAV and target in this Chapter. This research was extended in Chapter 5 by the implementation of evasive quadrotor target tracking. In Chapter 6, we implemented a strategy for cooperative tracking evasion using multiple UAVs while considering the effect of sensor noise as well as collision avoidance between the UAVs and the target.

Chapter 4

UAV Altitude Control

4.1 Introduction

In Chapter 3, we implemented an algorithm for tracking UAVs and a target evasion strategy. We also developed a vector transformation algorithm to extend a 2D target tracking engagement to a 3D scenario. The limitation of the 3D extension algorithm is that it is dependent on the target vector, implying that the UAV is not able to execute independent vertical manoeuvres. We consider that there may be scenarios where the UAV is required to execute independent vertical manoeuvres to adjust altitude and observation angle without utilising the target parameters. In such situations, an independent vertical control algorithm for the UAV becomes valuable. In this Chapter, we develop vertical control algorithms that can be used with the 2D target tracking strategy presented in Chapter 3 for executing a target tracking mission in 3D. To provide some background on fixed-wing vertical control strategies, we review some related literature. Before that, we will quickly notify the reader that, the terminologies vertical control and altitude control mean the same thing in this thesis and are used interchangeably.

4.1.1 Altitude control-related work

Treil et al. [339] developed a vertical control law based on GPS data for target tracking using a VTOL UAV which showed effective performance during simulation. However, the dependency on GPS data limits the control versatility especially when such data is not available. Similarly, [340] implemented a constant velocity vertical control command for landing a MAV on a target platform. This type of control however is not sufficient for dynamic targets that move or manoeuvre frequently. By decomposing UAV control into vertical and horizontal movements, [341] developed an altitude control strategy that uses visual guidance for network recovery. The vertical controller enables the fixed-wing

UAV to adjust its pitch angle to attain and maintain a desired stable altitude, by processing vision system information to generate control signals. The vertical control combines a reference model-based adaptive controller with a set of feed-forward dynamics for the UAV movement. In a similar study, [342] designed a fixed-wing UAV vertical controller that includes a forward and a vertical motion subsystem, using a neural network model that compensates for external uncertain perturbations and an adaptive sliding mode controller for fault-tolerant control. In [343, 344], they implemented a hybrid MPC vertical controller that reduces a fixed-wing UAV sink rate in proportion to the altitude. The UAV autopilot decouples the longitudinal and vertical control, by assuming that thrust and pitch controls are appropriately tuned to give suitable response signals. Li et al. [345], also designed an MPC-based vertical controller to hold UAV at constant altitude using a target zero pitch angle. However, the main focus of the aforementioned vertical controllers was either on vertical descent, maintaining a fixed altitude, or landing the UAV. A more robust vertical control strategy will be needed for UAV evasive target tracking.

In another related research, [346] designed an altitude control strategy that uses PI control law to eliminate static error and maintain the desired altitude of a ground target tracking UAV. The control law uses velocity feedback to calibrate pitch angle, enabling UAV altitude control. Bao et al.[347] also developed a variable-structure controller with multiple algorithm fusion that combines the backstepping sliding mode and adaptive controls for UAV altitude regulation within a holding area. A PID controller uses the target altitude to compute the required pitch angle which is then calibrated by adaptive backstepping sliding mode law. The pitch angle is continuously fed to the hybrid PID control and adaptive sliding mode controller to adjust the UAV altitude. When the UAV exceeds the upper limit, the coupled altitude controller trims the UAV pitch angle and speed until it reaches within allowable altitude limits. While the above literature research addresses the desired control outcome in the current research, it is dependent on preset variables and does not consider target altitude.

Despite the various research on fixed-wing UAV controls, there is no literature addressing altitude control for fixed-wing tracking of smart evasive ground or aerial targets. This gap is particularly important, given the complex and unpredictable nature of real-world scenarios, where targets could employ sophisticated evasion tactics, including rapid or meandering altitude changes, to avoid detection or interception. Consequently, there is a pressing need for in-depth studies for autonomously adjusting UAV altitude in response to both target evasion and altitude fluctuations. Addressing this gap holds great potential for enhancing the effectiveness of UAV-based target tracking systems across various domains such as military surveillance, law enforcement, and search and rescue operations. This Chapter

therefore addresses the highlighted literature limitation by designing a vertical control law that can be used in conjunction with longitudinal and lateral control to autonomously regulate UAV altitude based on target behaviour.

4.1.2 Contributions

The main contributions of this Chapter are as follows

- An altitude control law that uses the relationship between the desired altitude above the target, and the velocity vector in the 2D plane to compute the FPA for control of the vertical movement of the UAV is developed.
- A UAV altitude control that uses the relationship between the actual and projected size of the target image on the tracking camera plane is designed to automatically determine and adjust the altitude of the tracking optimal UAV.

The remaining part of this Chapter is outlined as follows. Section 4.2 presents UAV control using flight path angle. In section 4.3, a method of controlling the UAV altitude using target actual and image size is presented. The altitude control simulation results for the various controller options are presented and discussed in section 4.3 while section 4.5 summarises the main points presented in the Chapter.

4.2 UAV Altitude Control Using Flight Path Angle

Consider a scenario where a fixed-wing UAV is tracking a ground target that operates on an undulating terrain. If the UAV is to maintain an optimal altitude above the target at all times, it needs to be capable of adjusting its altitude in response to changes in target altitude. In addition, the UAV would need to operate within an altitude band within which its camera can effectively capture the target. The scenario is depicted in Fig. 4.1 where z_a is the UAV current altitude, z_g is the target altitude, and z_d is the desired UAV altitude. The optimal altitude band can be defined as vertical space between $z_d - h$ and $z_d + h$, where h is an altitude value determined by the camera focal length.

To design a vertical control law for a fixed UAV tracking an evasive ground target, a variety of methods could be applied. However, we assume that the only information available to us is UAV tracking variables in the 2D plane. Accordingly, we designed a vertical control law to automatically adjust the UAV altitude using the FPA represented by σ_a. The UAV σ_a is the angle between the UAV's velocity vector and the horizontal plane, which determines the UAV's climb or descent rate and is essential for maintaining a desired altitude. Other important angles to consider in relation to the FPA, are the Angle of Attack (AoA) and the pitch angle θ_{pa}. The AoA is the angle between the oncoming air

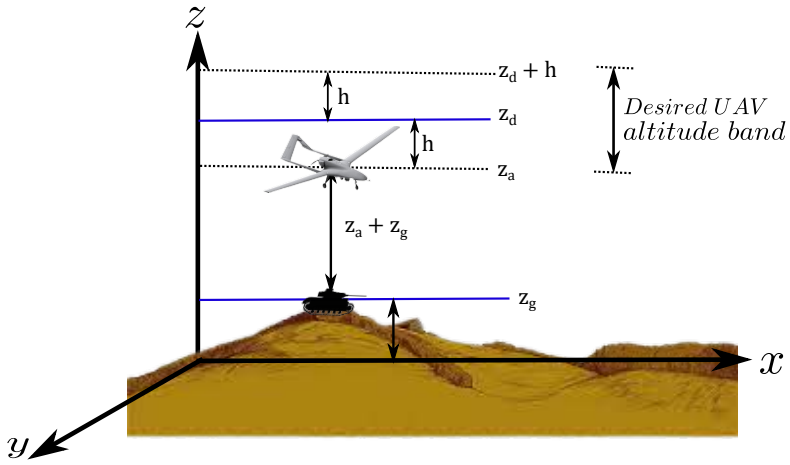

Fig. 4.1 UAV altitude constraint diagram

and the aircraft's longitudinal axis while the pitch angle is the angle between the aircraft's longitudinal axis and the horizon. As shown in Fig. 4.2a, the FPA, AoA, and pitch angles are related by the formula $\theta_{pa} = \sigma_a + \alpha_a$ [348]. We decided on FPA as the vertical control variable for our vertical controller as it simplifies our design for altitude regulation. The FPA encapsulates both pitch and angle of attack information and directly relates to the vertical speed component of the UAV, making it a more efficient control variable in terms of proportional response for maintaining altitude [349]. Thus, by controlling FPA, we can better achieve the desired rate of climb or descent.

In this section, we explore FPA determination using either the relationship between z_a, z_g, and z_d or the velocity magnitude in the horizontal plane. These FPA computation methods are discussed as options in the subsequent paragraphs. To ensure the UAV does not pitch up or nose down at very steep angles, the UAV FPA is constrained by the maximum and minimum limits as depicted in Fig. 4.4.

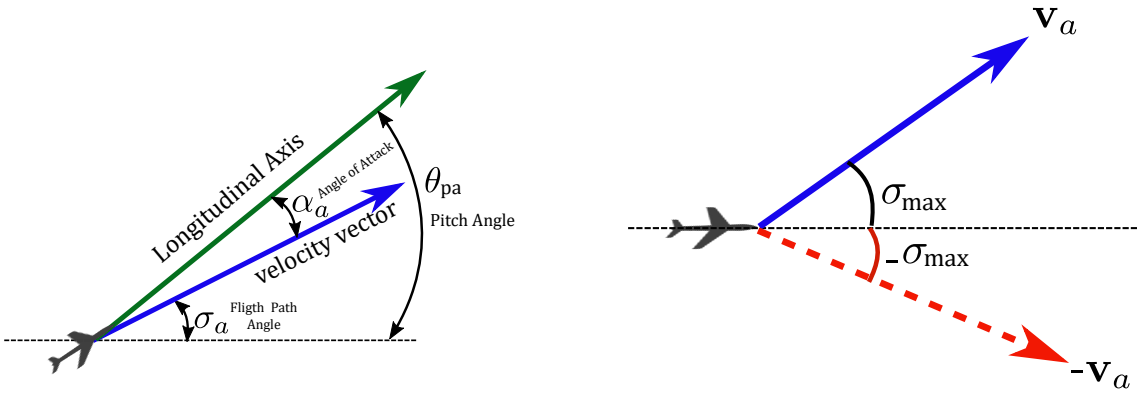

(a) Flight path angle vs pitch angle

(b) Flight path angle limits

Fig. 4.2 Representation of the UAV climb and decent angle dynamics

The three options for computing the FPA needed for the vertical control are designed and presented in the following subsection. Designing three distinct methods for computing FPA, is strategic as the multi-pronged methodology not only enhances the robustness and adaptability of the system but also contributes to the overall reliability of our research. This is because different scenarios and operational conditions may require varying methods to effectively compute FPA. Therefore, presenting multiple options, ensures that our system can handle a broader spectrum of real-world situations and is robust for deployment in various environments. Additionally, developing 3 options provides redundancy in our tracking system, especially in situations where one method encounters issues or limitations, the others can serve as reliable fallbacks, ensuring mission success. Moreover, our multiple methods approach allows for comprehensive comparative analysis as we can objectively evaluate the strengths, weaknesses, and trade-offs of each method, aiding in the selection of the most suitable approach.

The normal FPA design constraint for aircraft and UAVs can vary depending on the specific application and design requirements. However, in general, FPAs for level flight are typically small, on the order of a few degrees, typically around 2-3 degrees [350]. The UAV's FPA in this research is constrained to 0.06 radians, which means that the UAV's velocity vector is constrained by a maximum inclination to the horizontal plane of approximately 3.4^o, where σ_a is in radians.

4.2.1 Option 1 - Flight path angle calculation using relative altitudes

Assuming the UAV is tracking a target moving on the ground which suddenly climbs a hill, we want the UAV to increase its FPA above the target correspondingly to maintain an optimal altitude above the target. If on the other hand, the target enters a valley, the UAV should also be capable of descending downward to maintain an optimal tracking altitude. Using the relative UAV difference between the current UAV, desired UAV, and target altitudes, the FPA can be computed as shown in (4.1).

$$\sigma_a = \frac{(z_d - z_a)}{(z_d - z_g)} \tag{4.1}$$

where $\|\sigma_{\max}\|$ is the maximum allowed FPA, constrained by the physical limitation of the UAV as given by:

$$\sigma_a = \begin{cases} \sigma_{\max}, & \text{if } \dfrac{(z_d - z_a)}{(z_d - z_g)} > \sigma_{\max} \\ -\sigma_{\max}, & \text{if } \dfrac{(z_d - z_a)}{(z_d - z_g)} < -\sigma_{\max} \\ \dfrac{(z_d - z_a)}{(z_d - z_g)}, & \text{Otherwise} \end{cases} \tag{4.2}$$

When the FPA is calculated using the above equations, the velocity of the UAV along the vertical axis, v_{az} is calculated using the following equations:

$$\mathbf{v}_{a_{xy}} = [v_{ax}, v_{ay}]^T \tag{4.3a}$$

$$v_{a_{xy}} = \sqrt{{v_{ax}}^2 + {v_{ay}}^2} \tag{4.3b}$$

$$\sigma_a = \tan^{-1}\left(\frac{v_{az}}{v_{a_{xy}}}\right) \tag{4.3c}$$

$$v_{az} = v_{a_{xy}} \tan \sigma_a \tag{4.3d}$$

where $\mathbf{v}_{a_{xy}}$ is the velocity vector of the 2D plane, with a magnitude represented by $v_{a_{xy}}$.

4.2.2 Option 2 - Flight path angle using velocity vectors

While the method for computing the FPA in the previous subsection yields the desired outcome, the computation may not be feasible when z_d is not known. To address this limitation, we devised an alternative method for computing the FPA using vector geometry and the difference between UAV and target altitudes as shown in Fig. 4.3. To compute the FPA σ_a, we assume that the UAV flies in a straight line for a short period resulting in $v_a = \|v_{xy}\|$. With this, we can calculate σ_a as the ratio of the change in altitude to the change in horizontal distance, resulting in the actual climb rate of the UAV with respect to the ground as follows:

$$\sigma_a = \tan^{-1}\left(\frac{z_a - z_g}{v_a}\right) \tag{4.4}$$

where v_a is the magnitude of the UAV velocity in 3D space. The desired altitude of the UAV, is then computed by ensuring that the FPA is regulated by the following equation (4.5).

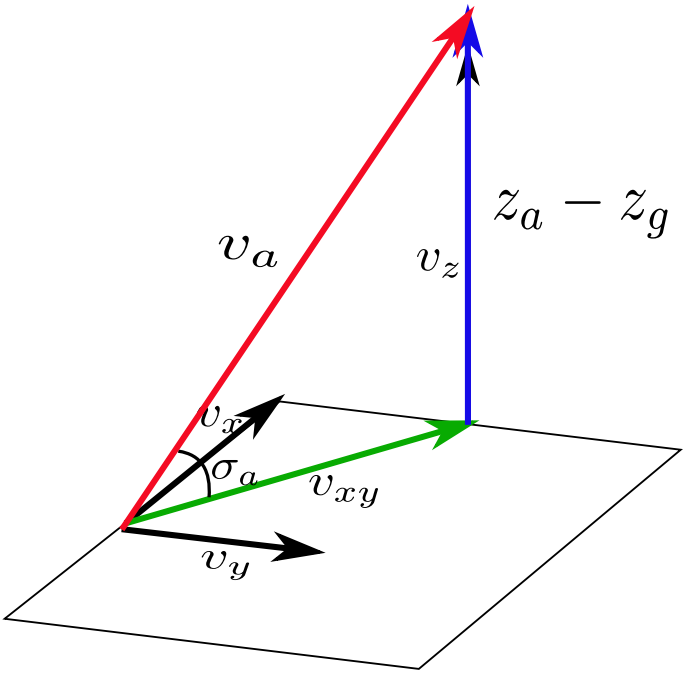

Fig. 4.3 Flight path angle geometric vector diagram

$$\sigma_a = \begin{cases} \sigma_{\max}, & \text{if } \sin^{-1}\left(\frac{Z_a - Z_g}{v_a}\right) > \sigma_{\max} \\ -\sigma_{\max}, & \text{if } \sin^{-1}\left(\frac{Z_a - Z_g}{v_a}\right) < -\sigma_{\max} \\ \sin^{-1}\left(\frac{Z_a - Z_g}{v_a}\right), & \text{Otherwise} \end{cases} \tag{4.5}$$

When σ_a is computed using the above equation, the v_{az} is determined using the formula given in (4.3).

4.2.3 Option 3 - Direct calculation of UAV vertical velocity component

In the third option, we consider the triangle defined by $\triangle ABC$ in Fig. 4.4.

Let d_h be the horizontal distance between the UAV and the target, and let $v_{a_{\text{xy}}}$ be the velocity component in the $x-y$ plane. Then, we can use the Pythagorean theorem to relate d_h, $v_{a_{\text{xy}}}$, and the total velocity v_a as follow:

$$v_a = \sqrt{v_{a_{\text{xy}}}^2 + v_{az}^2} \tag{4.6}$$

where v_{az} is the vertical velocity component. We compute the expression for the FPA in terms of the velocity components and the altitude difference between the UAV and the target:

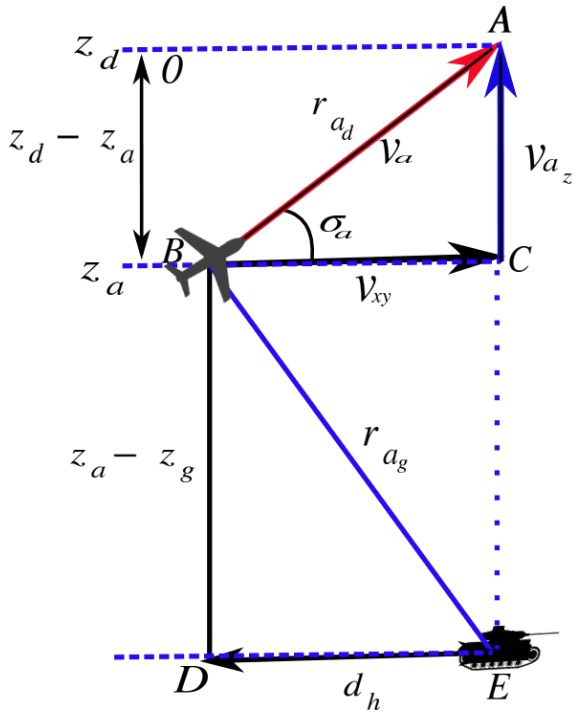

Fig. 4.4 UAV flight path computation triangles

$$\tan \sigma_a = \frac{v_{az}}{v_{a_{\text{xy}}}} \tag{4.7}$$

The first is $\triangle ABC$ in which the hypotenuse forms the side between the UAV current and desired altitudes, labelled as r_{a_d}. Next is triangle $\triangle BDE$, which is formed by the horizontal distance d_h and the altitude difference between UAV and target $z_a - z_g$. The hypotenuse of this triangle is the line connecting the UAV and the target r_{a_g}, and its length is given by the Pythagorean theorem:

$$r_{a_g}{}^2 = d_h{}^2 + (z_a - z_g)^2 \tag{4.8a}$$

$$z_a - z_g = \pm\sqrt{r_{a_g}{}^2 - d_h{}^2} \tag{4.8b}$$

Triangle $\triangle BCA$ is formed by the horizontal and vertical components of the UAV's velocity, $v_{a_{\text{xy}}}$ and v_{az}, respectively, and the total velocity v_a. The hypotenuse of this triangle is the direction of the UAV's velocity vector, which is the FPA σ_a. We can use the Pythagorean theorem to relate the horizontal and vertical velocity components to the total velocity, Using the definition of the FPA, we can express the vertical velocity component in terms

of the FPA and the horizontal velocity component:

$$v_a^2 = v_{a_{\text{xy}}}^2 + v_{az}^2 \tag{4.9a}$$
$$v_a^2 = v_{a_{\text{xy}}}^2 + v_{az}^2 \tag{4.9b}$$
$$v_{az} = v_a \sin \sigma_a \tag{4.9c}$$

Similarly, we can express the horizontal velocity component in terms of the FPA and the vertical velocity component:

$$v_{a_{\text{xy}}} = v_a \cos \sigma_a \tag{4.10}$$

Substituting these expressions into the Pythagorean theorem, we get:

$$v_a^2 = v_a^2 \sin^2 \sigma_a + v_a^2 \cos^2 \sigma_a \tag{4.11a}$$
$$\sin \sigma_a = \frac{v_{az}}{v_a} \tag{4.11b}$$
$$\cos \sigma_a = \frac{v_{a_{\text{xy}}}}{v_a} \tag{4.11c}$$
$$\tan \sigma_a = \frac{v_{az}}{v_{a_{\text{xy}}}} \tag{4.11d}$$
$$\tan \sigma_a = \frac{\sin \sigma_a}{\cos \sigma_a} \tag{4.11e}$$

We can now use the definition of the FPA and the expressions for the horizontal and vertical velocity components to relate the FPA to the other variables in the problem. The third $\triangle AOB$ is formed by the horizontal distance d_h and the altitude difference $z_d - z_a$. The hypotenuse of this triangle is the line connecting the desired altitude z_d and the UAV, and its length, r_{a_d} is given by the Pythagorean theorem:

$$r_{a_d}{}^2 = d_h^2 + (z_d - z_a)^2 \tag{4.12a}$$
$$z_d - z_a = \sqrt{r_{a_d}{}^2 - d_h^2} \tag{4.12b}$$

Using the altitude differences and the velocity components, we can now express the vertical velocity component v_{az} in terms of the FPA σ_a and the altitude differences:

$$v_{az} = v_a \sin \sigma_a \tag{4.13a}$$
$$v_{az} = \sqrt{v_a^2 - v_{a_{\text{xy}}}^2} \sin \sigma_a \tag{4.13b}$$

To remove the FPA σ_a from the final equation for v_{az}, we used the fact that $\sin \sigma_a$ appears in both the original equation and the substituted expressions for v_a and $v_{a_{xy}}$. Factoring out

$\sin\sigma_a$ from the original equation as follows:

$$v_a = \sqrt{(z_d - z_a)^2 + d_h^2} \tag{4.14a}$$

$$v_{a_{xy}} = \frac{d}{\sqrt{{d_h}^2 - (z_d - z_g)^2}} \sqrt{(z_d - z_a)^2 + {d_h}^2 - (z_d - z_g)^2} \tag{4.14b}$$

Substituting these expressions into the original equation gives us:

$$v_{az} = \sqrt{(z_d - z_a)^2 + {d_h}^2 - \frac{{d_h}^2}{{d_h}^2 - (z_d - z_g)^2}(z_d - z_a)^2} \sin\sigma_a \tag{4.15a}$$

$$v_{az} = \sin\sigma_a \sqrt{(z_d - z_a)^2 + {d_h}^2 - \frac{{d_h}^2}{{d_h}^2 - (z_d - z_g)^2}(z_d - z_a)^2} \tag{4.15b}$$

$$v_{az} = \sqrt{(z_d - z_a)^2 \left(\frac{{d_h}^2 - (z_d - z_g)^2 - (z_d - z_a)^2}{{d_h}^2 - (z_d - z_g)^2} \right)} \tag{4.15c}$$

Simplifying and rearranging the terms, we get:

$$v_{az} = \sqrt{(z_d - z_a)^2 \left(\frac{v_{a_{\text{xy}}}^2}{{d_h}^2 - (z_d - z_g)^2} - 1 \right)} \tag{4.16}$$

Note that we need to use the $\pm$ sign because the FPA can be positive or negative, depending on the direction of the UAV's velocity vector relative to the horizontal plane. Finally, we can use the above equation and the Pythagorean theorem to compute the FPA:

$$\sigma_a = \pm \tan^{-1} \left(\sqrt{\frac{(z_d - z_a)^2}{{d_h}^2 - (z_d - z_g)^2}} \right) \tag{4.17}$$

The equation for computing the FPA as shown above, utilises the variables z_a, z_g, z_d, and d_h. This formulation can be used to compute the FPA for any desired altitude z_d and horizontal distance d_h, even if the velocity components $v_{a_{\text{xy}}}$ and v_{az} of the UAV are not known.

In a situation where we are unable to compute the FPA, we need an alternative way of developing a vertical control law that is not dependent on the FPA. Consequently, we design a vertical control algorithm to ensure that the UAV can fly to an altitude where it can keep the target within its FOV, using a PD control method in the next subsection.

4.3 UAV Altitude Control Using PD and Image Sizes

Consider that a UAV with a camera pointed downward is flying at a certain altitude with the target within its field of view. We assume that the target is moving in a plane that is orthogonal to the camera's main axis, with an orthographic projected image. The goal of the guidance laws is to ensure that the UAV tracks the vehicles despite its evasive manoeuvres. Since the UAV follows 2D horizontal guidance laws to track an evasive ground target, the target may occasionally exit the camera's field of view. To address this scenario, our 2D horizontal guidance scheme will be supplemented with vertical guidance to keep the control area within the FOV and acceptable bounds.

Adjusting the altitude has a visual effect on the 2D target projection on the image plane. The apparent size of the target image increases with a decrease in UAV altitude and decreases as UAV altitude increases. Additionally, decreasing the UAV altitude has the effect of migrating the target image away from the centre of the image plane, whereas an increase in altitude tends to move the target image closer to the centre of the image plane. The size and distance of the target image, which is both inversely proportional to the UAV altitude. If the camera focal length is given by f_c, and the size of the ground target box frame in the world plane is x_{s_w}, then the size of the target box frame on the image plane x_{s_i} can be computed as follows:

$$x_{s_i} = x_{s_w}\left(\frac{f_c}{z_a}\right) \tag{4.18}$$

where z_a is the current UAV altitude. To control the UAV altitude using its projected image size, we define a control area for the UAV by the box bounding the projected target on the image plane. The extreme corners of the longer diagonal of the image box are defined as $x_{i_{\min}}$ and $x_{i_{\max}}$. The size of the control area is therefore computed as $x_{s_i} = \|x_{i_{\min}} - x_{i_{\max}}\|_2$. If we depict the midpoint of the image plane as $x_{p_{\text{cen}}}$ and the centre of the target on the image plane as $x_{i_{\text{cen}}}$, then the Euclidean distance between the midpoint of the UAV camera plane and the target image midpoint is represented by d_{c_i} as shown in Fig. 4.5 . Using the variables x_{s_i}, d_{c_i}, and z_a, we can develop a vertical guidance strategy for the tracking UAV that is dependent on the size of the image bounding box on the camera plane and the desired altitude [105].

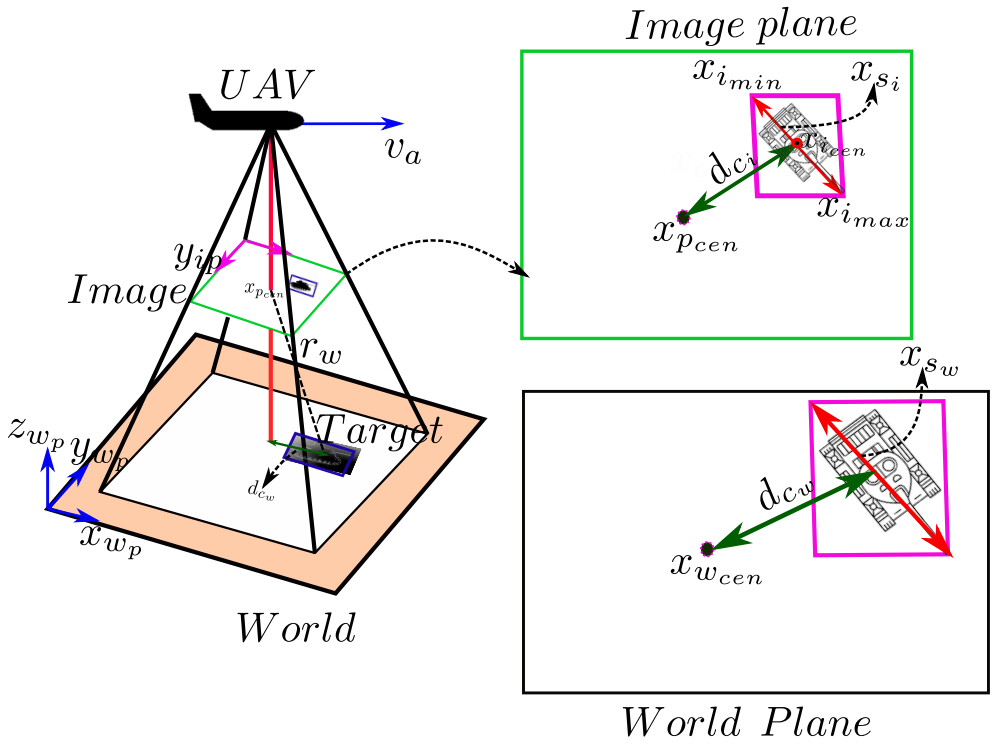

Fig. 4.5 Diagram explaining target size on world plane and Image plane

The size of the target image box is governed by the following equations:

$$x_{s_i} = x_{s_w}\left(\frac{f_c}{z_a}\right), \quad d_{c_i} = d_{c_w}\left(\frac{f_c}{z_a}\right) \tag{4.19}$$

where x_{s_w} and d_{c_w} denote the size of the control area and the planar Euclidean distance between the UAV and target centre in the world frame. Note that under orthographic projection assumptions, $d_{c_w} = r_w$, where r_w is the distance measured along the line of sight between the UAV and the centre of the target. Using the equation below, a relationship can be obtained for the vertical control as follows:

$$d_{c_i} = r_w\left(\frac{f_c}{z_a}\right) \tag{4.20}$$

Using the multi-variable chain rule, the double derivative of the equation above is obtained, resulting in the following equations:

$$\ddot{z}_a = -f_c x_{s_w}\left(\frac{\ddot{x}_{s_i}}{x_{s_i}^2} - \frac{2\dot{x}_{s_i}^2}{x_{s_i}^3}\right) \tag{4.21a}$$

$$\ddot{x}_{s_i} = -\left(\frac{x_{s_i}^2}{f_c x_{s_w}}\right)\ddot{z}_a + 2\frac{\dot{x}_{s_i}^2}{x_{s_i}} \tag{4.21b}$$

If we denote $\ddot{z}_a = u_{za}$ and $\ddot{x}_{s_i} = u_{si}$, then a PD controller can be designed to drive $x_{s_i} \rightarrow {x_{s_i}}^{des}$.

$$u_{za} = K_{p_{za}} e_{za} + K_{d_{za}}(\dot{z}_a) \tag{4.22}$$

where $K_{p_{za}}$ and $K_{d_{za}}$ and proportional and derivative respective gains for z_a and $e_{za} = z_d - z_a$. Similarly, the following holds:

$$u_{si} = -\left(\frac{f_c x_{s_w}}{x_{s_i}^2}\right) K_{p_i} e_{si} + \left(\frac{f_c x_{s_w}}{x_{s_i}^2}\right) K_{d_i}(\dot{x}_{s_i}) \tag{4.23}$$

where K_{p_i} and K_{d_i} and proportional and derivative respective gains for x_{i_l} and $e_{si} = {x_{s_i}}^{des} - x_{s_i}$. The vertical guidance law above generates altitude control commands with the lower bounds and upper constraints of ${}^{-}z_d \leq z_a \leq {}^{+}z_d$ and ${}^{-}{x_{s_i}}^{des} \leq x_{s_i} \leq {}^{+}{x_{s_i}}^{des}$ respectively.

4.4 Simulation and results

The simulation results comparing the vertical control laws in different scenarios are presented in this section. We used a Windows 10 system with an Intel Core i5-8700 CPU and 32 GB RAM to run the simulations. All the simulations to test the performance of the altitude controller utilised UAV minimum turn radius, $r_{\min}$, is set at 100m with the velocity limits of $v_{a_{\min}} = 15$m/s and $v_{a_{\max}} = 40$m/s. Similarly, the respective minimum and maximum acceleration limits of the UAV along x, y, and z axes are as follows:

$$\begin{aligned}
u_{ax_{\min}} &= -10\ [\text{m/s}^2],\ u_{ax_{\max}} = 8\ [\text{m/s}^2],\\
u_{ay_{\min}} &= -4\ [\text{m/s}^2]\ , u_{ay_{\max}} = 4\ [\text{m/s}^2],\\
u_{az_{\min}} &= -2\ [\text{m/s}^2],\ u_{az_{\max}} = 3\ [\text{m/s}^2]
\end{aligned}$$

The target velocity limits is set to $v_{g_{\max}} = 16.7m/s$, while its respective acceleration limits along x, y, and z axes are as follows:

$$\begin{aligned}
a_{gx_{\min}} &= -2\ [\text{m/s}^2],\ a_{gx_{\max}} = 4\ [\text{m/s}^2],\\
a_{gy_{\min}} &= -2\ [\text{m/s}^2],\ a_{gy_{\max}} = 2\ [\text{m/s}^2],\\
a_{gz_{\min}} &= -1\ [\text{m/s}^2],\ a_{gz_{\max}} = 2\ [\text{m/s}^2]
\end{aligned}$$

The simulation results are presented in the next subsections

4.4.1 Altitude control using FPA

The altitude control implemented above using 2D velocity vectors was simulated to evaluate the performance of the three FPA options. For this simulation, we use a desired altitude $z_d = 300$m. The UAV is initiated at position $[1000,\ 1000,\ 50]$ while the target $[0,\ 50,\ 0]$. The UAV and target velocity and acceleration initial inputs and magnitude limits are the same as the values used in Section 3.5. The maximum value of FPA was set to $\sigma_{a_{\max}} = 0.06$ *rads* and the algorithm comparing the various altitudes was simulated for 1200 s.

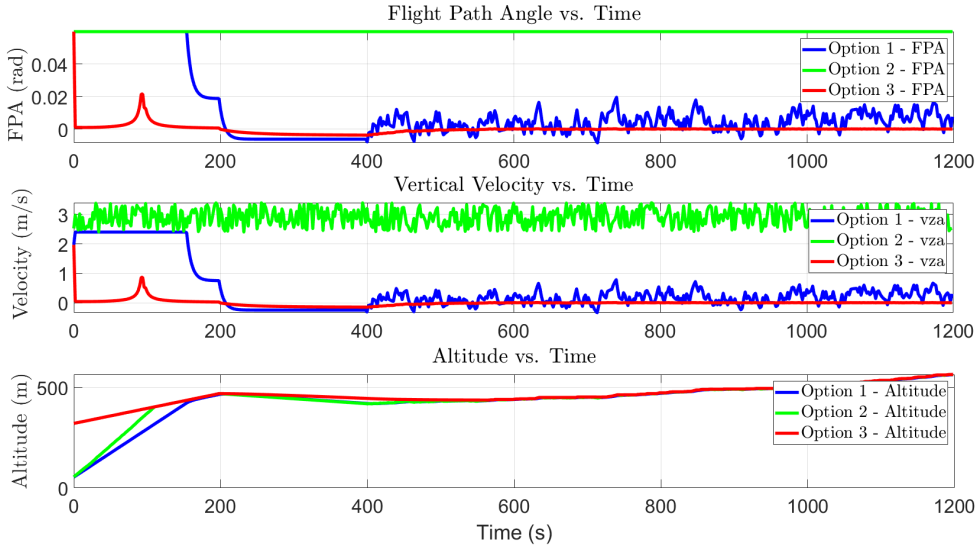

Fig. 4.6 Comparison of options 1, 2 and 3

In Fig. 4.6, the simulation output for the 3 altitude control options based on FPA is presented in a stacked plot comparing FPA, vertical velocity, and change in altitude throughout the simulation. In the comparison plot, it is observed that the FPA for option-1 responded to the control input by slowly adjusting its value from the maximum value to a regulated value as it smoothly attained the desired altitude. With option-2, the FPA remained at maximum value resulting in a stable velocity towards the desired altitude. With option-3, the response by the FPA was sharp but velocity was fairly stable. The altitude trajectory for option 3 showed it started adjusting to the desired altitude faster. The plot shows that the 3 options can be utilised for our target tracking problem. However, due to the simplicity and stability of option-1, it will be adopted for our FPA for the remainder of this thesis.

4.4.2 Altitude control using target size

For the PID altitude controller, we simulated a scenario where the UAV is at a lower altitude than the desired tracking altitude above the target. The UAV was initiated a position of $[1000\ , -1000\ , 180]$, while the target started at $[50\ , -50\ , 50]$. The target size

on the ground was set at $x_{s_w} = 10$m and the initial image size on the camera plane is set to $x_{s_i} = 0.5$m. The camera focal length was assumed to be $f_c = 200$mm. The simulation was run for 100s with the derived altitude controller aiming to get the UAV to the desired altitude, $z_d = zg + 150$m.

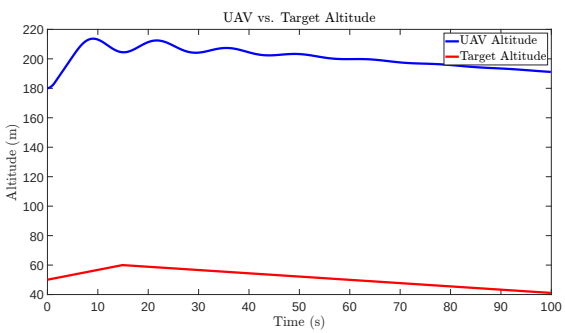

(a) UAV Altitude vs. Target Altitude

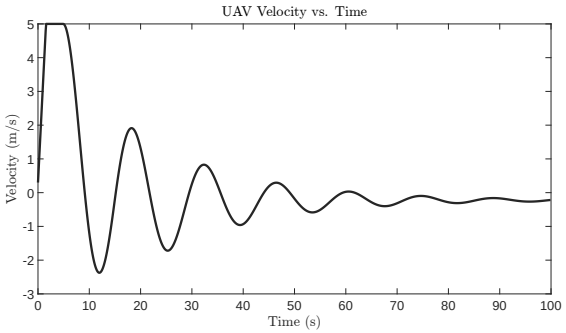

(b) UAV Velocity vs. Time

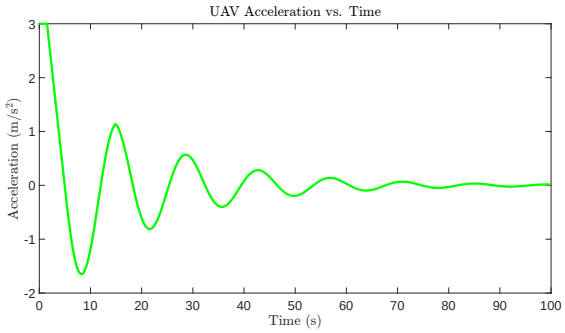

(c) UAV Acceleration vs. Time

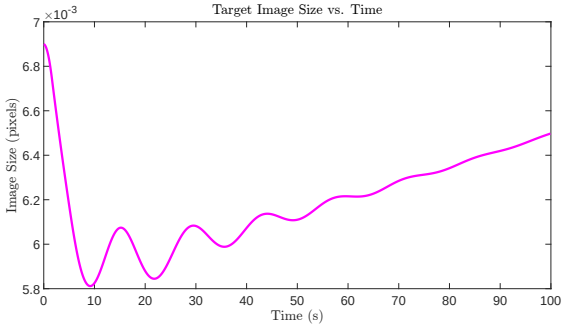

(d) Target Image Size vs. Time

Fig. 4.7 UAV altitude control simulation

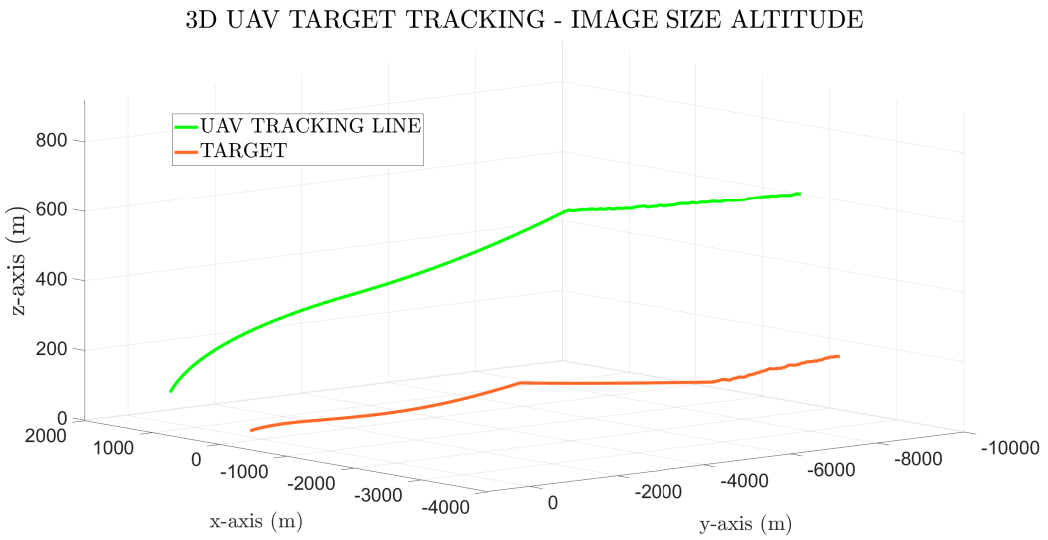

Fig. 4.8 Trajectory of target tracking using camera focal length and image size altitude control.

In Fig 4.7, we plot the velocity of the UAV and target, as well as the change of the image size x_{i_l}, the distance between the image plane midpoint and target image midpoint, x_c, and the altitude of the UAV z_a plots over the simulation time. Fig 4.7c depicts the plots of the UAV acceleration along the x axis, while Fig 4.8 depicts UAV and target 3D trajectories. The UAV was able to adjust its altitude from its initial position, gradually attaining the desired altitude and remaining within the designed upper and lower limits during the remaining part of its trajectory. The UAV acceleration can be compared to the rate of change in the size of the control area. The change in the UAV altitude is also observed to change the size of the target on the UAV camera plane.

4.4.3 Comparison and selection of altitude controls

The UAV vertical control strategies implemented in this section have shown the capability to adjust the UAV altitude as needed in response to an increase or decrease in target altitude during a tracking scenario. The vertical control laws based on FPA are computationally simpler to implement. However, we are also mindful of situations where we are unable to compute the FPA either due to sensor limitation, failure or non-availability of the needed measuring equipment. Accordingly, we implemented an altitude control strategy that is not dependent on the FPA. In our algorithm, we used the relationship between the camera focal length, the target actual size and the size of the target image on the camera plane to develop a control box that allows the UAV to adjust its altitude in response to target altitude. While the image size-dependent algorithm gives the desired outcome, it involves many variables and has higher complexity and computational cost than the FPA algorithm. Based on the above reason, we will adopt the FPA UAV control algorithm presented in option-1 in this section for the remaining part of this research.

4.4.4 Selected altitude control strategy

Based on the decision from our comparison, we carried out additional simulations to test the performance of option-1 in different mission scenarios. Consider a UAV that is below the target at the start of the simulation. In the first scenario, we assume that the UAV, while unable to access the target state, receives these details from another UAV overhead the target or a ground control station with the capability to obtain the target states using a satellite. Having received this information, the UAV should be able to fly and position over the target to get updated tracking information. The UAV and target trajectories, the FPA and the relative altitude of the UAV and target are shown in Fig. 4.9a and 4.9b.

In the second scenario, we assume that the UAV is above the target at the start of the simulation and away from the target. This scenario is typical and the goal is to get the UAV

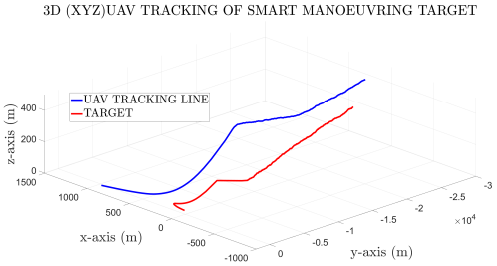

(a) UAV initial altitude is below the desired altitude

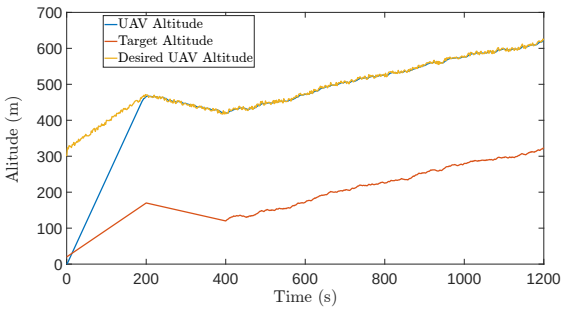

(b) UAV, target and desired altitude compared

Fig. 4.9 UAV below, desired and relative target altitude

to the desired altitude while tracking the target. As shown in Fig.4.10a and 4.10b, the UAV altitude control enables the UAV quickly arrive at the desired altitude and maintains the relative separation in response to target lateral and altitude manoeuvres.

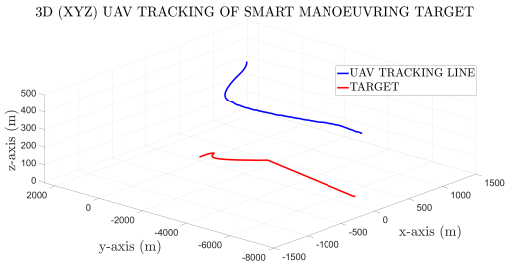

(a) UAV initial altitude is above the desired altitude

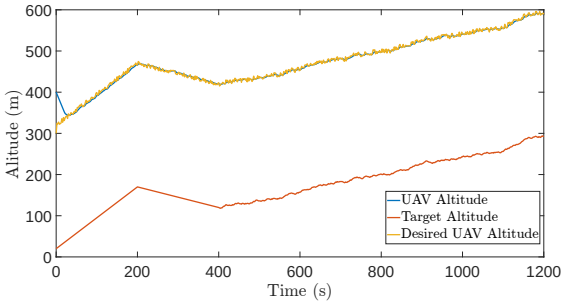

(b) UAV, target, and desired altitude compared

Fig. 4.10 UAV above desired and relative target altitude

4.5 Summary

We developed various vertical acceleration algorithms for generating altitude control for a fixed-wing UAV starting from the 2D plane. Essentially the vertical controller is combined with the 2D lateral and longitudinal control of the $x-y$ axis to form 3D control of the UAV. One of the options utilised the relationship between the target and desired UAV altitude to compute controlled FPA changes to control the UAV altitude. The second option set required using a relationship between UAV camera focal length, the size of the target image on the ground, and the desired size of the image on the camera lens to geometrically compute altitude control accelerations that control the UAV altitude above ground and the target. Both options were tested using simulation and the results show that the altitude control strategies are adequate for the research work. Due to its simplicity, effectiveness and lower computational cost, we adopted the vertical controller designed based on FPA for controlling the UAV altitude for the remaining Chapters of this research. Further

simulation of the adopted altitude controllers shows it is sufficient for our fixed-wing UAV target tracking problem.

Chapter 5

Single UAV Evasive Quadrotor Tracking

5.1 Introduction

Drones have become increasingly popular due to their versatility and affordability, making them an attractive option for various applications. These flying machines have become indispensable tools utilised in various roles, including aerial photography, target tracking, fire fighting, aerial surveillance, and medical emergency response. However, as with many technologies, there are downsides. The rapid technological advancement in drone technology has led to the widespread availability of drones, raising concerns about their potential misuse [351]. For instance, criminals and non-state actors have exploited drones to perpetrate various forms of crimes, including drug trafficking, smuggling, and espionage. Moreover, *Kamikaze* drones [352] pose a significant threat to air travel, with several near-misses reported between commercial aircraft and drones [353–356]. These concerns have emphasised the need for effective countermeasures that can detect, track, and intercept rogue drones. The ability to track and intercept evasive drones in real time is critical for ensuring the safety of our skies and mitigating the risks associated with the use of drones for nefarious purposes.

To address this issue, this Chapter combines the fixed-wing UAV control algorithms presented in Chapters 4 and 5 for persistent tracking of an evasive quadrotor to keep the target within the pursuer's camera field of view (FOV). The proposed algorithm can be utilised to develop various countermeasure applications, mitigating the risks associated with drones used for nefarious purposes, and contributing to military, law enforcement, and civilian applications. To ensure the current research makes meaningful contributions, we review some related literature on tracking evasive quadrotors to assess current knowledge and gaps.

5.1.1 Aerial target tracking - related work

Dogru and Marques [357] researched target drone detection and pursuit using a bigger drone mounted with a millimetre-wave radar antenna. However, the target developed for this research was a non-smart aerial target assumed to fly at a constant speed. A similar tracking strategy was implemented by [162, 358], however, the target was heuristically modelled to test the effectiveness of the tracking algorithm. Lee et al. [359], also designed an algorithm for tracking manoeuvring aerial targets but the tracking performance was tested against a simple drone model making a 90-degree turn during simulation. In a related study, Choi and Kim [360] addressed a vision-based aerial target tracking problem by implementing a nonlinear adaptive observer UAV guidance for fixed-wing UAV tracking of an aerial target. Similarly, [237, 361] proposed a vision-based fixed-time control for tracking an uncooperative aerial quadrotor-type target. However, unlike the evasive target consideration in this research, the reviewed study only implemented a constant velocity aerial target. A drone that operates autonomously and can follow and intercept an aerial target was also studied by [362].

In [363] a pursuer-evader game was implemented where a quadrotor UAV algorithm attempted to intercept an evader quadrotor by tracking and getting within a distance of 0.5m from the centre of the evader quadrotor. The evader target utilised an A^* search algorithm to iteratively navigate through a window to return to a predefined yellow region while avoiding the tracking quadrotor as an obstacle. However, the research only focused on the synthesis of an advisory controller for the pursuer quadrotor, without highlighting the tracking and evasion algorithm and their effectiveness. Similar research was carried out by Tsoukalas in [364] and [365], for visual tracking of an evading UAV using a pursuer-UAV. They combined principles of optical flow, deep learning, and intra-frame homography to execute correlation-based target tracking using a computer-controlled Pan-Tilt-Zoom (PTZ) camera. Like the previous research, the target evasion aspect was not fully addressed. In another related study, [352] presented a method for optimising multiple-drone pursuers' performance to intercept *Kamikaze* multiple-drone evader quadrotors, utilising a communication strategy where each pursuer can decide which evaders should be chased and immobilised. The Multiple-Pursuers Multiple-Evaders (MPME) problem was addressed using an Internet of Battlefield Things (IoBT) to track the evasive target. The research did not however address the evasion strategy of the targets. In another related study, [359] designed a strategy for quadrotor tracking a highly manoeuvrable drone aerial target with control input unknown to the tracker. They applied an impact angle control with prediction in combination with a weighting function that used Bayesian estimated variance data. The target evasion strategy was not presented and they only considered a quadrotor pursuer, without addressing a scenario where the pursuer is a fixed-wing UAV.

While existing algorithms may be effective in tracking stationary or predictable targets, only a few studies have addressed fixed-wing UAV tracking of manoeuvring targets performing sudden and unpredictable manoeuvres. However, none of the literature reviewed addressed the tracking of smart evasive quadrotor targets using fixed-wing UAVs. Considering the current capability of recent drone design and manufacture, and the possibility of adversarial drone pursuit using fixed-wing UAVs, this gap is important and needs to be addressed. This Chapter contributes to addressing the highlighted gap by extending the research from Chapters 3 and 4 and developing a quadrotor target algorithm that performs aerial manoeuvres. The fixed-wing UAV algorithm is modified to take into consideration the various types of manoeuvres that can be carried out by the quadrotor. Our approach represents a significant improvement over existing methods by anticipating evasive drone movement and adjusting the fixed-wing UAV's position and altitude accordingly, allowing it to stay within the field of view of the evasive drone even if it performs sudden and unpredictable manoeuvres.

5.1.2 Contributions

The contributions of this Chapter are as follows:

- We implemented a quadrotor dynamics and control algorithm to test the performance of our fixed-wing UAV in tracking evasive aerial targets.
- A safety controller for collision avoidance between the tracking UAV and the evasive target was designed and applied to the tracking-evasion mission.
- To enhance the UAV tracking algorithm developed in Chapter 2, we designed an adaptive optimisation algorithm that uses feedback from the UAV and target states during simulation to adaptively adjust the optimisation parameters of the tracking UAV.
- A performance assessment method was developed that computes and compares the energy consumed by the original and adaptively optimised UAV algorithm while tracking an evasive target.

The remaining part of this Chapter is organised as follows. We develop a quadrotor target by designing the mathematical representation for the vehicle dynamics in Section 5.2, while Section 5.3 discusses the quadrotor path following controllers. Our strategy for quadrotor evasion is highlighted in Section 5.4 while a discussion on safety measures and collision avoidance is presented in Section 5.5. In Section 5.6 we present our adaptive optimisation consideration and evaluate the UAV tracking performance against an evasive aerial target

in Section 5.7. Simulation results are presented in Section 5.8 followed by analysis and discussion in Section 5.9. This Chapter concludes with a summary in Section 5.10.

5.2 Quadrotor Dynamics

In this section, we focus our attention on the dynamics and control strategy of an evasive quadrotor, intending to develop path-following and evasive aerial targets to be tracked by our fixed-wing UAV. We consider a quadrotor design that manoeuvres and evades based on a PD control strategy in 3D space. Parameterised trajectories will be generated and the quadrotor control designed to follow a path using some preset waypoints. Our fixed UAV algorithm will then be applied to track the quadrotor while maintaining the desired altitude above.

Consider a quadrotor with fixed body frame x_B, y_B, z_B attached its centre of mass E_B as shown in Fig.5.1. The axis x_B is aligned with the desired forward direction of the quadrotor z_B points vertically upwards and is perpendicular to the plane of rotation when the quadrotor is in a hover position. The quadrotor operates in a global (inertial) frame defined by x, y, z. The quadrotor state consists of position and orientation. The position part of the state specifies the location of the quadrotor in space while the roll, pitch and yaw angles define its orientation [366]. Accordingly, the quadrotor state is represented by a six-dimensional vector $\mathbf{x}_{sq}$ while its rate of change $\dot{\mathbf{x}}_{sq}$ in (5.1).

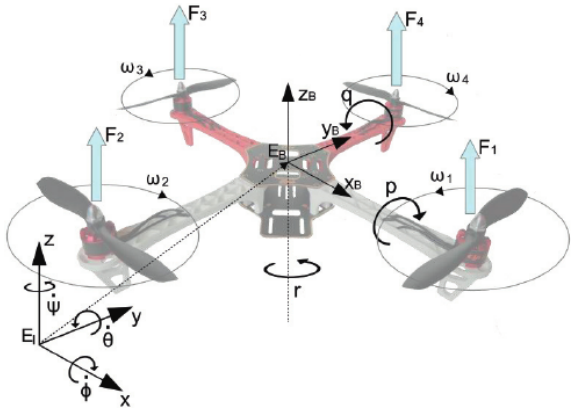

Fig. 5.1 Quadrotor dynamics [367].

$$\mathbf{x}_{\text{sq}} = \begin{bmatrix} x_q & y_q & z_q & \varphi_q & \theta_q & \psi_q \end{bmatrix}^T \tag{5.1}$$

The yaw angle rotates about the z-axis while the roll and pitch angles rotate about the x and y axes respectively. The body frame angular rates p, q, and r are related to the derivatives of the roll, pitch, and yaw angles The z-x-y Euler angles are used to model the rotation of

the quadrotor in the global frame and the rotation matrix for transforming components of vectors in the quadrotor body frame to the global frame is presented in (5.2).

$$\begin{bmatrix} p \\ q \\ r \end{bmatrix} = \begin{bmatrix} c\theta_q & 0 & -c\varphi_q s\theta_q \\ 0 & 1 & s\varphi_q \\ s\theta_q & 0 & c\varphi_q c\theta_q \end{bmatrix} \tag{5.2}$$

where c and s represent cosine and sine respectively. Also, the parameters φ_q, θ_q and ψ_q are the quadrotor row, pitch, and yaw angles respectively. Our goal is to track 3D trajectories represented by a position vector and a yaw angle that both change with time. The position and yaw angle are used to form a four-dimensional vector as in (5.3), which must be differentiable so we can calculate its derivative and second derivative.

$$A[R]_B = \begin{bmatrix} c\psi_q c\theta_q - s\varphi_q s\psi_q s\theta_q & -c\varphi_q s\psi_q & c\psi_q s\theta_q + c\theta_q s\varphi_q s\psi_q \\ c\theta_q s\psi_q + c\psi_q s\varphi_q s\theta_q & c\varphi_q c\psi_q & s\psi_q s\theta_q - c\psi_q c\theta_q s\varphi_q \\ -c\varphi_q s\theta_q & s\varphi_q & c\varphi_q c\theta_q \end{bmatrix} \tag{5.3}$$

Using (5.4), we compare the desired position and yaw angle with the actual values to obtain an error vector and its derivative. The objective is for the error vector to approach zero exponentially, allowing us to determine the required acceleration, which can be the second derivative of either the position vector or the yaw angle.

$$e_{p_q} = r_{tr}(t) - r_q \tag{5.4a}$$

$$e_{v_q} = \dot{r}_{tr}(t) - \dot{r_q} \tag{5.4b}$$

$$(\ddot{r}_{tr}(t) - \ddot{r}_{q_c}) = k_{d,x} e_{v_q} + k_{p,x} e_{p_q} \tag{5.4c}$$

where r_{tr} is the desired trajectory (position and yaw angle) vector and $\ddot{r}_{q_c}$ is the commanded acceleration to be computed by the controller. The rotor of the quadrotor are all equidistant to the centre of mass by a distance L. Let the vector that represents the position of the quadrotor in the global reference be represented by $\mathbf{x}_q$. The forces acting on the system are the force of gravity, acting in a direction that is opposite to the positive z_B axis, and the forces exerted by each rotor, represented as F_i, which act in the positive z_B direction. The equations that determine the acceleration of the centre of mass and the hovering control

are governed by the following forces:

$$m\ddot{r} = \begin{bmatrix} 0 \\ 0 \\ -mg \end{bmatrix} + R \begin{bmatrix} 0 \\ 0 \\ F_1 + F_2 + F_3 + F_4 \end{bmatrix} \tag{5.5}$$

The first control input will be defined as :

$$u_{q_1} = \sum_{i=-1}^{4} F_i \tag{5.6}$$

Each rotor in the quadrotor generates a moment perpendicular to the blade's plane of rotation, denoted as M_i. Rotors 1 and 3 rotate in the negative direction of z_B, while rotors 2 and 4 rotate in the positive direction of z_B. As a result, M_1 and M_3 act in the direction of z_B, while M_2 and M_4 act in the opposite direction of z_B. The distance from the centre of mass of the quadrotor to the axis of rotation of the rotors is represented by L. The angular acceleration determined by the Euler equations is:

$$I \begin{bmatrix} \dot{p} \\ \dot{q} \\ \dot{r} \end{bmatrix} = \begin{bmatrix} L(F_2 - F_4) \\ L(F_3 - F_1) \\ M_1 - M_2 + M_3 - M_4 \end{bmatrix} - \begin{bmatrix} p \\ q \\ r \end{bmatrix} \times \begin{bmatrix} p \\ q \\ r \end{bmatrix} \tag{5.7a}$$

$$I \begin{bmatrix} \dot{p} \\ \dot{q} \\ \dot{r} \end{bmatrix} = \begin{bmatrix} 0 & L & 0 & -L \\ -L & 0 & L & 0 \\ \delta & -\delta & \delta & -\delta \end{bmatrix} - \begin{bmatrix} p \\ q \\ r \end{bmatrix} \times \begin{bmatrix} p \\ q \\ r \end{bmatrix} \tag{5.7b}$$

where $\delta = \frac{kM}{kF}$ represents the relationship between the quadrotors lift and drag.

5.3 Quadrotor Controllers

In implementing the quadrotor controls, we consider the hover state as well as the position and attitude controls. These are discussed in the following subsections.

5.3.1 Nominal hover state

We design the quadrotor controllers by linearising the equations of motion presented in (5.9), at the hover state, where $\mathbf{x}_q = \mathbf{x}_{q_0}$, $\varphi_q = 0$ and $\theta_q = 0$. At this state, $\psi_q = \psi_0$, and $\dot{\theta} = \dot{\varphi}_q = \dot{\psi}_q = 0$, and the lift generated by the propellers is computed by:

$$F_{i,0} = \frac{mg}{4} \tag{5.8}$$

The nominal values of the position and attitude inputs at hover are $u_{1,0} = mg$ and $u_{2,0} = 0$. If we linearise (5.5), we get:

$$\ddot{x}_{sq1} = g(\theta_q \cos\psi_0 + \varphi_q \sin\psi_0) \tag{5.9a}$$

$$\ddot{x}_{sq2} = g(\theta_q \sin\psi_0 + \varphi_q \cos\psi_0) \tag{5.9b}$$

$$\ddot{x}_{sq3} = \frac{1}{m}(u_{q_1} - mg) \tag{5.9c}$$

Similarly, if we linearise (5.7), we arrive at:

$$\begin{bmatrix} \dot{p} \\ \dot{q} \\ \dot{r} \end{bmatrix} = I^{-1} \begin{bmatrix} 0 & L & 0 & -L \\ -L & 0 & L & 0 \\ \delta & -\delta & \delta & -\delta \end{bmatrix} \begin{bmatrix} F_1 \\ F_2 \\ F_3 \\ F_4 \end{bmatrix} \tag{5.10}$$

Essentially, the equations that describe motion are decoupled when considering angular acceleration. The specific component of angular acceleration is only affected by its corresponding component of u_{q_2}.

5.3.2 Position and attitude control

The goal of the control problem is to find the four inputs, u_{q_1}, and u_{q_2} that are necessary for either hovering or following a desired trajectory, z_{des}. To do so, the quadrotor's position errors are used to control its position through the use of a position controller, which directly determines u_{q_1}. The position controller also allows the derivation of a desired orientation, which is then controlled through an attitude controller. The process of converting inputs into u_{q_1}, u_{q_2} is detailed in [368].

Attitude control. We now introduce a control system for the quadrotor's orientation (roll, pitch, and yaw) to follow a desired path. The control system, known as a PD attitude controller, will be based on simplified equations of motion, and it will only work effectively when the quadrotor's orientation is close to a stable hovering position with small roll and pitch angles. The control laws for this system will have a specific form when the quadrotor is near the nominal hover state. The equation for computing the attitude control is given in (5.11)

$$\mathbf{u}_2 = \begin{bmatrix} k_{p,\varphi}(\varphi_{des} - \varphi_q) + k_{d,\varphi}(p_{des} - p) \\ k_{q,\theta}(\theta_{des} - \theta_q) + k_{d,\theta}(q_{des} - q) \\ k_{x,\psi}(\psi_{des} - \psi_q) + k_{d,\psi}(x_{des} - x) \end{bmatrix} \tag{5.11}$$

Position control. The next part of the discussion will focus on two methods for controlling the position of the quadrotor. These methods use the roll and pitch angles as inputs and aim to maintain the position or follow a specific trajectory in 3D space. The first method is for holding the position at a set point $\mathbf{x}_0$, while the second one is for tracking a specified trajectory $\mathbf{x}_{tr}(t)$. The desired yaw angle can be either constant ψ_q or change over time with $\psi_{tr}(t)$, and this will be separately defined in both methods. The desired roll and pitch angles, $\varphi_{q_{des}}$ and $\theta_{q_{des}}$, will be determined by the position control algorithm and will be used to calculate the desired speeds. The desired trajectory $\mathbf{z}_{des}$ is given as follows:

$$\mathbf{z}_{des} = \begin{bmatrix} \mathbf{x}_{tr}(t) \\ \psi_{tr}(t) \end{bmatrix} \tag{5.12}$$

5.3.3 Hover controller design

In the hover position, we have that $\mathbf{x}_{tr}(t) = \mathbf{x}_0$ and $\psi_{tr}(t) = \psi_0$. Accordingly, the command control acceleration, $\ddot{x}_{i,des}$ is computed using a PD controller. The position error is defined as $e_i = x_{tr_i} - x_{q_i}$. To ensure that the errors exponentially go to zero, the following must hold:

$$(\ddot{x}_{tr_i} - \ddot{x}_{i,des}) + k_{d,i}(\dot{x}_{tr_i} - \dot{x}_{q_i}) + k_{p,i}(x_{tr_i} - x_{q_i}) = 0 \tag{5.13}$$

where $\dot{x}_{tr_i} = \ddot{x}_{tr_i} = 0$. Using (5.9), we derive the relationship between the desired control acceleration and quadrotor roll and pitch angles. If $\delta_\theta = \theta_q - \theta_{q_0}$ and $\delta_\psi = \psi_q - \psi_{q_0} = \psi_q$, then we can arrive at the following:

$$\ddot{x}_{1,des} = g(\theta_q \cos\psi_q + \varphi_q \sin\psi_q) \tag{5.14a}$$

$$\ddot{x}_{2,des} = g(\theta_q \sin\psi_q + \varphi_q \cos\psi_q) \tag{5.14b}$$

$$\ddot{x}_{3,des} = \frac{1}{m}(u_{q_1} - g) \tag{5.14c}$$

In a hover situation, this results in the following:

$$u_{q_1} = mg + m\ddot{x}_{3,des} = mg - m(k_{d,3}\dot{x}_3 + k_{p,3}(x_3 - x_{3,0})) \tag{5.15}$$

The other two can be used to compute the desired attitude control from the roll and pitch angles as follows:

$$\varphi_{q_{des}} = \frac{1}{g}(\ddot{x}_{1,des}\sin\psi_{q_{des}} - \ddot{x}_{2,des}\cos\psi_{q_{des}}) \tag{5.16a}$$

$$\theta_{q_{des}} = \frac{1}{g}(\ddot{x}_{1,des}\cos\psi_{q_{des}} + \ddot{x}_{2,des}\sin\psi_{q_{des}}) \tag{5.16b}$$

The desired velocities for the roll and pitch are $p_{des} = 0$ and $q_{des} = 0$. The yaw is determined by the trajectory generator as follows:

$$\psi_{des} = \psi_{tr}(t) \tag{5.17a}$$

$$x_{des} = \dot{\psi}_{tr}(t) \tag{5.17b}$$

The trajectory controller is designed to follow complex 3D paths with moderate accelerations under the assumption that the UAV is hovering nearby. If the assumptions are valid and the system is linear with no saturation in inputs, the controller that generates the desired acceleration will drive the error towards zero exponentially. However, if the commanded path is too complex to follow precisely due to errors in the model or limitations on input thrust, a modification to the controller is proposed. This modification involves determining the closest point on the desired trajectory to the current position and using it to define the position and velocity errors. The unit tangent vector along the trajectory is found, and the unit normal and bi-normal vectors are then derived by differentiating the tangent vector with respect to time or arc length. The desired acceleration is then calculated using a PD feedback loop, as described in (5.18). Finally, the desired roll and pitch angles are computed using (5.17). Further details can be found in [63].

$$e_{p_c} = ((\mathbf{x}_{tr} - \mathbf{x}_q).\hat{n})\hat{n} + ((\mathbf{x}_{tr} - \mathbf{x}_q).\hat{b})\hat{b} \tag{5.18a}$$

$$e_{v_c} = (\mathbf{x}_{tr} - \mathbf{x}_q) \tag{5.18b}$$

$$(\dot{x}_{tr} - \dot{\mathbf{x}}_{des}) + \mathbf{k}_d\mathbf{e}_v + \mathbf{k}_p\mathbf{e}_p = 0 \tag{5.18c}$$

5.3.4 Trajectory design

Various trajectory paths can be developed using minimum snap, constructed by combining polynomials representing the motion between a pair of waypoints w_0 to w_n in a known duration. These trajectories can be designed for various shapes including, circular, diamond shape, helical and rectangular. Details on the trajectory generation can be found in

[368]. Using the equations presented above, we implemented two quadrotor controls and simulated scenarios for diamond and helix circle trajectories

5.4 Evasive Quadrotor Target

To test the effectiveness of the 3D UAV target tracking algorithm developed in Chapters 3 and 4, we designed a 3D evasive quadrotor to evade, while the UAV persistently tracks the target. We develop a quadrotor heuristic evasion algorithm, by assuming that the quadrotor is aware of the position and velocity of the UAV and then implement an algorithm to aid the quadrotor evasively manoeuvre based on the distance and direction to the UAV. The first step in our algorithm is to calculate the distance and direction of the quadrotor drone to the UAV. The norm function is then used to calculate the Euclidean distance between two points in 3D space. The direction of the UAV is calculated by subtracting the quadrotor position vector from the UAV position vector and normalising the resultant vector. This is used to determine the quadrotor's movement based on the distance and direction of the UAV.

$$\mathbf{d}_{uav} = \mathbf{x}_a - \mathbf{x}_q \tag{5.19a}$$

$$\mathbf{e}_{uav} = \frac{\mathbf{d}_{uav}}{\|\mathbf{d}_{uav}\|}; \tag{5.19b}$$

where, $\mathbf{d}_{uav}$ and $\mathbf{e}_{uav}$ are the displacement and direction of the quadrotor to the UAV, while $\mathbf{x}_a$ and $\mathbf{x}_q$ are the positions of the UAV and target quadrotor respectively. The next step in the sequence of the quadrotor is determined based on its distance and direction to the UAV. If the quadrotor is far away from the UAV $\|\mathbf{d}_{uav}\| > 50$, the quadrotor maintains its current velocity, and its position is updated using the velocity $\mathbf{v}_q$ and time step Δt variables. However, if the quadrotor is close to the UAV but not too close, i.e., $\|\mathbf{d}_{uav}\| > 20$, then the quadrotor accelerates towards the UAV with a magnitude of 2 m/s and updates its velocity and position accordingly. The velocity is also constrained within feasible limits, which are defined by the $\mathbf{v}_{q_{\mathbf{max}}}$ and $\mathbf{v}_{q_{\mathbf{min}}}$ variables. When the quadrotor is very close to the UAV for instance, $\|\mathbf{d}_{uav}\| \geq 20$, then, the quadrotor accelerates away from the UAV in the opposite direction, with a magnitude of $-4m/s^2$ and updates its velocity and position. The control input and velocity constraints are given in (5.20).

$$\mathbf{u}_q = \begin{cases} 0 & \text{if } \|\mathbf{d}_{uav}\| > 50\,, \\ 2\mathbf{e}_{uav} & \text{if } \|\mathbf{d}_{uav}\| > 10 \\ -4\mathbf{e}_{uav} & \text{if } \mathbf{x}_a - \mathbf{x}_q \leq 5 \end{cases} \tag{5.20a}$$

$$\mathbf{v}_q = \begin{cases} \mathbf{v}_{qc}, & \text{if } \mathbf{v}_{q_{\mathbf{min}}} \geq \mathbf{v}_q \leq \mathbf{v}_{q_{\mathbf{max}}} \\ \mathbf{v}_{q_{\mathbf{max}}}, & \text{if } \mathbf{v}_q \geq \mathbf{v}_{q_{\mathbf{max}}} \\ \mathbf{v}_{q_{\mathbf{min}}}, & \text{if } \mathbf{v}_q \leq \mathbf{v}_{q_{\mathbf{min}}} \end{cases} \tag{5.20b}$$

where $\mathbf{u}_q$ and $\mathbf{v}_q$ are the quadrotor control input and velocity vectors respectively while $\mathbf{v}_{qc}$ is the quadrotor velocity vector at current time step. When the simulation step reaches the 50s, the quadrotor is made to perform evasive manoeuvres consisting of three different sub-manoeuvres. The first sub-manoeuvre is a dive manoeuvre, where the quadrotor accelerates downwards for a duration of 4s. The second sub-manoeuvre is a controlled stall manoeuvre, where the quadrotor accelerates upwards for a duration between 6 and 8 seconds. The third sub-manoeuvre is an escape flight manoeuvre, where the quadrotor accelerates in the opposite direction of the UAV for a duration of between 10 seconds. The quadrotor velocity and position are updated based on the acceleration, maximum and minimum velocity constraints, and the time increment Δt. Additionally, if the timer variable is equal to 200, the quadrotor performs a random side-step manoeuvre. The quadrotor generates a random acceleration vector using the *randn* function and normalises it. The quadrotor then accelerates in the direction of the normalised acceleration vector with an acceleration magnitude of $1.5 m/s^2$. The quadrotor's position, velocity, and acceleration are updated at every time step to reflect its current manoeuvre.

5.5 Safety Controller for Collision Avoidance

To ensure safety and prevent a collision between the tracker and the evader from occurring, in case of unexpected events, such as wind gusts or sudden movements of the quadrotor, a safety margin is introduced between the fixed-wing UAV and the quadrotor. The controller safety measure adjusts the heading and velocity of the fixed-wing UAV to move away from the quadrotor while maintaining a safe distance. If the distance between the quadrotor and UAV is less than the minimum safe distance d_{safe}, the UAV's course is adjusted to avoid a collision. Our collision avoidance equation utilises three inputs. These are the velocity error between the UAV current and desired collision avoidance velocity, the distance between the UAV and the quadrotor and the head heading angle errors between the UAV and the obstacle. The mathematical equation for computing the collision avoidance

command is presented below. If the positions of the UAV and the target are denoted as $\mathbf{x}_a = (x_a, y_a, z_a)$ and $\mathbf{x}_q = (x_q, y_q, z_q)$ respectively. The direction vectors of the UAV and the target can be calculated as:

$$\mathbf{e}_a = \frac{\mathbf{x}_q - \mathbf{x}_a}{\|\mathbf{x}_q - \mathbf{x}_a\|} \tag{5.21a}$$

$$\mathbf{e}_q = \frac{\mathbf{x}_a - \mathbf{x}_q}{\|\mathbf{x}_a - \mathbf{x}_q\|} \tag{5.21b}$$

where $\mathbf{e}_a$ and $\mathbf{e}_q$ are the UAV and quadrotor target directions respectively. To ensure collision avoidance by adjusting the UAV's direction and increasing the error in terms of direction between the UAV and the target, we compute the heading error and formulate the control equation:

$$\theta_{\text{err}} = \arccos\left(\frac{\mathbf{e}_a \cdot \mathbf{e}_q}{\|\mathbf{e}_a\| \cdot \|\mathbf{e}_q\|}\right) \tag{5.22a}$$

$$d_{\text{err}} = \|\mathbf{x}_a - \mathbf{x}_q\| - d_{\text{safe}} \tag{5.22b}$$

$$\mathbf{u}_{\text{req}} = K_p\left(\frac{\mathbf{e}_q - \mathbf{e}_a\|\mathbf{e}_a - \mathbf{e}_q\|}{\Delta t}\right) + K_h\theta_{\text{err}} + K_d d_{\text{err}}\mathbf{e}_a \tag{5.22c}$$

where θ_{err} and d_{err} are the heading and distance errors respectively. Alternatively, we can also compute the collision avoidance command utilising the heading error in the PD controller to compute the required acceleration $\mathbf{u}_{\text{req}}$ as follows:

$$\mathbf{v}_{\text{des}} = \mathbf{e}_q v_{\max} \tag{5.23a}$$

$$\mathbf{v}_{\text{err}} = \mathbf{v}_{\text{des}} - \mathbf{v}_a \tag{5.23b}$$

$$\mathbf{u}_{\text{req}} = K_p\mathbf{v}_{\text{err}} + K_d\left(\frac{\mathbf{v}_{\text{des}} - \mathbf{v}_a}{\Delta t}\right) + K_h\theta_{\text{err}} \tag{5.23c}$$

where $K_h\theta_{\text{err}}$ represents the influence of the heading error θ_{err} controlled by the proportional gain K_h in the PD controller. This term adjusts the required acceleration based on the heading error to further refine collision avoidance manoeuvres. Also, $\mathbf{d}_q$ is the quadrotor distance vector, $\mathbf{v}_{des}$ is the desired velocity, and $\mathbf{v}_{err}$ is the error between the desired velocity and the current velocity of the UAV $\mathbf{v}_a$. The required acceleration of the UAV is $\mathbf{u}_{\text{req}}$ and $\mathbf{u}_{\text{prev}}$ is the previous acceleration, while the parameters k_p and k_d are the PD controller gains. The parameter Δt is the time step used in computing the required acceleration control.

5.6 Adaptive Optimisation

In this section, we present a method for implementing an online adaptive optimisation algorithm for a UAV-quadrotor system that is commonly used for aerial surveillance, reconnaissance, and other applications. The goal of online adaptive optimisation is to adjust the control parameters of a system in real time based on its current state. The modified hybrid optimal-adaptive control strategy will enhance target tracking robustness and achievement of improved performance. To this end, we consider the optimisation parameters v_{min}, v_{max}, r_{min}, and n_{sample}. We consider two ways of adaptively optimising the UAV performance as follows:

5.6.1 Heuristic adaptive optimisation

To achieve online adaptive optimisation, we have designed the optimise-performance function that adjusts the values of the optimisation variables based on the current state of the simulation. We use a simple approach for optimisation as follows:

$$\begin{bmatrix} v_{\min_{Op}} \\ v_{\max_{Op}} \\ r_{\min_{Op}} \\ n_{\text{sam}_{Op}} \end{bmatrix} = \begin{cases} \begin{bmatrix} v_{a_{\min}} - 1 & v_{a_{\max}} - 1 & r_{\min} + 0.5 & n_{\text{sam}} + 50 \end{bmatrix}^T & \text{if } d < 10 \\ \begin{bmatrix} v_{a_{\min}} + 1 & v_{a_{\max}} + 1 & r_{\min} - 0.5 & n_{\text{sam}} - 50 \end{bmatrix}^T & \text{if } d > 20 \\ \begin{bmatrix} v_{a_{\min}} & v_{a_{\min}} v_{a_{\max}} & r_{\min} & n_{sam} \end{bmatrix}^T & \text{otherwise} \end{cases} \tag{5.24}$$

$$v_{\min_{Op}} = \max(v_{\min_{Op}}, -10) \tag{5.25a}$$
$$v_{\max_{Op}} = \min(v_{\max}, 20) \tag{5.25b}$$
$$r_{\min_{Op}} = \max(r_{\min_{Op}}, 1) \tag{5.25c}$$
$$n_{\text{sam}_{Op}} = \max(n_{\text{sam}_{Op}}, 50) \tag{5.25d}$$

where $v_{a_{\min}}, v_{a_{\max}}, r_{\min}, n_{\text{sam}}$ are the initial values of the UAV minimum and maximum velocities, minimum turn radius and the number of control space search samples respectively. While, $v_{\min_{Op}}, v_{\max_{Op}}, r_{\min_{Op}}$ and $n_{\text{sam}_{Op}}$ are the adaptively optimised values, d is the distance between UAV and target.

Using (5.24), if the distance between the UAV and quadrotor is less than 10m, we decrease the minimum and maximum velocities of the UAV by 1m/s, increase the minimum range of the quadrotor by 0.5, and increase the number of samples by 50. If the distance is greater than 20m, we increase the minimum and maximum velocities of the UAV by 1m/s, decrease the minimum range of the quadrotor by 0.5, and decrease the number of samples by 50. Otherwise, we keep the values of optimisation variables unchanged. Regardless of

the relative distance between the UAV and quadrotor, the values of optimisation variables must satisfy some constraints in (5.25). These equations enable the adjustment of the UAV control parameters in real time, based on the current state of the simulation and target behaviour, thus achieving optimal performance for the system.

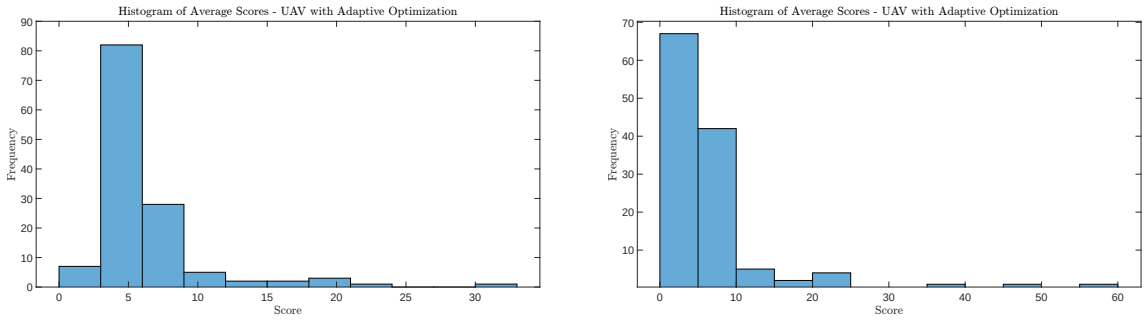

(a) Adaptively optimised performance score (b) Original optimised performance score

Fig. 5.2 Comparing original and adaptively optimised performance scores

Comparing the results from Fig. 5.2. A performance analysis was conducted to compare the original and adaptively optimised UAV controllers. The performance analysis showed that the UAV with adaptive optimisation showed better performance than the UAV with no optimisation. This does not show a strong improvement on the original algorithm. Hence, the adaptive optimisation was reviewed and updated to a PD controller type as discussed in the next subsection.

5.6.2 PD adaptive optimisation

The UAV tracking parameters can be adaptively optimised to perform better based on the current positions of the UAV and the quadrotor. A predictive PD controller is used to adjust the original target tracking parameters in real time and improve the performance of the UAV system. We utilise the UAV and quadrotor positions, $\mathbf{x}_a$ and $\mathbf{x}_q$, as well as the maximum UAV velocity and acceleration $v_{a_{\max}}$ and $u_{a_{\max}}$ to compute the required velocity and acceleration.

$$\mathbf{v}_{\mathrm{r}} = \mathbf{v}_a - \mathbf{v}_q \tag{5.26a}$$

$$v_{\mathrm{des}} = \mathbf{e}_{\mathrm{uav}} \times v_{a_{\max}} \tag{5.26b}$$

$$x_{\mathrm{pr}} = \mathbf{x}_a + \mathbf{v}_a \times t_{\mathrm{prd}} \tag{5.26c}$$

$$d_{\mathrm{pr}} = \left| \mathbf{x}_q - x_{\mathrm{apr}} \right| \tag{5.26d}$$

$$v_{\mathrm{rpr}} = \mathbf{v}_q - \left(\mathbf{v}_a + \mathbf{v}_{\mathrm{r}} \times t_{\mathrm{pr}} \right) \tag{5.26e}$$

where v_{r} is the relative velocity, v_{des} is the desired UAV velocity, while x_{prd}, d_{prd} and v_{rpr} are the predicted UAV position, distance and relative velocity between the quadrotor and

the predicted position of the UAV. The velocity error between the desired velocity and the current UAV velocity is calculated as follows:

$$v_{\text{aerr}} = v_{\text{des}} - \mathbf{v}_a + k_{\text{d}} \times v_{\text{rpr}} \tag{5.27a}$$

$$u_{\text{areq}} = k_{\text{p}} \times \left(v_{\text{aerr}} + k_{\text{d}} \times \frac{(v_{\text{aerr}} - v_{\text{aerrp}})}{t_{\text{pr}}} \right) \tag{5.27b}$$

where v_{aerr} is the error between the predicted velocity and the current velocity and u_{areq} is the required acceleration of the UAV, computed using the PD controller while v_{aerrp} is the previous velocity error. The control input calculated is updated as follows:

$$\mathbf{u}_{a_p} = \begin{cases} \dfrac{\mathbf{u}_{\text{areq}}}{|\mathbf{u}_{\text{areq}}|} \times u_{a_{\max}} & \text{if } |\mathbf{u}_{\text{areq}}| > u_{a_{\max}} \\ \mathbf{u}_{\text{areq}} & \text{otherwise} \end{cases} \tag{5.28}$$

where $\mathbf{u}_{a_p}$ is the updated constrained control input of the UAV. The velocity is computed as $\mathbf{v}_{req}$ and constrained to the maximum velocity as follows:

$$\mathbf{v}_{req} = \mathbf{v}_a + \mathbf{u}_{a_p} \times t_{prd} \tag{5.29a}$$

$$\mathbf{v}_{a_p} = \begin{cases} \dfrac{\mathbf{v}_{req}}{|\mathbf{v}_{req}|} \times v_{a_{\max}} & \text{if } |\mathbf{v}_{req}| > v_{a_{\max}} \\ \mathbf{v}_{req} & \text{otherwise} \end{cases} \tag{5.29b}$$

where $\mathbf{v}_{a_p}$ is the updated UAV velocity which is constrained to operate with maximum limits.

5.7 Performance Evaluation

In this section, we present 3 performance evaluation methods based on energy consumption, performance score metric, and performance during wind disturbance. We evaluated the performance of the tracking UAV under different scenarios, by varying its speed as well as the manoeuvre of the quadrotor. These are discussed in the following subsections.

5.7.1 Energy consumption assessment

One of the methods of assessing the performance of the tracking UAV against a manoeuvring target is by using the energy consumption metric. The UAV generally incorporates several energy-consuming components, including, data processing, communication, internal and external loads as well as motor controls [113]. For this research, we are only considering the energy consumption by the motor controls during various phases of the

tracking mission. To Calculate the total energy consumed by the UAV, we assume that the energy consumed is proportional to the distance travelled by the UAV during its flight. We compute the distances covered at various speeds and the time interval at maximum velocity, cruise travel by the UAV and while manoeuvring at maximum velocity,. The various phases considered in the energy consumption computation are presented below.

Energy consumed at maximum velocity. The energy consumed by the UAV while travelling at maximum velocity during the tracking mission can be computed using the equation in (5.30)

$$E_{v_{\max}} = \frac{1}{2}\left(\frac{{v_{a_{\max}}}^2}{u_{a_{\max}}}\right) \tag{5.30}$$

where $E_{v_{\max}}$ represents the energy consumed while flying at maximum velocity.

Energy during deceleration. Next, we consider that the UAV will decelerate in response to target deceleration, hover or abrupt turn. The equation for computing the energy consumed in this phase is given in (5.31)

$$t_{stp} = \frac{v_{a_{\max}}}{u_{a_{\max}}} \tag{5.31a}$$

$$E_{dec} = \frac{1}{2}\left(\frac{{v_{a_{\max}}}^2}{u_{a_{\max}}}\right) \times t_{stp} \tag{5.31b}$$

where t_{stp} is the time taken to decelerate from maximum velocity to minimum velocity and E_{dec} represents the energy consumed during the deceleration phase.

Energy consumed during travel. At some point during the target tracking mission, the UAV would operate at cruise speed. This will occur if the target being tracked travels continuously along a straight line. Accordingly, the energy consumed during cruise travel is computed using the set of equations in (5.32) below.

$$d_{dec} = 0.5 \times u_{a_{\max}} \times t_{stp}^2 \tag{5.32a}$$

$$d_{drd} = d_{rem} - d_{dec} - r_{tgt} \tag{5.32b}$$

$$E_{trv} = (d_{drd} \times u_{a_{\max}}) \tag{5.32c}$$

where d_{trv} is the distance travelled during the travel phase, d_{drd} is the remaining distance after deceleration and the target radius r_{tgt} while d_{dec} is deceleration distance and d_{rem} is the distance remaining from the current position to the target position. The energy

consumed during the travel phase is given as E_{trv}.

Energy during close manoeuvres. During the close manoeuvre, the UAV will take quick actions in response to target evasion. The energy utilised by the UAV during this phase of the mission can be computed using the equations in (5.33).

$$t_{ttg} = \frac{d_{rem}}{\|v_{a_i}\|} \tag{5.33a}$$

$$t_{vmx} = \begin{cases} \frac{d_{drd}}{v_{a\,\max}} & \text{if } d_{drd} > 0 \\ 0 & \text{otherwise} \end{cases} \tag{5.33b}$$

$$E_{tgt} = \frac{1}{2} \times ({r_{tgt}}^2 \times u_{a_{\max}}) \tag{5.33c}$$

where t_{ttg} is the time to target, t_{vmx} is the time during which the UAV is operating at maximum velocity and E_{tgt} represents the energy consumed during a close manoeuvre to the target.

Total energy consumed. Having computed the energy consumed during the various phases of the tracking mission, we now sum up to obtain the total energy expended for the scenario under consideration as shown in (5.34).

$$t_{tot} = t_{stp} + t_{ttg} + t_{vmx} \tag{5.34a}$$

$$E_{tot} = \sum_{t} (E_{v_{\max},t} + E_{dec,t} + E_{trv,t} + E_{tgt,t}) \tag{5.34b}$$

where t_{tot} is the total time of travel and E_{tot} represents the total energy consumed during the simulation.

To assess the performance of the PD adaptive controller, the UAV and target initial conditions were randomly varied within allowable limits and used to run 100 Monte Carlo simulations in which the energy consumed by the UAV in tracking the target was collated. The results are shown in the histograms in the Fig. 5.3

A comparison of the two histograms shows that the energy expenditure by the adaptively optimised UAV where concentrated within a few bars while the original algorithm had a broader spread including higher value bars. This indicates that the energy consumed by the UAV when utilising the original tracking algorithm is more than that consumed by the adaptively optimised algorithm.

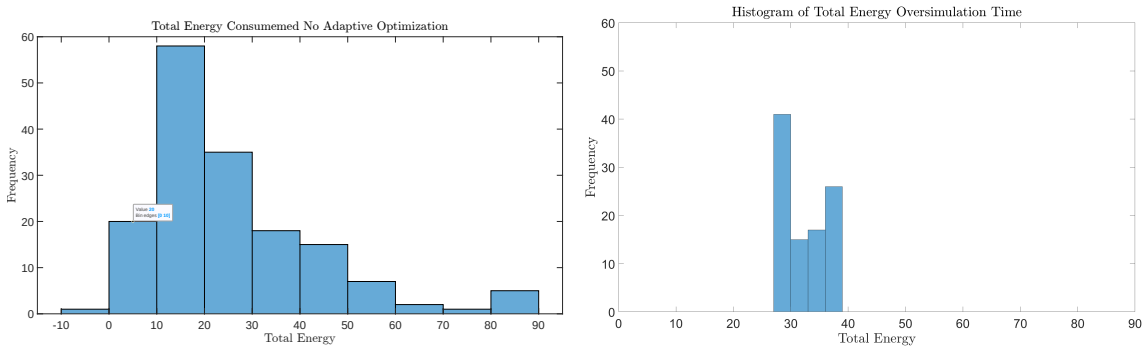

(a) Original - energy consumed (b) Adaptive - energy consumed

Fig. 5.3 Comparing original and adaptively optimised performance scores

#	Algorithm Type	Average energy	Average score	Average area
1	Original Algorithm	10.5	0.78	150
2	Adaptive Algorithm	8.9	0.92	175

Table 5.1 Comparison of average energy, performance score, and area covered by UAV to target

5.7.2 UAV performance metric score

In addition to the energy assessment presented above, we devised a second performance metric to further assess the UAV tracking algorithm over time. The performance score metric will compare the distance between the UAV and the target in the previous step with the relative distance at the current step while taking into consideration the velocity utilised in closing the relative distance as shown in (5.35).

$$t_{a_{\textbf{score-1}}} = \sum_{t} \left(1 - \frac{\|d_{\text{prv}}\| - \|d_{\text{cur}}\|}{\|d_{\text{prv}}\|}\right) \times \frac{\|\mathbf{v}_a\|}{\|\mathbf{v}_{a_{\max}}\|} \tag{5.35}$$

where d_{prv} is the distance covered in the previous time step and d_{cur} is the distance in the current step. A higher score implies that the UAV was more effective in tracking and closing the distance to the evasive target throughout the tracking scenario. It signifies that the UAV successfully reduced the distance to the evasive target, covered more distance relative to the maximum possible velocity, and accomplished a better percentage reduction in distance. Using this performance score, we compared the original and adaptively optimised UAV tracking algorithms and obtained their scores over 100 Monte Carlo simulations as shown in Fig. 5.4. Details of the comparison between the original and adaptive code are shown in Table 5.1.

From the histograms comparing the adaptively optimised UAV tracking algorithm with the original algorithm as shown in Fig. 5.4, it can be observed that the adaptively optimised

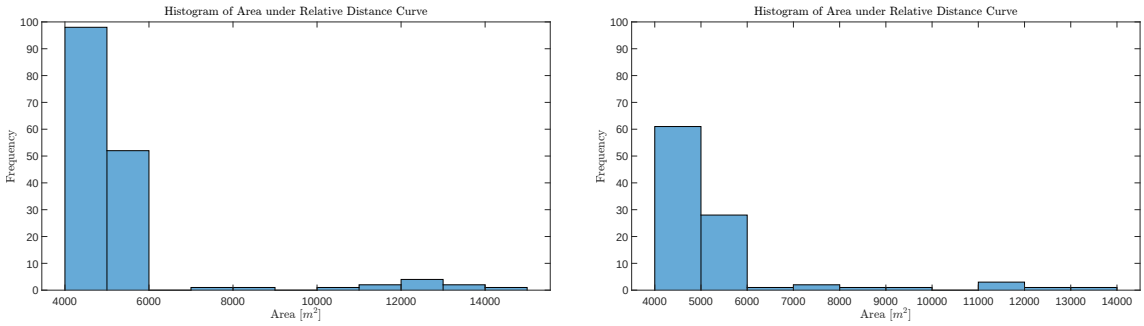

(a) Adaptive optimised performance score (b) Original optimised performance score

Fig. 5.4 Comparing original and adaptive optimised performance scores

UAV performed better in various scenarios in terms of energy consumption. The energy conservation is due a more precise tracking, reducing the distance travelled in each phase and the number of energy-sapping manoeuvres done by the UAV using the original algorithm in histogram Fig. 5.4b. This performance improvement by the adaptively optimised UAV is also seen in the histogram

5.7.3 Performance evaluation in wind disturbance

We also introduce a 5s wind gust to test how well the UAV recovers to tracking the target when displaced by a sudden wind gust. To score the UAV's performance, we used the ratio of the relative distance to the UAV's velocity as in (5.36).

$$t_{a_{\textbf{score-2}}} = \frac{\|d_{uav}\|}{\|\mathbf{v}_a\|} \tag{5.36}$$

The area histograms comparing the UAV tracking performance over 100 Monte Carlo simulations are as shown Fig. 5.5. Fig. 5.5a on the left shows tracking performance by the UAV without wind disturbance while Fig. 5.5b shows the tracking performance by the UAV when a short wind gust disturbance was introduced.

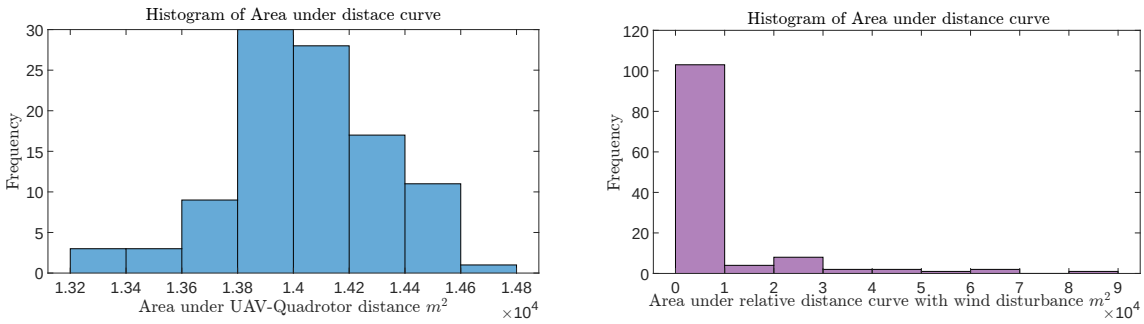

(a) Area - distance curve without disturbance (b) Area - distance curve with disturbance

Fig. 5.5 Histograms evaluating UAV performance against quadrotor target

The results show that the UAV tracking algorithm is robust to different scenarios and can track the quadrotor's trajectory accurately.

5.8 Scenario Simulations and Results

In this section, we test the performance of the UAV algorithm against non-manoeuvring and evasive moving quadrotors. The trajectories result from the behaviour of both vehicles. The simulation is executed on a Windows 10 computer running with an Intel Core i5 Processor and 32 GB of Memory. The UAV minimum turn radius, $r_{\min}$, is set at 10m with the velocity limits of $v_{a_{\min}} = 5$m/s and $v_{a_{\max}} = 10$m/s. Similarly, the respective minimum and maximum acceleration limits of the UAV along x, y, and z axes are as follows:

$$
\begin{aligned}
u_{ax_{\min}} &= -5\ [\text{m/s}^2],\ u_{ax_{\max}} = 5\ [\text{m/s}^2],\\
u_{ay_{\min}} &= -2\ [\text{m/s}^2]\ , u_{ay_{\max}} = 5\ [\text{m/s}^2],\\
u_{az_{\min}} &= -0.2\ [\text{m/s}^2],\ u_{az_{\max}} = 0.5\ [\text{m/s}^2]
\end{aligned}
$$

The target velocity limits is set to $v_{g_{\max}} = 7m/s$, while its respective acceleration limits along x, y,and z axes are as follows:

$$
\begin{aligned}
u_{qx_{\min}} &= -2\ [\text{m/s}^2],\ u_{qx_{\max}} = 5\ [\text{m/s}^2],\\
u_{qy_{\min}} &= -2\ [\text{m/s}^2],\ u_{qy_{\max}} = 2\ [\text{m/s}^2],\\
u_{qz_{\min}} &= -0.2\ [\text{m/s}^2],\ u_{qz_{\max}} = 0.4\ [\text{m/s}^2]
\end{aligned}
$$

5.8.1 UAV tracking target following predefined paths

To simulate mission scenarios where the UAV is tracking a target following a predefined helix trajectory path, we initiated the target at position [5, 0, 0], while the UAV was initiated at a [5, 5, 2].

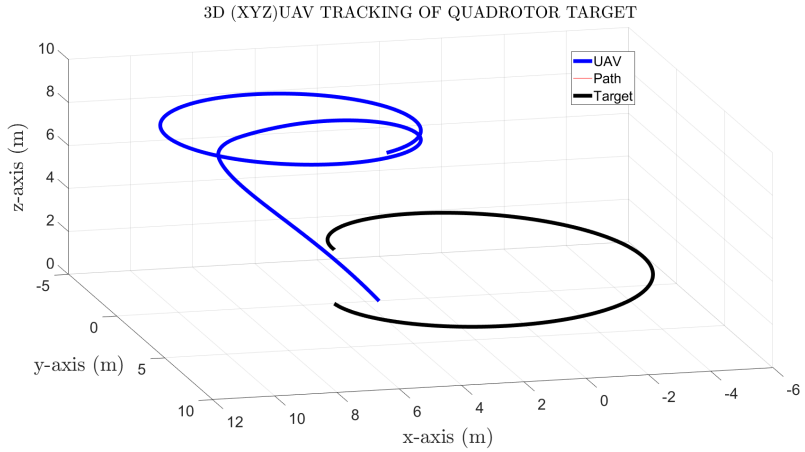

Fig. 5.6 UAV tracking helix path following quadrotor.

We also simulated a mission scenario where the UAV tracks a quadrotor target following a predefined diamond trajectory path with the UAV and target starting at the same positions as in the helix path scenario.

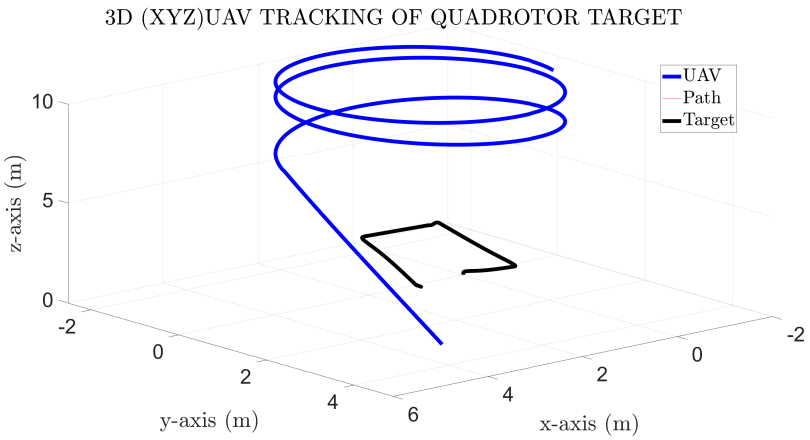

Fig. 5.7 UAV tracking helix path following quadrotor.

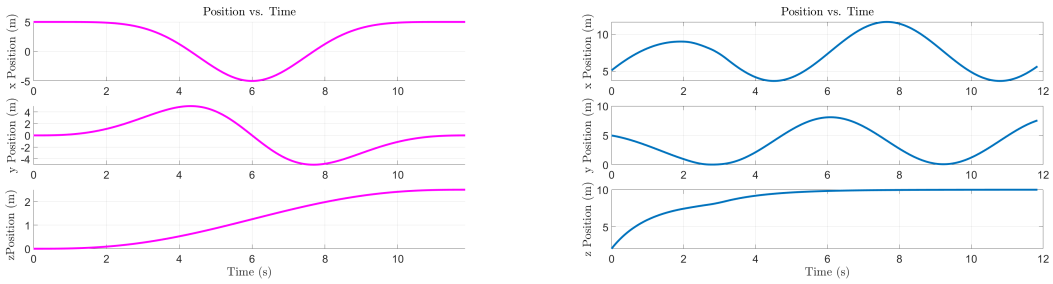

(a) Quadrotor position (b) UAV position

Fig. 5.8 Comparison of quadrotor and UAV positions

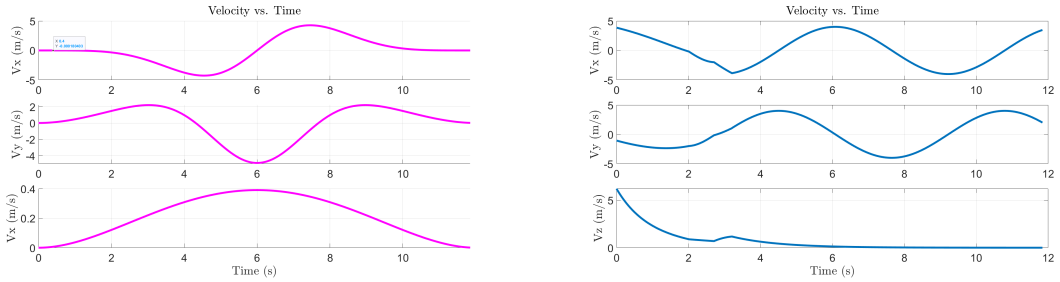

(a) Quadrotor velocity

(b) UAV velocity

Fig. 5.9 Comparison of quadrotor and UAV velocities

From Figs. 5.6 and 5.7, we observe that the target follows the helix and diamond path, steadily flying upward. To track the target effectively, the UAV is observed to fly upward with an angle within the limits of the maximum FPA. The UAV trajectory shows that it tracks the target position at each time step but does not follow the quadrotor predefined path. When the UAV reaches the desired altitude, it flies in a circular path while maintaining optimal tracking distance and keeping the quadrotor within its FOV. Comparing plots of the quadrotor path, Fig. 5.8a and UAV Fig. 5.8b position in the x, y, and z direction, we see the UAV is manoeuvring in response to the target's path tracking manoeuvre. These responses are also observed in the quadrotor and UAV velocities as shown in Fig. 5.9a and UAV Fig. 5.9b, indicating that the UAV responds to the path changes by the quadrotor target.

5.8.2 UAV tracking evading aerial target

To simulate mission scenarios where the UAV is tracking a simple evading target, the UAV minimum turn radius, $r_{\min}$, is set at 10m with the velocity limits of $v_{a_{\min}} = 5$m/s and $v_{a_{\max}} = 10$m/s. Similarly, the respective minimum and maximum acceleration limits of the UAV along x, y, and z axes are as follows:

$$
\begin{aligned}
u_{ax_{\min}} &= -5\ [\mathrm{m/s^2}],\ u_{ax_{\max}} = 5\ [\mathrm{m/s^2}],\\
u_{ay_{\min}} &= -2\ [\mathrm{m/s^2}]\ , u_{ay_{\max}} = 5\ [\mathrm{m/s^2}],\\
u_{az_{\min}} &= -0.2\ [\mathrm{m/s^2}],\ u_{az_{\max}} = 0.5\ [\mathrm{m/s^2}]
\end{aligned}
$$

The target velocity limits is set to $v_{g_{\max}} = 7m/s$, while its respective acceleration limits along x, y,and z axes are as follows:

$$u_{qx_{\min}} = -2\ [\text{m/s}^2],\ u_{qx_{\max}} = 5\ [\text{m/s}^2],$$
$$u_{qy_{\min}} = -2\ [\text{m/s}^2],\ u_{qy_{\max}} = 2\ [\text{m/s}^2],$$
$$u_{qz_{\min}} = -0.2\ [\text{m/s}^2],\ u_{qz_{\max}} = 0.4\ [\text{m/s}^2]$$

The simulation time was set to 60s in time steps of 0.1, resulting in a time vector of 600 steps.

Scenario 1: Tracking a quadrotor climbing at an angle.

In the first scenario, we implement the quadrotor at the initial position of $[0,0,0]$ and fly at a constant angle and velocity upward. The UAV is initiated with states as described earlier and position $[20,30,20]$. At the start of the simulation, the UAV flies downwards so to maintain the desired altitude separation of 10m above the quadrotor. However, as the target flies upwards the UAV is forced to adjust its trajectory back upward at an angle allowed by the design constraint. The continued upward flight of the quadrotor results in continuous adjustment and controlled manoeuvres by the UAV to keep the target within its FOV.

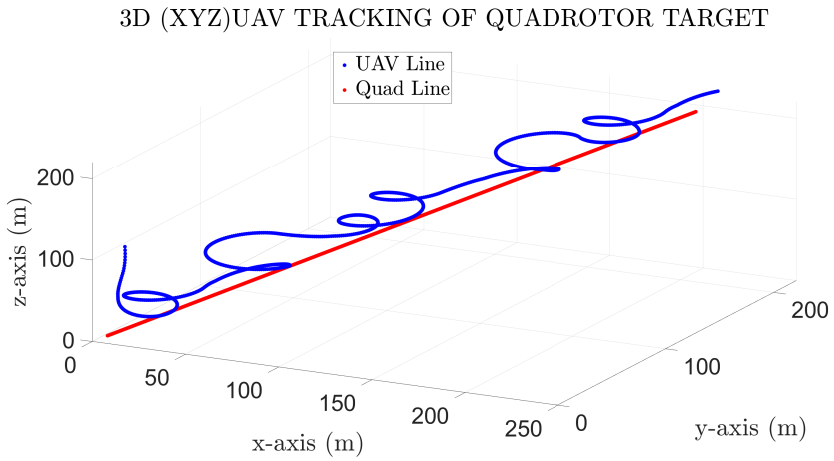

Fig. 5.10 UAV tracking a fast quadrotor.

Scenario 2: Tracking a quadrotor following a Z-shaped path and hovering at a predefined altitude.

In the second scenario Fig.5.11, the quadrotor starts at the origin and makes a z-like manoeuvre, hovering at instances during the flight. The UAV was observed to track the target quadrotor, following a circular path at the target's first hover point. When the quadrotor accelerates upward, the UAV quickly makes a turn, climbing in the process

to close up with the target, while maintaining the required separation distance. Having attained the desired altitude, the UAV is observed to fly in a circular path around the hovering quadrotor until the end of the simulation.

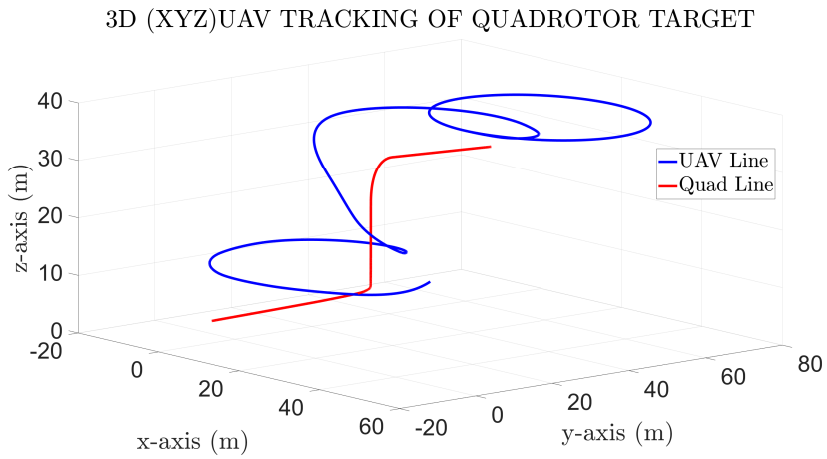

Fig. 5.11 UAV tracking a fast quadrotor making a z-manoeuvre.

Scenario 3: Tracking an evasive quadrotor in 3D space.

Using the same initial conditions in scenario 1, the quadrotor controller was modified to persistently evade the tracking UAV in 3D space. The UAV's goal is to maintain pursuit while observing a minimum distance of 20m above the target to enable FOV coverage and prevent a collision.

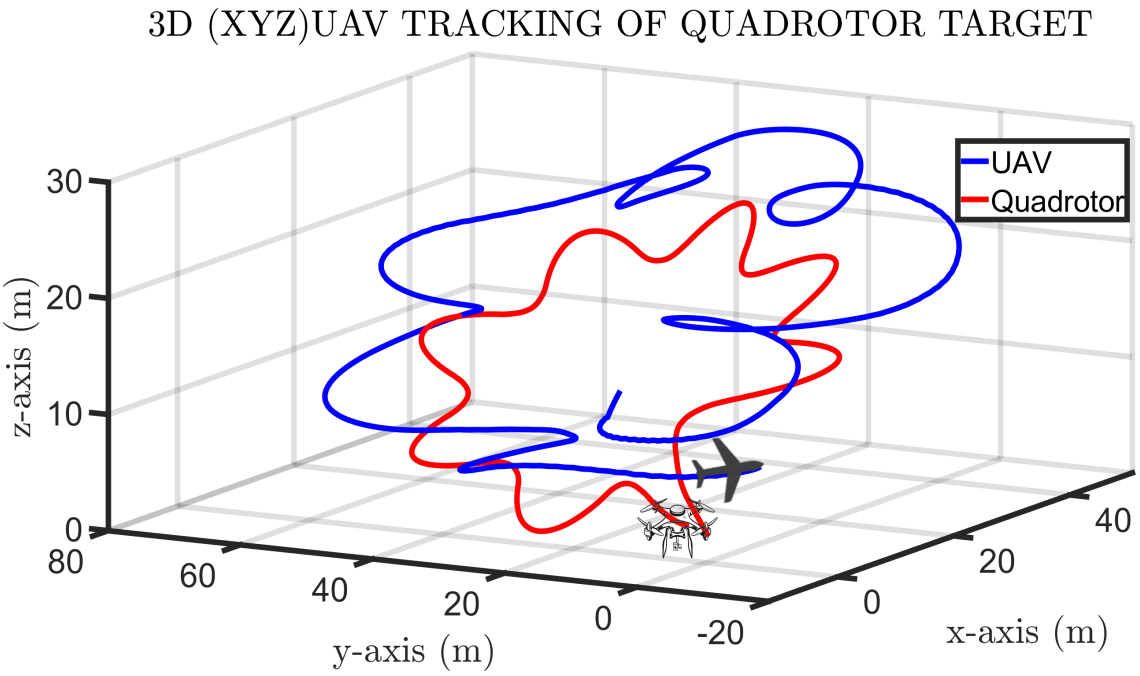

Fig. 5.12 UAV tracking an evasive quadrotor

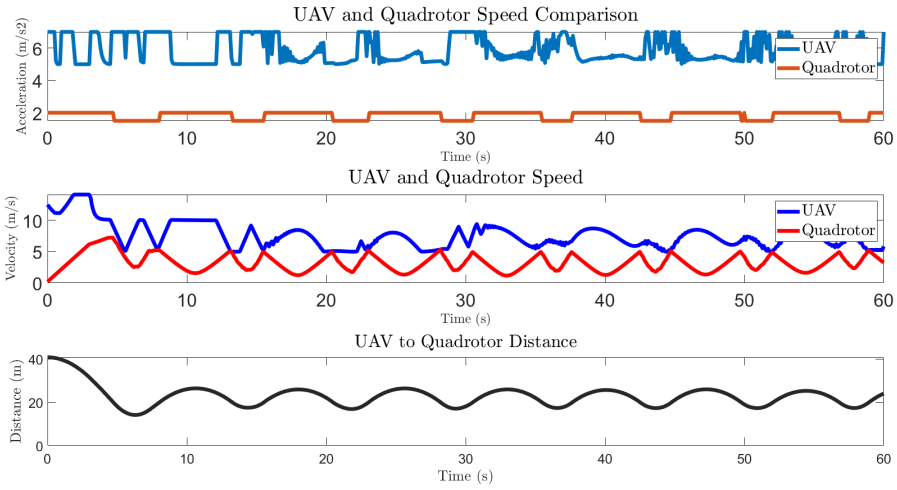

Fig. 5.13 UAV and target state parameters and relative distance

As shown in the trajectory plots in Fig.5.12, it is observed that the quadrotor takes evasive manoeuvres, flying upward and then making evasive turns leading to a downward manoeuvre. The UAV's response was a quick change in direction to close up with the quadrotor while maintaining the required altitude separation from the quadrotor. The comparison of the UAV and quadrotor acceleration and velocity as shown in Fig.5.13, shows the target maintaining a sequence of increase and decrease in acceleration while the UAV is forced to make rapid control input changes to change direction and close up with the quadrotor target. This trend is also observed in the velocity magnitudes of the UAV and quadrotor, indicating the pursuit and evasion of manoeuvres. The UAV can be observed to increase velocity while closing up to the target. The velocity is clipped when it reaches the maximum feasible limit of the UAV design.

To check the effectiveness of the UAV control, the relative distance between the UAV and the target is included in Fig.5.13 and shows an increase in separation distance when the target evades the UAV. The UAV quickly closes up to the target resulting in minimised separation. The process is repeated for every manoeuvre by the quadrotor, resulting in an undulating relative distance curve.

5.9 Analysis and Discussion

The simulation results for UAV tracking targets in various scenarios, starting from simple manoeuvres to more comprehensive evasion strategies indicate clearly that the UAV algorithm is sufficient for the tracking and target pursuit. When collision avoidance was applied, the controller showed that the fixed-wing UAV was able to track the quadrotor

safely while avoiding collision5.5a. With the application of adaptive optimisation, the tracking performance was observed to improve. To be sure that the results obtained are representative of the general mission scenarios, we conducted 100 Monte Carlo simulations with UAV and quadrotor initial positions and velocities varied randomly within feasible bounds. The histogram used to report the Monte Carlo simulations were generated by integrating the area under the UAV-quadrotor relative distance plot, which represents the total distance travelled by the UAV relative to the target during the simulation. The spread of the histogram bars as observed in Figs. 5.3 and 5.4 showed that the majority of simulations produced similar area values, implying that the UAV travelled a relatively consistent distance relative to the target. The shorter bars near the histogram's edges represent simulations that produced extreme area values, either significantly higher or lower than the majority of simulations. With more variation and the introduction of wind gust disturbance for 5s during the simulation, the area and performance plots showed clustered bars towards the left of Fig. 5.5, indicating that the UAV was performing consistently well at tracking the quadrotor with controlled speed. The few bars towards the right of the histogram show where the UAV applied more speed to reach the target. In terms of potential applications, the proposed approach has several practical uses in real-world scenarios. For example, the proposed approach can be used for surveillance and monitoring of aerial targets, such as quadrotors, gliders, birds, and other fixed-wing UAVs.

Future research could implement extensions to improve the proposed approach. Firstly, the proposed approach can be extended to track multiple aerial objects simultaneously, which would require the use of multiple UAVs mounted with cameras, other sensors such as lidar or radar, to improve tracking accuracy in adverse weather conditions, and advanced algorithms for object tracking and classification.

5.10 Summary

In this Chapter, we designed an evasive quadrotor algorithm to test the effectiveness of the UAV tracking algorithm against an evasive quadrotor-type target. Target evasion algorithms were designed for 3 scenarios, straight-line accelerated evasion, hover and evade manoeuvre, and continuous aerial evasion. To Prevent the UAV from colliding with the evasive target during aerial pursuit and evasion, we modified the UAV control algorithm designed in Chapters 3 and 4, to incorporate anti-collision measures. To further improve on the tracking algorithm, we introduced an adaptive optimisation and formulated a hybrid optimal-adaptive algorithm that utilises the optimisation parameters to optimise the control of the UAV which is dependent on the relative distance of the UAV from the target. We also designed a performance metric of energy consumption and time-to-target metrics to

assess the effectiveness of the UAV in tracking the target. The energy consumption metric was used to compare the original and adaptively optimised algorithm and the simulation results show that the adaptively optimised algorithm performed better in all scenarios. In Chapter 6, we extend our research by exploring cooperative tracking using multiple UAVs to track a single aerial target.

Chapter 6

Multi UAVs Evasive Quadrotor Tracking

6.1 Introduction

In Chapter 5, we discussed tracking an evasive target using a single UAV by designing a quadrotor model with an evasion strategy. We applied some modifications to the UAV control strategy developed in Chapters 3 & 4 and performed various simulations to test the performance of our control strategy against the target in ideal and disturbed environments. In this Chapter, we extend the research by looking into the tracking problem using multiple tracking UAVs. The main question we intend to answer is, how can our fixed-wing UAV control strategy be applied cooperatively to track an evasive target(s) while avoiding collisions? This is an important question because cooperative UAV tracking provides extended range and endurance for continuous tracking of evasive targets that may attempt to evade detection by manoeuvring in open space or behind obstacles [106]. Additionally, cooperative UAV tracking offers better accuracy in terms of estimation and robustness and redundancy against temporary sensor or UAV failure [106, 369]. Cooperative or multi-UAV tracking has the advantage of either decentralised or collaborative decision-making for effective target tracking. We review a few research efforts related to cooperative UAV tracking using fixed-wing UAVs and present the motivation for this Chapter. Note that we use the terms muli-UAV, coordinated, and cooperative interchangeably in this Chapter when referring to a group of UAVs working together to track single or multiple targets.

6.1.1 Multi UAV tracking - related research

Ragi and Chong [370] developed a multi-UAV strategy to track evasive ground targets based on POMDP that incorporates bank angle constraints, wind disturbance, and collision avoidance. While this study addresses some of our research considerations in this Chapter,

the UAVs were however assumed to fly at a fixed altitude and the simulations considered only 2D implementation. In another related study, Quintero et al. [371] implemented an evasive target-tracking optimisation-based, min-max MPC/moving horizon estimation strategy for two fixed-wing visual UAVs tracking a moving ground target. Similarly, [372], designed a guidance law that controls the heading rate based on a Lyapunov Guidance Vector Field (LGVF), for stand-off multi-UAV tracking of a ground-moving target in unknown wind conditions. In [373], their cooperative tracking research incorporated flocking constraints, collision avoidance, and Control Barrier Functions (CBFs) to formulate an LGVF UAV controller, regulated by Quadratic Programming (QP). Like previous research, these studies were also implemented for 2D UAVs and targets. In related research, [106] implemented a vector field guidance controller for coordinated UAV tracking of ground targets. This study also investigated localisation sensitivity to the target group to enable better angular separations between the tracking UAVs. However, this research was only implemented for 2D scenarios with constant altitude and UAV operation radius.

The research effort by Choi [318] implemented a control impact point/MPC strategy for fixed-wing UAV cooperative defence against intruding adversarial swarm target drones. The UAVs were assumed to have explosives on board to intercept the intruding swarm. However, this research did not address the aspect of evasive swarm targets. In [374], they developed a controller that estimates drone target states using a 3D instantaneous velocity vector and an MPC controller for the air-to-air tracking of aerial quadrotor targets.

While these studies have made immense contributions to the literature on target tracking using multi-UAV, none of the studies in the literature considered cooperative fixed-wing multi-UAV tracking of single or multiple evasive quadrotor targets. Considering the serious security threat posed by drones operated by mischievous persons, and the need for a robust security and defence strategy, the cooperative tracking and interception of evasive drones has become paramount. Hence, addressing the research gap highlighted above will contribute to enhancing C-UAS operations. In this Chapter, we intend to address this challenge by implementing a fixed-wing cooperative tracking strategy and evasive aerial target manoeuvre control. The contributions of this Chapter are outlined in the next subsection.

6.1.2 Contributions

The main contributions of this Chapter are as follows:

- A multi-UAV tracking strategy that incorporates collision avoidance is developed for tracking aerial evasive quadrotor-type targets.

- A modified controller is designed to group and cooperatively track a swarm of uncooperative evasive aerial target targets.
- We addressed the issue of autonomously controlling the altitude for each UAV on a cooperative search mission based on their distance to the individual targets, the area of the target cluster, and the balance between optimal FOV coverage and image quality requirements.

The remaining part of this Chapter is organised as follows. In Section 6.2, we discuss the problem we will be solving in this Chapter and present a mathematical model of our multi-UAV dynamics. We then present a cooperative control strategy for single evasive target tracking in Section 6.3. In Section 6.4, we extend our multi-UAV tracking by modifying our controller to track group or clustered swarm adversarial drones. Section 6.5 discusses task assignment considerations while simulations and results for the work done in this Chapter are presented in Section 6.6. We analyse and discuss the results obtained and conclude this Chapter by summarising the main findings in Section 6.7.

6.2 Problem formulation

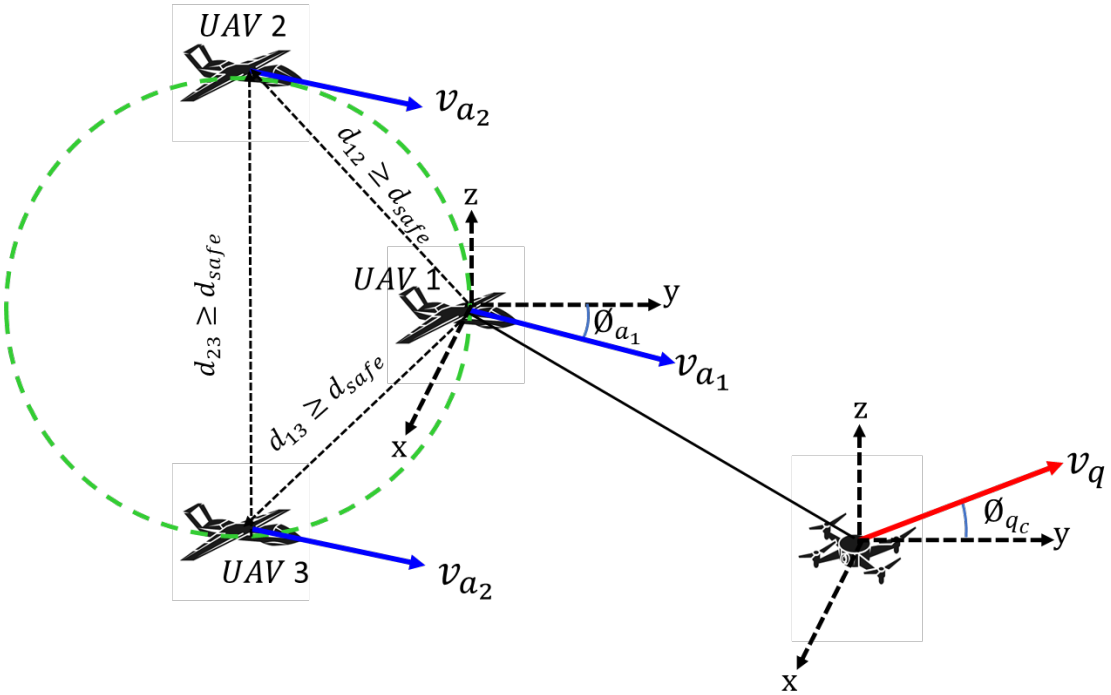

Fig. 6.1 Multi-UAV tracking single quadrotor engagement diagram

Consider a scenario, where multiple fixed-wing UAVs are used to cooperatively track an evasive moving aerial quadrotor target. This represents the tracking of non-cooperative or

adversarial targets such as Unmanned Ground Vehicles (UGVs) or drones, equipped with jamming or spoofing devices, that actively interfere with the UAVs' sensors or communication.

The UAV and target dynamics are represented as shown in Fig. 6.1. The UAV positions are represented by x_{a_i}, y_{a_i} and z_{a_i}. and the dynamic equations of the UAVs are represented by

$$\dot{x}_{a_i} = v_{ax_i}, \dot{y}_{a_i} = v_{ay_i}, \dot{z}_{a_i} = v_{az_i}, \tag{6.1a}$$

$$v_{ax_i} = \mathbf{v}_{a_i} \cos\sigma_{a_i} \sin\phi_{a_i} \tag{6.1b}$$

$$v_{ay_i} = \mathbf{v}_{a_i} \sin\sigma_{a_i} \cos\phi_{a_i} \tag{6.1c}$$

$$v_{az_i} = \mathbf{v}_{a_i} \sin\sigma_a \tag{6.1d}$$

$$\dot{v}_{ax_i} = u_{ax_i}, \dot{v}_{ay_i} = u_{ay_i}, \dot{v}_{az_i} = u_{az_i} \tag{6.1e}$$

where $(\dot{})$ is the derivative with respect to time, $\mathbf{v}_{a_i}$ is the i-th UAV velocity vector with respective components as v_{ax_i}, v_{ay_i} and v_{az_i} in the global reference frame, indicated by x-y-z in Fig. 6.1. Furthermore, σ_{a_i} and ϕ_{a_i} are the flight path and heading (course) for the i-th UAV angles respectively [328], while u_{ax_i}, u_{ay_i} and u_{az_i} are the control acceleration input of the UAV. The body frame is defined by $x_i{}^{Ba}$-yi^{Ba}-$z_i{}^{Ba}$ where $x_i{}^{Ba}$ is aligned with the UAV velocity vector, yi^{Ba} is towards the right-hand-side of the wing, and $z_i{}^{Ba}$ is given by the cross product of x_i^{Ba} and y_i^{Ba}. The state space representation is given by:

$$\dot{\mathbf{x}}_a = A_a\mathbf{x}_a + B_a\mathbf{u}_a = \begin{bmatrix} 0_3 & I_3 \\ 0_3 & 0_3 \end{bmatrix} \mathbf{x}_a + \begin{bmatrix} 0_3 \\ I_3 \end{bmatrix} \mathbf{u}_a \tag{6.2a}$$

$$\mathbf{y} = C_a\mathbf{x}_a = [I_3\, 0_3]\mathbf{x}_a \tag{6.2b}$$

where 0_3 is the 3×3 zero matrix, I_3 is the 3×3 identity matrix, A_a, B_a and C_a are defined appropriately in the above equation, $\mathbf{x}_a = [x_a, y_a, z_a, v_x, v_y, v_z]^T$ and $\mathbf{u}_a = [u_{ax}, u_{ay}, u_{az}]^T$.

6.3 Multi-UAV Cooperative Control Strategy

To persistently track an evasive quadrotor, the fixed-wing multi-UAVs are collaboratively controlled using a multi-UAV min-max optimal control strategy. A decentralised control strategy is adopted where each UAV utilises a joint cost function J_{comb} to determine optimal control action for tracking the target. The proposed cooperative control strategy aims to improve the tracking accuracy of UAVs against evasive air targets such as quadrotors while, maintaining the desired altitude above the target, avoiding collision and conserving energy

expenditure. Accordingly, the combined cost function uses a weight function to assign relative priority to the sub-functions as shown in (6.3)

$$J_{comb} = w_1 J_{tr} + w_2 J_{avd} + w_3 J_{alt} \tag{6.3}$$

where J_{comb} is the combined cost function for effective cooperative tracking by the multi-UAVs, J_{tr} is the min-max cost function to track the evasive target quadrotor, J_{avd} is the collision avoidance function to keep the UAVs from colliding with the target and maintain a safe distance between the UAVs, while J_{alt} controls the altitudes of the UAVs. The weights of the functions are represented by the constants w_1, w_2 and w_3 respectively. The weighting function for J_{comb}, determines weights based on the relative importance of each function in achieving the overall objective of the multi-UAV tracking strategy.

$$W_{comb} = w_1 + w_2 + w_3 = 1 \tag{6.4}$$

where W_{comb} is combined weight. Let us assume that we have determined the relative importance of the individual cost functions based on some domain knowledge or application-specific requirements. The sub-cost functions used in J_{comb} are discussed in more detail in the following subsections:

6.3.1 UAV tracking trajectory

This subsection highlights the cost function that tracks and closes up with the target during a mission scenario J_{tr}. This function same as the one presented in Chapter 3 for 2D target tracking with necessary adjustments made for multi-UAV tracking. Here, the main goal is to minimise the relative distance between the UAV and the target by minimising the worst-case target evasion. This cost function is presented in (6.5a).

$$\underset{\mathbf{w}(t)\in W}{\text{Maximise}} \ \underset{\mathbf{u}(t)\in U}{\text{Maximise}} \ J_{tr} = \int_{t_0}^{t_f} [y(t)i - z(t)i]^T [y(t)i - z(t)i] dt \tag{6.5a}$$

subject to

$$\dot{x}_{ai} = A_{ai} x_{ai} + B_{ai} \tag{6.5b}$$

$$\dot{x}_{ti} = B_{twi} \tag{6.5c}$$

$$y = C_{ai} x_{ai} \tag{6.5d}$$

$$z = C_t x_t \tag{6.5e}$$

and;

$$v_{a_{\min}} \leq v^2{}_{axi} + v_{ayi}^2 \leq v_{a_{\max}} \tag{6.6a}$$

$$u_{xi_{\min}} \leq u_{xi}\cos\phi + u_{yi}\sin\phi \leq u_{xi_{\max}} \tag{6.6b}$$

$$u_{yi_{\min}} \leq -u_{xi}\sin\phi + u_{yi}\cos\phi \leq u_{yi_{\max}} \tag{6.6c}$$

$$-\frac{1}{r_{\min i}}\left(v_{xi}^2 + v_{yi}^2\right)^{\frac{3}{2}} \leq v_{xi}u_{yi} - v_{yi}u_{xi} \leq \frac{1}{r_{\min i}}\left(v_{xi}^2 + v_{yi}^2\right)^{\frac{3}{2}} \tag{6.6d}$$

$$0 \leq v_{qx}^2 + v_{qy}^2 \leq v_{q_{\max}}^2 \tag{6.6e}$$

The minimum turn radius in the above equations can be set to the same value for all the UAVs, or specified for each of the UAVs to enhance collision avoidance. The cost used for the tracking in coordination with the altitude and anti-collision cost above is discussed in the succeeding paragraphs.

6.3.2 Collision avoidance

Considering that the multi-UAVs will be tracking an evasive aerial target, there is a likelihood of a collision between UAVs and the target. This is because our tracking UAVs do not operate on a fixed standoff circle with an angular separation between but more realistically track the highly manoeuvring targets independently. Our goal with collision avoidance cost function is to ensure a collision is prevented even in the event of the UAV trajectories being affected by external disturbances like wind. The avoidance cost therefore considers aspects of avoiding UAV-to-UAV collision and UAV-to-target collision as follows:

$$J_{adv} = J_{adv_{ij}} + J_{adv_{it}} \tag{6.7}$$

where $J_{adv_{ij}}$ and $J_{adv_{it}}$ are the respective functions for preventing collision between the UAVs and the target, and J_{adv} is the combined collision avoidance cost function.

Collision avoidance between UAVs. We now address the cost of avoiding collision between UAVs i and j. The cost for avoiding collision between the tracking UAVs is presented below in (6.8) :

$$J_{adv_{ij}} = \int_0^{t_f}\int_{i=1}^{N_u}\int_{j=i+1}^{N_u} \frac{k_a(v_{c_{ij}}^2)}{2d_{ij}} dt, di, dj \tag{6.8}$$

Here, t_f is the total simulation time, and we are integrating over the entire simulation period. The integral represents the average cost function $J_{adv_{ij}}$ over time, for preventing collision between the UAVs. The sum is over all unique pairs of vehicles i and j where $i < j$. N_u is the total number of UAVs, d_{ij}, $v_{c_{ij}}$ are the distance and closing velocity between UAVs

i and j respectively, k_a is a constant for the avoidance acceleration. This cost function represents the avoidance acceleration and velocity correction to prevent collisions between UAVs. The goal of minimising the potential for collisions UAV-to-UAV is achieved by maximising the minimum separation distance and is computed as follows:

$$\mathbf{d}_{ij} = \left[(x_{a_i} - x_{a_j}) \; (y_{a_i} - y_{a_j}) \right] \tag{6.9a}$$

$$\mathbf{s}_{ij} = \frac{\left[x_{a_i} \; y_{a_i} \right] - \left[x_{a_j} \; y_{a_j} \right]}{\|\mathbf{d}_{ij}\|} \tag{6.9b}$$

$$\mathbf{v}_{r_{ij}} = \left[([v_{ax_i} \; v_{ay_i}]) - ([v_{ax_j} \; v_{ay_j}]) \right] \tag{6.9c}$$

$$v_{c_{ij}} = \mathbf{v}_{r_{ij}} \cdot \mathbf{s}_{ij} \tag{6.9d}$$

where $\mathbf{d}_{ij}$, $\mathbf{s}_{ij}$, $\mathbf{v}_{r_{ij}}$ and $v_{c_{ij}}$ are the distance, separation vector, relative velocity and closing velocity between UAVs i and j respectively. The time to collision from UAV i to UAV j and the corresponding avoidance acceleration can then be computed as:

$$t_{c_{ij}} = \frac{d_{ij}}{v_{c_{ij}}} \tag{6.10a}$$

$$u_{avd_{ij}} = \frac{k_a v_{c_{ij}}^2}{2 d_{ij}} \tag{6.10b}$$

$$v_{avd_{ij}} = u_{avd_{ij}} t_{c_{ij}} \tag{6.10c}$$

where $t_{c_{ij}}$, $u_{avd_{ij}}$ and $v_{avd_{ij}}$ are the time to the collision between UAVs i and j, avoidance acceleration and correction velocity respectively. The i-th UAV velocity is adjusted by subtracting the product of the separation vector and correction velocity from its current velocity as follows:

$$v_{ax_{ni}} = v_{axi} - \mathbf{s}_{ij}(1) \times v_{avd_{ij}} \tag{6.11a}$$

$$v_{ay_{ni}} = v_{ay_i} - \mathbf{s}_{ij}(2) \times v_{avd_{ij}} \tag{6.11b}$$

where v_{ax_i} and v_{ay_i} are the x and y components of the UAV velocity with their updated values as $v_{ax_{ni}}$ and $v_{ay_{ni}}$. Having computed the UAV-to-UAV collision avoidance formula, we now address the problem of preventing collision between a tracking UAV and the aerial quadrotor target in the next subsection.

Collision avoidance between UAV and target. In the last subsection, we addressed the avoidance of collision between UAVs. In this subsection, we consider the possibility of a collision between any of the tracking UAVs and the aerial target. This could occur if a sudden wind gust pushed the UAV towards the target or vice versa. Another likelihood of

collision is that the target could intentionally try to collide with the UAV in a *kamikaze* style attack if in close proximity. We, therefore, present the cost function, $J_{adv_{it}}$, that needs to be minimised to avoid a collision between the i-th UAV and the aerial target as follows:

$$J_{adv_{it}} = \frac{1}{t_f}\int_0^{t_f} \left(k_d d_{e_{it}} \mathbf{s}_{it} \mathbf{v}_{r_{it}} + k_p s_{e_{it}} s_{d_{it}} + k_i i_{e_{it}} + \alpha_{it}(d_{it} - d_{it_o})\right) dt \tag{6.12}$$

where $d_{e_{it}}$ is the distance error, $\mathbf{s}_{it}$ is the separation vector, $\mathbf{v}_{r_{it}}$ is the relative velocity, $s_{d_{it}}$ is the desired separation vector, $s_{e_{it}}$ is the separation vector error, $i_{e_{it}}$ is the integral error, and k_d, k_p, and k_i are the gains of the PID controller. The optimal distance between UAV i and the target is given as d_{it_o}. The relative velocity $\mathbf{v}_{r_{it}}$ between UAV i and the target is calculated by subtracting the target velocity from the UAV i velocity while the closing velocity $v_{c_{it}}$ between UAV i and the target is calculated as the dot product between the relative velocity and the separation vector. The control input to correct the UAV positions is calculated as shown:

$$\mathbf{d}_{it} = [(x_{a_i} - x_q)\ (y_{a_i} - y_q)] \tag{6.13a}$$

$$\mathbf{s}_{it} = \frac{[x_{a_i}\ y_{a_i}] - [x_q\ y_q]}{\|\mathbf{d}_{it}\|} \tag{6.13b}$$

$$\mathbf{v}_{r_{it}} = \left[(v_{ax_i} - v_q)\ (v_{ay_i} - v_q)\right] \tag{6.13c}$$

$$v_{c_{it}} = \mathbf{v}_{r_{it}} \cdot \mathbf{s}_{it} \tag{6.13d}$$

The correction heading of UAV i, θ_{ci} can be computed as follows:

$$\theta_{ci} = \tan^{-1}\left(\frac{\mathbf{d}_{it}(2)}{\mathbf{d}_{it}(1))}\right) - \tan^{-1}\left(\frac{\mathbf{v}_{r_{it}}(2)}{\mathbf{v}_{r_{it}}(1))}\right) \tag{6.14a}$$

$$\mathbf{s}_{d_{it}} = [\cos(\theta_{ci})\sin(\theta_{ci})] \tag{6.14b}$$

$$\theta_{d_i} = (i-1)\frac{2\pi}{N_u} \tag{6.14c}$$

where $\mathbf{s}_{d_{it}}$ and θ_{d_i} are the desired separation vector and heading angle respectively. The control input to correct the UAV positions is calculated as follows:

$$\mathbf{s}_{e_{it}} = \mathbf{s}_{d_{it}} - \mathbf{s}_{it} \tag{6.15a}$$

$$d_{e_{it}} = \|\mathbf{d}_{it}\| - d_{it_o} \tag{6.15b}$$

$$l_{e_{it}}(i) = l_{e_{it}}(i) + d_{e_{it}} \cdot \Delta t \tag{6.15c}$$

$$u_{x_{it}} = k_p \mathbf{s}_{e_{it}}(1) + k_d d_{e_{it}} \mathbf{s}_{it}(1) + k_i i_{e_{it}}(i) \tag{6.15d}$$

$$u_{y_{it}} = k_p \mathbf{s}_{e_{it}}(2) + k_d d_{e_{it}} \mathbf{s}_{it}(2) + k_i i_{e_{it}}(i) \tag{6.15e}$$

where the parameters $u_{x_{it}}$ and $u_{y_{it}}$ are the respective x and y control input while k_p, k_d and k_i are the respective gains of the PID controller.

6.3.3 Altitude correction cost

In addition to preventing collision, the multi-UAV cost function incorporates an altitude control component. As the respective altitudes of UAVs increase, their FOVs tend to become larger, enabling coverage of a wider area. However, increasing the altitude also results provides poorer target visibility due to limitations of the onboard camera to capture quality images and limitations on the target state estimation by the sensors. To resolve the problem, the UAVs are constrained to fly within an optimal band, $z_d \pm n$ of altitude above the target where both visibility and state estimations sensors perform well. The cost function equation that summarises the altitude control algorithm can be expressed as:

$$J_{alt} = \sum_{i=1}^{N_u} \left[(z_d - z_{a_i})^2 + \lambda_a \left(\frac{d_{it}^2 - (z_d - z_{a_i})^2}{d_{it}^2} \right) + \lambda_v (v_{az_i})^2 \right] \tag{6.16}$$

where N_u is the number of UAVs, $z_d = 200 + z_q$ is the desired altitude, u_{az} is the desired vertical acceleration computed using the flight path equation, d_{it} is the distance between the i-th UAV and the target, σ_a is the FPA, v_{az} is the vertical velocity component, λ_a and λ_v are weighting coefficients for altitude and velocity, respectively and they control the relative importance of altitude and velocity control. The cost function is a sum of squared errors, where the first term penalises deviations from the desired altitude, the second term penalises deviations from the desired flight path angle, and the third term penalises deviations from the desired vertical velocity.

6.4 Cooperative UAV Tracking Quadrotor Swarm

In this section, we consider the scenario where our multi-UAVs are tracking a group of manoeuvring mini-drone swarms. The drone swarm would ideally be clustered together

on an adversarial mission to attack a remote protected facility, with a control strategy that enables the target cluster to evade interception. The cooperative UAVs would therefore aim to treat the drone swarm cluster as a geometrical object with a dynamic surface area and a central or focal point(s) [105]. In this group-to-group scenario, our task is to decide how the UAVs perceive and measure the size and speed of the adversarial drone swarm. This will facilitate the tracking and keep the target cluster within the FOV of the respective tracking UAVs.

Some of the work available in the literature on multi-target tracking includes the research by [375, 376, 128], in which a decentralised deep reinforcement learning algorithm was developed to learn cooperative tracking policies for a UAV swarm used for multi-target tracking. However, little attention was given to the target cluster and evasion strategy. In another related research. Wu et al. [377] developed a strategy for multi-fixed-wing UAVs intercepting a group evasive adversarial fixed-wing UAV target cluster. Their research focused on target isolation, clustering, and using the Apollonius circle evaluation for assigning tasks to the UAVs in the tracking group. This research however utilised a simple Dumbins curves path strategy for controlling the UAV interception. In [304], they investigated the Multi-Target Tracking (MTT) for a group of cooperative UAVs based on Lyapunov optimisation. Their multi-objective optimisation, incorporated execution delay, prediction accuracy, and physical collision avoidance. However, the target comprised decentralised aerial targets, ground-moving vehicles, and humans. Similarly [378] developed a heuristic search strategy to investigate how various intruder behaviours affect the search performance of a patrolling UAV swarm. The results suggest that multi-objective optimisation outperforms other techniques in providing patrolling performance. It will be observed that there is limited literature on multi-target aerial tracking by multi-UAV.

6.4.1 Multi-target tracking problem

The group tracking mission scenario is depicted in Fig. 6.2.

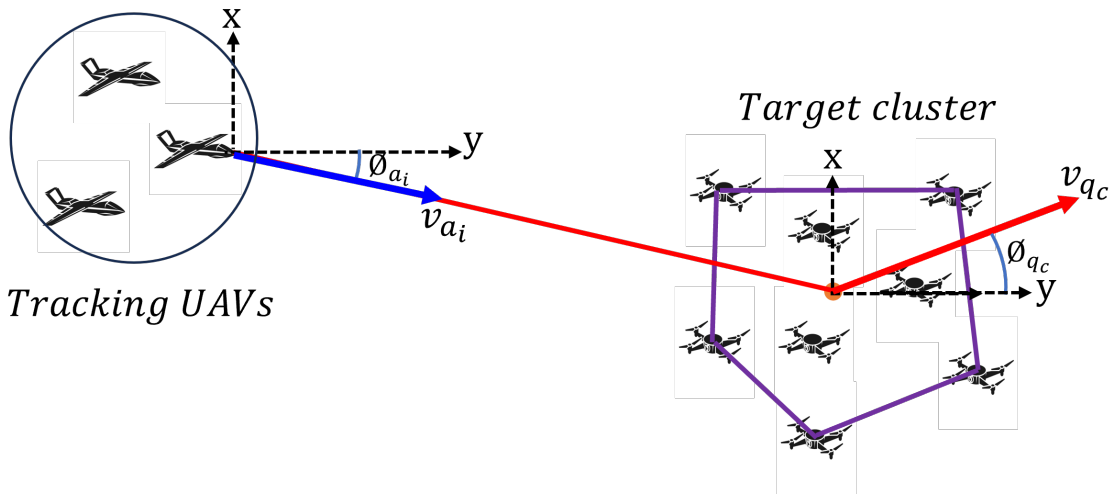

Fig. 6.2 Multi-UAV tracking clustered target

We assume that the drones in the target cluster are all adversarial and we aim to track the targets as a group by assuming that the number of tracking fixed-wing UAVs N_u is less than the number of quadrotors in the evasive drone swarm N_q, so that $(Nq > N_u)$. To ensure that the UAVs maintain the targets within desirable proximity, we compute the relative speed and position of the target cluster and apply a combination of the control law presented in Chapter 3 and the altitude controller presented in the next subsection to track the multi-target.

6.4.2 UAV altitude control for optimal multi-target tracking

This subsection addresses the strategy for autonomously adjusting the altitudes of the individual UAVs tracking a clustered multi-target. To ensure that the UAV can keep the target cluster within its camera FOV while avoiding poor image quality, we will utilise the optical range from the UAV to the target to enhance observation (visualisation) and optimal vertical altitude to allow full coverage of all targets as our calibration parameters. These parameters have been chosen because, without a vertical constraint, the UAV could produce poor image quality. Assuming our tracking UAVs all have downward-looking cameras installed under their fuselage, our design ensures that the UAVs are always at a higher altitude than the target cluster as follows:

$$h_{tc} < h_{\min} \leq h_{u_i} \geq h_{\max} \tag{6.17}$$

where h_{tc} is the altitude of the target cluster, measured from its centre point, h_{u_i} is the altitude of the i-th UAV, while $h_{\min}$ minimum altitude that optimises observation and image quality and $h_{\max}$ is the maximum altitude that maximises visibility coverage. Our goal is

to keep all the tracking UAVs between the operating altitudes bounds in (6.17). Our next consideration is to decide on how the centre of the multi-target dynamic swarm cluster is determined. If the targets are uniformly distributed within the cluster, the simple way of determining the central point is to compute the centre point of the circle (in 2D) or sphere (in 3D) enclosing all the targets. However, for a dynamic evasive multi-target cluster, there will be situations where one or two targets are further away from the others and simply using a circle centre would be unsuitable. To enable a more representative coverage of the target including the outer ones, a polygon centre (in 2D) or ellipsoid (in 3D) could be used. Let's consider the polygon scenario by assuming that the UAV camera sees the spread of the clustered targets from a vertical elevation as a polygon on the $x-y$ plane as depicted in Fig. 6.3.

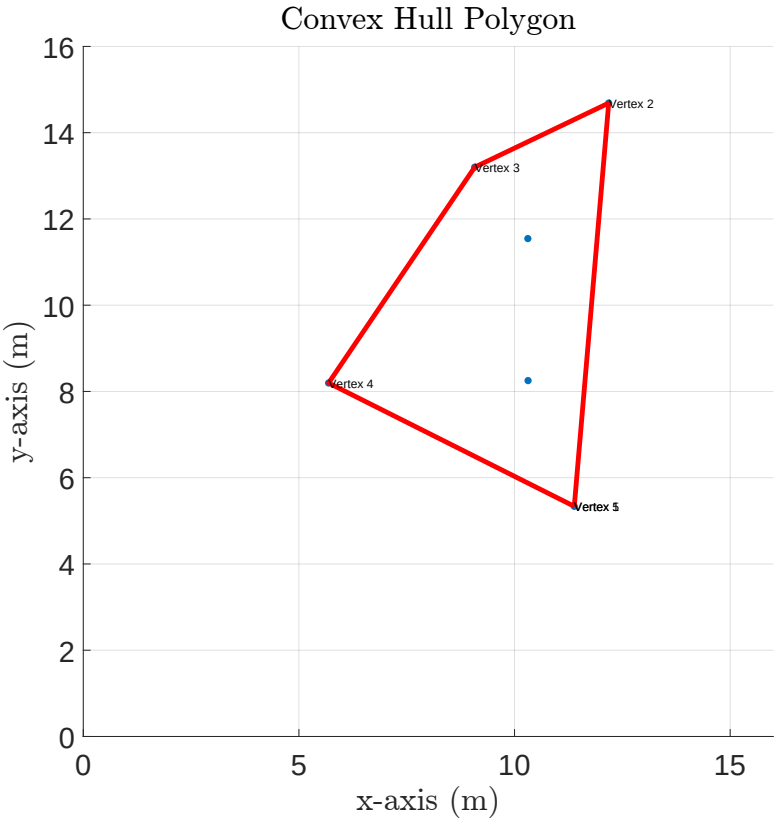

Fig. 6.3 Multi-target clustered polygon

If we assume that the polygon formed by the target cluster is a convex hull where none of the vertices points inward, then the equation for determining the centre of the polygon enclosing the target cluster can be determined using the positions of the various targets. The size (perimeter) of the polygon can be calculated as follows:

$$S = \sum_{i=1}^{N_q} \sqrt{(x_{q_i} - x_{q_{i+1}})^2 + (y_{q_i} - y_{q_{i+1}})^2} + \sqrt{(x_{q_{N_q}} - x_{q_1})^2 + (y_{q_{N_q}} - y_{q_1})^2} \tag{6.18}$$

where (x_{q_i}, y_{q_i}) is the position of the i-th target, while N_q is the number of targets. The surface area of the polygon can be computed using the formula for the area of a polygon A_p.

$$A_p = \frac{1}{2} \left| \sum_{i=1}^{N_q} (x_{q_i} y_{q_{i+1}} - x_{q_{i+1}} y_{q_i}) + (x_{q_{N_q}} y_{q_1} - x_{q_1} y_{q_{N_q}}) \right|, \tag{6.19a}$$

$$C_x = \frac{1}{6A_p} \sum_{i=1}^{N_q} (x_{q_i} + x_{q_{i+1}})(x_{q_i} y_{q_{i+1}} - x_{q_{i+1}} y_{q_i}) + (x_{q_{N_q}} + x_{q_1})(x_{q_{N_q}} y_{q_1} - x_{q_1} y_{q_{N_q}}), \tag{6.19b}$$

$$C_y = \frac{1}{6A_p} \sum_{i=1}^{N_q} (y_{q_i} + y_{q_{i+1}})(x_{q_i} y_{q_{i+1}} - x_{q_{i+1}} y_{q_i}) + (y_{q_{N_q}} + y_{q_1})(x_{q_{N_q}} y_{q_1} - x_{q_1} y_{q_{N_q}}). \tag{6.19c}$$

In Fig. 6.4, C is the centre of the target cluster, while l_{q1} and l_{q2} represent the horizontal distance between quadrotor targets 1 and 2 to the centre of the cluster. Additionally, h_{q1} represents the altitude of quadrotor target 1. The centre (centroid) of the polygon is represented by coordinates (C_x, C_y). Having determined the polygon centre, the next step is to determine how to adjust the altitudes of the various UAVs so they all operate within desirable bounds. If we depict the i-th UAV as being directly over the cluster polygon centre, then we compute and use the angle between its vertical separation from the centre of the target cluster and its Euclidean distances to the various target as an input for the vertical control as shown in Fig. 6.4.

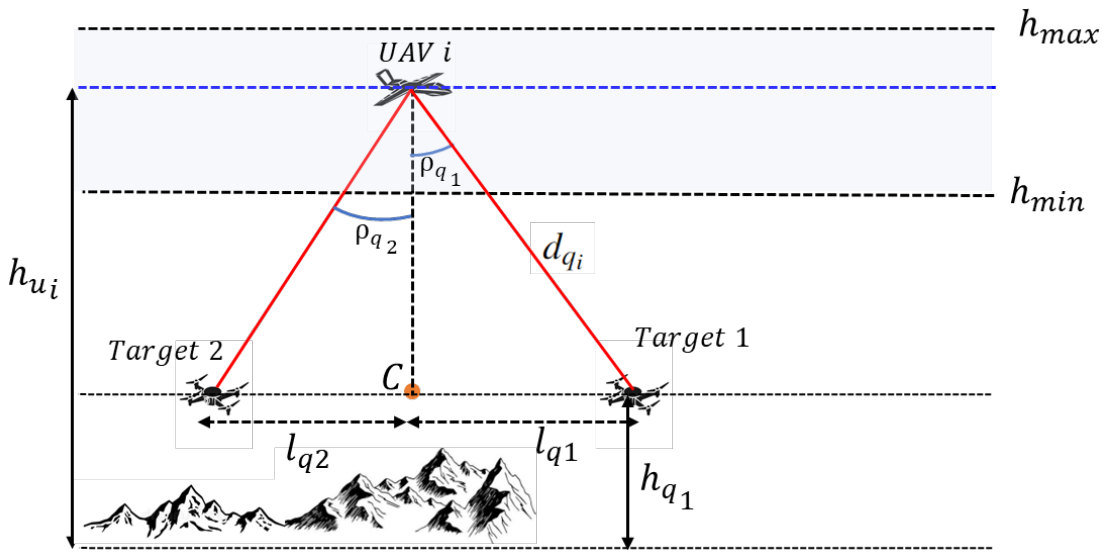

Fig. 6.4 Angle computation using outermost polygon targets

Our cost function for the UAV altitude control comprises two quadratic terms, one for the UAV distance to targets with the cluster and another term for the vertical separation above the target cluster as follows:

$$J_h = \sum_{i=1}^{n} \frac{1}{2}(J_{x_i} + J_{\rho_i}) \tag{6.20}$$

where J_h is the cost function for determining the altitude of the i-th UAV. This has two sub-costs to optimise the quality of target image observation and vertical coverage of the targets in the cluster. The term to optimise vertical observation is determined as follows:

$$J_{\rho_i} = e_\rho \tan^2(\rho_{q_i}) \tag{6.21a}$$

$$e_\rho = \frac{1}{\tan^2(\rho_{\text{lim}})} \tag{6.21b}$$

whereJ_{ρ_i} is the vertical control term dependent on the angle made by the UAV and i-th target ρ_{q_i}, while f_{c_i} is the focal length of the i-th tracking UAV and e_ρ is the coefficient weighting term for this minimisation index. The verticality term, J_{ρ_i}, defined above reaches a minimum value of 0, for optimal verticality and a normalised value, 1, that represents the worst admissible verticality limited by the ρ_{lim}. To enhance the optimal tracking for each UAV, we can define the optical range as the ratio between the Euclidean distance to the target and the focal length of the mounted tracking camera as follows:

$$d_{f_{c_i}} = \frac{d_{q_i}}{f_{c_i}} \tag{6.22}$$

where $d_{f_{c_i}}$ is the ratio of target distance to UAV focal length, which gives greater flexibility to the feasible optimal solutions, as the index can automatically trade larger Euclidean distances for longer focal lengths. The term d_{q_i} is the Euclidean distance between UAV and i-th target. To associate the size of the target cluster in the real world to the altitude of the i-th UAV, let's assume that the polygon shape enclosing the target cluster area $A_c[m^2]$. We can then develop an approximate equivalent measure that is independent of the polygon shape as the diameter of the cycle enclosing the polygon as:

$$d_p = 2\sqrt{A_c/\pi} \tag{6.23}$$

where d_p, is the diameter of the target cluster polygon. This enables us to design a projection ratio as the quotient p_{r_i}:

$$p_{r_i} = \frac{d_{ig_i}}{d_p} \tag{6.24}$$

where d_{ig_i} is the magnitude of the projected target cluster diameter on the i-th UAV camera image plane. The above ratio relationship depends on the distance of the UAV to the target cluster and its camera focal length and can be approximated as the inverse of the optical range as follows:

$$p_{r_i} \approx \frac{1}{d_{f_i}} \tag{6.25}$$

We can define limits for this parameter independent of the parameters of the tracking UAV camera with the projection ratio limits defined as $p_{r_{\min}}$, $p_{r_{\max}}$ as follows:

$$J_{x_i} = \frac{(d_{f_{c_i}} - \frac{1}{p_{r_{\max}}})^2}{\left(\frac{1}{p_{r_{\min}}} - \frac{1}{p_{r_{\max}}}\right)^2} \tag{6.26}$$

The optical range, J_{x_i} is defined in a way that balances the optical range with the verticality term introduced above. The term, J_{x_i} has a minimum value of zero which represents the optimal optical range and corresponds to the minimum altitude $h_{\min}$. The coefficient e_x is defined to reach the normalised unitary value for the admissible limit of the specified optical range. Since the minimum desirable altitude for any of the tracking UAVs should not be below $h_{\min}$, we can redefine the value of $p_{r_{\max}}$ in terms of the minimum altitude as follows:

$$p_{r_{\max}} = \frac{f_{c_i}}{h_{\min}} \tag{6.27}$$

Thus, the optical range optimisation term can be modified as follows

$$J_{x_i} = e_x \cdot \frac{(d_{q_i} - h_{\min})^2}{(f_{c_i} - p_{r_{\lim}} \cdot h_{\min})^2} \tag{6.28a}$$

$$e_x = p_{r_{\lim}}^2 \tag{6.28b}$$

where $p_{r_{\lim}}$ is an equivalent value of $p_{r_{\min}}$ introduced for calibration purposes. We conclude this UAV altitude control by computing the vertical acceleration a_{z_i} that minimises the cost function J_h based on the optimisation problem presented above while ensuring that the altitude h_{u_i} of the i-th UAV falls within the specified altitude bound of $h_{\min}$ and $h_{\max}$.

$$\begin{aligned} \min_{a_{z_i}} J_h &= \sum_{i=1}^{n} \frac{1}{2}(J_{x_i} + J_{\rho_i}) \\ \text{s.t. } & h_{\min} \leq h_{u_i} \leq h_{\max} \end{aligned} \tag{6.29}$$

The pseudocode for the altitude control of each UAV in the tracking mission is presented in Algorithm 3 below.

Algorithm 3 UAV Altitude Control for Multi-Target Tracking

Require:

Set of tracking UAVs $U = \{\mathbf{x}_{a_1}, \mathbf{x}_{a_2}, \ldots, \mathbf{x}_{a_n}\}$
Altitude bounds: $h_{\min}$ and $h_{\max}$
Maximum allowable angle for verticality: $\rho_{\lim}$
Maximum allowable projection ratio: $p_{r_{\lim}}$
Target positions: $\mathbf{x}_{q_i} = (x_{q_i}, y_{q_i})$ for $i = 1, 2, \ldots, n$
Target cluster polygon centre: (c_x, c_y)
Focal lengths of tracking cameras: f_{c_i} for $i = 1, 2, \ldots, n$
Coefficient e_ρ controlling verticality term
Coefficient e_x controlling optical range term
Equivalent value of $p_{r_{\min}}$ for calibration: $p_{r_{\lim}}$

Ensure:

Optimal vertical accelerations a_{z_i} for each UAV
procedure UAV ALTITUDE CONTROL
    for $i = 1$ to n **do**
        Calculate the angle ρ_{q_i} between $\mathbf{x}_{a_i}$ and target $\mathbf{x}_{q_i}$
        $J_{\rho_i} = e_\rho \cdot \tan^2(\rho_{q_i})$
        Calculate the optical range $d_{f_{c_i}}$ for each UAV
        $d_{f_{c_i}} = \dfrac{d_{q_i}}{f_{c_i}}$
        Calculate the projection ratio p_{r_i} for each UAV
        $p_{r_i} = \frac{d_{ig_i}}{d_p}$
        Calculate $p_{r_{\max}}$ based on $h_{\min}$: $p_{r_{\max}} = \frac{f_{c_i}}{h_{\min}}$
        Calculate J_{x_i} with $p_{r_{\max}}$ and $p_{r_{\lim}}$
        $J_{x_i} = e_x \cdot \frac{(d_{q_i} - h_{\min})^2}{(f_{c_i} - p_{r_{\lim}} \cdot h_{\min})^2}$
        Calculate the cost function J_h for each UAV
        $J_h = \frac{1}{2}(J_{x_i} + J_{\rho_i})$
    end for
    Minimise J_h to find optimal vertical accelerations
    subject to $h_{\min} \leq h_{u_i} \leq h_{\max}$
    Output: Optimal vertical accelerations a_{z_i} for each UAV
end procedure

6.4.3 Drone swarm evasion strategy

In this section, we describe the dynamic equations and evasion strategy for a group of clustered quadrotor targets. Each target has its velocity, acceleration, and position but

maintains a coordinated movement to evade a tracking UAV. The dynamic equations for the quadrotor targets are described as follows for each quadrotor target i:

$$\mathbf{x}_{q_i} = [x_{qx_i},\, x_{qy_i},\, x_{qz_i}] \tag{6.30a}$$

$$\mathbf{v}_{q_i} = [v_{qx_i},\, v_{qy_i},\, v_{qz_i}] \tag{6.30b}$$

$$\dot{\mathbf{x}}_{q_i} = \mathbf{v}_{q_i} \tag{6.30c}$$

$$\dot{\mathbf{v}}_{q_i} = \mathbf{a}_{q_i} \tag{6.30d}$$

where $\mathbf{x}_{q_i}$, $\mathbf{v}_{q_i}$ and $\mathbf{a}_{q_i}$ are the position, velocity, and acceleration vectors of the i-th of the target. To maintain a close fit while evading the tracking UAV, the quadrotor targets employ an evasion strategy to escape the UAVs based on the flocking controller that dynamically adjusts their velocities and positions to avoid detection while staying within a specified cluster radius as follows:

$$a_{q_i} = k_p \cdot (\mathbf{x}_{q_{des_i}} - \mathbf{x}_{q_i}) - k_v \cdot (v_{q_{des_i}} - v_{q_i}) \tag{6.31a}$$

$$\mathbf{x}_{q_{des_i}} = w_1 \cdot \mathbf{x}_{a_m} + \sum_{j \neq i} w_2 \cdot \mathbf{x}_{q_j} \tag{6.31b}$$

Where $\mathbf{x}_{q_{des_i}}$ is the desired position for the i-th target while w_1 and w_2 are weight coefficients that determine the influence of the UAV and neighbouring targets on the desired position. The term $\mathbf{x}_a$ is the current position of the UAV and $\mathbf{x}_{q_j}$ represents the positions of neighbouring targets $j \neq i$. This equation models the behaviour of target i in a flocking-based evasion strategy, where it adjusts its desired position to maintain certain relationships with the positions of neighbouring targets and the UAV. The weight coefficients w_1 and w_2 control the relative importance of these influences. For simplicity, we assume that the target utilises the mean of the various UAV positions $\mathbf{x}_{a_m}$.

6.5 Task Assignment

We consider the assignment of tasks to some of the UAVs during tracking by starting with the assumption that reliable communication exists between the multi-tracking UAVs. Consider a scenario during a multi-UAV to multi-target tracking mission, where a single target breaks away from its cluster and accelerates with high speed towards a protected facility or to execute a Kamakazi mission. If this happens, we will want the remaining clustered targets to be continuously tracked by some of the UAVs, while the UAV closest to the break-out target is autonomously tasked to pursue the solo quadrotor drone. Accordingly, we implement an algorithm that assigns a risk factor to each target based on their

proximity to a restricted area or protected facility and assigns the task of single pursuit and interception to the most suitable UAV.

Let X_q represent the set of all targets, including the break-away target, and X_a be the set of all available UAVs. We can formulate a risk factor for each of the targets based on the distance $d_r(x_{q_i})$ using an exponential function as follows:

$$R(x_{q_i}) = e^{-k \cdot d_r(x_{q_i})} \tag{6.32}$$

where, d_r represents the distance function between a target and a restricted area and $d_r(x_{q_i})$ is the distance from target x_{q_i} to the restricted area while k is a parameter that controls the rate at which the risk increases with proximity. To evaluate the suitability score $S(X_{aj})$ for each UAV, we consider multiple criteria, including its current position, velocity, and ability to intercept the target. The overall suitability score $S(X_{aj})$ is determined as a weighted combination of these criteria:

$$S(X_{aj}) = w_1 \cdot F_{\text{pos}}(\mathbf{x_{aj}}) + \mathbf{w_2} \cdot \mathbf{F}_{\text{vel}}(\mathbf{X_{aj}}) + \mathbf{w_3} \cdot \mathbf{F}_{\text{int}}(\mathbf{X_{aj}}) \tag{6.33}$$

where w_1, w_2, and w_3 are weighting factors that control the relative importance of each criterion. $F_{\text{pos}}(X_{aj})$ is a function that assesses the position-related suitability of the UAV based on its proximity to the target while $F_{\text{vel}}(X_{aj})$ is a function that evaluates the suitability related to the UAV's velocity, considering factors such as its speed. The function that measures the UAV's capability to intercept the target and is based on criteria of heading direction and acceleration of the UAVs is presented as $F_{\text{int}}(X_{aj})$. The weighting factors w_1, w_2, and w_3 can be adjusted based on the relative significance of each criterion in the assignment process. A pseudo-code that summarises the steps in the task assignment algorithm is presented in Algorithm 4.

Algorithm 4 Task Assignment Algorithm

Require:

Set of targets $X_q = \{\mathbf{x}_{q_1}, \mathbf{x}_{q_2}, \ldots, \mathbf{x}_{q_n}\}$
Set of available UAVs $X_a = \{\mathbf{x}_{a1}, \mathbf{x}_{a2}, \ldots, \mathbf{x}_{am}\}$
Distance function $d_r(\mathbf{x}_{q_i})$ for target $\mathbf{x}_{q_i}$
Parameter k controlling risk increase
Function to calculate suitability score $S(X_{aj})$ for UAV $\mathbf{x}_{aj}$

Ensure:

Assignment of pursuit task to UAV $\mathbf{x}_{ap}$
procedure TASK ASSIGNMENT
    Calculate risk factors for each target
    for each target $\mathbf{x}_{q_i}$ in X_q **do**
        Calculate risk factor $R(\mathbf{x}_{q_i})$ as: $R(\mathbf{x}_{q_i}) = e^{-k \cdot d_r(\mathbf{x}_{q_i})}$
    end for
    Sort targets by risk factor
    Sort X_q based on $R(\mathbf{x}_{q_i})$ in ascending order
    Select the break-away target
    $x_{q_b} = x_q[0]$ ▷ The first target after sorting
    Calculate suitability scores for UAVs
    for each UAV $\mathbf{x}_{aj}$ in X_a **do**
        Calculate suitability score $S(X_a)$ using the function
        $S(X_{aj}) =$ Some function of position, velocity, and interception capability of $\mathbf{x}_{aj}$
    end for
    Assign pursuit task to UAV
    $\mathbf{x}_{ap} = \mathbf{x}_a[0]$ ▷ The first UAV after sorting based on suitability scores
    Output: $\mathbf{x}_{ap}$ is assigned to pursue the break-away target x_{q_b}
end procedure

6.6 Simulation and Results

In this section, we present the initial conditions and results of simulating multi-UAV tracking single and multiple targets.

6.6.1 Multi-UAV tracking single target simulation

To assess the performance of the multi-UAV cooperative tracking strategy against an evasive aerial target, three UAVs tracking a single evasive aerial quadrotor target scenario were implemented. The UAVs were initialised at random positions with x_i , y_i and z_i positions as $10 \times \texttt{randn}(1,3) + [50;100;20]$. The initial velocity of each UAV is $v_a = 15m/s$ with the minimum and maximum velocities as $v_{a_{\min}} = 5m/s$ and $v_{a_{\max}} = 20m/s$ respectively. The minimum and maximum accelerations for the UAVs are set to $u_{a_{\min}} = 2m/s^2$ and $u_{a_{\max}} = 5m/s^2$ respectively. The target minimum and maximum velocities were constrained to $v_{q_{\min}} = -2m/s$ and $v_{q_{\max}} = 5m/s$ respectively while the target acceleration limits are $a_{q_{\min}} = -2m/s^2$ and $a_{q_{\max}} = 2m/s^2$. The quadrotor was initialised at position $[-3,\ 3,\ 3]$ and initial velocity of $rand(1)[-2,\ 4,\ 2]$. To prevent collision between the UAVs, a minimum safe distance of $d_{\min_{ij}} = 6m$ was utilised while the safety limits between each UAV and the target is $d_{\min} = 10m$ If a collision is imminent, the avoidance acceleration constant is set to $k_a = 2$ to nudge the UAVs away from each other or the target using the control avoidance equation presented earlier. The simulation for run for $60s$ using a sampling time of $0.2s$, giving 300 sample steps. Plots of the trajectories of the UAVs and target and their control input histories are shown in 6.5.

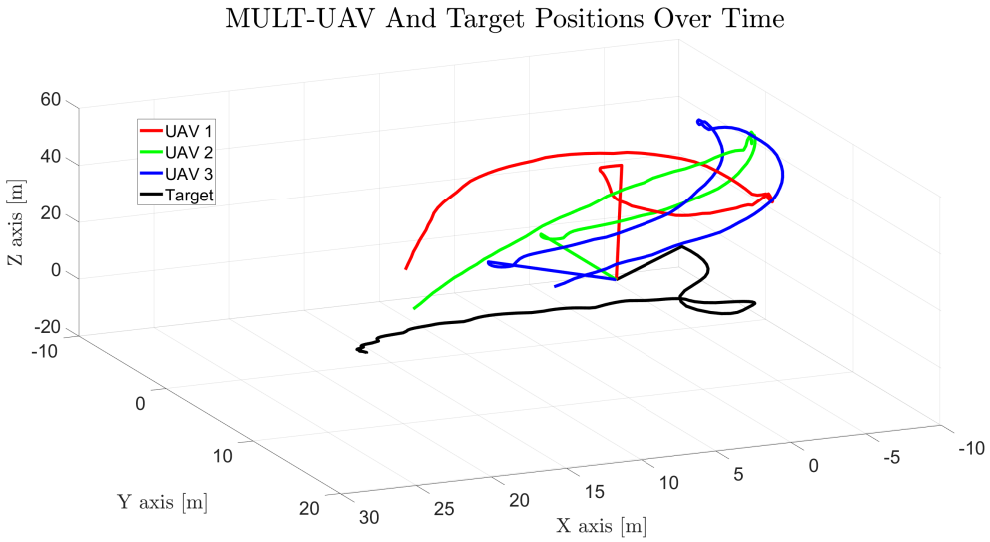

Fig. 6.5 Trajectories of multi-UAV tracking of an evasive aerial target

We compared the velocity of the UAVs and targets to see how they changed during the pursuit and evasion simulation.

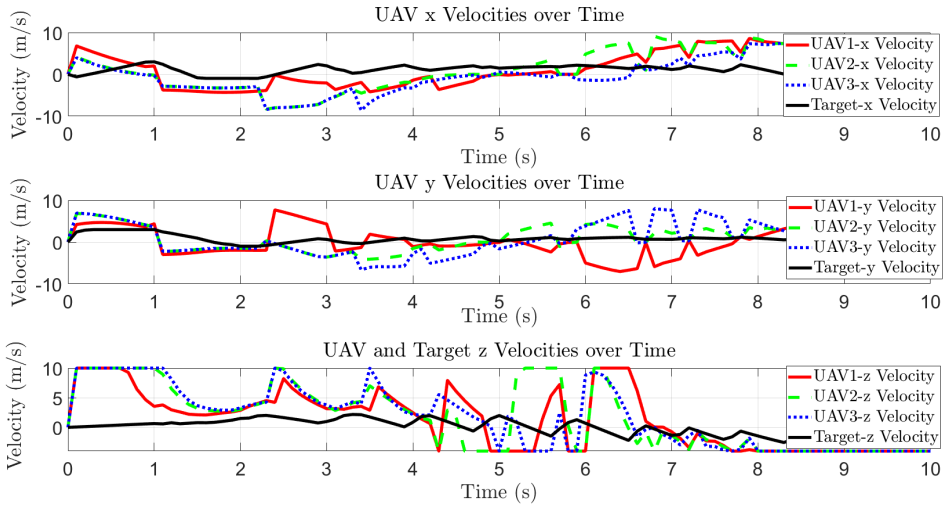

Fig. 6.6 Velocity histories of UAVs and target

Since the UAV velocity is dependent on the control input in the form of acceleration command from the UAV controller and target evasion strategy, we compared the acceleration of the UAVs along the x, y and z-axis to show the effect of the control input on the trajectories of the UAVs and the target during a simulation.

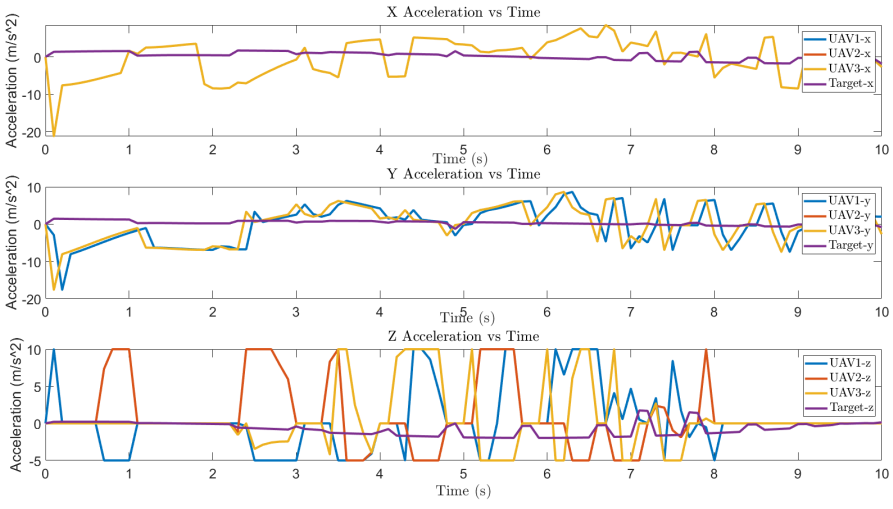

Fig. 6.7 Acceleration histories of UAVs and target

The plot in Fig. 6.5, shows that the 3 UAVs can track the single target independently using similar tracking algorithms. The target represented by the black line in the figure is observed to be evading the UAVs while UAVs 1, 2 and 3 are observed to continuously

adjust their control inputs, enabling them to track the target while maintaining a safe distance between the UAVs and target. The velocity histories of the 3 UAVs were overlaid on the same plot with the target velocity time history as shown in Fig.6.6. The UAV velocities show an increase and decrease in magnitude in response to the manoeuvres of the target velocities. A similar pattern is observed with the plot comparing the control inputs of the UAVs and the target in the x, y, z directions in Fig.6.7. The figures show that the target made a persistent effort to evade the mult-UAVs while the UAVs were able to track the target independently, adjusting their relative positions to prevent collision throughout the tracking period.

6.6.2 Multi-UAV tracking multi-target simulation

We simulated a scenario where 3 UAVs are tracking a target cluster comprising seven quadrotor targets, evading the tracking UAVs as a swarm. Similar initial values as implemented in the single target tracking were applied with modifications to enable the altitude controller implemented for the multi-UAV to autonomously track the targets at optimal altitude for each UAV. The constraints $h_{\min} = h_{qc} + 50$, and $h_{\max} = h_{qc} + 70$, where h_{qc} is the altitude of the target cluster measure from its centre. This was done to provide an altitude band of about 20m. Additionally, the value of $\rho_{\lim} = \frac{70\pi}{180}$ rad, $p_{r_{\lim}} = \frac{p_{r_{\max}}}{30}$, while the focal lengths of the 3 UAVs are $\mathbf{f}_c = [50 \times 10^{-3}\,\mathrm{m}, 60 \times 10^{-3}\,\mathrm{m}, 70 \times 10^{-3}\,\mathrm{m}]$. The plot in Fig. 6.8 shows the trajectories of the 3 UAVs tracking the multiple target quadrotor swarm.

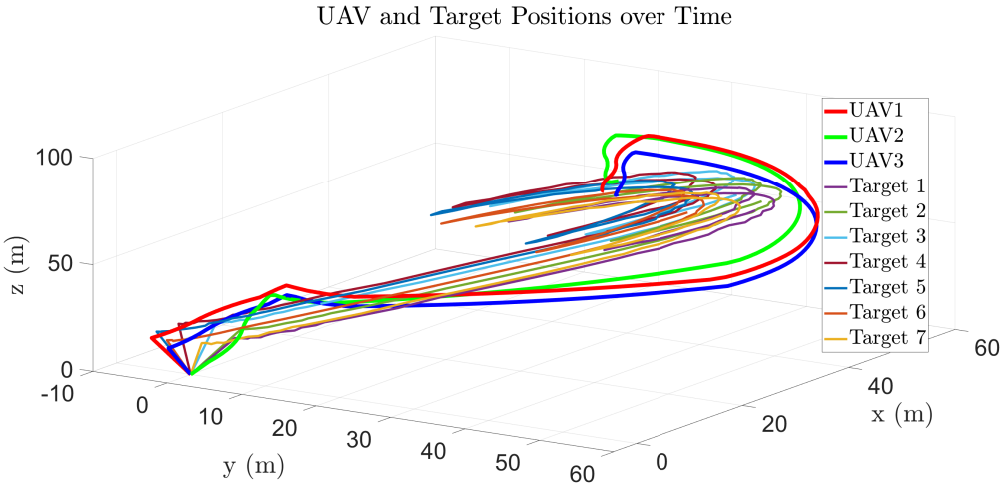

Fig. 6.8 Multi-UAV tracking clustered target

To compare the altitude control cost for the 3 UAVs, we plotted a histogram of their cost function responses over the simulation time as shown in Fig. 6.9.

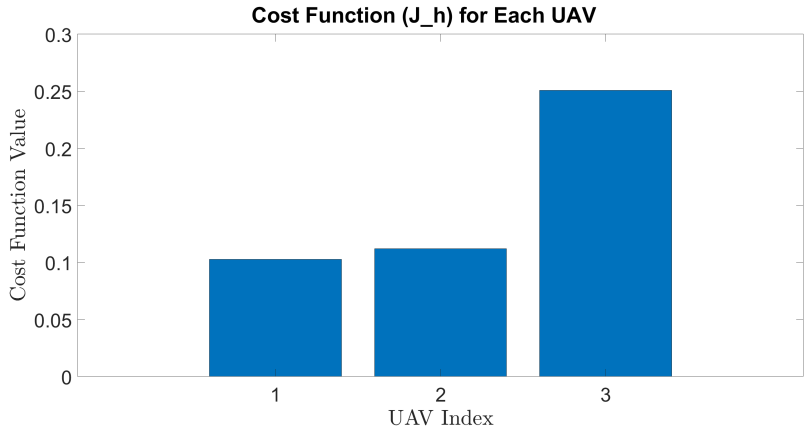

Fig. 6.9 Multi-UAV altitude control cost functions comparison

The tracking algorithm for the lateral, longitudinal, and altitude controls applied to co-operatively track single and multiple target quadrotors was observed to track the targets regardless of evasion. Additionally, the constraints applied to the tracking algorithms ensured that UAVs operated at an optimal altitude that balances the need for effective coverage and the need for quality of captured images by UAV cameras. The collision avoidance consideration was for the UAVs to maintain a minimum safe distance between each other and also avoid collision with targets being tracked. These cost functions were combined using weights that ensured they were all reflected in the target tracking mission. The Plot of the cost function output for the 3 UAVs in Fig. 6.9 shows that the focal length of the UAVs affected their cost function optimisation output and consequently affected the tracking altitudes of the respective UAVs. The cost performance histogram also showed that UAVs with high focal length cameras require less control input to attain desired altitudes as compared to low focal length UAV cameras.

6.7 Summary

This Chapter presented the control algorithm for tracking a single evasive quadrotor-type target by 3 cooperative UAVs, independently tracking the target with a decentralised control strategy. The multi-UAV control strategy incorporates a tracking cost function, collision avoidance cost function, and altitude control cost function, which are minimised to keep the UAVs tracking the target at an optimal altitude, while avoiding collision between the UAVs and between the UAVs and the target. To extend our cooperative tracking research, this Chapter also implemented a multi-UAV to multi-target mission scenario by designing an evasive target cluster, to evade the UAVs. Considering that the target cluster is dynamic and constantly changing in response to the target positions, we developed a new altitude control strategy that optimises the coverage and image capture quality relative to the cluster

area and target positions of each UAV. To apply real-world consideration to the multi-UAV to multi-target scenario in this research, we also presented a sample algorithm for task assignment to one or more tracking UAVs. In particular, we considered a scenario and implemented a logic to autonomously assign one of the tracking UAVs, the task of chasing and intercepting a break-out quadrotor from an adversarial swarm.

Simulations were conducted to assess the performance of the cooperative tracking control strategies for both single and multiple targets using various initial conditions and mission scenarios. The results show that the control strategies developed for the UAVs were able to persistently track the evading single and multiple aerial targets, at optimal altitudes while avoiding UAV-to-UAV and UAV-to-target collisions. In Chapter 7, we extend this thesis by exploring UAV-mounted countermeasures against adversarial single or multiple quadrotor-type aerial targets.

Chapter 7

Countermeasures against Drone Targets

7.1 Introduction

In Chapter 6, we explored multi-UAV tracking of both single and multiple quadrotor aerial targets to persistently capture the targets within the FOV of the tracking UAV camera. In the sequence of protecting vital assets from unauthorised drones, after effectively tracking the drones, the next step would be to prevent or stop the adversarial drones from causing damage or executing their planned mission [379]. Accordingly, in this chapter, we extend the research presented in this thesis by further considering countermeasure options. With the recent advancements in drone technology, various types of drones have been developed and deployed for a variety of roles, including security, commercial, and transportation purposes. The ease of acquisition and operation of drones also means that criminal individuals or groups can acquire and employ drones for illegal and adversarial purposes [15]. To protect vital and protected assets from being accessed, infiltrated, or damaged by unauthorised drones, various countermeasures are being employed. This includes stationary and mobile countermeasures as part of the C-UAS [380]. In this chapter, we focus on aerial countermeasures deployed by fixed-wing UAVs against adversarial targets due to the advantage of being able to pursue and close up to the target. We now review related literature on UAV-mounted countermeasures.

7.1.1 Related Literature

Several countermeasure options could be applied to intercept, disrupt, incapacitate, or capture rogue adversarial single or multiple drone swarms. Some of these methods are reviewed below:

Electro-Magnetic Net. This countermeasure is based on deploying a specialised net equipped with electromagnetic capabilities to disable the quadrotor's motors and electronics, causing it to fall or rendering it incapacitated [381]. The goal of the net could be to form an enclosed bag-like container upon contact with a group of target vehicles operating as a swarm.

Laser Dazzler. In this countermeasure method, a high-powered laser or microwave system is used to temporarily blind or disable the quadrotor's cameras or sensors, disrupting its flight and rendering it vulnerable to capture [382, 383].

Microwave Electromagnetic Weapons. UAV-mounted microwave electromagnetic weapons can be utilised as a countermeasure against adversary drones. Microwave electromagnetic weapons, also known as radio-frequency weapons or Directed Energy Weapons (DEWs), utilise microwave frequencies to generate and direct electromagnetic energy for various purposes. These weapons can be designed to emit High-power Microwave (HPM) pulses or Continuous Wave (CW) beams [384, 385]. When deployed against adversary drones, microwave electromagnetic weapons can target and interfere with the communication, navigation, and control systems of the UAV, causing temporary or permanent disruption. The range of such weapons can vary depending on the specific system, power output, and antenna design.

High-Precision Projectile. Employ a miniaturised projectile launcher on the UAV that can accurately launch projectiles to physically disable the quadrotor's propellers or vital components, causing it to crash [386].

Glue Dispenser. Equip the UAV with a glue dispenser that can release a quick-drying adhesive substance to disable the quadrotor's rotors or immobilise its moving parts, causing it to crash or be easily captured.

These are some examples of countermeasures that can be used to neutralise or disable a quadrotor drone. In the next section, we expand option 1 and develop the dynamics of UAV tracking evasive quadrotors.

7.1.2 Electro-Magnetic Net with UAV Deployment

The countermeasure involves equipping the UAV with a net launcher. When the target quadrotor is within range, the UAV will deploy the net to capture and disable the quadrotor using electromagnetic capabilities. To deploy countermeasures against an adversarial target, we assume that the UAV can identify the target quadrotor using sensors and tracking algorithms. Using onboard countermeasures, the UAV will then determine the optimal time and distance for net deployment based on the quadrotor's trajectory and position. When

the condition is right and the deployment parameters are met, the UAV activates the net deployment mechanism by launching a projectile containing the net towards the evasive quadrotor. Once the net makes contact with the quadrotor, the electromagnetic capabilities embedded in the net are activated which generates an Electromagnetic Field (EMF). The EMF interferes with the quadrotor's motors and electronics, causing it to fall or become incapacitated. Thereafter, the status of the captured quadrotor is observed to determine if necessary actions need to be taken for further containment or retrieval. The literature search shows they are scanty information on projectile-launched countermeasures against adversarial drones. This shows that despite literature contributions, gaps still exist in the area of UAV tracking and autonomous airborne countermeasure application. We intend to close this gap by designing an algorithm that tracks and gets the UAV within proximity to single or multiple aerial targets.

7.1.3 Contributions

The main contributions of this chapter are highlighted below:

- A task assignment logic is designed to enable the tracking UAV to decide on which target to track and a system for switching to the next target after neutralising the first target.
- A cost function is developed for the tracking UAV to close up and intercept the target using NMPC and optimal control solutions.
- We presented a high-precision projectile algorithm to destroy, incapacitate or deploy a projectile-launched net to capture aerial adversarial aerial targets.

The remainder of this chapter is organised as follows. In section 7.2, we formulate the countermeasure problem by designing a decision logic for the tracking UAV. Section 7.3 presents the UAV dynamics and control development while Section 7.4 highlights the target dynamics. To simulate the deployment of an electronic net, we develop a projectile guidance controller in Section 7.5 before presenting our simulation results and comparative plots in Section 7.6. The obtained results are discussed in Section 7.7 followed by a concluding summary in Section 7.8.

7.2 Problem Formulation

From the review of the various forms of UAV deployed anti-drone measures, we observe that the UAV needs to get within proximity to deploy the countermeasure. With this in mind, let us consider a scenario where a lone fixed-wing UAV is tasked with tracking and destroying or incapacitating 3 adversarial quadrotor targets operating independently within

the same environment. A decision problem arises for the UAV in deciding which of the 3 targets it should track and destroy first. The decision solution should also determine the sequence of tracking the remaining targets. We can simplify this complex mixed integer optimisation problem by designing a simple task assignment logic.

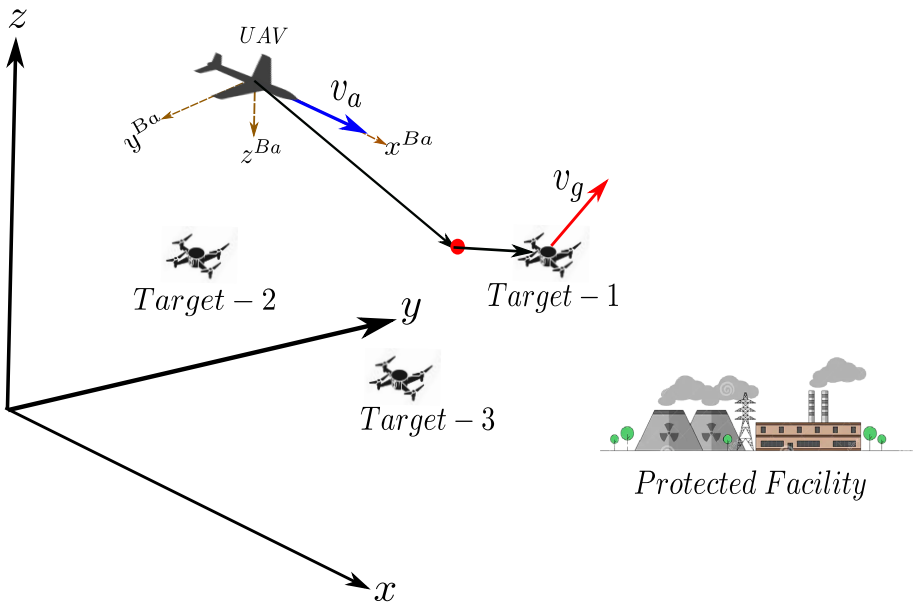

Fig. 7.1 Single UAV and multi-target engagement diagram

We begin by assuming that the UAV can estimate the current positions and velocities of various targets within the operating environment. To determine which target the UAV should track next, we calculate a weighted tracking score for each target based on their relative distances to the UAV, their distances to a static protected facility, and the estimated time it will take each target to reach this facility. Let X_q be the set of targets representing n number of targets in the sequence, and let (x_a, y_a, z_a) be the current position of the UAV. The relative distance between the UAV and a target $\mathbf{x}_{q_i}$ is denoted as $d_(\mathbf{x}_{q_i})$, and it is calculated as:

$$d_(\mathbf{x}_{q_i}) = \sqrt{(x_a - x_{q_i})^2 + (y_a - y_{q_i})^2 + (z_a - z_{q_i})^2} \tag{7.1}$$

The estimated time for each target to reach the facility is computed using the target's velocity v_{q_i} and the position of the facility (x_f, y_f, z_f):

$$t_{f_a}(\mathbf{x}_{q_i}) = \frac{d_{f_a}(\mathbf{x}_{q_i})}{v_{q_i}} \tag{7.2}$$

where $t_{f_a}(\mathbf{x}_{q_i})$ is the estimated time for target i to reach the facility, while $d_{f_a}(\mathbf{x}_{q_i})$ is the distance between the target and the facility, which is calculated as:

$$d_{f_a}(\mathbf{x}_{q_i}) = \sqrt{(x_{q_i} - x_f)^2 + (y_{q_i} - y_f)^2 + (z_{q_i} - z_f)^2} \tag{7.3}$$

If we define the threshold distance and time to the protected facility as d_{f_o} and t_{f_o} respectively, then we can compute the normalised values of our decision parameters as follows:

$$\hat{d}_r(\mathbf{x}_{q_i}) = \frac{d_(\mathbf{x}_{q_i})}{d_{\text{eng}}} \tag{7.4a}$$

$$\hat{d}_{f_a}(\mathbf{x}_{q_i}) = \frac{d_{f_a}(\mathbf{x}_{q_i})}{d_{f_o}} \tag{7.4b}$$

$$\hat{t}_{f_a}(\mathbf{x}_{q_i}) = \frac{t_{f_a}(\mathbf{x}_{q_i})}{t_{f_o}} \tag{7.4c}$$

where d_{eng} is the engagement distance of the UAV to the target, while $\hat{d}_r(\mathbf{x}_{q_i})$, $\hat{d}_{f_a}(\mathbf{x}_{q_i})$ and $\hat{t}_{f_a}(\mathbf{x}_{q_i})$ are the normalised distance of the UAV to the i-th target, normalised distance of the i-th target to the facility and the normalised time of the i-th target to the facility respectively. The decision score can therefore be computed as follows:

$$S_i = w_d \left(\hat{d}_r(\mathbf{x}_{q_i})\right) + w_f \left(\hat{d}_{f_a}(\mathbf{x}_{q_i})\right) + w_t \left(\hat{t}_{f_a}(\mathbf{x}_{q_i})\right) \tag{7.5}$$

where w_d, w_f, and w_t for the weights for UAV distance to target, target distance to facility and approximate time it will take target to get to facility respectively. The weights are used to assign relative importance to each of the scoring parameters. The next target to track, $\mathbf{x}_{track}$, can be determined as:

$$\mathbf{x}_{track} = \arg\min_i \{S_i\} \tag{7.6}$$

Where $\mathbf{x}_{track}$ is the target to be tracked next, and arg min is the operator that returns the index i corresponding to the target $\mathbf{x}_i$ with the maximum weighted tracking score. The scoring formulation enables the UAV to decide based on the calculated weighted scores, the order in which targets are tracked. Having determined the sequence of tracking the various targets, the next goal of the UAV is, to get within engagement range to the designated target d_{eng} to neutralise it. For simplicity, if the UAV is within the engagement range for 5 seconds or more, a high-level manoeuvre is initiated to mimic the launching of a countermeasure and destruction of the evading quadrotor as shown in (7.7).

$$\text{Countermeasure} = \begin{cases} \text{Launch}, & \text{if } d_{q_i} < d_{\text{eng}}, \text{ for } t > 5 \text{ seconds} \\ \text{Keep Tracking}, & \text{otherwise} \end{cases} \tag{7.7}$$

When the countermeasure has been applied to the first target in the tracking sequence, the UAV is automatically reassigned to track the second target in the sequence by calculating its relative distances to the targets and deciding which one to track next based on the target closest to the UAV and then the third target in that order. A sketch diagram describing the engagement scenario is shown in 7.1

7.3 UAV Dynamics and Control

To accurately and efficiently track an aerial target, it is essential to apply a control law capable of driving the UAV toward the desired outcome. This section presents the UAV dynamics and control options applied to persistently track and close up with an evasive target to deploy a countermeasure. Here, we consider the NMPC technique due to its ability to handle complex dynamics and optimise control inputs in real time. As a model-based control approach, the NMPC uses a dynamic model of the system to predict its future behaviour to optimise control actions over a finite time horizon. One of the advantages that the NMPC has over traditional control methods, is that it considers system constraints and optimisation objectives simultaneously, which allows for precise and robust control, even in the presence of disturbances and uncertainties.

We start by defining the UAV dynamic model and then, we formulate an NMPC for a tracking UAV, using its state and control vectors, defining an appropriate optimisation problem, and implementing the control algorithm. We will also discuss key considerations such as adaptive weighting and constraining the target movements to further enhance the performance and robustness of the tracking system. The dynamic equations of the UAV are the same as the set of equations provided in Chapter 3 of this work.

7.3.1 NMPC formulation

The NMPC control design below incorporates dynamic trajectory prediction that factors changes in the mission environmental conditions such as wind disturbance and the rogue quadrotor's dynamics. This involves continuously updating the predicted trajectory of the target drone within the prediction horizon. These updates consider evolving factors such as wind speed, direction changes, and any observed variations in the drone's flight behaviour. Additionally, our control parameters are dynamically adjusted based on the

detected drone's specific characteristics, including its speed, agility, and other attributes. This adaptability allows the NMPC controller to fine-tune its response strategy, ensuring optimal control inputs that are tailored to the behaviour and capabilities of different types of target quadrotors. The NMPC algorithm integrates these adaptations into its predictive control loop, enabling the fixed-wing UAV to track the rogue drone in 3D space while continuously optimising its trajectory prediction and adjusting control parameters to ensure effective countermeasures. The cost function aims to minimise the tracking error between the UAV and the rogue drone while considering control effort and ensuring convergence. The cost function penalises the deviation from the desired trajectory and control effort, while also accounting for the terminal state penalty to ensure proper convergence towards the final state. The optimisation problem takes the following form:

$$\min_{\mathbf{u},\mathbf{x}} \quad J = \int_{t_0}^{t_f} \left(w_1 Q_p \|\mathbf{e}_p\|^2 + w_2 R_u \|\mathbf{u}\|^2 \right) dt + w_3 Q_f \|\mathbf{e}_f\|^2 \tag{7.8a}$$

$$\text{subject to} \quad \dot{\mathbf{x}} = f(\mathbf{x}, \mathbf{u}) \tag{7.8b}$$

$$\mathbf{x}(t_0) = \mathbf{x}_0 \tag{7.8c}$$

$$\mathbf{x}(t_f) = \mathbf{x}_f \tag{7.8d}$$

$$\mathbf{u}_{\min} \leq \mathbf{u}(t) \leq \mathbf{u}_{\max} \tag{7.8e}$$

where w_1, w_2, and w_3 are weighting factors for position errors, control efforts, and final prediction errors, respectively, $\mathbf{x}$ is the state vector, $\mathbf{u}$ is the control input vector, $f(\cdot)$ represents the dynamic equations of the UAV, $\mathbf{e}_p$ is the position error vector and $\mathbf{e}_f$ signifies the final prediction error at t_f. Q_p and Q_f are positive definite weighting matrices for position errors and R_u is a positive definite weighting matrix for control efforts. The adaptive weighting matrices Q_p, Q_f and R_u are updated based on the tracking error during the optimisation process, allowing the controller to adjust the relative importance of position error and control effort based on the tracking performance. The position error to the target being tracked as follows:

$$e_p = \sqrt{(x_q - x)^2 + (y_q - y)^2 + (z_q - z)^2} \tag{7.9}$$

where e_p is the position error while the values (x_q, y_q, z_q) represent the target position. The problem is subject to constraints for the dynamics of the system $\dot{\mathbf{x}} = f(\mathbf{x}, \mathbf{u})$, initial state $\mathbf{x}(t_0) = \mathbf{x}_0$, final state: $\mathbf{x}(t_f) = \mathbf{x}_f$, control input constraints: $\mathbf{u}_{\min} \leq \mathbf{u}(t) \leq \mathbf{u}_{\max}$ and constraints on adaptive control parameters ϕ_{ua}, ψ_{ua}, and θ_{ua}. The time variables t_0 and t_f represent the initial and final times, respectively. To apply NMPC, we discretise the time horizon from t_0 to t_f into N equally spaced time intervals Δt, and we introduce

the control trajectory $\mathbf{U} = [\mathbf{u}(t_0), \mathbf{u}(t_0 + \Delta t), \ldots, \mathbf{u}(t_f - \Delta t), \mathbf{u}(t_f)]$ and the state trajectory $\mathbf{X} = [\mathbf{x}(t_0), \mathbf{x}(t_0 + \Delta t), \ldots, \mathbf{x}(t_f - \Delta t), \mathbf{x}(t_f)]$.

We now discretize the integral over the time horizon $[t_0, t_f]$ into N intervals. Let's denote the time step as $\Delta t = \frac{t_f - t_0}{N}$. The discretized cost function can be written as follows:

$$\min_{\mathbf{u},\mathbf{x}} \quad J = \sum_{k=0}^{N-1} \left(w_1 Q_p \|\mathbf{e}_p(k\Delta t)\|^2 + w_2 R_u \|\mathbf{u}(k\Delta t)\|^2 \right) \Delta t + w_3 Q_f \|\mathbf{e}_f\|^2 \tag{7.10}$$

where, k represents the discrete time steps, and $\|\mathbf{e}_p(k\Delta t)\|$ and $\|\mathbf{u}(k\Delta t)\|$ represent the position error and control input at each time step $k\Delta t$, respectively. The objective function is the sum of the individual costs over each time interval, while the last term $w_3 Q_f \|\mathbf{e}_f\|^2$ remains continuous, representing the final prediction error at time t_f.

The optimisation process is performed at each time step, and the first control input of the optimal trajectory is applied to the UAV. The process is then repeated in a receding horizon fashion, allowing the controller to adapt to changes in the UAV's state and environment over time. A pseudocode showing steps used in solving our NMPC problem, by iteratively updating the control inputs $\mathbf{u}$, using the gradient descent method is presented in Algorithm 5:

Algorithm 5 NMPC Solution

Step 1: Initialise control inputs and other parameters:
    $\mathbf{u}_0, \alpha, \varepsilon$
    where $\mathbf{u}_0$ is the initial guess for control inputs,
    α is the step size, and ε is the convergence criterion.
Step 2: Initialise the optimisation horizon and time index $k = 0$.
Step 3: Repeat
    Step 4: Predict the system's state trajectory over the optimisation horizon using the current control inputs:
        Compute $\mathbf{x}_1^k, \mathbf{x}_2^k, \ldots, \mathbf{x}_N^k$.
    Step 5: Compute the cost function for the predicted trajectory:
        $J_k = \sum_{i=1}^{N} \left(w_1 Q_p \|\mathbf{e}_p(i\Delta t)\|^2 + w_2 R_u \|\mathbf{u}(i\Delta t)\|^2 \right) \Delta t + w_3 Q_f \|\mathbf{e}_f\|^2$.
    Step 6: Compute the cost function gradient ∇J_k with respect to the control inputs:
        $\nabla J_k = \sum_{i=1}^{N} \frac{\partial J}{\partial \mathbf{u}}(\mathbf{x}_i^k, \mathbf{u}_i^k)$.
    Step 7: Update the control inputs using the gradient descent update rule:
        $\mathbf{u}_{k+1} = \mathbf{u}_k - \alpha \nabla J_k$.
    Step 8: Increment the time index: $k \leftarrow k + 1$.
    Step 9: Until convergence criterion is met.
Step 10: Consider the optimal control inputs: $\mathbf{u}_{\text{opt}} = \mathbf{u}_k$.

7.3.2 Optimal Control Formulation

The NMPC controller developed in the previous section needs to be assessed for performance. For the assessment to be valuable, a reference controller is needed. Accordingly, we implement an optimal control algorithm using the same cost function in the NMPC solution to compare the two control algorithms. The Gradient descent-based optimal control is an iterative optimisation method that searches for the optimal control inputs by iteratively updating the control inputs in the direction of the steepest descent of the cost function [259]. In relation to our target tracking problem, the optimal control problem aims to find the control inputs $\mathbf{u}^*(t)$ that minimise the cost function J_{um}.

$$\min_{\mathbf{u},\mathbf{x}} \quad \int_{t_0}^{t_f} \left(w_1 Q_p \|\mathbf{e}_p\|^2 + w_2 R_u \|\mathbf{u}\|^2 \right) dt + w_3 Q_f \|\mathbf{e}_f\|^2 \tag{7.11}$$

where $\mathbf{e}p$ represents the position error vector. The adaptive weighting matrices Q_p, R_u are updated based on the tracking error during the optimisation process. To find the optimal solution, we can use optimisation techniques such as gradient descent or numerical solvers to solve the problem numerically. The solution involves iteratively updating the control inputs and propagating the dynamics until convergence. The detailed solution can be obtained by applying the necessary optimisation algorithms to minimise the cost function J while satisfying the given constraints. The simplified UAV tracking cost function was chosen for its quadratic form, which enables efficient optimisation, and its ability to balance position error and control effort using weighting matrices. It considers the cumulative effect over the entire time horizon and accommodates constraints, providing a flexible framework for various UAV tracking applications.

To solve the optimal control problem and find the control inputs $\mathbf{u}$ that minimise the cost function J, we will use the Euler-Lagrange equation. The Euler-Lagrange equation states that the partial derivatives of the Lagrangian concerning the state variables and their derivatives must be equal to the time derivative of the corresponding partial derivatives with respect to the derivatives of the state variables.

Let's define the Lagrangian L as follows:

$$L = w_1 Q_p \|\mathbf{e}_p\|^2 + w_2 R_u \|\mathbf{u}\|^2 + w_3 Q_f \|\mathbf{e}_f\|^2 \tag{7.12}$$

where $\mathbf{e}_p = [e_{px}, e_{py}, e_{pz}]^T$ is the position error vector, $\mathbf{u} = [u_x, u_y, u_z]^T$ is the control input vector, Q_p is the positive definite weighting matrix for the position error vector, and R_u is the positive definite weighting matrix for the control input vector.

The gradient descent algorithm iteratively updates the control inputs $\mathbf{u}(t)$ using the following update rule:

$$\mathbf{u}_{k+1}(t) = \mathbf{u}_k(t) - \alpha \cdot \nabla J \tag{7.13}$$

where $\mathbf{u}_k(t)$ is the control input vector at iteration k, α is the learning rate, and ∇J is the gradient of the cost function with respect to the control inputs. A pseudocode summarising the steps for solving the optimal control problem is presented in Algorithm 6.

Algorithm 6 Optimal Control using Gradient Descent

Step 1: Initialisation

Initialise control inputs and parameters:

u_0, α, ε

// u_0: Initial guess for control inputs

// α: Step size

// ε: Convergence criterion

Step 2: Compute Gradient

Compute the cost function gradient with respect to control inputs:

$$\nabla J = \begin{bmatrix} \frac{\partial J}{\partial V} \\ \frac{\partial J}{\partial \omega_x} \\ \frac{\partial J}{\partial \omega_y} \\ \frac{\partial J}{\partial \omega_z} \end{bmatrix}$$

Step 3: Iterative Update

Iteratively update control inputs using the gradient descent rule:

For $k = 0, 1, 2, \ldots$:

$u_{k+1} = u_k - \alpha \nabla J$

// u_{k+1}: Control inputs at iteration $k+1$

// u_k: Control inputs at iteration k

Step 4: Compute New Cost

Compute the new cost function value $J(u_{k+1})$ with updated control inputs.

Step 5: Check Convergence

Check for convergence by comparing changes in the cost function:

$\Delta J = |J(u_{k+1}) - J(u_k)|$

// ΔJ: Change in cost function

// $J(u_{k+1})$: Cost function value with updated control inputs

// $J(u_k)$: Cost function value with previous control inputs

If $\Delta J < \varepsilon$:

Stop iteration and consider u_{k+1} as the optimal solution.

Else:

Go back to **Step 2**.

Repeat Steps 2 to 5 until convergence is achieved.

7.4 Target Dynamics

To implement a scenario where a UAV intercepts 3 evasive targets that are operating independently, we need to design the target algorithms so they operate in the space. The dynamics and equations of motion for the target-1 in the tracking sequence are defined as

follows. Position and velocity equations:

$$\dot{x}_{q1} = v_{qx1}, \dot{y}_{q1} = v_{qy1}, \dot{z}_{q1} = v_{qz1}, \tag{7.14a}$$

$$v_{qx1} = \frac{1}{m}(F_{xq} - g\sin\theta_{uaq1}) \tag{7.14b}$$

$$v_{qy1} = \frac{1}{m}(F_{yq} + g\cos\theta_{uaq1}\sin\phi_{uaq1}) \tag{7.14c}$$

$$v_{qz1} = \frac{1}{m}(F_{zq} + g\cos\theta_{uaq1}\cos\phi_{uaq1}) - g \tag{7.14d}$$

$$u_{qx1} = \dot{v}_{qx1}, u_{qy1} = \dot{v}_{qy1}, u_{qz1} = \dot{v}_{qz1} \tag{7.14e}$$

where (x_{q1}, y_{q1}, z_{q1}) represents the quadrotor's position in the world frame, and $(v_{qx1}, v_{qy1}, v_{qz1})$ represents the quadrotor's linear velocity in the world frame, m denotes the mass of the quadrotor, and (F_{xq}, F_{yq}, F_{zq}) represent the forces acting on the quadrotor in the body frame along the quadrotor's x, y, and z axes, respectively. The term g represents the acceleration due to gravity while $(\phi_{uaq1}, \theta_{uaq1}, \psi_{uaq1})$ represent the roll, pitch, and yaw angles of the quadrotor, respectively, and $(\omega_{xq1}, \omega_{yq1}, \omega_{zq1})$ represent the angular velocities around the body-fixed x, y, and z axes, respectively. ω_z represents the angular velocity around the vertical axis (yaw rate). The attitude equations is as shown below:

$$\dot{\phi_{uaq1}} = \omega_{xq1} \tag{7.15a}$$

$$\dot{\theta_{uaq1}} = \omega_{yq1} \tag{7.15b}$$

$$\dot{\psi_{uaq1}} = \omega_{zq1} \tag{7.15c}$$

where u_qx, u_qy, and u_qz represent the control inputs for the quadrotor

Position control:

$$u_{qx1} = K_p(x_a - x_{q1}) + K_d(\dot{x}_a - \dot{x}_{q1}) \tag{7.16a}$$

$$u_{qy1} = K_p(y_a - y_{q1}) + K_d(\dot{y}_a - \dot{y}_{q1}) \tag{7.16b}$$

$$u_{qz1} = K_p(z_a - z_{q1}) + K_d(\dot{z}_a - \dot{z}_{q1}) \tag{7.16c}$$

The equations for quadrotor target-2 and target-3 are computed similarly to (7.14a) to (7.15a).

7.5 Countermeasure Projectile

In this section, we consider a scenario where a UAV is within close range of a target being tracked and is prepared to deploy a countermeasure. The countermeasure deployed is an

electromagnetic net propelled by a guided rocket projectile equipped with a proximity sensor, activating the net's deployment within 2m of a single or group of aerial targets, as depicted in Fig 7.2.

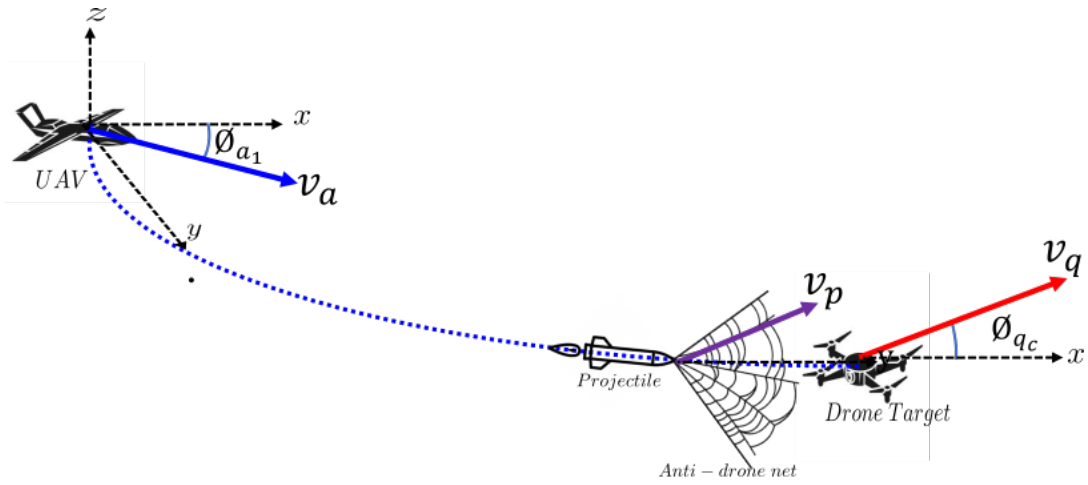

Fig. 7.2 Sketch of UAV-launched projectile anti-drone net deployment

The countermeasure needs to be agile and evasive, requiring the guided projectile to autonomously manoeuvre within the deployment range. Therefore, a control algorithm based on the proportional navigation guidance law is developed to guide the projectile to the target in 3D space. The guidance law is represented by the following equations:

$$\dot{\gamma}_p = \frac{v_q}{r_p}\sin(\gamma_p) \tag{7.17a}$$

$$\dot{\psi}_{ua_p} = \frac{v_q}{r_p}\cos(\gamma_p)\cos(\psi_{ua_p}) \tag{7.17b}$$

$$\dot{\theta}_{ua_p} = \frac{r_p}{v_q}\cos(\gamma_p)\cos(\psi_{ua_p}) \tag{7.17c}$$

$$\dot{\phi}_{ua_p} = \frac{r_p}{v_q}\sin(\gamma_p) \tag{7.17d}$$

Here, γ_p is the Line of Sight (LOS) angle between the projectile and the target, ψ_{ua_p} denotes the projectile's course angle, v_q is the target's velocity, and r_p represents the LOS range between the projectile and the target. The angles θ_{ua_p} and ϕ_{ua_p} correspond to the projectile's elevation and azimuth angles, respectively.

To control the projectile and achieve target proximity, a proportional control law is applied:

$$u_p = N_p \cdot \dot{\gamma}_p \cdot v_c - k_{pr} \cdot (d_{\text{eng}} - r_p) \tag{7.18}$$

Here, u_p denotes the projectile's acceleration command, N_p represents the proportional gain, $\dot{\gamma}_p$ is the LOS angle rate, v_c is the closing velocity of the projectile, k_{pr} is a positive constant for retardation, and d_{eng} denotes the engagement distance.

The calculation of γ_p and r_p involves:

$$\gamma_p = \tan^{-1}\left(\frac{y_q - y_p}{x_q - x_p}\right) \tag{7.19a}$$

$$r_p = \sqrt{(x_q - x_p)^2 + (y_q - y_p)^2 + (z_q - z_p)^2} \tag{7.19b}$$

$$\theta_{ua_p} = \tan^{-1}\left(\frac{(x_q - x_p)}{\sqrt{(y_q - y_p)^2 + (z_q - z_p)^2}}\right) \tag{7.19c}$$

$$\phi_{ua_p} = \tan^{-1}\left(\frac{(y_q - y_p)}{(x_q - x_p)}\right) \tag{7.19d}$$

Here, (x_p, y_p, z_p) represents the current projectile position, and (x_q, y_q, z_q) denotes the quadrotor target's position.

The objective is to integrate the projectile's dynamic equations along with the guidance law, updating the course angle using the proportional control law, to iteratively adjust the projectile's position and velocity in 3D space. This aims to achieve the projectile's proximity within 2m of the target.

7.6 Simulation and Results

7.6.1 Target interception simulation

To simulate the behaviour of the NMPC-controlled UAV in tracking the independent multi-targets, we initialised a scenario with the following parameters for the UAV and the target quadrotors:

UAV parameters: The UAV's initial position was set as $x_a = 30$, $y_a = 10$, and $z_a = 20$. Its initial velocities were $v_{xa} = 5$, $v_{ya} = 3$, and $v_{za} = 2$. Additionally, the UAV had control inputs $u_{ax} = 2$, $u_{ay} = 2$, and $u_{az} = 2$.

Target quadrotor 1 parameters: The first target quadrotor's initial position was $x_{q1} = 15$, $y_{q1} = 30$, and $z_{q1} = 40$. Its initial velocities were $v_{qx1} = 2$, $v_{qy1} = 1$, and $v_{qz1} = 2$. The target quadrotor's control inputs were $u_{qx1} = 1.5$, $u_{qy1} = 2$, and $u_{qz1} = 1$.

Target quadrotor 2 parameters: The second target quadrotor's initial position was $x_{q2} = 20$, $y_{q2} = 60$, and $z_{q2} = 20$. Its initial velocities were $v_{qx2} = 2$, $v_{qy2} = 1$, and $v_{qz2} = 2$. The target quadrotor's control inputs were $u_{qx2} = 1.5$, $u_{qy2} = 2$, and $u_{qz2} = 1$.

Target quadrotor 3 parameters: The third target quadrotor's initial position was $x_{q3} = 50$, $y_{q3} = 60$, and $z_{q3} = 40$. Its initial velocities were $v_{qx3} = 2$, $v_{qy3} = 1$, and $v_{qz3} = 2$. The target quadrotor's control inputs were $u_{qx3} = 1.5$, $u_{qy3} = 2$, and $u_{qz3} = 1$.

By specifying these parameter values, we were able to simulate the behaviour and interactions between the UAV and the target quadrotors. The subsequent analysis and results provide insights into the performance and effectiveness of the implemented control and evasion strategies.

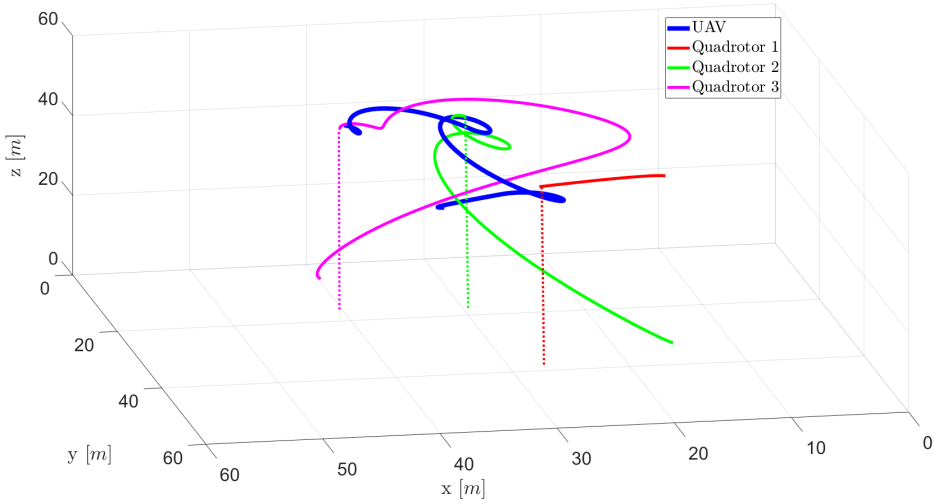

Fig. 7.3 Single UAV and multi-target positions

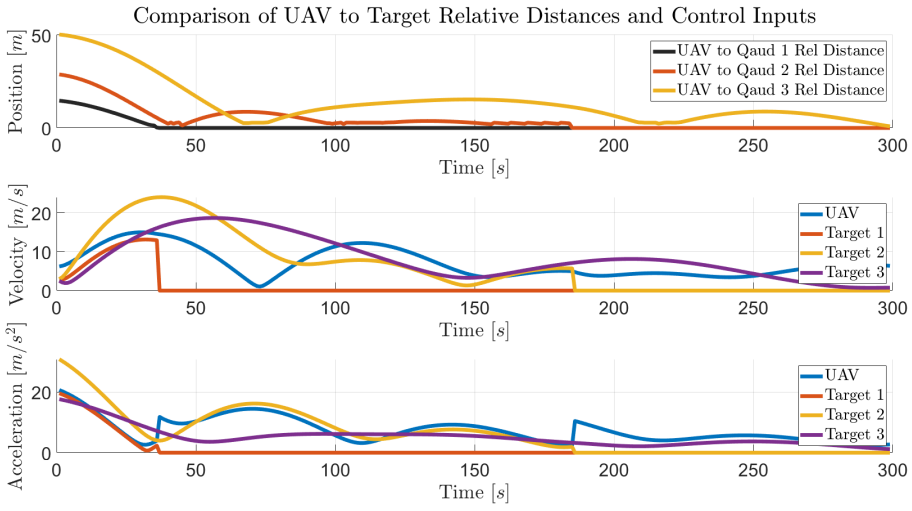

Fig. 7.4 Single UAV and multi-target position, velocity and acceleration comparison

From the plot of the UAV and multi-target trajectories in Fig.7.3, The UAV represented by the blue line, started by tracking and closing up to the target-1, depicted by the red line. When the UAV was within a 2m radius of target-1, the quadrotor was deemed as

captured. The UAV then switched to tracking the second target to track target-2, the green line, closing up to within 2m before a final switch to track target-3 represented by the pink line. The relative distance between the UAV and the 3 targets when plotted alongside their velocities and control input accelerations is shown in Fig.7.4. The relative distance between the UAV and target-1 started from 13m and gradually reduced as the UAV accelerated towards the target and eventually closed up to capture the target. In the same vein, the UAV acceleration was observed to have a sharp increase as it changed direction to track target-2. Again, the relative distance between the UAV and target-2 reduced as the UAV got closer to the target and increased when the target evaded the UAV. A similar pattern is observed as the UAV changes direction to track target-3 after intercepting target-2.

7.6.2 Tracking comparison and performance assessment

To test the performance of the UAV control algorithm in various mission scenarios, we modified some parameters using random variables within the allowable range. We utilised the average relative distance d_{rel} of the UAV to the target as an efficiency factor computed as the ratio of the total distance covered by the target currently being chased to the total distance covered by the UAV. The performance metric p_{met}, was developed using the relationship between the UAV to target relative distance, which represents the UAV's ability to maintain proximity to the target while tracking it, the total time taken to neutralise the 3 targets t_{nt}, and the total distance covered by the UAV. The closer the UAV can stay to the target within that threshold, the higher the efficiency factor would be. The equation for computing the efficiency and performance metric is as follows:

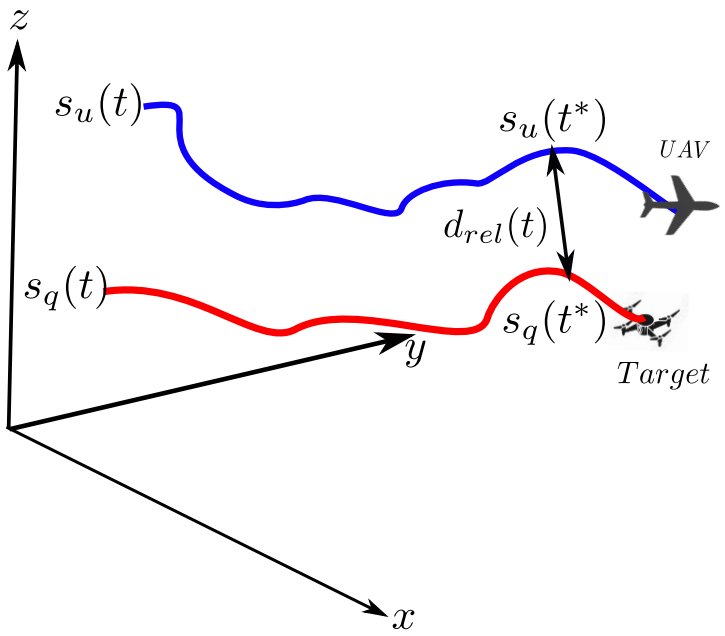

Fig. 7.5 UAV and target path length and relative distance

$$s_{u_{\text{tot}}} = \sum s_u(t) \tag{7.20a}$$

$$s_{q_{\text{tot}}} = \sum s_q(t) \tag{7.20b}$$

$$\varepsilon_f = \frac{s_{q_{\text{tot}}}}{s_{u_{\text{tot}}}} \tag{7.20c}$$

$$d_{\text{tot}} = \frac{1}{t_{\text{tot}}} \cdot \int_0^{t_{\text{tot}}} d_{rel}(t)\, dt \tag{7.20d}$$

$$p_{\text{met}} = \frac{s_{\text{utot}}}{\varepsilon_f \cdot t_{\text{tot}} \cdot d_{\text{rel}}} \tag{7.20e}$$

where $s_u(t)$ and $s_q(t)$ are the UAV and target paths at each time t while $d_{rel}(t)$ is the relative distance between UAV and target a particular time t^*. The efficiency factor ε_f represents the overall efficiency of the tracking algorithm or system. Also, s_{utot} is the total length of the path travelled by the UAV while s_{qtot} is the total path length of the tracked target trajectory cumulatively during the simulation. The simulation time t_{tot} is the total duration of the simulation. The purpose of this efficiency factor is to assess the efficiency of the UAV's movements in relation to the tracked target's movements. It provides a measure of how far the UAV has travelled compared to the target. A higher value of ε_f indicates that the UAV has covered a larger distance relative to the target's movement, suggesting more active tracking behaviour. Conversely, a lower value suggests that the UAV has covered a shorter distance compared to the target.

This metric takes into account the relative distance d_{rel} between the UAV and the target, which represents the UAV's ability to maintain proximity to the target while tracking it. A high score for the performance metric p_{met} indicates that the UAV control algorithm has performed well in terms of tracking efficiency and effectiveness. It suggests that the UAV has covered a large portion of the target's cumulative distance while maintaining proximity to the target within the defined threshold. This implies that the algorithm is efficient in tracking the target, achieving a good balance between distance covered and proximity maintained. On the other hand, a low score for p_{met} suggests that the UAV control algorithm struggled to track the target efficiently. It may have covered less distance or deviated significantly from the desired proximity, indicating a lower level of tracking performance.

Comparison between NMPC and optimal control tracking and performances

To compare the NMPC and optimal control algorithms presented in the problem formulation section, we designed a scenario where the two UAVs operating independently with the different controllers, are initiated with the same initial conditions used in the previous section to track and neutralise the 3 quadrotor targets. A sample simulation plot showing

the trajectories of the 2 UAVs in tracking the targets are superimposed on the same plot, while their control inputs and position histories are compared as shown in Fig. 7.6.

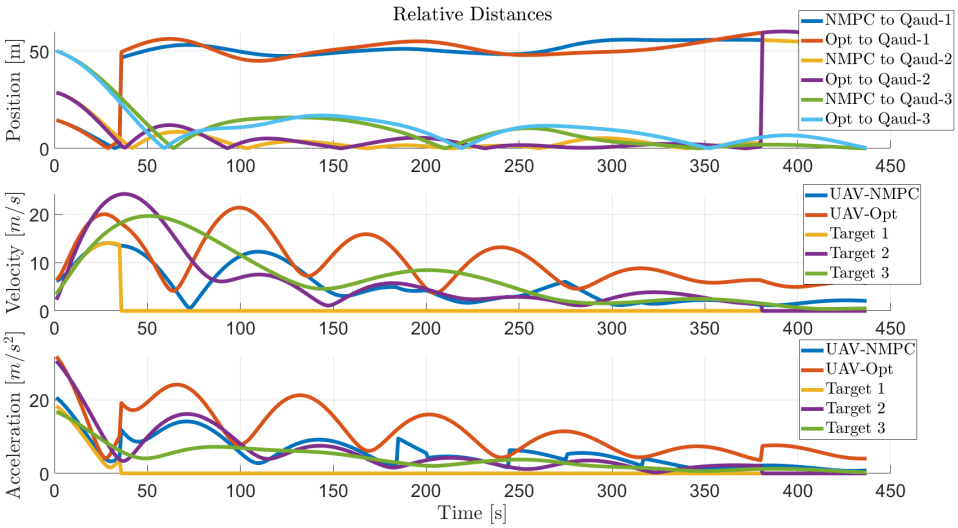

Fig. 7.6 NMPC and optimal control tracking trajectories

In addition to simulation UAV tracking using two control types, we also compared the NMPC control and the optimal control algorithms, using the performance metric developed earlier. By randomly varying the initial conditions and control parameters within allowable limits, we ran 100 Monte Carlo simulations to test the performance of the two control types in tracking and neutralising the 3 targets in sequence, starting from quadrotor target-1, followed by target-2 and then target-3. For all the simulations conducted, we computed the tracking algorithm efficiency factor and the performance metrics and recorded the average results in Table 7.1 below:

Table 7.1 Tracking metrics comparison for NMPC and optimal control UAV tracking strategies

Control Type	d_{utot}	d_{qtot}	ε_f	Average d_{rel}	t_{tot}	p_{met}
NMPC	957.2	947.6	0.65	33.3	101	0.49
Optimal	800.2	700.5	0.80	28.7	85	0.65

A histogram showing the comparative performance of the 2 control laws is shown in figure 7.7 below:

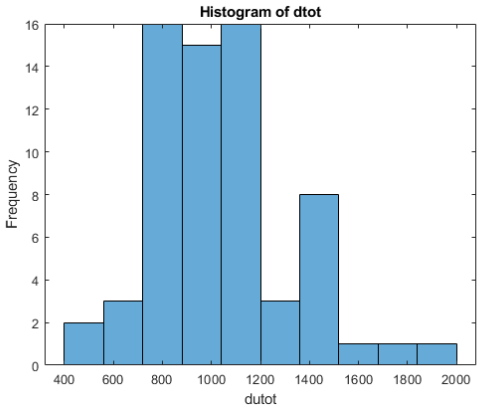

(a) Histogram of NMPC total distance tracking performance

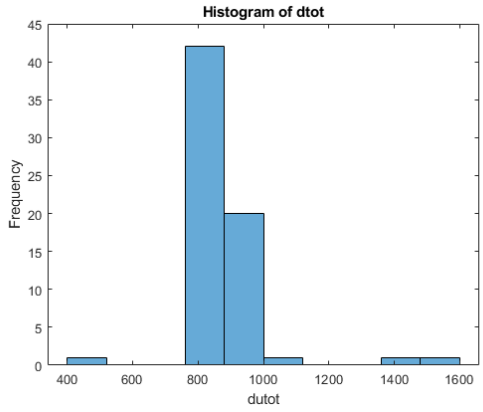

(b) Histogram of optimal control total distance tracking performance

Fig. 7.7 Histograms of total distance tracking performance for NMPC and optimal control

As shown in the histogram in Fig. 7.7, the cumulative distance covered by the NMPC controller in tracking the targets over 100 Monte Carlo simulations is greater than that of the optimal control. While the optimal control total distance covered was concentrated around 800 and 1000m, the NMPC controller had a wider spread with results concentrating between 800 - 1200m. This implies that while both controllers could track the targets, the NMPC controller was adapting to the variations in the initial conditions during the simulations. On the other hand, the optimal control gave more consistency in the distance travelled.

7.6.3 Projectile deployment simulation

The projectile was launched from the UAV when it got within 50m of the target and had a maximum acceleration $u_{p_{\max}} = 10m/s$ and a maximum velocity limit of $v_{p_{\max}} = 20m/s$. Considering the projectile is being launched from the same position as the UAV at the time of launch, its initial position was simulated as the position and speed of the UAV at a launch threshold of 50m to the target. The simulation result showing the performance of the projectile is as shown in Fig. 7.8.

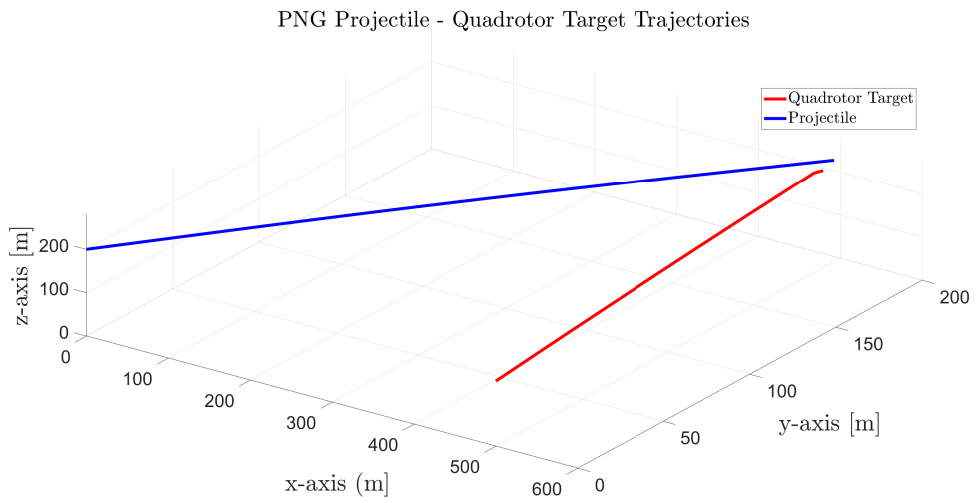

Fig. 7.8 Trajectory of projectile to target

7.7 Analysis and Discussion

It can be observed that the relative distance between the UAV and the target fell to zero as soon as the target was captured as shown in Figs. 7.4 and 7.6. This is also depicted in the trajectory plots by the dotted lines showing that the captured quadrotor has fallen to the ground. In reality, the relative distance does not remain at zero throughout the simulation but because we assume that the target is no longer available for tracking, its relative distance is depicted as zero. It was also shown that even when the UAV was close to target-2, it maintained tracking of target-1 and only moved on to track the next adversary target in its control sequence.

while both controllers tracked and closed up with the 3 independent targets in our mission scenario, the comparison, 7.7 of the total distance covered during target tracking over 100 Monte Carlo simulations with varied initial conditions showed different results for both controllers. The difference in performance is also reflected in Table 7.1 with the optimal control algorithm performing averagely better than the NMPC controller in terms of distances covered by UAV and target, efficiency score, and performance metric. In addition to the performance, the NMPC also consumed longer computation time when compared to the optimal control. This is because of the repeated optimisation at each time step in the NMPC controller. However, the adaptive performance of the NMPC shows its robustness, and tracking accuracy. The optimal control law exhibited superior tracking abilities concerning the overall distance travelled during tracking, efficiency, and enhanced performance. Despite the NMPC requiring more simulation time due to its optimisation horizon, it demonstrated increased adaptability to changes, a crucial aspect for ensuring robustness.

The results from the net dispensing projectile simulation as seen in Fig. 7.8, indicate the projectile can respond and close up with the target. The simulation was terminated when the projectile got to within 2m of the target, as we expected that the proximity sensor within the projectile would deploy the net. For further research, an algorithm could be developed to simulate and optimise the net deployment in the presence of disturbances like wind and precipitation.

7.8 Summary

This chapter developed a countermeasure strategy for the UAV to track and neutralise a non-cooperative adversarial target, intruding into restricted air space. The countermeasure algorithm assumes that the UAV is tracking 3 different targets, one target at a time. We implemented a decision logic to aid the UAV in deciding which target to track first and the next target using the same logic. We also implemented an NMPC controller for tracking UAVs and an optimal controller using the same cost function to compare their performances. The UAV controllers penalise the position error between the UAV and the target, while the target is evading using a smart PD control law. We also developed a performance metric to compare the performances of the NMPC and optimal control. Simulation results show that the UAV NMPC and optimal control laws were able to track the target. However, the optimal control law showed better tracking performance in terms of total distance covered during tracking, efficiency, and better performance. Although the NMPC consumed more time during simulation due to its optimisation horizon, it was observed to be more adaptive to changes which is essential for robustness.

Chapter 8

Conclusions and Future Work

Consider a scenario where we received credible intelligence information that a mischievous adversarial group is planning to attack a protected high-value facility using a ground-based vehicle and single or multi-quadrotor swarm. In addition to other security arrangements, we have been tasked to design algorithms to identify, track, and intercept the adversarial platforms before they intrude or access a protected facility. To simplify the problem, in this thesis, we assumed that the identification aspect has been solved and focused on the tracking aspect. Accordingly, we started by reviewing and modifying a min-max optimal control algorithm designed for planar UAV tracking of a ground-based target, by incorporating bank angle and turn rate constraints to reduce the chance of actuator failure on our UAV when tracking an evasively agile target. To ensure the tracking UAV can perform the task, we also designed an evasive control strategy for the target to intelligently and persistently evade.

Since 3D space is more representative of the real world, we devised a method to extend the 2D tracking and evasion strategies to 3D space using vector manipulation. Having done this, we considered that the UAV controller would require a more flexible altitude controller. Accordingly, we implemented 3 controller options for autonomously controlling the altitude of the UAV. Since some of the intruding vehicles are likely to be agile drones, we designed a quadrotor dynamics and evasion algorithm and further modified the UAV tracking controller to track the adversarial aerial target. We also considered the advantages of multi-UAV tracking and developed an algorithm for tracking single and multiple quadrotor swarms while optimally adjusting the UAV altitudes depending on the cluster size and relative distances of the individual quadrotors to the tracking UAV. Having considered these fixed-wing UAV tracking control strategies, we proceeded to explore and implement strategies to drive the UAVs close to the target to apply countermeasures and also developed

a control algorithm to launch and deliver a net-bearing projectile to within 2m proximity of the evasive single or multiple quadrotors, to deploy an electromagnetic net upon activation by an embedded proximity sensor. The remainder of this Chapter provides a summary of the technical chapters of this thesis and outlines the major contributions and future direction of the research.

8.1 Research Summary

In Chapter 3, we presented a fixed-wing UAV optimal target tracking strategy with the minimum turn radius varying with the bank angle, which enables the generation of realistic tracking paths for the tracking UAV. The optimal UAV control was based on a 2 step predictive min-max cost function where the UAV tries to persistently minimise its relative distance to the track a target assumed to be evading with its best control effort within the limits of the design constraints. Traditionally, most research focuses on the development of algorithms and controllers for the pursuing UAVs and implements a simplistic model like a curved path, or predefined or random target manoeuvres. In a few studies, evasive targets have been developed to manoeuvre away from the tracking UAV using a semi-smart controller. However, there are scanty studies on evasive aerial target pursuit and neutralisation. To address this, the chapter implemented a smart evasive target that is capable of initiating and persistently evading the tracker, thus enabling realistic tests, optimisation, and simulation of the pursuing UAV for robust performance. The evasive target control strategy was developed by maximising the same cost function, to generate smart evasive manoeuvres for the target. A method for extending the 2D target tracking algorithm to 3D cases using a vector transformation and direction cosine matrix derived from the UAV and target instantaneous velocity vectors was also implemented while avoiding the complexity of implementing a new design. The simulation results obtained show that the UAV persistently tracked the evading target in various scenarios and mission configurations.

In Chapter 4, we developed 3 vertical acceleration algorithms for generating altitude control for a fixed-wing UAV starting from the 2D plane. Essentially the vertical controller is combined with the 2D lateral and longitudinal control of the x and y axis to form 3D control of the UAV. One of the options utilised the relationship between the target and desired UAV altitude to compute controlled FPA changes to control the UAV altitude. The second option utilised the relationship between the UAV camera focal length, the size of the target image on the ground, and the desired size of the image on the camera lens to geometrically compute altitude control accelerations that control the UAV altitude above the target. Both options were tested using simulation and the results show that the

altitude control strategies are adequate for the research work. Due to its simple design demand, effectiveness and lower computational cost, we adopted the vertical controller designed based on FPA for controlling the UAV altitude for the remaining chapters of this research. Further simulation of the adopted altitude controllers shows it was sufficient for our fixed-wing UAV target tracking problem.

Chapter 5 presented a design for an evasive quadrotor algorithm to test the effectiveness of the UAV tracking algorithm against an evasive quadrotor-type target. Simple target evasion algorithms were designed for 3 scenarios, straight-line accelerated evasion, hover and evade manoeuvre, and continuous aerial evasion. To Prevent the UAV from colliding with the evasive target during aerial pursuit and evasion, we modified the UAV control algorithm designed in Chapters 3 and 4, to incorporate anti-collision measures. We also designed a performance metric to measure and test the effectiveness of the UAV in tracking the target. To further improve on the tracking algorithm, we introduced an adaptive optimisation algorithm that utilises the optimisation parameters to optimise the control of the UAV which was dependent on the relative distance of the UAV from the target. Energy consumption comparison was used to compare the original and adaptively optimised algorithm. The simulation results show that the adaptively optimised algorithm perfumed better in all scenarios.

In Chapter 6, we implemented an algorithm for tracking of a single evasive quadrotor-type target by 3 cooperative UAVs, independently tracking the target with a decentralised control strategy. The multi-UAV control strategy incorporated a tracking cost function, collision avoidance cost function, and altitude control cost function, which were minimised to keep the UAVs tracking the target at an optimal altitude, while avoiding collision between the UAVs and the target. To extend our cooperative tracking research, this Chapter also implemented a multi-UAV to multi-target mission scenario by designing an evasive target cluster, to evade the UAVs. Considering that the target cluster is dynamic and constantly changing in response to the target positions, we developed a new altitude control strategy that optimises the coverage and image capture quality relative to the cluster area and target positions of each UAV. To apply real-world consideration to the multi-UAV to multi-target scenario in this research, we also presented a sample algorithm for task assignment to one or more tracking UAVs. In particular, we designed and implemented a logic to autonomously assign one of the tracking UAVs, the task of chasing and intercepting a break-out quadrotor from an adversarial swarm.

In Chapter 7, we developed a countermeasure strategy for the UAV to track and neutralise a non-cooperative adversarial target, intruding into restricted air space. The countermeasure algorithm assumed that the UAV was tracking 3 different targets, one after the other. We implemented a decision logic to aid the UAV in deciding which target to track first and to determine the next target in the sequence using the same logic. We also implemented an NMPC controller to drive the tracking UAV within countermeasure deployment distance and an optimal controller using the same cost function to compare their performances. The UAV controllers penalise the position error between the UAV and the target, while the target is evaded using a smart PD control law. A performance metric was also designed to assess the performances of the NMPC and optimal control. Simulation results show that the UAV NMPC and optimal control laws were able to track the target. However, the optimal control law showed better tracking performance in terms of total distance covered during tracking, efficiency, and better performance. Although the NMPC consumed more time during simulation due to its optimisation horizon, it was observed to be more adaptive to changes which is essential for robustness.

8.1.1 Application in real world

The proposed approach has several practical uses in real-world scenarios as follows:

- **Surveillance and Security**: The algorithms developed for tracking the ground-based and aerial targets in this thesis can be employed in surveillance and security systems. This would enable autonomous tracking and interception of potential adversarial platforms, such as intruding vehicles or evasive drones, to protect critical infrastructure and secure key facilities.
- **Drone Defence Systems**: As the use of drones for various purposes becomes more rampant, the ability to track and intercept or capture evasive hostile or unauthorised drones is paramount. The research presented in this thesis can be adapted for drone defence systems to protect sensitive facilities like airports, security installations, events centres and routes and government facilities.
- **Search and Rescue Operations**: The research findings will also be valuable in search and rescue missions, where locating and tracking individuals or objects is paramount. The algorithms designed can be used and modified to suit specific mission requirements to aid in efficient search and tracking of missing persons or vehicles in challenging environments, such as urban areas, remote deserts or open sea.
- **Agriculture and Environmental Monitoring**: The algorithms developed in this research can also find applications in agriculture and wildlife tracking and envi-

ronmental monitoring. UAVs equipped with tracking and evasion strategies can be applied to enhance precision agriculture and tracking wildlife like birds and nocturnal animals.

- **Autonomous Delivery Systems**: The algorithms developed for tracking and interception could be utilised in autonomous delivery systems. UAVs delivering packages or medical supplies can navigate through dynamic environments like water bodies or evasive targets such as speedboats.

8.2 Future Research Directions

The research conducted in this thesis lays a foundation for future research in the following areas:

1. **Adaptive Evasive Strategies**: The evasive target algorithm developed in Chapter 3 could be modified by considering more advanced and self-tuning adaptive evasion strategies to enable targets to make smarter decisions to create more challenging scenarios for tracking algorithms robustness modification.
2. **Collaborative UAV Swarms**: The cooperative fixed-wing UAV tracking algorithm introduced in Chapter 5 could be extended in further research to include improved coordination and communication capabilities between the collaborative UAVs, to allow for more efficient task assignment and tracking of multiple targets.
3. **Machine Learning Integration**: Future research could leverage machine learning techniques to improve the adaptability and learning capabilities of tracking algorithms to optimise performance energy consumption, tracking time and countermeasure deployment in dynamic and complex evolving mission scenarios.
4. **Integration of Sensor Technologies**: Future studies could explore the use of more sophisticated tracking sensors highlighted in the review. Integrating advanced sensors like lidar, radar and hyperspectral imaging systems to enhance tracking precision and robustness in diverse environments. Furthermore, using sensors like infrared and thermal cameras will enable tracking in low-light conditions and enhance detection capabilities, particularly for nocturnal operations.
5. **Real-World Testing**: Lastly future work could explore building fixed-wing UAVs and conducting field experiments to validate or enhance the target tracking and countermeasure algorithms presented in this thesis in practical applications while addressing real-world disturbances such as wind, precipitation, poor visibility and sensor noise.

References

[1] Hisham O Khogali and Samir Mekid. The blended future of automation and ai: Examining some long-term societal and ethical impact features. *Technology in Society*, 73:102232, 2023.

[2] Michael Hood and Tom Jenkins. *Pathway to the Stars: 100 Years of the Royal Canadian Air Force*. University of Toronto Press, 2023.

[3] Mahmood A Al-Shareeda, Murtaja Ali Saare, and Selvakumar Manickam. Unmanned aerial vehicle: a review and future directions. *Indonesian Journal of Electrical Engineering and Computer Science (IJEECS)*, 30(2):778–786, 2023.

[4] Hazim Shakhatreh, Ahmad H Sawalmeh, Ala Al-Fuqaha, Zuochao Dou, Eyad Almaita, Issa Khalil, Noor Shamsiah Othman, Abdallah Khreishah, and Mohsen Guizani. Unmanned aerial vehicles (uavs): A survey on civil applications and key research challenges. *Ieee Access*, 7:48572–48634, 2019.

[5] Syed Agha Hassnain Mohsan, Nawaf Qasem Hamood Othman, Yanlong Li, Mohammed H Alsharif, and Muhammad Asghar Khan. Unmanned aerial vehicles (uavs): Practical aspects, applications, open challenges, security issues, and future trends. *Intelligent Service Robotics*, 16(1):109–137, 2023.

[6] Muaz Al Radi, Maryam Nooman AlMallahi, Ameena Saad Al-Sumaiti, Concetta Semeraro, Mohammad Ali Abdelkareem, and Abdul Ghani Olabi. Progress in artificial intelligence-based visual servoing of autonomous unmanned aerial vehicles (uavs). *International Journal of Thermofluids*, 21:100590, 2024.

[7] Jason Knight. *Countering unmanned aircraft systems*. PhD thesis, Monterey, CA; Naval Postgraduate School, 2019.

[8] Jian Wang, Yongxin Liu, and Houbing Song. Counter-unmanned aircraft system(s) (c-uas): State of the art, challenges, and future trends. *IEEE Aerospace and Electronic Systems Magazine*, 36(3):4–29, 2021.

[9] UK Government. UK Counter-Unmanned Aircraft Strategy. *Policy paper UK Counter-Unmanned Aircraft Strategy*, 2022. Accessed: January 18, 2024.

[10] Joint Air Power Competence Centre. A comprehensive approach to countering unmanned aircraft systems. Technical report, Joint Air Power Competence Centre, Kalkar, Germany, Year. Accessed: Date.

[11] Jingbo Wang, Kaiwen Zhou, Wenbin Xing, Huanhuan Li, and Zaili Yang. Applications, evolutions, and challenges of drones in maritime transport. *Journal of Marine Science and Engineering*, 11(11):2056, 2023.

[12] Peng Yan, Jifeng Guo, Xiaojie Su, and Chengchao Bai. Long-term tracking of evasive urban target based on intention inference and deep reinforcement learning. *IEEE Transactions on Neural Networks and Learning Systems*, 2023.

[13] Promit Panja, Jesse B Hoagg, and Sabur Baidya. Control barrier function based uav safety controller in autonomous airborne tracking and following systems. *arXiv preprint arXiv:2312.17215*, 2023.

[14] Jongrae Kim. *Dynamic System Modeling and Analysis with MATLAB and Python: For Control Engineers*. IEEE Press Series on Control Systems Theory and Applications. Wiley, 2022.

[15] Douglas Brown and Liang Sun. Dynamic exhaustive mobile target search using unmanned aerial vehicles. *IEEE Transactions on Aerospace and Electronic Systems*, 55(6):3413–3423, 2019.

[16] Jianguo Chen, Wenjun Zhang, Shuaishuai Wang, Yawei Li, and Kun Wang. Ground target guidance method for oriented overhead tracking of fixed-wing uav. In *2019 IEEE International Conference on Power, Intelligent Computing and Systems (ICPICS)*, pages 1–5. IEEE, 2019.

[17] Reza Shakeri, Mohammed Ali Al-Garadi, Ahmed Badawy, Amr Mohamed, Tamer Khattab, Abdulla Khalid Al-Ali, Khaled A Harras, and Mohsen Guizani. Design challenges of multi-uav systems in cyber-physical applications: A comprehensive survey and future directions. *IEEE Communications Surveys & Tutorials*, 21(4):3340–3385, 2019.

[18] Carlos Paucar, Lilia Morales, Katherine Pinto, Marcos Sánchez, Rosalba Rodríguez, Marisol Gutierrez, and Luis Palacios. Use of drones for surveillance and reconnaissance of military areas. In *Developments and Advances in Defense and Security: Proceedings of the Multidisciplinary International Conference of Research Applied to Defense and Security (MICRADS 2018)*, pages 119–132. Springer, 2018.

[19] Faris A Almalki and Ben Othman Soufiene. Modifying hata-davidson propagation model for remote sensing in complex environments using a multifactional drone. *Sensors*, 22(5):1786, 2022.

[20] Norbert Tuśnio and Wojciech Wróblewski. The efficiency of drones usage for safety and rescue operations in an open area: A case from poland. *Sustainability*, 14(1):327, 2021.

[21] Bart Engberts and Edo Gillissen. Policing from above: Drone use by the police. *The future of drone use: Opportunities and threats from ethical and legal perspectives*, pages 93–113, 2016.

[22] Douglas W Murphy and James Cycon. Applications for mini vtol uav for law enforcement. In *Sensors, C3I, information, and training technologies for law enforcement*, volume 3577, pages 35–43. SPIE, 1999.

[23] George Eftychidis, Ilias Gkotsis, Panayiotis Kolios, and Costas Peleties. Uavs and their use in servicing the community. *Community-oriented policing and technological innovations*, pages 119–131, 2018.

[24] Svetlana Ivanova, Alexander Prosekov, and Anatoly Kaledin. A survey on monitoring of wild animals during fires using drones. *Fire*, 5(3):60, 2022.

[25] Zongyao Yang, Xueying Yu, Simon Dedman, Massimiliano Rosso, Jingmin Zhu, Jiaqi Yang, Yuxiang Xia, Yichao Tian, Guangping Zhang, and Jingzhen Wang. Uav remote sensing applications in marine monitoring: Knowledge visualization and review. *Science of The Total Environment*, 838:155939, 2022.

[26] Jesús Jiménez López and Margarita Mulero-Pázmány. Drones for conservation in protected areas: Present and future. *Drones*, 3(1):10, 2019.

[27] Shreeram Marathe. Leveraging drone-based imaging technology for pipeline and rou monitoring survey. In *SPE Asia Pacific Health, Safety, Security, Environment and Social Responsibility Symposium?*, page D021S006R001. SPE, 2019.

[28] Dammika Seneviratne, Lorenzo Ciani, Marcantonio Catelani, Diego Galar, et al. Smart maintenance and inspection of linear assets: An industry 4.0 approach. *Acta Imeko*, 7:50–56, 2018.

[29] Bushra Jalil, Giuseppe Riccardo Leone, Massimo Martinelli, Davide Moroni, Maria Antonietta Pascali, and Andrea Berton. Fault detection in power equipment via an unmanned aerial system using multi modal data. *Sensors*, 19(13):3014, 2019.

[30] Pradeep Kumar Singh and Amit Sharma. An intelligent wsn-uav-based iot framework for precision agriculture application. *Computers and Electrical Engineering*, 100:107912, 2022.

[31] Parthasarathy Velusamy, Santhosh Rajendran, Rakesh Kumar Mahendran, Salman Naseer, Muhammad Shafiq, and Jin-Ghoo Choi. Unmanned aerial vehicles (uav) in precision agriculture: Applications and challenges. *Energies*, 15(1):217, 2021.

[32] Dan Popescu, Florin Stoican, Grigore Stamatescu, Loretta Ichim, and Cristian Dragana. Advanced uav–wsn system for intelligent monitoring in precision agriculture. *Sensors*, 20(3):817, 2020.

[33] Rogerio Bonatti, Cherie Ho, Wenshan Wang, Sanjiban Choudhury, and Sebastian Scherer. Towards a robust aerial cinematography platform: Localizing and tracking moving targets in unstructured environments. In *2019 IEEE/RSJ International Conference on Intelligent Robots and Systems (IROS)*, pages 229–236. IEEE, 2019.

[34] Naqqash Dilshad, JaeYoung Hwang, JaeSeung Song, and NakMyoung Sung. Applications and challenges in video surveillance via drone: A brief survey. In *2020 International Conference on Information and Communication Technology Convergence (ICTC)*, pages 728–732. IEEE, 2020.

[35] Eric Cheng. *Aerial photography and videography using drones*. Peachpit Press, 2015.

[36] Zhi Zheng and Xinze Chen. A game based path planning method for dual uavs in complex environments. In *2019 Chinese Control And Decision Conference (CCDC)*, pages 5431–5437. IEEE, 2019.

[37] Michael Jones, Soufiene Djahel, and Kristopher Welsh. Path-planning for unmanned aerial vehicles with environment complexity considerations: A survey. *ACM Computing Surveys*, 55(11):1–39, 2023.

[38] Haibin Duan, Jianxia Zhao, Yimin Deng, Yuhui Shi, and Xilun Ding. Dynamic discrete pigeon-inspired optimization for multi-uav cooperative search-attack mission planning. *IEEE Transactions on Aerospace and Electronic Systems*, 57(1):706–720, 2020.

[39] Guoqiang Xu, Weilai Jiang, Zhaolei Wang, and Yaonan Wang. Autonomous obstacle avoidance and target tracking of uav based on deep reinforcement learning. *Journal of Intelligent & Robotic Systems*, 104(4):60, 2022.

[40] Fan Li, Wen-Ping Song, Bi-Feng Song, and Jun Jiao. Dynamic simulation and conceptual layout study on a quad-plane in vtol mode in wind disturbance environment. *International Journal of Aerospace Engineering*, 2022, 2022.

[41] Wenhong Zhou, Jie Li, and Qingjie Zhang. Joint communication and action learning in multi-target tracking of uav swarms with deep reinforcement learning. *Drones*, 6(11):339, 2022.

[42] Peyman Abeshtan and Fariborz Saghafi. An innovative integrated path planning and trajectory tracking framework for a quadrotor slung load system in an urban environment. *Proceedings of the Institution of Mechanical Engineers, Part G: Journal of Aerospace Engineering*, page 09544100231166033, 2023.

[43] Yifei Shu, Yang Chen, Mian Hu, Huaiyu Wu, and Xingang Zhao. Uav path planning based on simultaneous optimization of monitoring frequency and security. In *2022 34th Chinese Control and Decision Conference (CCDC)*, pages 3808–3814. IEEE, 2022.

[44] Seok-ho Jang, Youyoung Yang, and Henzeh Leeghim. Angular rate constrained sliding mode control of uavs for path following. *Electronics*, 10(22):2776, 2021.

[45] Zi-Quan Wang, Cheng-Wei Yang, Xiao-Lin Hu, Jing Xiong, Juan Li, and Chang Liu. A design of simulation environment for small fixed-wing aircraft. In *Journal of Physics: Conference Series*, volume 1584, page 012066. IOP Publishing, 2020.

[46] Jia Huang, Sijiang Chang, and Shengfu Chen. A hybrid proportional navigation based two-stage impact time control guidance law. *Journal of Systems Engineering and Electronics*, 33(2):461–473, 2022.

[47] Kazuo Tanaka, Motoyasu Tanaka, Yutoku Takahashi, Arimasa Iwase, and Hua O Wang. 3-d flight path tracking control for unmanned aerial vehicles under wind environments. *IEEE Transactions on Vehicular Technology*, 68(12):11621–11634, 2019.

[48] Qiming Yang, Jiandong Zhang, Guoqing Shi, Jinwen Hu, and Yong Wu. Maneuver decision of uav in short-range air combat based on deep reinforcement learning. *IEEE Access*, 8:363–378, 2019.

[49] Federico Mason, Martina Capuzzo, Davide Magrin, Federico Chiariotti, Andrea Zanella, and Michele Zorzi. Remote tracking of uav swarms via 3d mobility models and lorawan communications. *IEEE Transactions on Wireless Communications*, 21(5):2953–2968, 2021.

[50] Lele Xu, Teng Wang, Wenzhe Cai, and Changyin Sun. Uav target following in complex occluded environments with adaptive multi-modal fusion. *Applied Intelligence*, pages 1–17, 2022.

[51] Santiago Garrido, Javier Muñoz, Blanca López, Fernando Quevedo, Concepción A Monje, and Luis Moreno. Fast marching techniques for teaming uav's applications in complex terrain. *Drones*, 7(2):84, 2023.

[52] Christophe De Wagter, Rick Ruijsink, Ewoud JJ Smeur, Kevin G van Hecke, Freek van Tienen, Erik van der Horst, and Bart DW Remes. Design, control, and visual navigation of the delftacopter vtol tail-sitter uav. *Journal of Field Robotics*, 35(6):937–960, 2018.

[53] Florian-M Adolf, Franz Andert, Lukas Goormann, and Jörg Dittrich. Vision-based target recognition and autonomous flights through obstacle arches with a small uav. In *Proceedings of the 65th AHS Annual Forum, Grapevine, TX, USA*, volume 42, 2009.

[54] Robin Lloyd Henderson Deits. *Learning contact-aware robot controllers from mixed integer optimization*. PhD thesis, Massachusetts Institute of Technology, 2019.

[55] Huili Yu, Kevin Meier, Matthew Argyle, and Randal W Beard. Cooperative path planning for target tracking in urban environments using unmanned air and ground vehicles. *IEEE/ASME transactions on mechatronics*, 20(2):541–552, 2014.

[56] Amirreza M Khaleghi, Dong Xu, Sara Minaeian, Mingyang Li, Yifei Yuan, Jian Liu, Young-Jun Son, Christopher Vo, Arsalan Mousavian, and Jyh-Ming Lien. A comparative study of control architectures in uav/ugv-based surveillance system. In *IIE Annual Conference. Proceedings*, page 3455. Institute of Industrial and Systems Engineers (IISE), 2014.

[57] Yuting Wan, Yanfei Zhong, Ailong Ma, and Liangpei Zhang. An accurate uav 3-d path planning method for disaster emergency response based on an improved multi-objective swarm intelligence algorithm. *IEEE Transactions on Cybernetics*, 53(4):2658–2671, 2022.

[58] R Prazenica, A Kurdila, R Sharpley, and J Evers. Vision-based geometry estimation and receding horizon path planning for uavs operating in urban environments. In *2006 American Control Conference*, pages 6–pp. IEEE, 2006.

[59] Stefan Hrabar. 3d path planning and stereo-based obstacle avoidance for rotorcraft uavs. In *2008 IEEE/RSJ International Conference on Intelligent Robots and Systems*, pages 807–814. IEEE, 2008.

[60] Benjamin Morrell, Rohan Thakker, Gene Merewether, Robert Reid, Marc Rigter, Theodore Tzanetos, and Gregory Chamitoff. Comparison of trajectory optimization algorithms for high-speed quadrotor flight near obstacles. *IEEE Robotics and Automation Letters*, 3(4):4399–4406, 2018.

[61] Markus Ryll, John Ware, John Carter, and Nick Roy. Efficient trajectory planning for high-speed flight in unknown environments. In *2019 International Conference on Robotics and Automation (ICRA)*, pages 732–738. IEEE, 2019.

[62] Ted J Steiner, Robert D Truax, and Kristoffer Frey. A vision-aided inertial navigation system for agile high-speed flight in unmapped environments: Distribution statement a: Approved for public release, distribution unlimited. In *2017 IEEE Aerospace Conference*, pages 1–10. IEEE, 2017.

[63] Antonios Tsourdos, Brian White, and Madhavan Shanmugavel. *Cooperative path planning of unmanned aerial vehicles*, volume 32. John Wiley & Sons, 2010.

[64] J-P Ramirez-Paredes, Emily A Doucette, J Willard Curtis, and Nicholas R Gans. Urban target search and tracking using a uav and unattended ground sensors. In *2015 American Control Conference (ACC)*, pages 2401–2407. IEEE, 2015.

[65] Sarthak Bhagat and PB Sujit. Uav target tracking in urban environments using deep reinforcement learning. In *2020 International Conference on Unmanned Aircraft Systems (ICUAS)*, pages 694–701. IEEE, 2020.

[66] Leonardo AA Pereira, Arthur HD Nunes, Adriano MC Rezende, Vinicius M Gonçalves, Guilherme V Raffo, and Luciano CA Pimenta. Collision-free vector field guidance and mpc for a fixed-wing uav. In *2021 IEEE International Conference on Robotics and Automation (ICRA)*, pages 176–182. IEEE, 2021.

[67] Herath Mpc Jayaweera and Samer Hanoun. Real-time obstacle avoidance for unmanned aerial vehicles (uavs). In *2021 IEEE International Conference on Systems, Man, and Cybernetics (SMC)*, pages 2622–2627. IEEE, 2021.

[68] Myoung Hoon Lee and Jun Moon. Deep reinforcement learning-based model-free path planning and collision avoidance for uavs: A soft actor–critic with hindsight experience replay approach. *ICT Express*, 9(3):403–408, 2023.

[69] Mahya Ramezani, Hamed Habibi, Jose Luis Sanchez-Lopez, and Holger Voos. Uav path planning employing mpc-reinforcement learning method considering collision avoidance. In *2023 International Conference on Unmanned Aircraft Systems (ICUAS)*, pages 507–514. IEEE, 2023.

[70] Hui Xiong, Yaozu Ding, and Jinzhen Liu. Compact and ordered swarms of unmanned aerial vehicles in cluttered environments. *Bioinspiration & Biomimetics*, 2023.

[71] Youfang Huang, Wen Liu, Bo Li, Yongsheng Yang, and Bing Xiao. Finite-time formation tracking control with collision avoidance for quadrotor uavs. *Journal of the Franklin Institute*, 357(7):4034–4058, 2020.

[72] Amala Sonny, Sreenivasa Reddy Yeduri, and Linga Reddy Cenkeramaddi. Autonomous uav path planning using modified pso for uav-assisted wireless networks. *IEEE Access*, 2023.

[73] Qingfeng Yao, Zeyu Zheng, Liang Qi, Haitao Yuan, Xiwang Guo, Ming Zhao, Zhi Liu, and Tianji Yang. Path planning method with improved artificial potential field—a reinforcement learning perspective. *IEEE access*, 8:135513–135523, 2020.

[74] Rachit Prasad, Gwonyeol Lee, Jae-Young Choi, Junki Shim, Nicholas C Song, and Seongim Choi. Data-driven target tracking methods of uas/uam in dynamic environment. In *AIAA SciTech 2023 Forum*, page 2660, 2023.

[75] Marcin Odelga, Paolo Stegagno, and Heinrich H Bülthoff. Obstacle detection, tracking and avoidance for a teleoperated uav. In *2016 IEEE International Conference on Robotics and Automation (ICRA)*, pages 2984–2990. IEEE, 2016.

[76] Bryant Eldon Chandler. *Robust Object Tracking: A Path-Planning Approach*. Brigham Young University, 2017.

[77] Rui Song, Teng Long, Zhu Wang, Yan Cao, and Guangtong Xu. Multi-uav cooperative target tracking method using sparse a search and standoff tracking algorithms. In *2018 IEEE CSAA Guidance, Navigation and Control Conference (CGNCC)*, pages 1–6. IEEE, 2018.

[78] Aditya Hegde and Debasish Ghose. Multi-uav collaborative transportation of payloads with obstacle avoidance. *IEEE Control Systems Letters*, 6:926–931, 2021.

[79] Alexey A Munishkin, David W Casbeer, and Dejan Milutinović. Scalable navigation for tracking a cooperative unpredictably moving target in an urban environment. In *2022 IEEE Conference on Control Technology and Applications (CCTA)*, pages 484–490. IEEE, 2022.

[80] Bryan Penin, Paolo Robuffo Giordano, and François Chaumette. Vision-based reactive planning for aggressive target tracking while avoiding collisions and occlusions. *IEEE Robotics and Automation Letters*, 3(4):3725–3732, 2018.

[81] Kevin Eckenhoff, Indrajeet Yadav, Guoquan Huang, and H Tanner. Dynamic target interception in cluttered environments. In *RT-DUNE ICRA 2018 Workshop*, 2018.

[82] Nikhil Kumar Singh and Sikha Hota. Three-dimensional waypoint following for fixed-wing unmanned aerial vehicles in obstacle-filled environments. *Proceedings of the Institution of Mechanical Engineers, Part G: Journal of Aerospace Engineering*, 234(3):640–654, 2020.

[83] Qianyu Lin, Xiaoli Wang, and YuTong Wang. Cooperative formation and obstacle avoidance algorithm for multi-uav system in 3d environment. In *2018 37th Chinese Control Conference (CCC)*, pages 6943–6948. IEEE, 2018.

[84] Zhiyuan Sun, Hanbing Sun, Ping Li, and Jin Zou. Cooperative strategy for pursuit-evasion problem in the presence of static and dynamic obstacles. *Ocean Engineering*, 279:114476, 2023.

[85] Yufeng Gao, Jun Yang, Ke Zhang, Huaizhen Peng, Yin Wang, Na Xia, and Gang Yao. A new method of conductor galloping monitoring using the target detection of infrared source. *Electronics*, 11(8):1207, 2022.

[86] Alexander C Woods. *An Extended Potential Field Controller for use on Aerial Robots*. University of Nevada, Reno, 2016.

[87] Shaimaa Ahmed, Amr Mohamed, Khaled Harras, Mohamed Kholief, and Saleh Mesbah. Energy efficient path planning techniques for uav-based systems with space discretization. In *2016 IEEE Wireless Communications and Networking Conference*, pages 1–6. IEEE, 2016.

[88] Zichao Zhang, Shubo Wang, Jian Chen, and Yu Han. A bionic dynamic path planning algorithm of the micro uav based on the fusion of deep neural network optimization/filtering and hawk-eye vision. *IEEE Transactions on Systems, Man, and Cybernetics: Systems*, 2023.

[89] Takumi Wakabayashi, Yukimasa Suzuki, and Satoshi Suzuki. Dynamic obstacle avoidance for multi-rotor uav using chance-constraints based on obstacle velocity. *Robotics and Autonomous Systems*, 160:104320, 2023.

[90] ZHOU Yaoming, SU Yu, XIE Anhuan, and KONG Lingyu. A newly bio-inspired path planning algorithm for autonomous obstacle avoidance of uav. *Chinese Journal of Aeronautics*, 34(9):199–209, 2021.

[91] Yiguo Yang, Liefa Liao, Hong Yang, and Shuai Li. An optimal control strategy for multi-uavs target tracking and cooperative competition. *IEEE/CAA Journal of Automatica Sinica*, 8(12):1931–1947, 2020.

[92] Qijie Chen, Tinglong Yan, Taoyu Wang, and Tong Zhang. Path planning algorithm for uav in complex environment based on state change. In *2020 International Conference on Intelligent Computing and Human-Computer Interaction (ICHCI)*, pages 310–315. IEEE, 2020.

[93] Yang Ji. Target tracking trajectory generation for quadrotors in static complex environments. In *2022 4th International Conference on Industrial Artificial Intelligence (IAI)*, pages 1–6. IEEE, 2022.

[94] Anthony B Muccio and T Bryan Scruggs. Moving target indicator (mti) applications for unmanned aerial vehicles (uavs). In *2003 Proceedings of the International Conference on Radar (IEEE Cat. No. 03EX695)*, pages 541–546. IEEE, 2003.

[95] Nathaniel Ray Olsen. *Information-Based Mobile Sensor Network Coordination for Localizing and Tracking of an Uncooperative Target*. PhD thesis, The University of Utah, 2022.

[96] Ali K Raz, Michael Hieb, Jair Ferrari, Lance Sherry, and Paulo Costa. Exploiting information fusion for cybersecurity of small unmanned aerial vehicles. In *AIAA SCITECH 2023 Forum*, page 2582, 2023.

[97] Naveen Kumar S, Rohit V Nanavati, and Shashi Ranjan Kumar. Robust nonlinear guidance strategies for survival of cooperating unmanned aerial vehicles against pursuing attackers. *Proceedings of the Institution of Mechanical Engineers, Part G: Journal of Aerospace Engineering*, 237(5):1025–1040, 2023.

[98] Piotr Samczynski, Mateusz Malanowski, Grzegorz Krawczyk, Janusz Kulpa, and Marcin Żywek. Passive radar as a part of critical infrastructure protection system. In *2018 International Conference on Radar (RADAR)*, pages 1–5. IEEE, 2018.

[99] Lin Gao, Stefano Selleri, Giorgio Battistelli, Luigi Chisci, and Giuseppe Pelosi. Passive target detection and tracking from electromagnetic field measurements. *International Journal of RF and Microwave Computer-Aided Engineering*, 30(9):e22321, 2020.

[100] José Lopes Esteves. Electromagnetic watermarking: Exploiting iemi effects for forensic tracking of uavs. In *2019 International Symposium on Electromagnetic Compatibility-EMC EUROPE*, pages 1144–1149. IEEE, 2019.

[101] Teodor Balaz, Jaroslav Krejci, Miroslav Svec, and Martin Drahansky. Uav range measurement by impulse laser rangefinder. In *2019 International Conference on Military Technologies (ICMT)*, pages 1–7. IEEE, 2019.

[102] Vladimir Dobrokhodov, Isaac Kaminer, Kevin Jones, Ioannis Kitsios, Chengyu Cao, Lili Ma, Naira Hovakimyan, and Craig Woolsey. Rapid motion estimation of a target moving with time-varying velocity. In *AIAA Guidance, Navigation and Control Conference and Exhibit*, page 6746, 2007.

[103] Jacob M Perron, Rui Huang, Jack Thomas, Lingkang Zhang, Ping Tan, and Richard T Vaughan. Orbiting a moving target with multi-robot collaborative visual slam. In *Proceedings of the Workshop on Multi-View Geometry in Robotics (MVIGRO), Rome, Italy*, pages 1339–1344, 2015.

[104] Jacob Michael Perron. Enabling autonomous mobile robots in dynamic environments with computer vision. M.sc. thesis, Simon Fraser University, 2018.

[105] Kashish Dhal, Pritam Karmokar, Animesh Chakravarthy, and William J Beksi. Vision-based guidance for tracking multiple dynamic objects. *Journal of Intelligent & Robotic Systems*, 105(3):1–23, 2022.

[106] Hyondong Oh, Seungkeun Kim, Hyo-sang Shin, and Antonios Tsourdos. Coordinated standoff tracking of moving target groups using multiple uavs. *IEEE Transactions on Aerospace and Electronic Systems*, 51(2):1501–1514, 2015.

[107] Andrey V Savkin and Hailong Huang. Navigation of a uav network for optimal surveillance of a group of ground targets moving along a road. *IEEE Transactions on Intelligent Transportation Systems*, 23(7):9281–9285, 2021.

[108] Andrey V Savkin and Hailong Huang. Multi-uav navigation for optimized video surveillance of ground vehicles on uneven terrains. *IEEE Transactions on Intelligent Transportation Systems*, 2023.

[109] Jiandong Zhang, Yuyang Chen, Qiming Yang, Yi Lu, Guoqing Shi, Shuo Wang, and Jinwen Hu. Dynamic task allocation of multiple uavs based on improved a-qcdpso. *Electronics*, 11(7):1028, 2022.

[110] Zhihao Liu, Yuanyuan Shang, Timing Li, Guanlin Chen, Yu Wang, Qinghua Hu, and Pengfei Zhu. Robust multi-drone multi-target tracking to resolve target occlusion: A benchmark. *IEEE Transactions on Multimedia*, 2023.

[111] Moulay A Akhloufi, Sebastien Arola, and Alexandre Bonnet. Drones chasing drones: Reinforcement learning and deep search area proposal. *Drones*, 3(3):58, 2019.

[112] ZHANG Min, ZHENG Chenming, and HUANG Kun. Fixed-wing uav guidance law for ground target over-flight tracking. *Journal of Systems Engineering and Electronics*, 30(2):384–392, 2019.

[113] Mouna Elloumi, Benoit Escrig, Riadh Dhaou, Hanen Idoudi, and Leila Azouz Saidane. Designing an energy efficient uav tracking algorithm. In *2017 13th International Wireless Communications and Mobile Computing Conference (IWCMC)*, pages 127–132. IEEE, 2017.

[114] Shulong Zhao, Xiangke Wang, Daibing Zhang, and Lincheng Shen. Curved path following control for fixed-wing unmanned aerial vehicles with control constraint. *Journal of Intelligent & Robotic Systems*, 89:107–119, 2018.

[115] Shulong Zhao, Xiangke Wang, Zhiyun Lin, Daibing Zhang, and Lincheng Shen. Integrating vector field approach and input-to-state stability curved path following for unmanned aerial vehicles. *IEEE Transactions on Systems, Man, and Cybernetics: Systems*, 50(8):2897–2904, 2018.

[116] Yueqian Liang, Yingmin Jia, Junping Du, and Jun Zhang. Vector field guidance for three-dimensional curved path following with fixed-wing uavs. In *2015 American Control Conference (ACC)*, pages 1187–1192. IEEE, 2015.

[117] Tagir Z Muslimov and Rustem A Munasypov. Multi-uav cooperative target tracking via consensus-based guidance vector fields and fuzzy mrac. *Aircraft Engineering and Aerospace Technology*, 93(7):1204–1212, 2021.

[118] Hamed Jabbari Asl and Hossein Bolandi. Robust vision-based control of an underactuated flying robot tracking a moving target. *Transactions of the Institute of Measurement and Control*, 36(3):411–424, 2014.

[119] Antoni Kopyt, Janusz Narkiewicz, and Paweł Radziszewski. An unmanned aerial vehicle optimal selection methodology for object tracking. *Advances in Mechanical Engineering*, 10(12):1687814018814085, 2018.

[120] Stanley S Baek, Hyukseong Kwon, Josiah A Yoder, and Daniel Pack. Optimal path planning of a target-following fixed-wing uav using sequential decision processes. In *2013 IEEE/RSJ International conference on intelligent robots and systems*, pages 2955–2962. IEEE, 2013.

[121] Kazuki Hirota, Yasuyuki Satoh, Norizumi Motooka, Yuta Asano, Shota Kameoka, and Toshiyuki Ohtsuka. Nonlinear receding-horizon differential game between a multirotor uav and a moving object. In *2017 11th Asian Control Conference (ASCC)*, pages 2137–2142. IEEE, 2017.

[122] Ross Anderson. *Uncertainty-Anticipating Stochastic Optimal Feedback Control of Autonomous Vehicle Models*. PhD thesis, UC Santa Cruz, 2014.

[123] Zhihao Cai, Mingjun Li, Jiang Zhao, and Yingxun Wang. Reinforcement learning for uav autonomous tracking random moving target. In *Advances in Guidance, Navigation and Control: Proceedings of 2020 International Conference on Guidance, Navigation and Control, ICGNC 2020, Tianjin, China, October 23–25, 2020*, pages 1109–1121. Springer, 2022.

[124] Hu Duoxiu, Dong Wenhan, Xie Wujie, and He Lei. Proximal policy optimization for multi-rotor uav autonomous guidance, tracking and obstacle avoidance. *International Journal of Aeronautical and Space Sciences*, 23(2):339–353, 2022.

[125] Binbin Xu, Zhuoning Dong, and Zehao Jia. The multi-uavs cooperative observation and tracking considering communication interference and transmission loss. In *2016 IEEE International Conference on Aircraft Utility Systems (AUS)*, pages 227–232. IEEE, 2016.

[126] Mingjun Li, Zhihao Cai, Jiang Zhao, Yibo Wang, Yingxun Wang, and Kelin Lu. Mnnms integrated control for uav autonomous tracking randomly moving target based on learning method. *Sensors*, 21(21):7307, 2021.

[127] Yaohong Qu, Ying Sun, Kai Wang, and Feng Zhang. Multi-uav cooperative search method for a moving target on the ground or sea. In *2019 Chinese Control Conference (CCC)*, pages 4049–4054. IEEE, 2019.

[128] Maryam Kouzeghar, Youngbin Song, Malika Meghjani, and Roland Bouffanais. Multi-target pursuit by a decentralized heterogeneous uav swarm using deep multi-agent reinforcement learning. *arXiv preprint arXiv:2303.01799*, 2023.

[129] Sami El-Ferik. Biologically based control of a fleet of unmanned aerial vehicles facing multiple threats. *IEEE Access*, 8:107146–107160, 2020.

[130] André Brandenburger, Folker Hoffmann, and Alexander Charlish. Co-training an observer and an evading target. In *2021 IEEE 24th International Conference on Information Fusion (FUSION)*, pages 1–8. IEEE, 2021.

[131] Sean Wolfe, Sidney Givigi, and Camille-Alain Rabbath. Distributed multiple model mpc for target tracking uavs. In *2020 International Conference on Unmanned Aircraft Systems (ICUAS)*, pages 123–130. IEEE, 2020.

[132] Mouhyemen Khan, Karel Heurtefeux, Amr Mohamed, Khaled A Harras, and Mohammad Mehedi Hassan. Mobile target coverage and tracking on drone-be-gone uav cyber-physical testbed. *IEEE Systems Journal*, 12(4):3485–3496, 2017.

[133] Emily Beatty and Eric Dong. Multi-agent reinforcement learning for uav sensor management. In *Open Architecture/Open Business Model Net-Centric Systems and Defense Transformation 2023*, volume 12544, pages 103–112. SPIE, 2023.

[134] Mahendra Mallick, Vikram Krishnamurthy, and Ba-Ngu Vo. *Integrated tracking, classification, and sensor management: theory and applications*. John Wiley & Sons, 2012.

[135] Mengjie Hu, Xiaotong Zhu, Haotian Wang, Shixiang Cao, Chun Liu, and Qing Song. Stdformer: Spatial-temporal motion transformer for multiple object tracking. *IEEE Transactions on Circuits and Systems for Video Technology*, 2023.

[136] Bo Wang, Jinghong Liu, Shengjie Zhu, Fang Xu, and Chenglong Liu. A dual-input moving object detection method in remote sensing image sequences via temporal semantics. *Remote Sensing*, 15(9):2230, 2023.

[137] Hend Gedawy, Abdulla Al-Ali, Amr Mohamed, Aiman Erbad, and Mohsen Guizani. Uavs smart heuristics for target coverage and path planning through strategic locations. In *2021 International Wireless Communications and Mobile Computing (IWCMC)*, pages 278–284. IEEE, 2021.

[138] Philip Dames, Pratap Tokekar, and Vijay Kumar. Detecting, localizing, and tracking an unknown number of moving targets using a team of mobile robots. *The International Journal of Robotics Research*, 36(13-14):1540–1553, 2017.

[139] Xiaolong Zhu, Fernando Vanegas, and Felipe Gonzalez. Decentralised multi-uav cooperative searching multi-target in cluttered and gps-denied environments. In *2022 IEEE Aerospace Conference (AERO)*, pages 1–10. IEEE, 2022.

[140] Senqiang Zhu, Danwei Wang, and Chang Boon Low. Ground target tracking using uav with input constraints. *Journal of Intelligent & Robotic Systems*, 69:417–429, 2013.

[141] Karl Engelbert Wenzel, Andreas Masselli, and Andreas Zell. Automatic take off, tracking and landing of a miniature uav on a moving carrier vehicle. *Journal of intelligent & robotic systems*, 61:221–238, 2011.

[142] Quan Xiao, Linghua Kong, Cheng Zou, Guowei Cai, and Kun Yu. Development of a yolo-kcf coupling algorithm for miniature fixed-wing uavs in target detection and tracking. *Unmanned Systems*, pages 1–12, 2023.

[143] Qiusheng He, Weifeng Zhang, Wei Chen, Gang Xie, and Yanxin Yao. Target tracking algorithm combined part-based and redetection for uav. *EURASIP Journal on Wireless Communications and Networking*, 2020(1):1–17, 2020.

[144] Wen-Chieh Chen, Chun-Liang Lin, Yang-Yi Chen, and Hsin-Hsu Cheng. Quadcopter drone for vision-based autonomous target following. *Aerospace*, 10(1):82, 2023.

[145] CP Warren, WR Pfister, DM Even, A Velasco, and J Naungayan. Conference 8020: Airborne intelligence, surveillance, reconnaissance (isr) systems and applications viii. *Connecting minds for global solutions*, 14:112, 2011.

[146] Rob O'Gorman and Chris Abbott. Remote control war. *Open Briefing, September*, 82, 2013.

[147] Shan Mufti et al. *Path planning algorithm for multiple unmanned aerial vehicles with parallel implementation on a graphics processing unit*. PhD thesis, Royal Military Collge of Canada, 2019.

[148] Thibault Maillot, Ugo Boscain, Jean-Paul Gauthier, and Ulysse Serres. Lyapunov and minimum-time path planning for drones. *Journal of Dynamical and Control Systems*, 21:47–80, 2015.

[149] Ugo Boscain, Jean-Paul Gauthier, Thibault Maillot, and Ulysse Serres. Lyapunov and minimum time path planning for drones. *Journal of Dynamical and Control Systems*, 2014.

[150] Sudhir Kumar Chaturvedi, Raj Sekhar, Saikat Banerjee, and Hutanshu Kamal. Comparative review study of military and civilian unmanned aerial vehicles (uavs). *INCAS bulletin*, 11(3):181–182, 2019.

[151] Andrew George Pollock. *Optimal algorithm design for transfer path planning for unmanned aerial vehicles*. PhD thesis, University of Glasgow, 2014.

[152] Wonkeun Youn, Hyoungsik Choi, Am Cho, Sungyug Kim, and Matthew B Rhudy. Accelerometer fault-tolerant model-aided state estimation for high-altitude long-endurance uav. *IEEE Transactions on Instrumentation and Measurement*, 69(10):8539–8553, 2020.

[153] Sang Wook Park, Jeong Woo Shin, and Tae-Uk Kim. Development of the main wing structure of a high altitude long endurance uav. *International Journal of Aeronautical and Space Sciences*, 19:53–71, 2018.

[154] Wonkeun Youn, Hyoung Sik Choi, Hyeok Ryu, Sungyug Kim, and Matthew B Rhudy. Model-aided state estimation of hale uav with synthetic aoa/ssa for analytical redundancy. *IEEE Sensors Journal*, 20(14):7929–7940, 2020.

[155] Alain Ajami, Iwan Pranoto, and Jean-Paul Gauthier. Hale uav: Output stabilization with the minimum time strategy. In *2023 IEEE Aerospace Conference*, pages 1–6. IEEE, 2023.

[156] Yazdi Ibrahim Jenie, Gerald Yohanes Pardomoan, and Mochammad Agoes Moelyadi. Development of an automatic solar tracker control system for a tandem-winged uav and its implementation strategies. *Drones*, 7(7):442, 2023.

[157] Bin Li, Shi Qiu, Wei Jiang, Wei Zhang, Mingnan Le, et al. A uav detection and tracking algorithm based on image feature super-resolution. *Wireless Communications and Mobile Computing*, 2022, 2022.

[158] Rohit Sharma and Rajeev Arya. Uav-based long-range environment monitoring system with industry 5.0 perspectives for smart city infrastructure. *Computers & Industrial Engineering*, 168:108066, 2022.

[159] Zhaoyue Xia, Jun Du, Chunxiao Jiang, Jingjing Wang, Yong Ren, and Gang Li. Multi-uav cooperative target tracking based on swarm intelligence. In *ICC 2021-IEEE International Conference on Communications*, pages 1–6. IEEE, 2021.

[160] Kumar Garvit, Hariom Goyal, VK Dwivedi, VK Mehta, and Rama Mehta. Designing of quad copter for surveillance and hydrological data collection: Maximizing target acquisition. In *Proceedings of the International Conference on Soft Computing for Problem Solving (SocProS 2011) December 20-22, 2011: Volume 2*, pages 425–436. Springer, 2012.

[161] Qifeng Shen, Linfeng Jiang, and Huilin Xiong. Person tracking and frontal face capture with uav. In *2018 IEEE 18th International Conference on Communication Technology (ICCT)*, pages 1412–1416. IEEE, 2018.

[162] Xuancen Liu, Yueneng Yang, Chenxiang Ma, Jie Li, and Shifeng Zhang. Real-time visual tracking of moving targets using a low-cost unmanned aerial vehicle with a 3-axis stabilized gimbal system. *Applied Sciences*, 10(15):5064, 2020.

[163] MY Zakaria, Moatassem M Abdallah, and M Adnan Elshafie. Design and production of small tailless unmanned aerial vehicle. In *The International Conference on Applied Mechanics and Mechanical Engineering*, volume 15, pages 1–26. Military Technical College, 2012.

[164] Matthias Mueller, Neil Smith, and Bernard Ghanem. A benchmark and simulator for uav tracking. In *Computer Vision–ECCV 2016: 14th European Conference, Amsterdam, The Netherlands, October 11–14, 2016, Proceedings, Part I 14*, pages 445–461. Springer, 2016.

[165] Jin Liu, Ying Lu, Yusi Chen, Qianqian Zhao, Zilu Qin, and Yanfang Fu. Research on low-altitude uav aerial photography target detection. In *2022 International Conference on Computer Network, Electronic and Automation (ICCNEA)*, pages 369–372. IEEE, 2022.

[166] Bahri Maraş, Nafiz Arica, and Ayşın Ertüzün. A robust vehicle tracking in low-altitude uav videos. *Machine Vision and Applications*, 34(5):77, 2023.

[167] Ershen Wang, Wansen Shu, Junjie Zhu, Song Xu, Pingping Qu, and Tao Pang. Low-altitude uav recognition and classification algorithm based on machine learning. In *2021 IEEE 16th Conference on Industrial Electronics and Applications (ICIEA)*, pages 1136–1141. IEEE, 2021.

[168] Hongguang Li, Wenrui Ding, Xianbin Cao, and Chunlei Liu. Image registration and fusion of visible and infrared integrated camera for medium-altitude unmanned aerial vehicle remote sensing. *Remote Sensing*, 9(5):441, 2017.

[169] Ruonan Yu, Hongguang Li, Yalong Jiang, Baochang Zhang, and Yufeng Wang. Tiny vehicle detection for mid-to-high altitude uav images based on visual attention and spatial-temporal information. *Sensors*, 22(6):2354, 2022.

[170] Themistoklis Giitsidis, Evangelos G Karakasis, Antonios Gasteratos, and G Ch Sirakoulis. Human and fire detection from high altitude uav images. In *2015 23rd euro micro international conference on parallel, distributed, and network-based processing*, pages 309–315. IEEE, 2015.

[171] Yanlong Chang, Dong Li, Yunlong Gao, Yun Su, and Xiaoqiang Jia. An improved yolo model for uav fuzzy small target image detection. *Applied Sciences*, 13(9):5409, 2023.

[172] Myung Hwangbo. *Vision-based navigation for a small fixed-wing airplane in urban environment*. Carnegie Mellon University, 2012.

[173] Niccolo'Carlo Martello. Modelling and integration of an evtol uav. M.sc. thesis, Polytechnic University of Milan, 2021.

[174] Ferit Çakıcı. *Control and guidance of a multi-mode unmanned aerial vehicle for increased versatility*. PhD thesis, Middle East Technical University, 2016.

[175] W.Y.H. Adoni, S. Lorenz, J.S. Fareedh, R. Gloaguen, and M. Bussmann. Classification of uncrewed aerial vehicles. Encyclopedia, Year. Available online: https://encyclopedia.pub/entry/43656 (accessed on Day Month Year).

[176] Song-lin Liao, Rong-ming Zhu, Nai-qi Wu, Tauqeer Ahmed Shaikh, Mohamed Sharaf, and Almetwally M Mostafa. Path planning for moving target tracking by fixed-wing uav. *Defence Technology*, 16(4):811–824, 2020.

[177] Kun Wu, Zhihao Cai, Jiang Zhao, and Yingxun Wang. Target tracking based on a nonsingular fast terminal sliding mode guidance law by fixed-wing uav. *Applied sciences*, 7(4):333, 2017.

[178] Shun Sun, Kai Dong, Chen Guo, and Daning Tan. A wind estimation based on unscented kalman filter for standoff target tracking using a fixed-wing uav. *International Journal of Aeronautical and Space Sciences*, 22(2):366–375, 2021.

[179] Chaoying Pei, Jingjuan Zhang, Xueyun Wang, and Qian Zhang. Research of a non-linearity control algorithm for uav target tracking based on fuzzy logic systems. *Microsystem Technologies*, 24:2237–2252, 2018.

[180] Lingjie Yang, Zhihong Liu, Xiangke Wang, and Yinbo Xu. An optimized image-based visual servo control for fixed-wing unmanned aerial vehicle target tracking with fixed camera. *IEEE Access*, 7:68455–68468, 2019.

[181] Prakrit Tyagi, Cunjia Liu, and PB Sujit. Energy optimal 3d target tracking using fixed-wing uav. In *2022 International Conference on Unmanned Aircraft Systems (ICUAS)*, pages 1404–1410. IEEE, 2022.

[182] Yong Zhou, Dengqing Tang, Han Zhou, Xiaojia Xiang, and Tianjia Hu. Vision-based online localization and trajectory smoothing for fixed-wing uav tracking a moving target. In *Proceedings of the IEEE/CVF International Conference on Computer Vision Workshops*, pages 0–0, 2019.

[183] Dongmin Shin, Yeongho Song, Jinwoo Oh, and Hyondong Oh. Nonlinear disturbance observer-based standoff target tracking for small fixed-wing uavs. *International Journal of Aeronautical and Space Sciences*, 22(1):108–119, 2021.

[184] Zhihong Liu, Xiangke Wang, Lincheng Shen, Shulong Zhao, Yirui Cong, Jie Li, Dong Yin, Shengde Jia, and Xiaojia Xiang. Mission-oriented miniature fixed-wing uav swarms: A multilayered and distributed architecture. *IEEE Transactions on Systems, Man, and Cybernetics: Systems*, 52(3):1588–1602, 2020.

[185] Xin Zhao, Zhihui Xu, Yifeng Fu, Shoupeng Xu, Shasha Xiong, et al. Motion control and tracking control of uav based on adaptive sensor. *Journal of Sensors*, 2023, 2023.

[186] Ha Sier, Xianjia Yu, Iacopo Catalano, Jorge Pena Queralta, Zhuo Zou, and Tomi Westerlund. Uav tracking with lidar as a camera sensor in gnss-denied environments. In *2023 International Conference on Localization and GNSS (ICL-GNSS)*, pages 1–7. IEEE, 2023.

[187] Jingcheng Zhang, Yuqiang An, Jianing Cao, Shibo Ouyang, and Lei Wang. Uav trajectory planning for complex open storage environments based on an improved rrt algorithm. *IEEE Access*, 11:23189–23204, 2023.

[188] Shuyan Hu, Xin Yuan, Wei Ni, Xin Wang, and Abbas Jamalipour. Visual camouflage and online trajectory planning for unmanned aerial vehicle-based disguised video surveillance: Recent advances and a case study. *IEEE Vehicular Technology Magazine*, 2023.

[189] Cesare Donati, Martina Mammarella, Lorenzo Comba, Alessandro Biglia, Paolo Gay, and Fabrizio Dabbene. 3d distance filter for the autonomous navigation of uavs in agricultural scenarios. *Remote Sensing*, 14(6):1374, 2022.

[190] Aicha Idriss Hentati and Lamia Chaari Fourati. Framework for uav mobile object tracking based on ue4sim. In *2019 international conference on software, telecommunications and computer networks (softcom)*, pages 1–6. IEEE, 2019.

[191] Mohammed Rabah, Ali Rohan, Sherif AS Mohamed, and Sung-Ho Kim. Autonomous moving target-tracking for a uav quadcopter based on fuzzy-pi. *IEEE Access*, 7:38407–38419, 2019.

[192] Yanhua Shao, Xianfeng Tang, Hongyu Chu, Yanying Mei, Zhiyuan Chang, Xiaoqiang Zhang, Huayi Zhan, and Yunbo Rao. Research on target tracking system of quadrotor uav based on monocular vision. In *2019 Chinese Automation Congress (CAC)*, pages 4772–4775. IEEE, 2019.

[193] Xudong Wang, Bo Luo, and Zhiyuan Zhang. Application of uav target tracking based on computer vision. In *Journal of Physics: Conference Series*, volume 1881, pages 042–053. IOP Publishing, 2021.

[194] Mirko Leomanni, Francesco Ferrante, Nicholas Cartocci, Gabriele Costante, Mario Luca Fravolini, Kadriye Merve Dogan, and Tansel Yucelen. Robust output feedback control of a quadrotor uav for autonomous vision-based target tracking. In *AIAA SCITECH 2023 Forum*, page 1632, 2023.

[195] Jun Hou, Liming Dai, Chunhui Zhao, Xiaolei Hou, Jinwen Hu, and Yang Lyu. Dynamic target tracking and localization for small uav in unstructured outdoor environment. In *International Conference on Autonomous Unmanned Systems*, pages 203–213. Springer, 2022.

[196] Wentao Xue, Xunnan Zhu, Xiaofei Yang, Hui Ye, and Xuan Chen. A moving target tracking control of quadrotor uav based on passive control and super-twisting sliding mode control. *Mathematical Problems in Engineering*, 2021:1–17, 2021.

[197] Kangli Wang, Swee King Phang, Yijie Ke, Xudong Chen, Kehong Gong, and Ben M. Chen. Vision-aided tracking of a moving ground vehicle with a hybrid uav. In *2017 13th IEEE International Conference on Control & Automation (ICCA)*, pages 28–33, 2017.

[198] Nihal Dalwadi, Dipankar Deb, and Stepan Ozana. Multi-observer based adaptive controller for hybrid uav. In *Adaptive Hybrid Control of Quadrotor Drones*, pages 87–108. Springer, 2023.

[199] P Panagiotou, I Tsavlidis, and K Yakinthos. Conceptual design of a hybrid solar male uav. *Aerospace Science and Technology*, 53:207–219, 2016.

[200] Hang Zhang, Bifeng Song, Haifeng Wang, and Jianlin Xuan. A method for evaluating the wind disturbance rejection capability of a hybrid uav in the quadrotor mode. *International Journal of Micro Air Vehicles*, 11:1756829319869647, 2019.

[201] Shanfei Su, Yihan Mei, Yan Zhou, Xiaowen Shan, Peng Yu, and Hao Wang. Flight performance characteristics of a modified quadcopter with and without a wing based on flight test. In *AIAA SCITECH 2023 Forum*, page 2103, 2023.

[202] Siddhant Panigrahi, Yenugu Siva Sai Krishna, and Asokan Thondiyath. Design, analysis, and testing of a hybrid vtol tilt-rotor uav for increased endurance. *Sensors*, 21(18):5987, 2021.

[203] Adnan S Saeed, Ahmad Bani Younes, Chenxiao Cai, and Guowei Cai. A survey of hybrid unmanned aerial vehicles. *Progress in Aerospace Sciences*, 98:91–105, 2018.

[204] Kyung-Jae Nam, Joosang Joung, and Dongsoo Har. Tri-copter uav with individually tilted main wings for flight maneuvers. *IEEE Access*, 8:46753–46772, 2020.

[205] Davide Invernizzi, Marco Lovera, and Luca Zaccarian. Dynamic attitude planning for trajectory tracking in thrust-vectoring uavs. *IEEE Transactions on Automatic Control*, 65(1):453–460, 2019.

[206] Bodi Ma, Zhenbao Liu, Wen Zhao, Jinbiao Yuan, Hao Long, Xiao Wang, and Zhirong Yuan. Target tracking control of uav through deep reinforcement learning. *IEEE Transactions on Intelligent Transportation Systems*, 2023.

[207] Xun Wang, Huayong Zhu, Daibing Zhang, Dianle Zhou, and Xiangke Wang. Vision-based detection and tracking of a mobile ground target using a fixed-wing uav. *International Journal of Advanced Robotic Systems*, 11(9):156, 2014.

[208] Jiwei Fan, Xiaogang Yang, Ruitao Lu, Weipeng Li, and Yueping Huang. Long-term visual tracking algorithm for uavs based on kernel correlation filtering and surf features. *The Visual Computer*, 39(1):319–333, 2023.

[209] Zhao Zhang, Yongxiang He, Hongwu Guo, Jiaxing He, Lin Yan, and Xuanying Li. Towards robust visual tracking for unmanned aerial vehicle with spatial attention aberration repressed correlation filters. *Drones*, 7(6):401, 2023.

[210] Sedat Ozer et al. Visual object tracking in drone images with deep reinforcement learning. In *2020 25th International Conference on Pattern Recognition (ICPR)*, pages 10082–10089. IEEE, 2021.

[211] Paraskevi Nousi, Ioannis Mademlis, Iason Karakostas, Anastasios Tefas, and Ioannis Pitas. Embedded uav real-time visual object detection and tracking. In *2019 IEEE International Conference on Real-time Computing and Robotics (RCAR)*, pages 708–713. IEEE, 2019.

[212] Iason Karakostas, Ioannis Mademlis, Nikos Nikolaidis, and Ioannis Pitas. Shot type constraints in uav cinematography for autonomous target tracking. *Information Sciences*, 506:273–294, 2020.

[213] SWEE KING Phang and XUDONG Chen. Autonomous tracking and landing on moving ground vehicle with multi-rotor uav. *J. Eng. Sci. Technol.(JESTEC)*, 16:2795–2815, 2021.

[214] Bor-Horng Sheu, Chih-Cheng Chiu, Wei-Ting Lu, Chun-Chieh Lien, Tung-Kuan Liu, and Wen-Ping Chen. Dual-axis rotary platform with uav image recognition and tracking. *Microelectronics Reliability*, 95:8–17, 2019.

[215] Zhang Chi, Guang-yan Dong, Heng-kuo Qu, Zhi-yuan Zhao, Feng-chao Peng, Yi-jun Lan, Ning-bo Gao, and Guang-fu Si. Realization of target recognition and tracking by single photon array imaging lidar. In *AOPC 2021: Optical Sensing and Imaging Technology*, volume 12065, pages 891–896. SPIE, 2021.

[216] Peikun Zhu, Jing Liang, Zihan Luo, and Xiaofeng Shen. Cognitive radar target tracking using intelligent waveforms based on reinforcement learning. *IEEE Transactions on Geoscience and Remote Sensing*, 2023.

[217] Oliviero Vouch, Yihan Guo, Simone Zocca, Alex Minetto, and Fabio Dovis. Improved outdoor target tracking via ekf-based gnss/uwb tight integration with online time synchronisation. In *Proceedings of the 35th International Technical Meeting of the Satellite Division of The Institute of Navigation (ION GNSS+ 2022)*, pages 2409–2422, 2022.

[218] Abulasad Elgamoudi, Hamza Benzerrouk, G Arul Elango, and René Landry Jr. A survey for recent techniques and algorithms of geolocation and target tracking in wireless and satellite systems. *Applied Sciences*, 11(13):6079, 2021.

[219] Negm Eldin Mohamed Shawky. Accuracy enhancement of gps for tracking multiple drones based on mcmc particle filter. *International Journal of Security and Privacy in Pervasive Computing (IJSPPC)*, 12(1):1–16, 2020.

[220] Abhishek Gupta and Xavier Fernando. Simultaneous localization and mapping (slam) and data fusion in unmanned aerial vehicles: Recent advances and challenges. *Drones*, 6(4):85, 2022.

[221] Ju-Hyeon Hong, Chang-Kyung Ryoo, Hyo-Sang Shin, and Antonios Tsourdos. Integrated guidance, navigation, and control system for a uav in a gps denied environment. In *ICINCO (2)*, pages 450–457, 2018.

[222] John L Crassidis. What is navigation? *Journal of Guidance, Control, and Dynamics*, 45(5):792–794, 2022.

[223] Hao Zhou, Jerome Lynch, and Dimitrios Zekkos. Autonomous wireless sensor deployment with unmanned aerial vehicles for structural health monitoring applications. *Structural Control and Health Monitoring*, 29(6):e2942, 2022.

[224] Liu Yubo, Bei Haohan, Li Wenhao, and Huang Ying. Survey of uav autonomous landing based on vision processing. In *Advances in Intelligent Networking and Collaborative Systems: The 12th International Conference on Intelligent Networking and Collaborative Systems (INCoS-2020) 12*, pages 300–311. Springer, 2021.

[225] WANG Shizhuang, ZHAN Xingqun, ZHAI Yawei, CHI Cheng, and SHEN Jiawen. Highly reliable relative navigation for multi-uav formation flight in urban environments. *Chinese Journal of Aeronautics*, 34(7):257–270, 2021.

[226] Xiaolong Hui, Jiang Bian, Yongjia Yu, Xiaoguang Zhao, and Min Tan. A novel autonomous navigation approach for uav power line inspection. In *2017 IEEE International Conference on Robotics and Biomimetics (ROBIO)*, pages 634–639. IEEE, 2017.

[227] Soumya Vasisht and Mehran Mesbahi. A data-driven approach for uav tracking control. In *Dynamic Systems and Control Conference*, volume 58271, page V001T02A001. American Society of Mechanical Engineers, 2017.

[228] Soumya Vasisht. *Data-Guided Estimation and Tracking Methods for Unmanned Aerial Vehicles*. PhD thesis, University of Washington, 2019.

[229] Jin Tang, Nianhao Xie, Kebo Li, Yangang Liang, and Xinjie Shen. Trajectory tracking control for fixed-wing uav based on ddpg. *Journal of Aerospace Engineering*, 37(3):04024012, 2024.

[230] Jingyi Xie, Xiaodong Peng, Haijiao Wang, Wenlong Niu, and Xiao Zheng. Uav autonomous tracking and landing based on deep reinforcement learning strategy. *Sensors*, 20(19):5630, 2020.

[231] Aytaç Altan and Rıfat Hacıoğlu. Model predictive control of three-axis gimbal system mounted on uav for real-time target tracking under external disturbances. *Mechanical Systems and Signal Processing*, 138:106548, 2020.

[232] Mateusz Zarudzki, Hyo-Sang Shin, and Chang-Hun Lee. An image-based visual servoing approach for multi-target tracking using a quad-tilt rotor uav. In *2017 International Conference on Unmanned Aircraft Systems (ICUAS)*, pages 781–790, 2017.

[233] Hui Cheng, Lishan Lin, Zhuoqi Zheng, Yuwei Guan, and Zhongchang Liu. An autonomous vision-based target tracking system for rotorcraft unmanned aerial vehicles. In *2017 IEEE/RSJ international conference on intelligent robots and systems (IROS)*, pages 1732–1738. IEEE, 2017.

[234] Nguyen Xuan-Mung and Sung-Kyung Hong. Improved altitude control algorithm for quadcopter unmanned aerial vehicles. *Applied sciences*, 9(10):2122, 2019.

[235] Chuxiao Zhang, Jincheng Li, and Zifan Gao. Attitude control of quadrotor uav based on fuzzy pid control under small disturbance. *Highlights in Science, Engineering and Technology*, 53:199–207, 2023.

[236] DJ Regner, JD Salazar, PV Buschinelli, M Machado, D Oliveira, JM Santos, CA Marinho, and TC Pinto. Object tracking control using a gimbal mechanism. *The International Archives of the Photogrammetry, Remote Sensing and Spatial Information Sciences*, 43:189–196, 2021.

[237] Peng Sun, Bing Zhu, Zongyu Zuo, and Michael V Basin. Vision-based finite-time uncooperative target tracking for uav subject to actuator saturation. *Automatica*, 130:109708, 2021.

[238] Kyubin Kim, Jaehong Kim, Han-Gyeol Lee, Jihoon Choi, Jiancun Fan, and Jingon Joung. Uav chasing based on yolov3 and object tracker for counter uav systems. *IEEE Access*, 2023.

[239] Sherif I Abdelmaksoud, Musa Mailah, and Ayman M Abdallah. Control strategies and novel techniques for autonomous rotorcraft unmanned aerial vehicles: A review. *IEEE Access*, 8:195142–195169, 2020.

[240] Erjiang Liu, Yueneng Yang, and Ye Yan. Spacecraft attitude tracking for space debris removal using adaptive fuzzy sliding mode control. *Aerospace Science and Technology*, 107:106310, 2020.

[241] Kyunghyun Lee, Sangkyeum Kim, Seongwoo Kwak, and Kwanho You. Quadrotor stabilization and tracking using nonlinear surface sliding mode control and observer. *Applied Sciences*, 11(4):1417, 2021.

[242] Junseo Heo and Dongkyoung Chwa. Robust tracking control using integral sliding mode observer for quadrotors considering motor and propeller dynamics and disturbances. *Journal of Electrical Engineering & Technology*, 16(6):3247–3260, 2021.

[243] Xuan Chen, Wentao Xue, Haiyang Qiu, and Hui Ye. A moving target tracking control and obstacle avoidance of quadrotor uav based on sliding mode control using artificial potential field and rbf neural networks. In *2020 39th Chinese Control Conference (CCC)*, pages 3828–3833. IEEE, 2020.

[244] Qi Wang, Wei Wang, Satoshi Suzuki, Akio Namiki, Hongxun Liu, and Ziran Li. Design and implementation of uav velocity controller based on reference model sliding mode control. *Drones*, 7(2):130, 2023.

[245] Hamza Bouzerzour, Mohamed Guiatni, Mustapha Hamerlain, and Mohamed Taha Boudali. Robust uncooperative ground target surveillance using vision-based sliding mode control of quadrotor uav. In *IECON 2022–48th Annual Conference of the IEEE Industrial Electronics Society*, pages 1–8. IEEE, 2022.

[246] Hamza Bouzerzour, Mohamed Guiatni, Ahmed Allam, Yasser Bouzid, and Mustapha Hamrelain. Robust vision-based sliding mode control for uncooperative ground target searching and tracking by quadrotor. *Unmanned Systems*, pages 1–21, 2023.

[247] Paul Acquatella, Wouter Falkena, Erik-Jan van Kampen, and Q Ping Chu. Robust nonlinear spacecraft attitude control using incremental nonlinear dynamic inversion. In *AIAA Guidance, Navigation, and Control Conference*, page 4623, 2012.

[248] Tru Hoang, Enkhmurun Bayasgalan, Ziyin Wang, Gavriil Tsechpenakis, and Dimitra Panagou. Vision-based target tracking and autonomous landing of a quadrotor on a ground vehicle. In *2017 American Control Conference (ACC)*, pages 5580–5585. IEEE, 2017.

[249] Ghulam Farid, HW Mo, Asad H Baqar, and Syed M Ali. Comprehensive modelling and static feedback linearization-based trajectory tracking control of a quadrotor uav. *Mechatron. Syst. Control*, 46(3):97–106, 2018.

[250] Huanqing Wang, Xiaoping Liu, and Kefu Liu. Robust adaptive neural tracking control for a class of stochastic nonlinear interconnected systems. *IEEE Transactions on neural networks and learning systems*, 27(3):510–523, 2015.

[251] Christopher Sconyers, Ioannis A Raptis, and George J Vachtsevanos. Rotorcraft control and trajectory generation for target tracking. In *2011 19th Mediterranean Conference on Control & Automation (MED)*, pages 1235–1240. IEEE, 2011.

[252] Giovanni F Salierno and Guilherme V Raffo. Whole-body backstepping control with integral action of a quadrotor uav. *XIII Simpósio Brasileiro de Automaçao Inteligente*, pages 2157–2164, 2017.

[253] Xiaoyu Shi, Yuhua Cheng, Chun Yin, Sara Dadras, and Xuegang Huang. Design of fractional-order backstepping sliding mode control for quadrotor uav. *Asian Journal of Control*, 21(1):156–171, 2019.

[254] Bing Jiang, Kaiyu Qin, Tong Li, Boxian Lin, and Mengji Shi. Robust cooperative control of uav swarms for dual-camp divergent tracking of a heterogeneous target. *Drones*, 7(5):306, 2023.

[255] Tiago Oliveira, A Pedro Aguiar, and Pedro Encarnação. Three dimensional moving path following for fixed-wing unmanned aerial vehicles. In *2017 IEEE International Conference on Robotics and Automation (ICRA)*, pages 2710–2716. IEEE, 2017.

[256] Puneet Jain and Cameron K Peterson. Encirclement of moving targets using relative range and bearing measurements. In *2019 International Conference on Unmanned Aircraft Systems (ICUAS)*, pages 43–50. IEEE, 2019.

[257] Abin Alex Pothen and Ashwini Ratnoo. Curvature-constrained lyapunov vector field for standoff target tracking. *Journal of Guidance, Control, and Dynamics*, 40(10):2729–2736, 2017.

[258] Niki Regina and Matteo Zanzi. Uav guidance law for ground-based target trajectory tracking and loitering. In *2011 Aerospace Conference*, pages 1–9. IEEE, 2011.

[259] Daniel Liberzon. Calculus of variations and optimal control theory - a concise introduction.

[260] RS Sharp and Huei Peng. Vehicle dynamics applications of optimal control theory. *Vehicle System Dynamics*, 49(7):1073–1111, 2011.

[261] Mohamad Norherman Shauqee, Parvathy Rajendran, and Nurulasikin Mohd Suhadis. Proportional double derivative linear quadratic regulator controller using improvised grey wolf optimization technique to control quadcopter. *Applied Sciences*, 11(6):2699, 2021.

[262] Mohsen Majnoon, Kiarash Samsami, Mehran Mehrandezh, and Alex Ramirez-Serrano. Mobile-target tracking via highly-maneuverable vtol uavs with eo vision. In *2016 13th Conference on Computer and Robot Vision (CRV)*, pages 260–265. IEEE, 2016.

[263] Haider AF Almurib, Premeela T Nathan, and T Nandha Kumar. Control and path planning of quadrotor aerial vehicles for search and rescue. In *SICE Annual Conference 2011*, pages 700–705. IEEE, 2011.

[264] Yiheng Liu, Honglun Wang, Na Li, Zikang Su, Yue Yu, and Jiaxuan Fan. Novel anti-disturbance trajectory tracking controller for uav autonomous aerial refueling docking. In *2018 IEEE CSAA Guidance, Navigation and Control Conference (CGNCC)*, pages 1–6. IEEE, 2018.

[265] C Sallé Moreno, S Bertrand, T Lang, N Piasco, and R Bonalli. Uav trajectory generation on a semi-sphere for a fly-around observation mission of a moving target. *ResearchGate*, 12 2016.

[266] Alicia Arce Rubio, Alexandre Seuret, Yassine Ariba, and Alessio Mannisi. Optimal control strategies for load carrying drones. *Delays and Networked Control Systems*, pages 183–197, 2016.

[267] Constance D Hendrix, Michael J Veth, and Ryan W Carr. Lqg control design for a hovering micro air vehicle using an optical tracking system. In *2009 IEEE Aerospace conference*, pages 1–14. IEEE, 2009.

[268] Chao Huang and Heng Zhang. Comparison of disturbance rejection performance between three types of uav linear controllers. In *2020 7th International Conference on Information Science and Control Engineering (ICISCE)*, pages 1768–1773. IEEE, 2020.

[269] Methaq Hadi Lafta. Path scheduling and target trajectory optimization in uavs based on dragonfly and firefly algorithm. *Advances in Engineering and Intelligence Systems*, 1(03), 2022.

[270] Xiaocheng Song, Xiaopei Liu, and Jie Lu. Dynamic local laplacian potential field for uav navigation in unknown environments. *IEEE Transactions on Control System Technology (TCST)*, 2020.

[271] Troi Williams, Po-Lun Chen, Sparsh Bhogavilli, Vaibhav Sanjay, and Pratap Tokekar. Dynamically finding optimal observer states to minimize localization error with complex state-dependent noise. *arXiv preprint arXiv:2211.16721*, 2022.

[272] Soon-Seo Park, Youngjae Min, Jung-Su Ha, Doo-Hyun Cho, and Han-Lim Choi. A distributed admm approach to non-myopic path planning for multi-target tracking. *IEEE Access*, 7:163589–163603, 2019.

[273] Yi Feng, Cong Zhang, Stanley Baek, Samir Rawashdeh, and Alireza Mohammadi. Autonomous landing of a uav on a moving platform using model predictive control. *Drones*, 2(4):34, 2018.

[274] Max Edin Jakobsson and Muhamed Faraj. Trajectory planning for a fleet of autonomous transport robots. M.sc. thesis, Chalmers University of Technology Gothenburg, Sweden, 2022.

[275] Alireza Mohammadi, Yi Feng, Cong Zhang, Samir Rawashdeh, and Stanley Baek. Vision-based autonomous landing using an mpc-controlled micro uav on a moving platform. In *2020 International Conference on Unmanned Aircraft Systems (ICUAS)*, pages 771–780. IEEE, 2020.

[276] Abolfazl Eskandarpour, Mehran Mehrandezh, Kamal Gupta, Alejandro Ramirez-Serrano, and Mohammad Soltanshah. A constrained robust switching mpc structure for tilt-rotor uav trajectory tracking problem. *Nonlinear Dynamics*, pages 1–29, 2023.

[277] Weifeng Zhou et al. *Modelling and controlling of an autonomous tail-sitter vertical take-off and landing (VTOL) unmanned aerial vehicle (UAV)*. Ph.d. thesis, Hong Kong Polytechnic University, 2021.

[278] Erfan Nejabat and Amirhosein Nikoofard. Hybrid robust model predictive based controller for a class of multi-agent aerial dynamic systems. *AUT Journal of Electrical Engineering*, 54(2):209–224, 2022.

[279] Charles Philippe. *Reliable and safe control Navigation for Autonomous Vehicles in Dynamic Urban Environments*. PhD thesis, Université Clermont Auvergne [2017-2020], 2020.

[280] Ignacio Torres Herrera, Lanh Van Nguyen, Trung Le, Ricardo P Aguilera, and Quang Ha. Uav target tracking using nonlinear model predictive control. In *2022 International Conference on Electrical, Computer and Energy Technologies (ICECET)*, pages 1–7. IEEE, 2022.

[281] Baozhe Zhang, Xinwei Chen, Zhehan Li, Giovanni Beltrame, Chao Xu, Fei Gao, and Yanjun Cao. Coni-mpc: Cooperative non-inertial frame based model predictive control. *arXiv preprint arXiv:2306.11259*, 2023.

[282] Morteza Aliyari, Wing-Kwong Wong, Yassine Bouteraa, Sepideh Najafinia, Afef Fekih, and Saleh Mobayen. Design and implementation of a constrained model predictive control approach for unmanned aerial vehicles. *IEEE Access*, 10:91750–91762, 2022.

[283] Hoseong Seo, Suseong Kim, and H Jin Kim. Aerial grasping of a cylindrical object using visual servoing based on stochastic model predictive control. In *2017 IEEE International Conference on Robotics and Automation (ICRA)*, pages 6362–6368. IEEE, 2017.

[284] Qian Wang, Beshah Ayalew, and Thomas Weiskircher. Predictive maneuver planning for an autonomous vehicle in public highway traffic. *IEEE Transactions on Intelligent Transportation Systems*, 20(4):1303–1315, 2018.

[285] Ofir Avni, Francesco Borrelli, Gadi Katzir, Ehud Rivlin, and Hector Rotstein. Scanning and tracking with independent cameras—a biologically motivated approach based on model predictive control. *Autonomous Robots*, 24:285–302, 2008.

[286] Animesh K Shastry, Harsh Sinha, and Mangal Kothari. Autonomous detection and tracking of a high-speed ground vehicle using a quadrotor uav. In *AIAA Scitech 2019 Forum*, page 1188, 2019.

[287] Aytaç Altan, Özgür Aslan, and Rıfat Hacıoğlu. Model reference adaptive control of load transporting system on unmanned aerial vehicle. In *2018 6th International Conference on Control Engineering & Information Technology (CEIT)*, pages 1–5. IEEE, 2018.

[288] Zhi Wei Lee, Wai Hoe Chin, and Hann Woei Ho. Air-to-air micro air vehicle interceptor with an embedded mechanism and deep learning. *Aerospace Science and Technology*, 135:108192, 2023.

[289] Ziyang Zhen, Gang Tao, Ju Jiang, and Liuqing Yang. An adaptive control scheme for carrier landing of uav. In *2018 37th Chinese Control Conference (CCC)*, pages 9872–9876. IEEE, 2018.

[290] Peng Chen, Yunfeng Zhang, Jianhong Wang, Ahmad Taher Azar, Ibrahim A Hameed, Ibraheem Kasim Ibraheem, Nashwa Ahmad Kamal, and Farah Ayad Abdulmajeed. Adaptive internal model control based on parameter adaptation. *Electronics*, 11(23):3842, 2022.

[291] Tagir Z Muslimov and Rustem A Munasypov. Adaptive decentralized flocking control of multi-uav circular formations based on vector fields and backstepping. *ISA transactions*, 107:143–159, 2020.

[292] Lunan Zheng, Feiqi Deng, Zhuliang Yu, Yamei Luo, and Zhijun Zhang. Multilayer neural dynamics-based adaptive control of multirotor uavs for tracking time-varying tasks. *IEEE Transactions on Systems, Man, and Cybernetics: Systems*, 52(9):5889–5900, 2021.

[293] Andrea Cesetti, Emanuele Frontoni, Adriano Mancini, Primo Zingaretti, and Sauro Longhi. A vision-based guidance system for uav navigation and safe landing using natural landmarks. *Journal of intelligent and robotic systems*, 57:233–257, 2010.

[294] Aurelio G Melo, Fabio AA Andrade, Ihannah P Guedes, Guilherme F Carvalho, Alessandro RL Zachi, and Milena F Pinto. Fuzzy gain-scheduling pid for uav position and altitude controllers. *Sensors*, 22(6):2173, 2022.

[295] Narsimlu Kemsaram, TVR Thatiparti, Devendra Rao Guntupalli, and Anil Kuvvarapu. A hybrid autonomous visual tracking algorithm for micro aerial vehicles. *International Journal of Engineering Sciences & Research Technology*, 5(8):524–535, 2016.

[296] Alireza Modirrousta, Mohsen Sohrab, and Seyyed M Mehdi Dehghan. A modified guidance law for ground moving target tracking with a class of the fast adaptive second-order sliding mode. *Transactions of the Institute of Measurement and Control*, 38(7):819–831, 2016.

[297] Kangli Wang, Swee King Phang, Yijie Ke, Xudong Chen, Kehong Gong, and Ben M Chen. Vision-aided tracking of a moving ground vehicle with a hybrid uav. In *2017 13th IEEE International Conference on Control & Automation (ICCA)*, pages 28–33. IEEE, 2017.

[298] Alireza Modirrousta, Mohsen Sohrab, and Seyed Mohammad Mehdi Dehghan. Free chattering sliding mode control with an adaptive algorithm for ground moving target tracking. In *2014 Second RSI/ISM International Conference on Robotics and Mechatronics (ICRoM)*, pages 101–106. IEEE, 2014.

[299] Jose-Ernesto Gomez-Balderas, Gerardo Flores, LR García Carrillo, and Rogelio Lozano. Tracking a ground moving target with a quadrotor using switching control: nonlinear modelling and control. *Journal of Intelligent & Robotic Systems*, 70:65–78, 2013.

[300] Hanran Shi, Faxing Lu, Jiangxin Qi, and Haotian He. Coordinated target tracking of two uavs based on game theory approach and lyapunov guidance vector fields. In *Journal of Physics: Conference Series*, volume 1887, page 012006. IOP Publishing, 2021.

[301] Steven AP Quintero and Joao P Hespanha. Vision-based target tracking with a small uav: Optimization-based control strategies. *Control Engineering Practice*, 32:28–42, 2014.

[302] Sean Wolfe, Sidney Givigi, and Camille-Alain Rabbath. Multiple model distributed ekf for teams of target tracking uavs using t test selection. *Journal of Intelligent & Robotic Systems*, 104(3):1–18, 2022.

[303] Nick-Marios T. Kokolakis, Aris Kanellopoulos, and Kyriakos G. Vamvoudakis. Bounded rational unmanned aerial vehicle coordination for adversarial target tracking. In *2020 American Control Conference (ACC)*, pages 2508–2513, 2020.

[304] Longyu Zhou, Supeng Leng, Qiang Liu, and Qing Wang. Intelligent uav swarm cooperation for multiple targets tracking. *IEEE Internet of Things Journal*, 9(1):743–754, 2021.

[305] Ya Xiao. Multi-location cryptographic code repair with neural-network-based methodologies. In *Proceedings of the 29th ACM Joint Meeting on European Software Engineering Conference and Symposium on the Foundations of Software Engineering*, pages 1640–1644, 2021.

[306] Yudi Chen, Yiwen Jiao, Min Wu, Hongbin Ma, and Zhiwei Lu. Group target tracking for highly maneuverable unmanned aerial vehicles swarms: A perspective. *Sensors*, 23(9):4465, 2023.

[307] Md Ali Azam. Uav control optimization via decentralized markov decision processes. *arXiv preprint arXiv:2107.04593*, 2021.

[308] Nan Jiang, Kuiran Wang, Xiaoke Peng, Xuehui Yu, Qiang Wang, Junliang Xing, Guorong Li, Guodong Guo, Jian Zhao, and Zhenjun Han. Anti-uav: A large multi-modal benchmark for uav tracking. *ArXiv*, abs/2101.08466, 2021.

[309] Haoxin Jin, Shengde Jia, Yanni Deng, and Wenlin Wang. Uav recognition system based on machine vision. In *2022 37th Youth Academic Annual Conference of Chinese Association of Automation (YAC)*, pages 1007–1012, 2022.

[310] Hong Wang, Yu Peng, Liansheng Liu, and Jun Liang. Study on target detection and tracking method of uav based on lidar. In *2021 Global Reliability and Prognostics and Health Management (PHM-Nanjing)*, pages 1–6, 2021.

[311] Amy R Wagoner. *A monocular vision-based target surveillance and interception system demonstrated in a counter unmanned aerial system (UCAS) application*. PhD thesis, Purdue University, 2017.

[312] Ghazlane Yasmine, Gmira Maha, and Medromi Hicham. Survey on current anti-drone systems: process, technologies, and algorithms. *International Journal of System of Systems Engineering*, 12(3):235–270, 2022.

[313] VU Castrillo, A Manco, D Pascarella, and G Gigante. A review of counter-uas technologies for cooperative defensive teams of drones. drones 2022, 6, 65.

[314] RK Narang. Armed suas swarm: Big threat of small uas–c-suas development and threat mitigation by india. *Asian Defence Review*, pages 75–100, 2019.

[315] Jacob Tewes. Lasers, jammers, nets, and eagles: Drone defence is still illegal. *Available at SSRN 3304914*, 2017.

[316] Dr James et al. *A Comprehensive Approach to Countering Unmanned Aircraft Systems*. Joint Air Power Competence Centre, Germany, 2021.

[317] Wahab Khawaja, Vasilii Semkin, Naeem Iqbal Ratyal, Qasim Yaqoob, Jibran Gul, and Ismail Guvenc. Threats from and countermeasures for unmanned aerial and underwater vehicles. *Sensors*, 22(10):3896, 2022.

[318] Joonwon Choi, Minguk Seo, Hyo-Sang Shin, and Hyondong Oh. Adversarial swarm defence using multiple fixed-wing unmanned aerial vehicles. *IEEE Transactions on Aerospace and Electronic Systems*, 58(6):5204–5219, 2022.

[319] Savvas Papaioannou, Panayiotis Kolios, and Georgios Ellinas. Downing a rogue drone with a team of aerial radio signal jammers. In *2021 IEEE/RSJ International Conference on Intelligent Robots and Systems (IROS)*, pages 2555–2562. IEEE, 2021.

[320] Chengwei Ruan, Zhongliang Zhou, Hongqiang Liu, and Haiyan Yang. Task assignment under the constraint of timing sequential for cooperative air combat. *Journal of Systems Engineering and Electronics*, 27(4):836–844, 2016.

[321] Fei Yan, Xiaoping Zhu, Zhou Zhou, and Yang Tang. Heterogeneous multi-unmanned aerial vehicle task planning: Simultaneous attacks on targets using the pythagorean hodograph curve. *Proceedings of the Institution of Mechanical Engineers, Part G: Journal of Aerospace Engineering*, 233(13):4735–4749, 2019.

[322] Marina Moreira, Endre Papp, and Rodrigo Ventura. Interception of non-cooperative uavs. In *2019 IEEE International Symposium on Safety, Security, and Rescue Robotics (SSRR)*, pages 120–125. IEEE, 2019.

[323] Jan Tozicka, Erika Benvegnu, David Šišlák, Michal Pechoucek, and Niranjan Suri. Autonomous ucav coordination in dynamic search and destroy missions. In *Proe. Knowledge Sys. for Coalition Ops 2012*, pages 15–17, 2012.

[324] Jiangbo Jia, Xin Chen, Min Zhang, Weizhen Wang, and Zhen Li. Circular formation control for the cooperative ground target tracking of unmanned aerial vehicle. In *2021 40th Chinese Control Conference (CCC)*, pages 414–420. IEEE, 2021.

[325] Jason Brown and Nawin Raj. The impact of initial swarm formation for tracking of a high capability malicious uav. In *2021 IEEE International IOT, Electronics and Mechatronics Conference (IEMTRONICS)*, pages 1–6. IEEE, 2021.

[326] Jianguo Chen, Wenjun Zhang, Shuaishuai Wang, Yawei Li, and Kun Wang. Ground target guidance method for oriented overhead tracking of fixed-wing uav. In *2019 IEEE International Conference on Power, Intelligent Computing and Systems (ICPICS)*, pages 1–5, 2019.

[327] Peng Yao, Honglun Wang, and Zikang Su. Real-time path planning of unmanned aerial vehicle for target tracking and obstacle avoidance in complex dynamic environment. *Aerospace Science and Technology*, 47:269–279, 2015.

[328] Yueqi Hou, Xiaolong Liang, Lyulong He, and Jiaqiang Zhang. Time-coordinated control for unmanned aerial vehicle swarm cooperative attack on ground-moving target. *IEEE Access*, 7:106931–106940, 2019.

[329] Affiani Machmudah, Madhavan Shanmugavel, Setyamartana Parman, Teh Sabariah Abd Manan, Denys Dutykh, Salmia Beddu, and Armin Rajabi. Flight trajectories optimization of fixed-wing uav by bank-turn mechanism. *Drones*, 6(3):69, 2022.

[330] Jarurat Ousingsawat and Mark E Campbell. Optimal cooperative reconnaissance using multiple vehicles. *Journal of Guidance, Control, and Dynamics*, 30(1):122–132, 2007.

[331] Tahirovic Adnan and Avdagic Zikrija. Tracking style adjustment in automatic cruise control. In *2006 World Automation Congress*, pages 1–6. IEEE, 2006.

[332] Daniel Mellinger, Michael Shomin, and Vijay Kumar. Control of quadrotors for robust perching and landing. In *Proceedings of the International Powered Lift Conference*, pages 205–225, 2010.

[333] Daniel Mellinger, Nathan Michael, and Vijay Kumar. Trajectory generation and control for precise aggressive manoeuvres with quadrotors. *The International Journal of Robotics Research*, 31(5):664–674, 2012.

[334] Giuseppe Ambrosino, Marco Ariola, Umberto Ciniglio, Federico Corraro, Alfredo Pironti, and M Virgilio. Algorithms for 3d uav path generation and tracking. In *Proceedings of the 45th IEEE Conference on Decision and Control*, pages 5275–5280. IEEE, 2006.

[335] Myung Hwangbo, James Kuffner, and Takeo Kanade. Efficient two-phase 3d motion planning for small fixed-wing uavs. In *Proceedings 2007 IEEE International Conference on Robotics and Automation*, pages 1035–1041. IEEE, 2007.

[336] Dongqing Shi, Majura F Selekwa, EG Collins, and Carl A Moore. Fuzzy behavior navigation for an unmanned helicopter in unknown environments. In *2005 IEEE International Conference on Systems, Man and Cybernetics*, volume 4, pages 3897–3902. IEEE, 2005.

[337] Kwangjin Yang and Salah Sukkarieh. 3d smooth path planning for a uav in cluttered natural environments. In *2008 IEEE/RSJ International Conference on Intelligent Robots and Systems*, pages 794–800. IEEE, 2008.

[338] Peng Yan, Zhuo Yan, Hongxing Zheng, and Jifeng Guo. A fixed-wing uav path planning algorithm based on genetic algorithm and dubins curve theory. In *MATEC Web of Conferences*, volume 179, page 03003. EDP Sciences, 2018.

[339] Aurélie Treil, Philippe Mouyon, Tarek Hamel, Alain Piquereau, and Yoko Watanabe. Target tracking and obstacle avoidance for a vtol uav using optical flow. *ViCoMoR 2012*, page 19, 2012.

[340] Alexandre Borowczyk, Duc-Tien Nguyen, André Phu-Van Nguyen, Dang Quang Nguyen, David Saussié, and Jerome Le Ny. Autonomous landing of a multirotor micro air vehicle on a high-velocity ground vehicle. *Ifac-Papersonline*, 50(1):10488–10494, 2017.

[341] E Akshaya Sai Chandar. A review on longitudinal control law design for a small fixed-wing uav. *Int. Res. J. Eng. Technol.(IRJET)*, 9:197–202, 2022.

[342] Junfeng Wu, Huan Wang, Shanshan Li, and Shuguang Liu. Distributed adaptive path-following control for distance-based formation of fixed-wing uavs under input saturation. *Aerospace*, 10(9):768, 2023.

[343] Linnea Persson and Bo Wahlberg. Variable prediction horizon control for cooperative landing on moving target. In *2021 IEEE Aerospace Conference (50100)*, pages 1–10. IEEE, 2021.

[344] Linnea Persson. *Model Predictive Control for Cooperative Rendezvous of Autonomous Unmanned Vehicles*. PhD thesis, KTH Royal Institute of Technology, 2021.

[345] Can Li, Wei Jin, Dewei Li, and Yugeng Xi. Vision-aided automatic landing design for small twin-engine fixed wing uav. In *2019 IEEE 15th International Conference on Control and Automation (ICCA)*, pages 435–440. IEEE, 2019.

[346] Wei Xiao, Qiongjian Fan, Xiaolong Li, Zhiguo Xiong, and Ji Zhang. Control strategy of ground target tracking for fixed-wing uav. In *2018 IEEE CSAA Guidance, Navigation and Control Conference (CGNCC)*, pages 1–4. IEEE, 2018.

[347] Changchun Bao, Yufei Guo, Leru Luo, and Guanqun Su. Design of a fixed-wing uav controller based on adaptive backstepping sliding mode control method. *IEEE Access*, 9:157825–157841, 2021.

[348] Thomas Lombaerts, John Kaneshige, and Michael Feary. Control concepts for simplified vehicle operations of a quadrotor evtol vehicle. In *AIAA aviation 2020 forum*, page 3189, 2020.

[349] Doyoung Kim and Sanghyuk Park. Vision-assisted deep stall landing for a fixed-wing uav. *Journal of Field Robotics*, 39(7):1136–1150, 2022.

[350] Stephan Theil, Markus Schlotterer, Michael Conradt, Marcus Hallmann, Markus Markgraf, and Inge Vanschoenbeek. Hybrid navigation system for the shefex-2 mission. In *AIAA Guidance, Navigation and Control Conference and Exhibit*, page 6991, 2008.

[351] Christian Enemark. *Moralities of Drone Violence*. Edinburgh University Press, 2023.

[352] Ario Yudo Husodo, Grafika Jati, Amarulla Octavian, and Wisnu Jatmiko. Switching target communication strategy for optimizing multiple pursuer drones performance in immobilizing kamikaze multiple evader drones. *ICT Express*, 6(2):76–82, 2020.

[353] Ryan J Wallace and Jon M Loffi. Examining unmanned aerial system threats & defenses: A conceptual analysis. *International Journal of Aviation, Aeronautics, and Aerospace*, 2(4):1, 2015.

[354] Aaron R Schmersahl. Fifty feet above the wall: cartel drones in the us-mexico border zone airspace, and what to do about them. Technical report, Naval Postgraduate School Monterey United States, 2018.

[355] Garik Markarian and Andrew Staniforth. *Countermeasures for Aerial Drones*. Artech House, 2020.

[356] Yannick Veilleux-Lepage and Emil Archambault. A comparative study of non-state violent drone use in the middle east. *International Centre for Counter-Terrorism (ICCT)*, 2022.

[357] Sedat Dogru and Lino Marques. Pursuing drones with drones using millimetre wave radar. *IEEE Robotics and Automation Letters*, 5(3):4156–4163, 2020.

[358] Saulius Rudys, Andrius Laučys, Paulius Ragulis, Rimvydas Aleksiejūnas, Karolis Stankevičius, Martynas Kinka, Matas Razgūnas, Domantas Bručas, Dainius Udris, and Raimondas Pomarnacki. Hostile uav detection and neutralization using a uav system. *Drones*, 6(9):250, 2022.

[359] Hanseob Lee, Dasol Lee, Sunggoo Jung, and David Hyunchul Shim. Design of tracking system using bayesian position prediction for highly manoeuvrable aerial target. In *2018 AIAA Guidance, Navigation, and Control Conference*, page 1593, 2018.

[360] Hyunjin Choi and Youdan Kim. Uav guidance using a monocular-vision sensor for aerial target tracking. *Control Engineering Practice*, 22:10–19, 2014.

[361] Peng Sun, Siqi Li, Bing Zhu, Zongyu Zuo, and Xiaohua Xia. Vision-based fixed-time uncooperative aerial target tracking for uav. *IEEE/CAA Journal of Automatica Sinica*, 10(5):1322–1324, 2023.

[362] Manuel García, Rafael Caballero, Fidel González, Antidio Viguria, and Aníbal Ollero. Autonomous drone with the ability to track and capture an aerial target. In *2020 International Conference on Unmanned Aircraft Systems (ICUAS)*, pages 32–40. IEEE, 2020.

[363] Zhe Xu, Sayan Saha, Botao Hu, Sandipan Mishra, and A Agung Julius. Advisory temporal logic inference and controller design for semiautonomous robots. *IEEE Transactions on Automation Science and Engineering*, 16(1):459–477, 2018.

[364] Athanasios Tsoukalas, Nikolaos Evangeliou, Nikolaos Giakoumidis, and Anthony Tzes. Airborne visual tracking of uavs with a pan-tilt-zoom camera. In *2020 International Conference on Robotics, Computer Vision and Intelligent Systems, ROBOVIS 2020*, pages 90–97. SciTePress, 2020.

[365] Athanasios Tsoukalas, Daitao Xing, Nikolaos Evangeliou, Nikolaos Giakoumidis, and Anthony Tzes. Deep learning assisted visual tracking of evader-uav. In *2021 International Conference on Unmanned Aircraft Systems (ICUAS)*, pages 252–257. IEEE, 2021.

[366] V Kumar. Robotics: aerial robotics. *Coursera, University of Pennsylvania, izdano*, 2016.

[367] Cai Luo, Zhenpeng Du, and Leijian Yu. Neural network control design for an unmanned aerial vehicle with a suspended payload. *Electronics*, 8(9):931, 2019.

[368] Nathan Michael, Daniel Mellinger, Quentin Lindsey, and Vijay Kumar. The grasp multiple micro-uav testbed. *IEEE Robotics & Automation Magazine*, 17(3):56–65, 2010.

[369] Jiawen Shen, Shizhuang Wang, and Xingqun Zhan. Multi-uav cluster-based cooperative navigation with fault detection and exclusion capability. *Aerospace Science and Technology*, 124:107570, 2022.

[370] Shankarachary Ragi and Edwin KP Chong. Uav path planning in a dynamic environment via partially observable markov decision process. *IEEE Transactions on Aerospace and Electronic Systems*, 49(4):2397–2412, 2013.

[371] Steven AP Quintero, David A Copp, and Joao P Hespanha. Robust coordination of small uavs for vision-based target tracking using output-feedback mpc with mhe. *Cooperative Control of Multi-Agent Systems: Theory and Applications*, pages 51–83, 2017.

[372] Zhong Liu, Lingshuang Xiang, and Zemin Zhu. Cooperative standoff target tracking using multiple fixed-wing uavs with input constraints in unknown wind. *Drones*, 7(9):593, 2023.

[373] Weizhen Wang, Xin Chen, Li Li, and Min Zhang. Cooperative target search and tracking for multi-uavs based on control barrier functions. *Transactions of the Institute of Measurement and Control*, page 01423312231158677, 2023.

[374] Wee Kiat Chan and Sutthiphong Srigrarom. Image-based visual-servoing for air-to-air drone tracking & following with model predictive control. In *2023 SICE International Symposium on Control Systems (SICE ISCS)*, pages 1–7. IEEE, 2023.

[375] Wenhong Zhou, Zhihong Liu, Jie Li, Xin Xu, and Lincheng Shen. Multi-target tracking for unmanned aerial vehicle swarms using deep reinforcement learning. *Neurocomputing*, 466:285–297, 2021.

[376] ZHOU Wenhong, LI Jie, LIU Zhihong, and SHEN Lincheng. Improving multi-target cooperative tracking guidance for uav swarms using multi-agent reinforcement learning. *Chinese Journal of Aeronautics*, 35(7):100–112, 2022.

[377] Xinning Wu, Mengge Zhang, Xiangke Wang, Yongbin Zheng, and Huangchao Yu. Hierarchical task assignment for multi-uav system in large-scale group-to-group interception scenarios. *Drones*, 7(9):560, 2023.

[378] Ali Moltajaei Farid, Lim Mei Kuan, Md Abdus Samad Kamal, and KokSheik Wong. Effective uav patrolling for a swarm of intruders with heterogeneous behavior. *Robotica*, 41(6):1673–1688, 2023.

[379] Vinay Chamola, Pavan Kotesh, Aayush Agarwal, Navneet Gupta, Mohsen Guizani, et al. A comprehensive review of unmanned aerial vehicle attacks and neutralization techniques. *Ad hoc networks*, 111:102324, 2021.

[380] Joongsup Yun, David Anderson, and Francesco Fioranelli. Estimation of drone intention using trajectory frequency defined in radar's measurement phase planes. *IET Radar, Sonar & Navigation*, 2023.

[381] Jian Wang, Yongxin Liu, and Houbing Song. Counter-unmanned aircraft system (s)(c-uas): State of the art, challenges, and future trends. *IEEE Aerospace and Electronic Systems Magazine*, 36(3):4–29, 2021.

[382] Ronald O'Rourke. Navy lasers, railgun, and gun-launched guided projectile: Background and issues for congress. *CRS Report*, 2(R44175), 2020.

[383] Commander Dr Jayakrishnan N Nair. *Emerging Defence, Maritime and Aerospace Technologies by DRaS*. Highlyy Publishing LLP, 2023.

[384] Matthieu J Guitton. Fighting the locusts: Implementing military countermeasures against drones and drone swarms. *Scandinavian Journal of Military Studies*, 4(1), 2021.

[385] Fan Tianfeng, Meng Xiaojing, and Zhang Chi. Development status of anti-uav swarm and analysis of new defence system. In *Journal of Physics: Conference Series*, volume 2478, page 092011. IOP Publishing, 2023.

[386] Lee Weinstein and Jay Gainsboro. Method and apparatus for drone detection and disablement, January 9 2018. US Patent 9,862,489.